UNIVERSITY OF SOUTHAMPTON

# THE CONJUNCTIVAL EPITHELIUM AND GRASS POLLEN ALLERGEN ASSOCIATED INTERACTIONS IN ATOPIC EYE DISEASE

James L. Hughes

Doctor of Philosophy

SCHOOL OF MEDICINE

FACULTY OF MEDICINE, HEALTH AND LIFE SCIENCES

June 2006

# ABSTRACT

Seasonal Allergic Conjunctivitis (SAC) is a type I hypersensitivity reaction that effects approximately 1 in 10 of the population. It follows a distinct annual pattern of occurrence with the natural release of aeroallergens in the environment, therefore the patient population maybe sub-divided into two subject groups. Those subjects studied during the period of allergen release, therefore then the disease is active, are classed as SACa (active). Subjects studied during no allergen released are classed as SACq (quiescent). The first ocular tissue contact of these aeroallergens is the conjunctival epithelium, which forms the largest part of the ocular surface. Contact with the aeroallergens in susceptible individuals results in the local hypersensitivity response, which is characterised by the release of histamine from degranulated mast cells during the early phase response. The immune cascade following mast cell degranulation has been well studied and documented, but the role that the epithelial layer has within the pathogenesis of SAC is still poorly understood. The hypothesis of this thesis is that the epithelial layer of SAC subjects is altered, thus facilitating the passage of allergen to the immune system and therefore further contributing to disease progression. The aims of this thesis were, therefore, to investigate structural aspects of the conjunctival epithelium, develop and expand experimental models of the conjunctival, investigate the effects that Timothy grass pollen allergen has on the polarised epithelial barrier and finally detect the paracellular movement of the allergen.

Evidence is presented of certain structural alterations in the epithelial layer of subjects who suffer from SAC. By examining thin sections of conjunctiva, using immunohistochemistry, immunoreactivity for epithelial adhesion proteins and keratin filaments, were investigated. The epithelium from SAC subjects showed reduced expression of these protein targets and re-distribution of said proteins within the epithelial layer, suggesting that fundamentally the conjunctival epithelium from SAC provided a reduced barrier to endogenous antigens.

Epithelial model systems of the conjunctival epithelium were developed and characterised by their specific morphology, immunoreactivity and barrier function for experimental purposes. Models assessed were, immortalised cell lines, primary cell cultures and whole stratified tissue. All model systems displayed epithelial characteristics. Primary cell culture proved to be logistically expensive and therefore cell line models were preferred for further allergen-epithelial interaction study. Stratified tissue provided valuable insight into tissue polarity but further investigations in this model were unfeasible due to time constraints.

Re-creating the allergen challenge model of SAC facilitated investigations into the mode of allergen entry into the epithelial layer. The affect that Timothy grass has on the tight junctions, inducers of the polarised barrier function of epithelial tissues, was monitored by recording the trans-epithelial electrical resistance generated by the cell layer during challenges. Physical paracellular movements were assessed by the detection of inert molecules on the basal side of the epithelium after their addition above the apical membrane. Tight junctions were suggestively, affected by Timothy grass pollen allergen in a cysteine protease action, supported by the use of protease inhibitors.

Localisation studies were undertaken in the challenged models, to further investigate the paracellular movement of allergen through the epithelial layer. Then conjunctiva from subjects, whom had taken part in ocular challenges were used to detect allergen within the epithelium. Restrictive stock of specific antibodies resulted in no tangible data from either of these avenues of investigation.

# CONTENTS

# List of figures

# LIST OF ACCOMPANYING MATERIAL

Reduced structural proteins in the conjunctival epithelium in allergic eye disease.
J.L. Hughes, P.M. Lackie, S.J. Wilson, M.K. Church and J.I. McGill.
Allergy 2006; 61(11): 1268-74.

# DECLARATION

All work within this thesis was designed, carried out and analysed by the author with the exception of

- Immunohistochemical staining of CD44 and E-Cadherin was carried out jointly with Miss Carley Bowman-Burns.
- Immunohistochemical staining of Desmoplakin 1-2 was carried out jointly with Miss Si-Lee Yeoh.
- Immunohistochemical staining of Keratin 5/6, 7, 8, 13, 14, 18 and Pan was carried out jointly with Miss Siti Yossef.

Archival conjunctival biopsies were provided by Mr D.F. Anderson.

Technical assistance with the sectioning the Glycolmathacrylate blocks were provided by members of the Immunohistochemistry Research Unit.

The work was completed whilst I was a registered postgraduate student within the Infection, Inflammation and Repair Division of the School of Medicine, University of Southampton. This work has not, to my knowledge, been submitted by myself, or any other person, for another degree.

# ACKNOWLEDGEMENTS

I would firstly like to thank Peter Lackie for his invaluable supervision and scientific guidance, without which there would have been no project. I would also like to thank James McGill for his constant energetic and enthusiastic approach to this project and especially his ability to infuse inspiration into every aspect of this work.

The School of Medicine and charities that made this work possible by funding my position and research expenses.

My Brooke Laboratory family deserve a mention, for their ability of provide distractions as and when required throughout my time with them.

Without the love, support and constant badgering of my family I would never have been able to carry out this project, thank you Mum, Stu, Jo, Nana and Granddad!

And a little mention for my D. x

# ABBREVIATIONS

| | |
|---|---|
| 16HBE 14o- | Human bronchial epithelial cell line |
| AKC | Atopic keratoconjunctivitis |
| APC | Antigen presenting cell |
| BSA | Bovine serum albumin |
| CD | Cluster of Differentiation |
| ChWk | Chang epithelial cell line |
| DAB | Diaminobenzedine |
| Der p | *Dermatophagoides pteronyssinus* |
| DMSO | Dimethyl Sulfoxide |
| EDTA | Ethylenediaminetetraacetic acid |
| FcεRI | High affinity IgE receptor |
| FBS | Foetal bovine serum |
| FITC | Fluorescein Isothiocyanate |
| GMA | Glycolmathacrylate |
| GM-CSF | Granulocyte-macrophage colony stimulating factor |
| IgE | Immunoglobulin-E |
| IFN | Interferon |
| IL | Interleukin |
| IOBA-NHC | Conjunctival epithelial cell line |
| MC | Mast cell |
| PAC | Perennial allergic conjunctivitis |
| Phl p | *Phleum pratense* |
| RT | Room temperature |
| SAC | Seasonal allergic conjunctivitis |
| SACa | Active seasonal allergic conjunctivitis |
| SACq | Quiescent seasonal allergic conjunctivitis |
| SEM | Scanning electron microscopy |
| TEER | Trans-epithelial electrical resistance |
| TEM | Transmission electron microscopy |
| TNF | Tumour necrosis factor |
| VKC | Vernal keratoconjunctivitis |
| ZO | Zonula occludin |

# 1. Introduction

## 1.1 Seasonal Allergic Conjunctivitis (SAC)

Seasonal allergic conjunctivitis is often associated with allergic rhinitis and termed rhinoconjunctivitis (Easty and Wyse (Eds) 2002). For the purpose of this thesis, only the involvement of the eye will be dealt with.

Allergic eye disease is common and affects approximately 10-15% of the UK population (McGill *et al* 1998, Anderson 2001 (a)). Allergic eye disease, along with all atopic diseases are increasing in prevalence (Kosunen *et al* 2002, Ninan and Russell 1992), many factors such as; socioeconomic class, increased allergen exposure, lifestyle changes and heredity / intrauterine / infancy factors have been linked to this increase and have been widely cited (Sly 1999, Howarth 1998, Woolcock and Peat 1997, Norrman *et al* 1994, Herrstrom and Hogstedt 1994, Rind 1994, Lebowitz *et al* 1984). SAC is caused by inappropriate inflammation of the ocular surface to normally innocuous antigens, and is part of a spectrum of allergic eye diseases, which share a similar inflammatory response to allergen, that can manifest in a local or systemic response (Ono 2000). The variety of allergic eye diseases, range from the mild and irritating conditions to severe and sight threatening disorders. Disease classification and diagnosis is predominantly made upon the clinical symptoms presented. A confirmatory test to identify the offending allergen, can be used, commonly this is the skin-prick test. Another confirmatory test measures and quantifies the increased IgE levels within either blood or tear samples (Buckley 1998, Nomura and Takamura 1998).

The mild, symptomatic diseases are Seasonal Allergic Conjunctivitis (SAC) and Perennial Allergic Conjunctivitis (PAC). SAC is self-limiting, producing slightly milder symptoms and is more common affecting about 15% of the population, and represents the leading cause of red eye presentation to both hospital and general practice (Anderson 2001 (a), Magone *et al* 2000). Both SAC and PAC are not usually complicated by more serious corneal involvement (Leonardi *et al* 1999). Although symptomically mild, SAC and PAC can impair daily activities, causing inconvenience and compromising the quality of life of sufferers, also impacting economically, with working days lost each year (Joss

and Craig 1999, Buckley 1998). The two diseases share common pathologies, but as their names imply they follow different annual disease patterns. The incidences of the seasonal form are exclusively linked to the naturally occurring increases in air-bourne pollen levels, during the pollination period. PAC is chronic therefore incidences are seen throughout the year, with a slight increase seen in the autumnal months (Dart *et al* 1986, McGill *et al* 1998). The severe forms of allergic conjunctivitis are Vernal Keratoconjunctivitis / Vernal Catarrh (VKC) and Atopic Keratoconjunctivitis (AKC). VKC usually affects males more than females until puberty at which point the ratio between males and females reduces. AKC on the other hand develops during, and persists from the teenage years and has links with other disorders such as asthma and atopic dermatitis. Both VKC and AKC can lead to conjunctival fibrosis / scarring, symblepharon and corneal epithelial damage, leading to possible corneal fibrosis resulting in blindness (Roat *et al* 1993).

The common allergen involved in SAC is grass pollen, although other pollens may cross-react to cause the onset of symptoms in a sensitised individual. The main grass species connected with SAC are those found in temperate zones such as *Phleum pratense* (Timothy grass) and *Lolinum perenne* (rye grass). Within the UK, Timothy grass is the common instigator of SAC.

The clinical presentation of SAC includes a plethora of symptoms that are usually bilateral. The main symptom is irritation, manifesting as itch, lacrimation also occurs but is largely seen in cases of rhinoconjunctivitis. Eyelids become swollen which is further exacerbated by the action of rubbing. The conjunctival epithelium takes a reddish-pink appearance due to hyperaemia of the vessels. Small tarsal papillae can form in the tarsal conjunctiva; this is due to the oedema around the blood vessels being restricted in spread, caused by the lack of malleable tissue found between the conjunctiva and tarsal plate (Buckley 1998, Holgate *et al* 2001).

SAC is a type I (immediate) hypersensitivity reaction, therefore sufferers have been previously sensitised to a specific allergen. Development of the hypersensitivity reaction is the interactions of allergen, antigen presenting cells (APC), T cells, B cells and the effector immune cells; mast cells, basophils, macrophages and other APCs. Upon allergen exposure, APCs express small peptide fragments in conjunction with the major histocompatibility complex

(MHC) class II molecules to the T cells (Lambrecht 2001). These T cells interact with B cells and this leads to the production of allergen-specific IgE locally (Jackson *et al* 2002). The IgE molecules then bind to mast cells and basophils that have surface receptors for the FcεRI portion of the IgE molecule. These cells are then pre-programmed ready for the next episode of allergen exposure, upon which allergen is cross linked with two bound, adjacent IgE molecules, subsequently leading to cell degranulation and the release of mediators including histamine, tryptase, chymase, heparin, chrondroitin sulfate, postaglandins, thromboxanes and leukotrienes (Bannon 2002, Reischl *et al* 1999, Galli 1997).

## 1.2 Immunological aspects of the type one hypersensitivity

**Sensitisation**

For an evoked type one allergic reaction, recognition of the specific antigen must occur the first sampling of foreign antigens is called sensitisation. The first step of sensitisation is dependent upon the presentation of antigen to the T and B cells, located within the lymph tissues for the generation of IgE.

Within the eye, circulating non-phagocytic constitutive antigen presenting cells such as Langerhans' and dendritic cells sample any foreign material found within the tissue. These cells degrade intact proteins into processed peptides that bind to MHC II molecules, within intracellular organelles, which are then expressed on the surface of the cell. Activation of the $TH_2$ cell takes place in the nearest lymph node to the infection or site of sampling. Co-stimulatory molecules are also expressed on the surface of the APC in order to ensure that when the T cell and APC bind T cell proliferation is sanctioned. Antigen presentation through the MHC II molecule can be spilt into four stages: adhesion, antigen-specific activation, co-stimulation and cytokine signalling. The important factors involved in the four stages mentioned previously are, adhesion; ICAM 1/2 on the APC and LFA-1 on the T cell, antigen-specific activation; CD58 / MHC on the APC and CD2 / CD4 on the T cell, co-stimulation; B7 on the APC and CD28 on the T cell and finally cytokine signalling; IL-5 / IL-2 on the APC and IL-1R / CD25 on the T cell. The main co-stimulatory factor involved in the MHC/peptide – TCR interaction is the B7 – CD28 interaction. The sensitivity of

the T cell to the antigenic peptide is increased via the binding of CD4 to the tyrosine kinase lck.

T cell activation is the result of the clustering of receptors upon ligand binding, this leads to the activation of associated tyrosine kinases, which phosphorylates tyrosine kinase residues in the cytoplasmic tails of the clustered receptors, followed by recruitment of additional kinases and signalling molecules, in cascades. The end result of which is induction of gene synthesis by the activation of transcription factors predominantly IL-2.

As the activation of the $TH_2$ cells occur, the B cell will follow a similar pattern of activation. Two processes are the major influence on B cell activation; interaction with antigen and the B cell Ig receptor and stimulating signal cytokines from the TH cell released by antigen processing for presentation via bind to the MHC II molecule. When antigen is taken up by the B cell, it too is processed and expressed bound to MHC II molecules on the surface of the B cell. $TH_2$ also interact with these MHC II molecules leading to further activation of further $TH_2$ and therefore increased release of co-stimulating cytokines from the T cell, which induce proliferation and differentiation of the B cells into antibody forming cells (AFCs). The cytokines released from the TH cells which induce proliferation are IL-2, 4, 5 and 6. The cytokines involved in the differentiation of B to AFC are IL-2, 4, 5, 6 and 10, and also IFN$\gamma$. Excess Il-4 has been shown to have a role in the producing of IgE. Within the AFCs somatic hypermutation occurs in order to diversify the rearranged variable region genes, thus allowing sub-clones that contains variants with different affinities for the antigen of interest. The cells with the higher affinity immunoglobulin, express Bcl-2 and are saved from apoptosis via interaction with T cells, also promoting class switching for further antibody production. In the case the type one hypersensitivity reaction, IgE molecules are produced and released from the AFC cell either to remain as soluble molecules circulating around the site of the reaction or are sequestered to the high affinity receptor (Fc$\varepsilon$RI) on the surface of mast cells and basophils. The subsequent allergen cross-linkage of IgE is involved in causing inflammatory cell activation/degranulation.

The structure of IgE has a high molecular weight $\varepsilon$ chain, 72500 KDa, due to a large number of amino acid residues distributed over five the five

domains (VH, Cε1, Cε2, Cε3 and Cε4). It is distinct from the other dimeric immunoglobulins due to its extra constant region domain and binding site for the high and low affinity receptors (FcεRI and FcεRII).

Mast cells with surface bound IgE can be classed as programmed ready for the next episode of allergen presents.

**Evoked allergic response**

The central effector cell involved in the pathogenesis is the mast cell. Mast cells (MC) are responsible for the manufacture, storage and release of cytokines and other inflammatory factors that induce the inflammatory cascade.

During active periods of disease increases in mast cell numbers have been reported, these have been shown to form two different populations. Those found exclusively in the mucosal tissue contain only tryptase, and are classed as MCt, whereas those found in the underlying tissue contain other compounds such as chymase, cathepsin-G and carboxypeptidase-A (Morgan *et al* 1991, Baddeley *et al* 1995) and are classified as MCtc. Mast cells are regulated in terms of development and function by cytokine regulators, of which, stem cell factor is a major influence on the increased number of MCt and MCtc populations found in seasonal allergic conjunctivitis (Zhang *et al* 1998, Morgan *et al* 1991).

Histamine is the hallmark of both mast cell / basophil activation / degranulation and is responsible for increased vascular permeability, vasodilation, and increased mucus secretion.

Other primary mediators released from the degranulated mast cell are neutral proteases and arachidonic acid, both of which lead to the production of the proinflammatory cytokines; interleukin (IL) -4 / 5 / 6 / 8, prostagladins, leukotrienes, granulocyte-macrophage colony stimulating factor (GM-CSF), tumour necrosis factor-alpha (TNFα) and Interferon-gamma (IFN-γ) (Anderson *et al* 2001 (b), Leonardi *et al* 2000, Macleod *et al* 1997, Gamache *et al* 1997, Ohkawara *et al* 1992, Schwartz and Austen 1984).

The conjunctival epithelium has also been cited as a source of proinflammatory mediators *in vitro* possibly linked to the demonstration of the histamine receptors $H_1$ and $H_2$ on the conjunctival surface (Anderson 2001 (a), Gamache *et al* 1997). The endothelium acts, under the influence of the released

cytokines, as a potent paracrine stimulatory for the immune reaction. During acute inflammation, endothelial cells transform into a proinflammatory phenotype, facilitating chemo-attraction and leukocyte adhesion / activation / migration, with the endothelial layer increasing further in terms of permeability from its already freely diffuse nature (Stefanovic *et al* 1998, Raviola 1983).

The recruitment of cell types such as eosinophils and neutrophils in SAC during active disease periods, was not found to be statistically significant; although if present they may contribute physiologically (Anderson *et al* 1997).

Levels of Substance P have been found to be elevated in allergic eye disease compared to levels found in non-atopic controls (Fujishima *et al* 1997), and it has been suggested that it has a role in the severity of the disease.

Several other markers have also been found to be increased in the tears of patients; these markers include eosinophil cationic protein, neurotoxin, and IL-2 receptor (Leonardi *et al* 2000).

The type I immediate hypersensitivity reaction has a bi-phasic pattern; the early and late phase responses. Due to the rapid degrading of histamine, the early response is due to the release of histamine from mast cells, the late response is thought to be due to infiltrating basophil-derived histamine (Bacon *et al* 2000, Leonardi *et al* 2000). Cellular interactions during the inflammatory response are controlled and regulated by complex mechanisms that include the inter-play between cell surface receptors, cytokines and components of the extra-cellular matrix, therefore any disturbance to these factors can affect the progression of the inflammatory response (Bacon *et al* 1998, Carreno *et al* 1995).

Inhibition of the immediate hypersensitivity and the late-response cellular infiltrates has been suggested due to the release of type 1 cytokines (Magone *et al* 2000). GM-CSF has been found to induce apoptosis of mast cells and antigen presenting cells that have undergone change due to stress or injury, possibly as a result of the inflammatory reaction, the removal of the cells is postulated to homeostasis in cell populations (Breuhaln *et al* 2000). IL-4 has been shown to cause a dampening effect on the cellular component of active inflammation through retarded leukocyte migration into epithelial tissue (Colgan *et al* 1994).

The role that the mast cell and other inflammatory cells have in the progression of disease has been investigated in great depth, but the effects that

this inflammatory response has on the surrounding tissues especially the epithelial layer remain poorly understood.

## 1.3 *Phleum pratense* (Timothy grass pollen)

The Timothy grass species *Phleum pratense* is a cool-season, short-lived perennial bunchgrass, originally a native Eurasian plant it is now globally distributed throughout temperate regions (Duke 1978). It grows on heavy, deep and moist soil types and is mainly cultivated for agricultural proposes most importantly for animal foodstuff such as hay production or silage. It grows to approximately 150 cm long with leaf-blades of 4-20 cm in length and 3-9 mm in width (Clayton *et al* 2002). Seed yields from Timothy grass can range from 6 – 600 kilogram per hectare according to cultivation and farming techniques applied (Duke 1978). The pollen grain from Timothy grass can vary in diameter from 25 to 60 μm (Motta *et al* 2004) (figure 1.1). A pollen grain is constructed of two or three cells; the vegetative cell, which provides the major bulk of the grain, and either a generative cell or two sperm cells. The grain protoplasm is encased by the cell wall whose outer portion is a tough, resistant and highly elaborate sculptured, but incomplete in grain surface coverage, coat called the exine composed of sporopollenin. This provides protection from the external environment for the internal reproductive cells and is also involved in the adhesion to pollinator and stigmatic surfaces. The inner portion, intine, is composed of pectin and cellulose (Twell 2001). Pollen grains are released in a highly dehydrated state and upon rehydration the exine undergoes structural re-modeling allowing the release of allergen loaded starch / pollen cytoplasmic granules. These starch / pollen cytoplasmic granules are approximately 5 μm or less in diameter and offer allergen and associated proteins a better vehicle for gaining entry into biological tissue either as allergen-containing aerosols or directly through mucosal tissues (Motta *et al* 2004). Grass pollens are typically released during the spring to autumn months (May – mid August), with peak pollen release occurring in the months of June and July (figure 1.2).

### 1.3.1. Timothy grass allergens

Allergens are types of antigens that are otherwise harmless but elicit an allergic response in certain sensitised populations. Sensitisation occurs when an allergen is sampled by the immune system, which then builds and expands its potential to react to the allergen upon its next contact. In order for the immune system to see the allergen, the allergen has to gain access into the body. Classically allergens enter the body through either the skin or mucosal membranes, entry can also be facilitated by injection or parasitically (Aalberse and Kapsenberg 2001). Upon the next episode of immune contact with an allergen, the immune reaction and subsequent release of mediators results in the symptoms being experienced by the individual. Grass pollen allergens are proposed to gain entry via the mucosal membranes of the body. Allergens are released from the pollen grain directly upon hydration (Ball *et al* 2005, Grote *et al* 2001, Vrtala *et al* 1993). The mechanisms by which the allergen then physically penetrates through the mucosal membrane is still not fully understood. One proposed model is via cleavage of the junctional components between cells, through the proteolytic nature of some the of the allergens (Grobe *et al* 1999, 2002), but this is not universally accepted (Lian-Chao and Cosgrove 2001). Timothy grass has the most complete set of isolated and cloned grass pollen allergens. About 20 species of allergens have been implicated as the most frequent causes of allergy, with more being characterised constantly (Andersson and Lidholm 2003). Allergens are classified as either major or minor, this definition is based upon the number of individuals which show sensitivity to a particular allergen, if greater than 50% of the sensitised population reaction to an allergen then it is termed a major allergen (Mari 2003, Aalberse and Kapsenberg 2001). The term atopic allergens are those that are IgE-inducing antigens. The allergenic properties of these proteins is though to be linked to speed of solubility and therefore amount present, rather than the intrinsic properties of the allergen (Vrtrala *et al* 1993). The molecular masses of grass pollen allergens mostly range from 10-50 kDa. The most well defined allergens are group 1 and 5 and also data based on the prevalence of IgE recognition, shows that these groups dominate the immune reaction (Ball *et al* 2004, Andersson and Lidholm 2003, Suck *et al* 1999). Phl p1 is one of the most important allergens implicated in allergy disease. Phl p1 is a 33 / 35 kDa glycoprotein, which contains seven cysteines and

four independent IgE-binding regions and one continuous epitope, which would explain its 'major' allergen status via its ability to cross bind with two cytotropic IgE molecules via the FcεRI receptors on mast cells (Ball *et al* 2005, Suck *et al* 1999). Phl p1 is a cysteine protease, demonstrated by specific substrates and inhibitors and therefore could be the allergen that facilitates allergen paracellular movement (Petersen *et al* 1999). The other functions of the Phl p allergens are RNase (Phl p5b), $Ca^{2+}$ binding (Phl p7), Profilin (Phl p12) and Polygalacturonase (Phl p13) (Behrendt and Becker 2001). The immunogenicity of several of the major Phl p allergens have been shown to be Phl p 5>Phl p 1>Phl p 6>Phl p2 (Linhart *et al* 2002).

## 1.4 Structure of the external eye

As an extension of the nervous system, the eye acts as the visual sensory organ of the body. The eye is located within a thin bony socket called the orbit, which also contains fat deposits, nerves, blood vessels and the ocular muscles. The eye is composed of several soft tissue bodies; these bodies have both protective and light transmitting functions. The portion of the eye that is not enclosed by the orbit has tissues that allow the transmittance of light into the chambers of the inner eye to the retina. Light travels through firstly, the cornea, then through the aqueous humour, then the lens, passing through the vitreous humour before reaching the retina. The cornea is vital to the focusing of sight and therefore requires a specialised environment for it to function properly. The cornea's environment is supplied and maintained by the conjunctiva, which is a thin, transparent, vascular tissue layer that forms the mucosal membrane covering the white, tough body known as the sclera and continuing to the eyelid margins. The conjunctiva is an epithelial tissue that runs anti-parallel and closely apposed to the corneal epithelium, supports the tear film, and as such is constantly exposed to air-bourne allergens (figure 1.3). Anatomically the conjunctival epithelium has been divided into four regions, running from the corneal epithelium margin to the eyelids margin are the bulbar, fornix, orbital and tarsal regions.

## 1.5 Conjunctival epithelium

The conjunctiva is a vascular polarised tissue that runs from the lid margin becoming confluent with the corneal epithelium, covering the white sclera of the external eye. It is similar to mucus membranes from other parts of the body, is constantly exposed to aeroallergens, and can be considered as fully equiped to capture, process and present antigen to immunocompetent cells (Scott *et al* 1997). The names of the sub-divisions, bulbar, fornix, orbital and tarsal of the conjunctival epithelium are reflective in the structures they approximate (figure 1.4). It is the bulbar portion of the conjunctival epithelium that is loosely connected to the episclera, covering the sclera allowing the movement of the eyelids over the body of the eye. The conjunctiva has several features in common with other epithelial mucosa surfaces such as the upper airways, which it is continuous with, through the nasoacrimal canal. It is the major site of the first interaction of allergens and aero-irritants. Within the body the different epithelial structures are classified according to their morphology. Two distinct variables are used for classification, cell layer number and cell shape. Layers are categorised as simple, stratified or pseudo-stratified; cell shape can be squamous, cubiodal or columnar. In the conjunctiva the epithelial layer is composed of non-keratinised non-ciliated stratified columnar epithelium, of 3 to 5 cell layers thick (fig 1.5a Conjunctival epithelium). The epithelial layer is subject to abrasive pressure from epithelial-epithelial interactions from eyelid movement and it is the presence of the tear film and especially its mucus content that reduce the frictional forces (Gipson *et al* 1995). The epithelial layer supports the tear film, which is produced by the lacrimal gland located near the conjunctival fornix. The tear film is composed of three layers, directly supported by the superficial epithelial layer is the glycocalyx layer. The next layer is the largest layer of the tear film and is the aqueous layer, the most anterior and last layer of the film is the lipid layer. The tear film maintains the stable environment of the two epithelial tissues, namely the corneal and conjunctival. The tear film also fulfils a special role in the prevention of potential pathogens reaching the tissue of the eye, by presence and by the action of blinking. The tear film also contains important protective proteins such as lysozyme, $\beta$-lysin and lactoferrin, all of which have anti-bacterial properties. Mucin secreting cells are found in the

apocrine or holocrine glands and line the crypts of Henle; they form basally and migrate to the superficial layer. They attach via desmosome spot junctions to the epithelial cells of the conjunctival layer. A secondary mucus secreting system has also been postulated, a mucin-like glycoprotein has been isolated that is produced by the stratified epithelium of the conjunctiva (Watanabe *et al* 1995). Although some literature reports that it is only a small proportion of these superficial cells ~ 10%, that have secretory functions (Steuhl and Knorr 1990). The Mucin-like molecule is present on cytoplasmic vesicles in subapical cells, and then when the cells differentiate and form the superficial cell layer, the molecule is transported to the membrane and is located on microplicae folds (Gipson *et al* 1995). Release of the mucin-like glycoproteins has been shown in vitro, via the binding of platelet-activating factor (PAF) to receptors on the surface of the epithelial cells, via an autocrine or paracrine mechanism (Alder *et al* 1992).

As mentioned briefly above, the conjunctival epithelium has extensive desmosome spot junctions throughout, the desmosome spot junction is one part of the adherence system that epithelial tissues have, other major junctions are the tight junction, intermediate junction and located along the basement membrane are hemi-desmosomes, which as the name suggests resemble half desmosome spot junctions. Throughout the epithelial layer are also non-junctional molecules that achieve cell-cell adhesion and cell-matrix adhesion (figure 1.5b conjunctival epithelium). Regulation and modulation of these junctions and or the epithelial junctional complex can affect specific function of the epithelial tissue (Thei *et al.* 1996).

## 1.6 Cell-Cell adhesion

Epithelial tissues provide a protective barrier from physical, chemical and microbial damage; this is facilitated by the maintenance of structural integrity, via organisation and differentiation of cells and the subsequent expression of structural / adhesion proteins (Presland and Jurevic 2002, Presland and Dale 2000).

The organisation of an epithelium depends greatly upon the epithelial cell layers and their pattern of cell-cell junctions and therefore cell-cell adhesion, which also mediates layer maintenance. Running from the apical membrane, the

junctional complex found in epithelial tissue consists of three distinct types of junction; firstly, a tight junction (zonula occludens) followed by an intermediate junction (zonula adherens) then a desmosome spot junction. Desmosomes are found throughout the epithelium on the lateral (beneath the junctional complex) surfaces of the superficial cells, the apical and baso-lateral surfaces of the intermediate layer of cells and on the lateral membranes of basal cells. Connecting the basal epithelial layer with the basement layer are the hemi-desmosomes junctions. The formation of cellular junctions involves highly orchestrated cellular interactions, including the expression of adhesion proteins leading to the addition and assembling of junction proteins to form cell-cell junctions (Cyr *et al* 1995). These cell adhesion systems are also being increasingly implicated in cell-cell and intracellular signalling pathways (Magee 1995).

### 1.6.1 Tight junctions

Tight junctions (zonula occludens) create a paracellular permeability barrier also acting as a fence preventing the movement of proteins and lipids at mucosal surfaces (Ryeom *et al* 2000, Nusrat *et al* 2000, Inai *et al* 1999, Zahraoui *et al* 1994). Junctions are constructed of transmembrane and plaque proteins, forming a belt of proteins just beneath the apical membrane surface of the superficial cells, encircling the apical surface. They can be identified at the ultra-structural level by appearance; the opposing lateral cell membranes appear to fuse together or kiss (Gasbarrini and Montalto 1999, Kubota *et al* 1999). Tight junctions act as a barrier between the intercellular spaces and the external environment of the epithelium. This structured regulation of ionic solutions gives the epithelium its polarity, and therefore regulates protein and lipid distribution within the epithelium.

The predominant transmembrane proteins are the occludins and claudins (Latin, claudere = close), also associated are tight junction proteins that belong to the immunoglobulin superfamily.

Occludins have four transmembrane domains, two extracellular loops and three cytoplasmic domains, with a molecular weight ranging from 62-82kDa. The second extracellular loop has been cited as a requirement for the stable assembly of the occludin molecule within the tight junction (Medina *et al* 2000).

Claudins have four transmembrane domains and two extracellular loops, 24 members of the claudin family have been cloned with molecular weights ranging from 20-27kDa. Claudins are thought to be the primary adhesive protein that ensures the tightness of the junction, identified as the obliteration of the intercellular space (Anderson and Itallie 1999, Kubota *et al* 1999). The extra-cytoplasmic domains, in conjunction with other junctional proteins, regulate paracellular permeability (Heiskala *et al* 2001, Lippoldt *et al* 2000, Balda *et al* 2000).

The immunoglobulin-like proteins located in the tight junction are the junctional adhesion molecule (JAM), the coxsackievirus and adenovirus receptor (CAR) and protein 0 (P0) (Liang *et al* 2000) (figure 1.6). JAM is becoming the most important protein in this family. It is a 35-39kDa transmembrane homolog of the murine junction adhesion molecule, its cited role in the regulation of the latter assembly stages of tight junctions, via its interaction of recruiting occludin to the tight junctional site is growing. It may also function as a signalling element of the tight junction (Liu *et al* 2000).

Plaque proteins include a multitude of organised proteins such as MAGUK (membrane associated guanylate kinase homologues), MAGI (MAGUK inverted proteins), PAR (partitioning defection proteins), Cingulin, Symplekin and Pilt (protein incorporated later in TJ's) (Cereijdo *et al* 2000, Gonzalez-Mariscal *et al* 2003). Three of the major MAGUK proteins localised at the tight junction are ZO-1 (~220 kDa), -2 (~160 kDa) and -3 (~130 kDa), these PDZ domain containing proteins bind directly with occludin protein, but they can also be recruited to the tight junction even with the absence of the occludin molecule (Itoh *et al* 2001, 1999).

Tight junctions play an important role in the regulation of the passive transepithelial movement of molecules; these signalling molecules, have been implicated in the regulation of the formation of the junction. These molecules include $Ca^{2+}$, protein kinase C, G proteins and Phospholipase A2 (Saha *et al* 2001, Hopkins *et al* 2000, Lippoldt *et al* 2000, Gasbarrini and Montalto 1999). Formation of the junction is in a $Ca^{2+}$ dependent fashion, removal of $Ca^{2+}$ leads to the disruption of the junction via protein kinase A activation, further leading to increased barrier permeability (Ma *et al* 2000, Kilnger *et al* 2000). Phosphorylation of several of the junctional proteins in the tight junction have

been postulated as having roles in junction formation (Chen *et al* 2000). The actin cytoskeleton has also been implicated in the regulation, possibly through the involvement of Rho kinase (ROCK), of recruiting proteins to the per-junctional forming plaque portion of the tight junction, during junction construction (Walsh *et al* 2001, Ma *et al* 2000).

Several components of the tight junction have been shown to have roles in gene expression, ZO-1 have been shown to control the expression of the epithelial cell differentiational molecule, ErbB-2, through ZO-1-associated nucleic acid-binding protein (ZONAB) in a cell density-dependent manner, also mutants of ZO-1 have been found to influence cell differentiation pathways (Balda and Matter 2000, Ryeom *et al* 2000).

### 1.6.2 Intermediate (adherens) junctions

The intermediate junction was identified using ultrastructural analysis as, closely apposed plasma membrane domains reinforced by an electron dense cytoplasmic plaque to which actin microfilaments attach (Chitaev and Troyanovsky 1998). Molecular analysis shows that intermediate junctions are sites of cell-to-cell adhesion, where E-cadherin functions as a cell adhesion molecule, and where actin-based cytoskeleton and other cytoplasmic constitutes are assembled (Montefort *et al* 1993). The cytoplasmic domain of the cadherin protein is bound to three proteins, catenin- α, β, and γ, (102, 88 and 80 kDa respectively) which bind directly to the actin microfilament network. Several less described 'linker' proteins also facilitate further actin binding (Kee and Steinert 2001, Nagafuchi 2001, Goto *et al* 2000, El-Bahrawy *et al* 1998, Ozawa *et al* 1990) (figure 1.7). The catenin proteins are vital for cadherin function with loss of cadherin function correlating with catenin alterations (Ozawa and Kemler 1998). α-catenin is homologous to vinculin, β-catenin is homologous to the product of the drosphila gene armadillo and γ-catenin is identical to plakoglobin (Furukawai *et al* 1997). As briefly stated above it is the catenin proteins that mediate junction-cytoskeleton binding. β-catenin binds to the cytoplasmic tail of the cadherin, and serves as the linker protein to α-catenin. Therefore α-catenin should be thought of as the necessary protein for adhesion; also under the influence of actin filaments in the cytoskeleton in a vice-versa fashion, β-catenin

has many more functions connected with the regulation of the E-Cadherin molecule (Kee and Steinert 2001, Quinlan and Hyatt 1999). One of the main rate-limiting steps in epithelial cellular adhesion is the anchoring of the cadherin-catenin complex to the actin filaments (Moreno *et al* 2003).

β-catenin also plays a crucial and critical role in cell morphology, proliferation, migration, structural and adhesion re-modelling, through its participation in the Wnt-beta-catenin pathway. The intra-cellular levels of β-catenin have to be carefully balanced. Under normal physiological conditions β-catenin, ensures cell-cell adhesion via E-Cadherin in the intermediate junction, but is also involved in activating transcription factors involved in the normal and controlled proliferation and differentiation of cells via the Wnt-beta-catenin signalling cascade. De-regulation of these functions have been found to correlate greatly with human malignancies. β-catenin, under normal conditions is mainly located near the plasma membrane, in association with the cadherin-catenin complex and actin filaments. But when levels are elevated, β-catenin accumulates within the cell nucleus and induces the activation of gene transcription, in association with the transcription factors Lefs / Tefs, which lead to the abnormal proliferation and differentiation of cells. Wnt ligands bind to frizzled receptors, present on the cell surface, which in turn regulates the beta-catenin degradation component, thus regulating cellular levels. Wnts are combinations of discoveries in drosphila (wingless) and the MMTV proto-oncogene (int-1) in mammalian cells. Currently, 19 Wnts have been identified, which fall into two classes, classical and non-classical, and 10 known frizzled receptors have been classified. If mutations occur in the pathway, promotion of β-catenin occurs and its levels increase (Widelitz 2005, Brembeck *et al* 2006).

### 1.6.3 E-Cadherin

The cadherins are a super-family of transmembranous, calcium dependent adhesion proteins that mediate homophilic interactions between cells (Ozawa and Kemler 1998). The cadherin super-family consists of classical cadherins (E-Cadherin was also known as uvomorulin), desmosomal cadherins, protocadherins and some cadherin-related molecules. Cadherins are required for the assembly of

cells into multiple layers and the establishment and maintenance of these polarised barriers of epithelial tissue (Furukawa *et al* 1997, Braga *et al* 1997).

E-Cadherin has a molecule weight of 120 to 130 kDa and contains five cadherin ectodomains (EC1-5) (El-Bahrawy *et al* 1998) (figure 1.8). It has stable confirmation when calcium binds with the extra-cellular polypeptide portion of the molecule. The calcium binding regions are short highly conserved amino acid sequences located between neighbouring repeats. Cell-cell adhesion is mediated by the interaction of the extra-cellular domains of the proteins located on the membranes of neighbouring cells. They bind cells homophilically; the pattern of binding is still disputed but is generally thought to be the distinctive zipper-like structure that can be seen running parallel to the opposing membranes in the extracellular portion of the intermediate junction (Ivanov *et al* 2001).

E-cadherin is encoded on chromosome 16p11-16qter / 16q.22.1 (El-Bahrawy *et al* 1998, Kreis *et al* 1994, Pigott *et al* 1993,). Its expression is regulated cytoplasmically, by the stage of cell development via growth factors and peptide hormones (Ozawa and Kemler 1998). The PKC pathway has been shown to mediate activation of E-cadherin, although the direct interaction cascade has yet to be established (Winkel *et al* 1990). The strength of the cell-cell interaction is affected by activation and clustering of E-cadherin molecules at the junction complex (Ivanov *et al* 2001).

E-cadherin and its functions have been shown to be involved in many epithelial tissue disease processes such as carcinomas and skin dis-orders. Cadherin dysfunction may induce many skin diseases such as bullous disease (Furukawa *et al* 1997). The area in which it receives most attention is in cancer and the development of metastatic cells in several cancer types such as esophageal, pancreatic, gastric, colonic and adenocarcinomas. Reduced or even absent expression was associated with metastasis and several factors including poorly differentiated phenotype, infiltrative growth and lymph node involvement (Kallakury *et al* 2001, El-Bahrawy *et al* 1998).

In the normal human conjunctiva E-cadherin, expression has been confirmed in all the layers on the neighbouring epithelial cells especially in the adherens junctions (Scott *et al* 2002, Kobayashi *et al* 1998, Scott *et al* 1997, Cyr *et al* 1995).

### 1.6.4 Desmosome junctions

Desmosome (Greek, desmo = bound), junctions are located throughout epithelial tissues; anchored to the intermediate filament network of the cell they are involved in cell-cell communication and organisation of multi-layered epithelial tissues (Franke *et al* 1983, Montefort *et al* 1993, Pasdar *et al* 1995, Kowalczyk *et al* 1997, North *et al* 1999). Desmosome junctions are identifiable from transmission electron micrographs via their characteristic appearance. They consist of two regions. The transmembrane region contains the desmosome cadherin proteins (Desmoglein and Desmocollin), is also known as the Desmoglein, and is usually 10nm in width (Bannon *et al* 2001). The non-transmembrane region contains the anchoring protein complexes that can be further sub-divided into two segments, the outer dense plaque containing plakophilin and plakogloblin, and the inner dense plaque that contains the desmoplakin molecule, measuring 14 to 20nm thick (Mueller and Franke 1983) (figure 1.9). The desmosome cadherins are cited as mediating cell adhesion via calcium-dependent mechanisms within the extracellular domains, these bond to domains from opposite desmosomes on adjacent cells (Presland and Jurevic 2002, North *et al* 1999, Franke *et al* 1982). Studies into the structure of the desmosome junctions have shown that tissue heterogeneity occurs (Rubinstein and Stanley 1987). In addition, expression of desmosomes within an epithelial tissue is also dependent of the differentiational stage of the epithelial cells (Carmichael *et al* 1991)

### 1.6.5 Desmoplakin

Desmoplakin is one of seven identified proteins within the plakin family. Plakins are cytolinker proteins that function to bridge cytoskeletal filaments and the junctional complexes of organised tissues. The other members of the plakin family are bullous pemphigoid antigen-1, epiplakin, envoplakin, micro-actin crosslinking factor, periplakin and plectin (Leung *et al* 2002). The desmoplakin locus is encoded on chromosome 6p21/24/13 and the molecule is constructed of four domains; the plakin domain, coiled-coil domain, plakin repeat domain and the glycine-serine-arginine domain. It also has a single sub-domain, the linker sub-domain. It associates with the other constitutes of the desmosome junction, directly binding to the plakogloblin and plakophilin molecules in the intracellular

portion and the desmocollins of the transmembrane portion of the junction. The C terminus of the desmoplakin associates with the N terminus on the keratin filaments, especially the head domains of the type II intermediate filaments (Kowalczyk *et al* 1994, kouklis *et al* 1994, Green *et al* 1990). Two splice variants of desmoplakin exist, dpl and dp2 with molecular weights of 322kDa (Mr 250,000, 285,000[1]) and 259kDa (Mr 215,000, 225,000[1]) respectively; dp2 has a 599-residue rod missing in the coiled-coil rod domain (Green *et al* 1992, [1]O'Keefe *et al* 1989, Mueller and Franke 1983, Franke *et al* 1982). Studies have also shown that the present of dp2 is not constant in the desmosome junctions of all epithelial tissues (Angst *et al* 1990).

Cultured epithelial models have shown that desmoplakins are synthesized and accumulate at steady state in a ratio of 3-4:1. Once synthesized, the proteins are pooled for up to 8 hours at which time unless they are recruited to the junction they are degraded (Pasdar and Nelson 1988(a), 1988(b)). Extra-cellular calcium levels act via the phosphorylation of protein kinase and protein phosphatases in the assembly and disassembly of desmosome junction regulation, and therefore could induce the recruitment of the desmoplakin molecules as well as other factors (Pasdar *et al* 1995, Sheu *et al* 1989, Cowin *et al* 1985).

Mis-function or absence of the desmoplakin molecules have been investigated in keratinocytic diseases such as blistering skin disease, Naxos disease, paraneoplastic pemphigus and palmoplantar keratoderma. In the case of palmoplantar keratoderma, it is thought to be connected with desmoplakin haploinsufficiency (North *et al* 1999, Hatsell *et al* 2001).

### 1.6.6 CD44

CD44 is a transmembrane acidic glycoprotein that is expressed on cell membrane surfaces; previously it was termed as H-CAM, $GP90^{HERMES}$, Pgp-1 and ECRM III (Pigott *et al* 1993, Underhill 1992) and is a member of the hyaladherins (Toole 1990). Coded on chromosome 11p13, it forms a single chain sub-divided into three distinct regions the 72 amino acid cytoplasmic domain, which interacts with the actin cytoskeleton, the trans-membrane domain, which facilitates lymphocyte homing and the 250 amino acid amino-terminal end, which facilitates extra-cellular binding. It has a molecular weight of about 80-

95kDa, although many variant forms also exist with molecular weights ranging up to 250kDa (figure 1.10). CD44's adhesion properties stem from its binding to hyaluronan (HA) (Goetinck *et al* 1987). HA is a high molecular weight, highly anionic polysaccharide found in the extra-cellular matrix and on the surfaces of cell membranes.

CD44 is expressed on a multitude of cell types that include T and B lymphocytes, monocytes, mesenchymal, and epithelial tissue. The CD44 molecule is anchored cytosolically to the actin cytoskeletal filaments via adaptor proteins, although the distribution of CD44 is independent from its association with the cytoskeleton (Neame and Isacke 1993). The close interaction between the actin filament network and CD44 is influenced largely by post-translational modifications in the molecule's structure, and therefore can directly regulate its function (Lesley *et al* 1992). Other studies have shown different regulating pathways also influence CD44's function.

CD44 has been shown to function as a potent lymphocyte homing molecule, a binding molecule, a leucocyte-activating molecule and has a role in cell migration. The specific function greatly depends upon its structure; the variant/larger isoforms with inserted amino acid groups change the manner in which the molecule works.

Due to its multi-functional role in cell biology, CD44 has been investigated in several different tissues / diseases. In inflammatory renal diseases particularly, on tubular epithelial cells CD44 has been shown to be markedly up regulated (Wüthrich 1999). In systemic sclerosis, pancreatic cancer and atherosclerosis, CD44 expression has been shown to be up regulated and is a marker used evaluation of upper urinary tract transitional cell carcinoma (UTTCC), in conjunction with cytological tumour grading (Weaver *et al* 2001, Savani *et al* 1995, Takada *et al* 1994, Koch *et al* 1993,). CD44 expression and binding with HA has been shown to be increased during inflammation, through the inducement of activation pathways via the cytokines IL-2, TNF-$\alpha$, IFN-$\gamma$ and GM-CSF (Pur and Cuff 2001).

## 1.7 Keratin cytoskeletal filaments

Higher eukaryotic cells contain a complex intra-cytoplasmic cytoskeleton, composed of three principle groups of proteins: actin microfilaments, tubulin microtubules and intermediate filaments (IF). These cytoskeletal proteins are under continuous cycles of monomer addition and subtraction via polymerization / depolymerisation, and therefore should not be thought of as a static entity (Maciver 2001). Changes in the physical shape / structure of the cell and cell motility are achieved by these cycles, under the regulation of intra and extra cellular signals. Intermediate filaments are the least dynamic of the three cytoskeletal protein groups, leading to speculation that intermediate filaments were relatively stable, with very little soluble protein existing in the cell. Contrary to this notion, intermediate filaments are in fact motile within the cell. In many cell types the intermediate filaments and microtubule systems co-localise and destruction of either leads to the collapse of the other. The correct balance and maintenance of these elements of the cell's cytoskeleton are essential for normal growth, maturation, differentiation, integrity and function (Kivela and Uusitalo 1998).

IF's were originally termed intermediate due to their intermediate diameter (10nm) when compared to other filaments found in the cell such as actin filaments (6nm) and contractile filaments such as tubulin (23nm). IF's were first identified in wool samples, they form a super-family of protein filaments (Fuchs and Weber 1994 [plus reference therein], Sun *et al* 1983)

| IF type | Name | Example |
|---|---|---|
| I/II | Keratins | K1-20 |
| III | IF proteins | Vimentin |
| IV | Neuro / α-Internexin filament | Human NF-L |
| V | Nuclear lamina specific IF proteins | Lamins |

Keratins are a highly heterogeneous group and constitute the largest and most complex family of proteins in the IF super-family (Nelson and Sun 1983). The keratin family can be categorised into two branches as demonstrated using immunological, peptide mapping, mRNA hybridization and primary amino acid

sequence data (Quinlan *et al* 1985). The water-soluble proteins fall into two distinct groups, type I keratins are acidic (pI = 4-6) whereas type II keratins are more basic (pI = 6-8). Type I keratins are classified as K9-20 and are further sub-divided according to their carboxyl-terminus sequence, they are encoded on chromosome 17q, type II are classified as K1-8, they are encoded on chromosome 12q (Fuchs and Weber 1994, Chu *et al* 2002).

### 1.7.1 Keratin family

| Keratin Name | Chromosomal localisation | Mol. Wt. ($x10^{-3}$) | Type | pI |
|---|---|---|---|---|
| 1 | 12 | 67 | II | 7.8 |
| 2 | 12 | 65 | II | 6.1 |
| 3 | 12 | 64 | II | 7.5 |
| 4 | 12 | 59 | II | 7.3 |
| 5 | 12 | 58 | II | 7.4 |
| 6 | 12 | 56 | II | 7.8 |
| 7 | 12 | 54 | II | 6.0 |
| 8 | 12 | 52 | II | 6.1 |
| 9 | 17 | 64 | I | 5.4 |
| 10 | 17 | 56.5 | I | 5.3 |
| 11 | 17 | 56 | I | 5.3 |
| 12 | 17 | 55 | I | 4.9 |
| 13 | 17 | 51(54*) | I | 5.1 |
| 14 | 17 | 50 | I | 5.3 |
| 15 | 17 | 50 | I | 4.9 |
| 16 | 17 | 48 | I | 5.1 |
| 17 | 17 | 46 | I | 5.1 |
| 18 | 17 | 45 | I | 5.1 |
| 19 | 17 | 40 | I | 5.7 |
| 20 | 17 | 46 | I | 5.7 |

pI = isoelectric point. Table taken from Moll *et al* 1982.

(* van Muijen *et al* 1986)

### 1.7.2 Structure

Keratins are a primary two-chain α-helical polypeptide molecule that intertwine in a coiled-coil fashion on an imperfect helical lattice to form the subunit structure of the 10nm filament (Stewart 1993) (figure 1.11).

IF proteins are predicted to share a common secondary structure. They comprise a heterotypic tetramer, the central α-helical domain, the rod, is flanked by non-helical head and tail domains (Wilson *et al* 1992). Specific structural residue repeats enable the coiling of the two IF proteins to be hydrophobically sealed assuring stability. This principle of tetrameric organization is thought to be the model involved in the structure of all IF's (Quilan *et al* 1985).

Intermediate filament structure is influenced by phosphorylation during post translational modification, which in turn influences their behaviour, and possibly via depolymerisation in situ. In the case of keratin 18, phosphorylation is regulated by K18 ser33 and therefore affects the ability of K18 to bind to 14-3-3 during mitotic cellular division (Ku *et al* 2002, Omary *et al* 1998).

### 1.7.3 Expression

Members of each sub-family, e.g. acidic type I and basic type II, show related antigenicity and are therefore co-expressed in different epithelial cell types (Hatzfeld and Franke 1985).

| Keratin partnerships (Mol. Wt) | Examples of proposed markers |
|---|---|
| 45 – 52 | Simple epithelia |
| 48 – 56 | Hyper-proliferation / de-differentiated |
| 50 – 58 | Keratinocyte |
| 51 – 59 | Stratified squamous (mostly internal organs) |
| 55 – 64 | Corneal type differentiation |
| 56.5 – 65/67 | Keratinsation |

adapted from Sun *et al* 1985.

Supporting data demonstrates that keratin 1, 4, 5/6, 10, 13, 14, 15, 16 and 17 are found in columnar epithelium and keratin 7, 8, 18, 19 and 20 are found in simple epithelial (Nishimata *et al* 2005, Lu *et al* 2002, Chu and Weiss 2002, Oshima *et al* 1996).

### 1.7.4 Regulation of expression

The regulatory factors involved in gene expression are still poorly understood. In most stratified squamous epithelium, differential expression is dependent upon the specific epithelial developmental stage of the cell without the requirement of cell-cell contact or presence of desmoplakins for keratin assembly (von Koskull and Virtanen 1987). In keratinocytes, the intermediate filament (IF)-associated protein filaggrin has been shown to have a role in the aggregation of filaments during differential stages in the cell cycle (Presland *et al* 2001). Filaggrin also exerts an influence over the other structural filaments of the cell suggesting a more generalised non-intermediate filament interaction. Patterns of gene expression could be altered in response to immune-mediated mechanisms (Bloor *et al* 2000). Oncogenic activation pathways have been shown to stimulate the transcription of keratin proteins via the ras signal transduction factors (Oshima *et al* 1996). Cellular ionic fluxes and therefore cellular signaling via sodium channels can modulate differentiation, thus influencing the synthesis/expression of keratins (Mauro *et al* 2002).

In vitro experiments have shown a heteropolymer ratio of 1:1, and filaments generated from different proteins have distinct physical properties, which suggests differential expression may occur in response to specific tissue requirements e.g. tensile strength, flexibility and dynamics (Hatzfeld *et al* 1985, 1987).

Keratin bind to the C terminus (tail) of the desmoplakin molecule, located in the inner dense plaques of the junctions, but the formation of a desmosome junction or indeed any cell-cell contacts is not thought to be an initiator of intermediate filament assembly specifically within the area of the junction / cell-cell adhesion (Kouklis *et al* 1994, von Koskull and Virtanen 1987, Green *et al* 1987, Jones and Goldman 1985). The interaction between the two species of protein in terms of assembly and binding is still unclear. It should also be remembered that the intermediate filament network is not a static entity, and is in

fact motile and dynamic to accommodate the stress cells are under and retain the appropriate cell shape to ensure correct cell function (Galou *et al* 1997, Maciver 2001).

### 1.7.5 Tissue specific expression

The distribution of keratins has been shown that expression of specific keratins correlates with different morphological features of in *vivo* epithelial differentiation (Nelson and Sun 1983).

Due to the specific keratin expression in the differentiated epithelial tissues, keratins have been extensively studied, particularly in the human bronchial tissue, where several keratins including 4, 7, 8, 13, 14, 18 and 19 have been identified. Studies of fetal and adult tissue show that keratins 7, 8 and 18 were localised in the bronchial cells and 14 in basal cells during early development, this expression pattern was found to change with increases in K 7 expression, with the basal cells remaining negative, during the later stages of lung development. In fetal alveolar epithelial tissue, expression changed from K 7, 8, 18 and 19 to 7, 8, 13, 14, 18 and 19 within adult alveolar cells (Broers *et al* 1989, Lu *et al* 2002). Indeed, in the conjunctival epithelium, both animal and human studies have shown that the keratins found (Keratins 4, 5, 7, 8, 13, 14, 18, 19, but not 1, 2, 3, 12, 10, 16) and their patterns depend upon the specific region of interest, making it ideal for investigating keratin function and tissue specificity, (Kivela and Uusitalo 1998, Krenzer and Freddo 1997, Kurpakus *et al* 1992, Kapser 1991, Ryder and Weinreb 1990), although conflicting evidence exists for the 'simple' keratin 8 (Zhang *et al* 2000). In the human conjunctiva, it was shown that the most abundant keratin gene transcript was for keratin 13 (Dota *et al* 2001).

Further to the link of keratins and the desmosome junction, the further roles that keratins play within epithelial tissues give insight to their presence. In complex columnar epithelial layers, keratins 7, 8, 18 and 20 have suggested roles in cell contact / cell-matrix adhesion, 8 and 14 have roles in Golgi apparatus structure, 10 in basal cells anchors the nucleus of the cell and 13 is involved in cell-cell and cell-matrix contacts (Ogawa *et al* 2001). In simple epithelia the keratin pair 8 / 18 function in anti-stress role in the epithelial layer (Marceau *et al* 2001).

Mutations in the keratin genes have been shown to result in a multitude of diseases that effect skin, hair, and mucosal epithelial, in general, study of the epithelial cells has found them to be fragile and lyse, clump or disaggregate under mild stress, suggesting an altered cytoskeleton or constitutes, that are unable to cope with the stresses that normal epithelial tissue undergoes (Whitlock *et al* 2000, Fuchs and Weber 1994). Further studies have postulated that, changes in the keratin gene expression pattern may be also due to cellular responses to physical stress, pathogenic stimuli or immune-mediated mechanisms (Bloor *et al* 2000, Waseem *et al* 1998). It is through the study of keratin dis-orders that further understanding of function is enhanced, associating the different physical properties of the proteins with the different tissues that they are found (Porter and Lane 2003).

## 1.8 Thesis hypothesis

The conjunctival epithelium is altered in allergic eye disease and in the context of an inflammatory response; this facilitates the passage of allergen through the epithelium, contributing to the pathogenesis of the disease.

## 1.9 Thesis aims

Experiment Chapter One

- Characterise the structure of the conjunctival epithelium from non-atopic subjects.
- Characterise the structure of the conjunctival epithelium from patients, diagnosed with seasonal allergic conjunctivitis, during active and quiescent disease periods.
- Compare the structure of the non-atopic epithelium against the atopic epithelium.

Experiment Chapter Two

- Compare the epithelial characteristics of cell line models of the human conjunctival epithelium, (ChWk and IOBA-NHC), with an established epithelial cell line (16HBE 14o-).

- Develop a method for culturing conjunctival epithelial cells from patient donated biopsy material.
- Characterise and compare the epithelial cell cultures against cell line experimental models of the conjunctival epithelium.
- Develop a method for harvesting conjunctival tissue from an animal model.

Experiment Chapter Three

- Investigate the effects that Timothy grass pollen extract has on the permeability of the epithelial *in vitro* model systems.
- Investigate the effects that Timothy grass pollen extract has on the architecture of the epithelial *in vitro* model systems.

Experiment Chapter Four

- Detect and localise Timothy grass pollen extract in allergen challenged *in vitro* epithelial models systems.
- Detect, localise and compare Timothy grass pollen extract in SAC model *in vivo* allergen challenged subjects.

# Figure 1.1 Phleum pratense

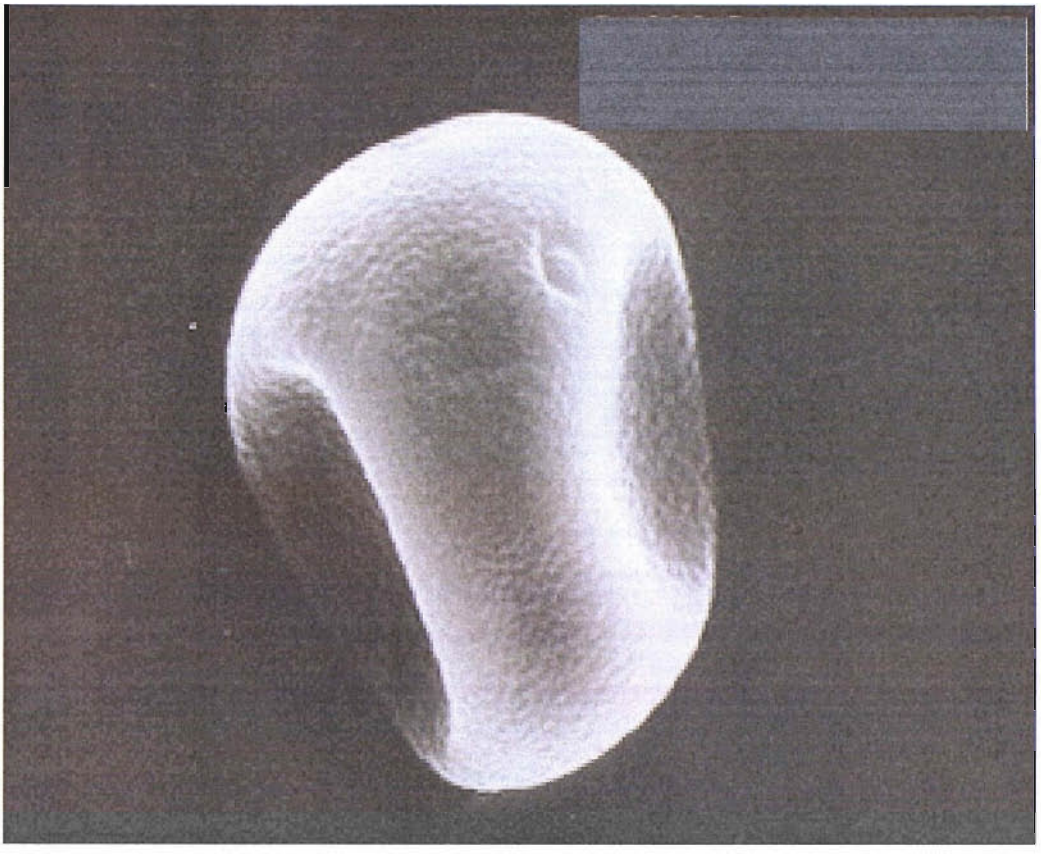

The micrograph shows the pollen grain of the timothy grass species (*Phleum pratense*). It is this grass species which is native to the United Kingdom and is the major causative allergen involved in seasonal allergic conjunctivitis. Pollens differ greatly in terms of size, shape and their surface features. Sizes can vary between 5 to 200 μm. Typically grass pollen range from 25 to 60 μm in diameter. The wall of the pollen is constructed of two layers, the exine and the intine, whose roles are protection of the internal cell.

# Figure 1.2 Calendar of pollen release

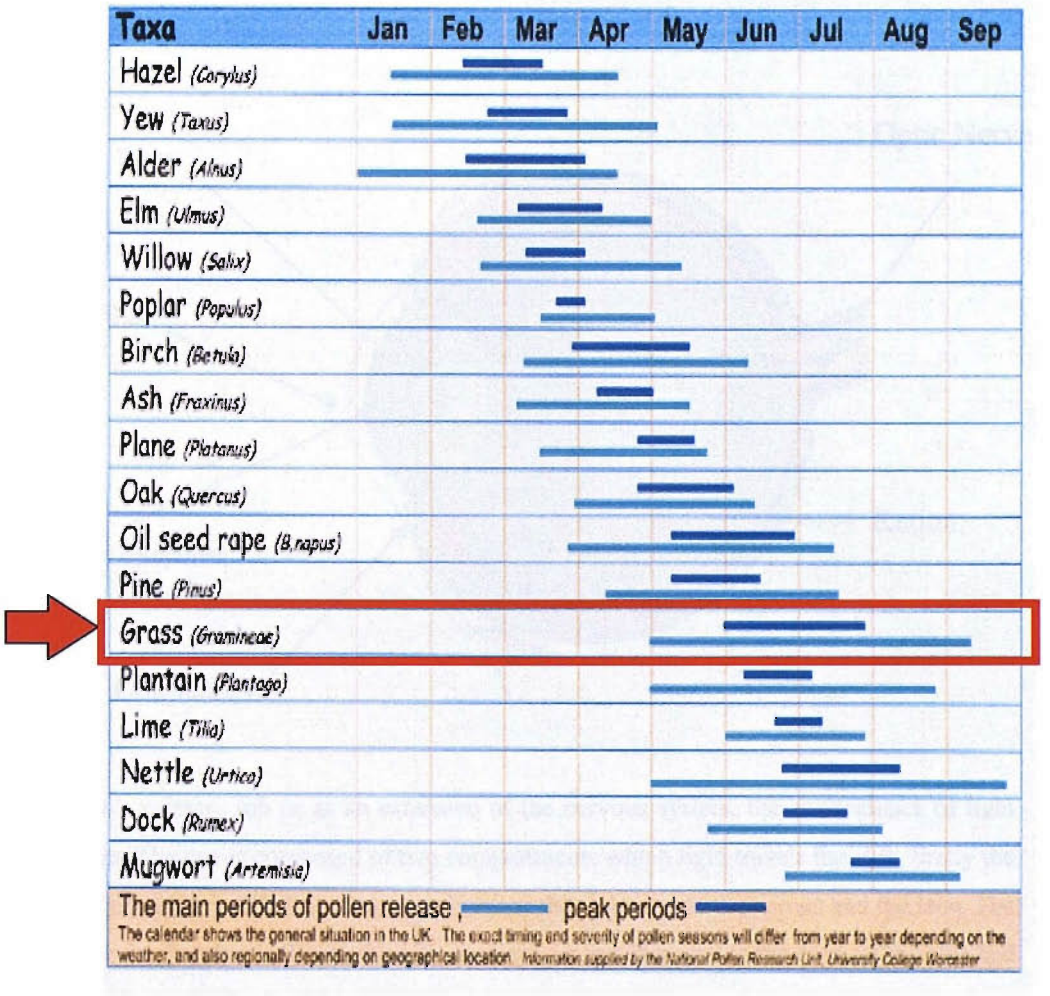


Timothy grass pollen release occurs roughly from the beginning of May to mid-September, with the peak release starting in June then continuing on until the end on July (Grass line marked with red arrow).

This data is calculated to demonstrate a generalised summary of pollen release across the UK.

Data was calculated by the National Pollen Research Unit, University College Worcester. The original graph can be found on the website : http://www.pollenuk.co.uk/aero/pm/calendar.html

# Figure 1.3 General anatomy of the human eye

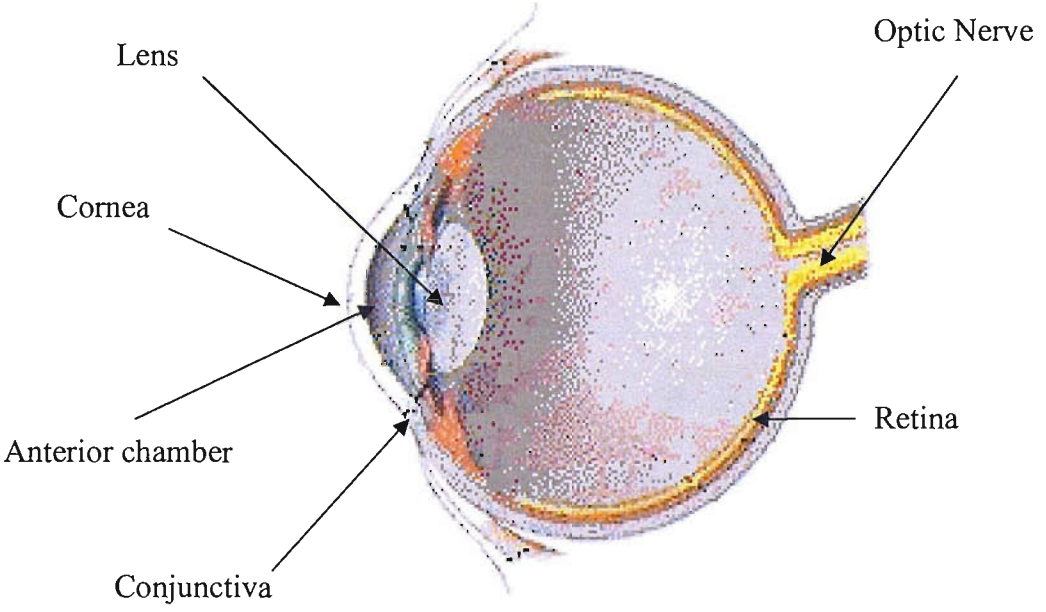


The eye's primary job is, as an extension of the nervous system, the conductance of light radiation. The eye is composed of two compartments which light travels through, firstly the smaller chamber is filled with aqueous humour that is bound to the cornea and the lens. The next, larger chamber is filled with vitreous humour that is bound to the back of the lens and to the retina at the back of the eye.

The eye is protected by a bony orbit, bound by the orbit septum and the eyelids.

The conjunctiva is the thin membrane that connects the eyelids and the eyeball, its principle role is to support and protect the cornea, the light transduction organ of the eye, and covers the entire sclera.

# Figure 1.4 Anatomy of the Conjunctiva

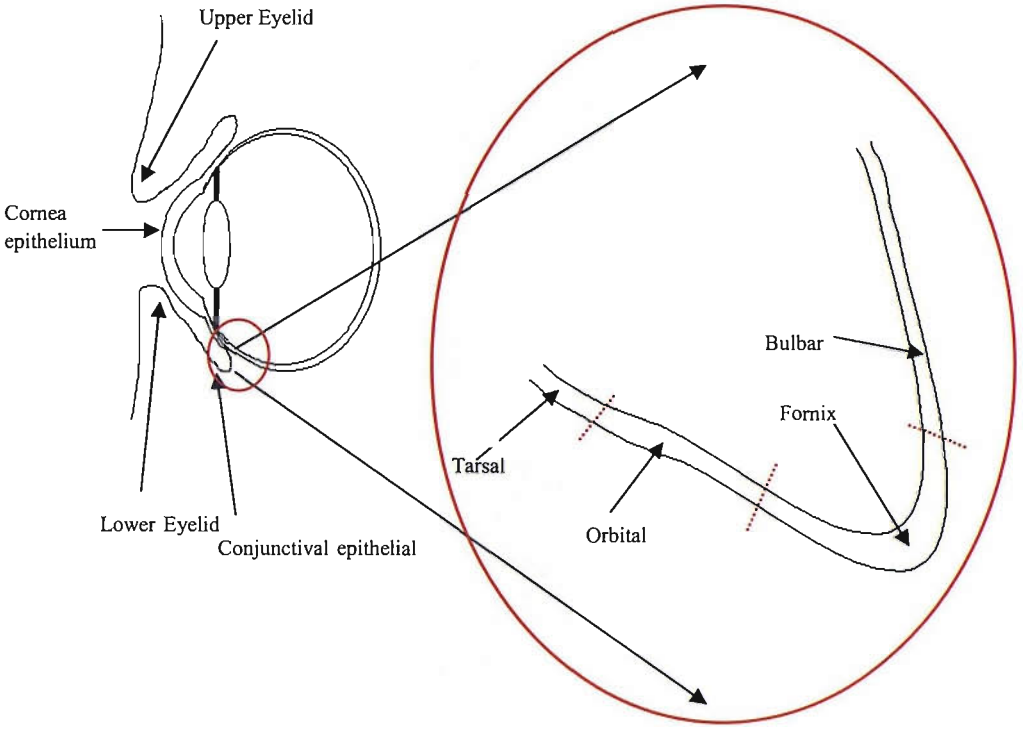


The conjunctival epithelium is broadly spilt into four divisions. Running from corneal epithelial margin to the eyelid margin are the Bulbar, Fornix, Orbital and Tarsal regions. The parts of the conjunctiva are named by the structures they approximate. Each region's epithelial structure is reported to differ slightly according to its specific location and therefore function. The bulbar conjunctiva covers the globe of the eye overlying the sclera, and is less firmly attached allowing the movement of the eyelids and the eyeball. The conjunctiva has several features in common with other epithelial mucosa surfaces such as the upper airways, which it is continuous with through the nasoacrimal canal. It is the major site of the first interaction of allergens and aero-irritants.

# Figure 1.5a Conjunctival epithelium

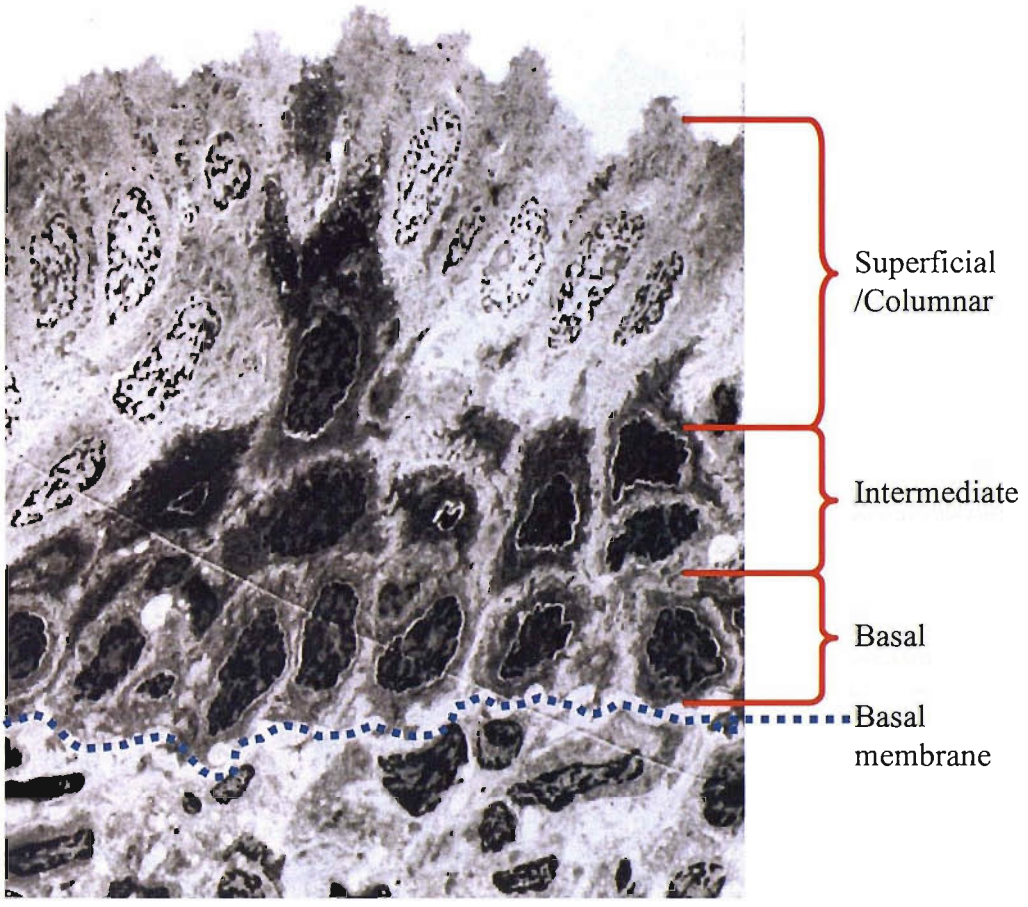


Above is a representative transmission electron micrograph of the human bulbar conjunctival epithelial layer.

The conjunctival epithelium is classified as a non-ciliated non-keratinised stratified columnar epithelium divided into three layers, the three layers are classified as the superficial, intermediate and basal. The epithelial layer is 3 to 5 cells thick. Mucin secreting cells can be found in apocrine or holocrine glands past the subtarsal groove, lining the crypts of Henle. The superficial cells form a semi-permeable lipophillic membrane via the tight junctions of the junctional complex, that are found at the anterior border of the cells. Basal cell are attached to the basal lamina (basal membrane) via hemi-desmosome junctions.

The superficial act as physical support for the several layers that make up the aqueous tear film.

# Figure 1.5b Conjunctival epithelium

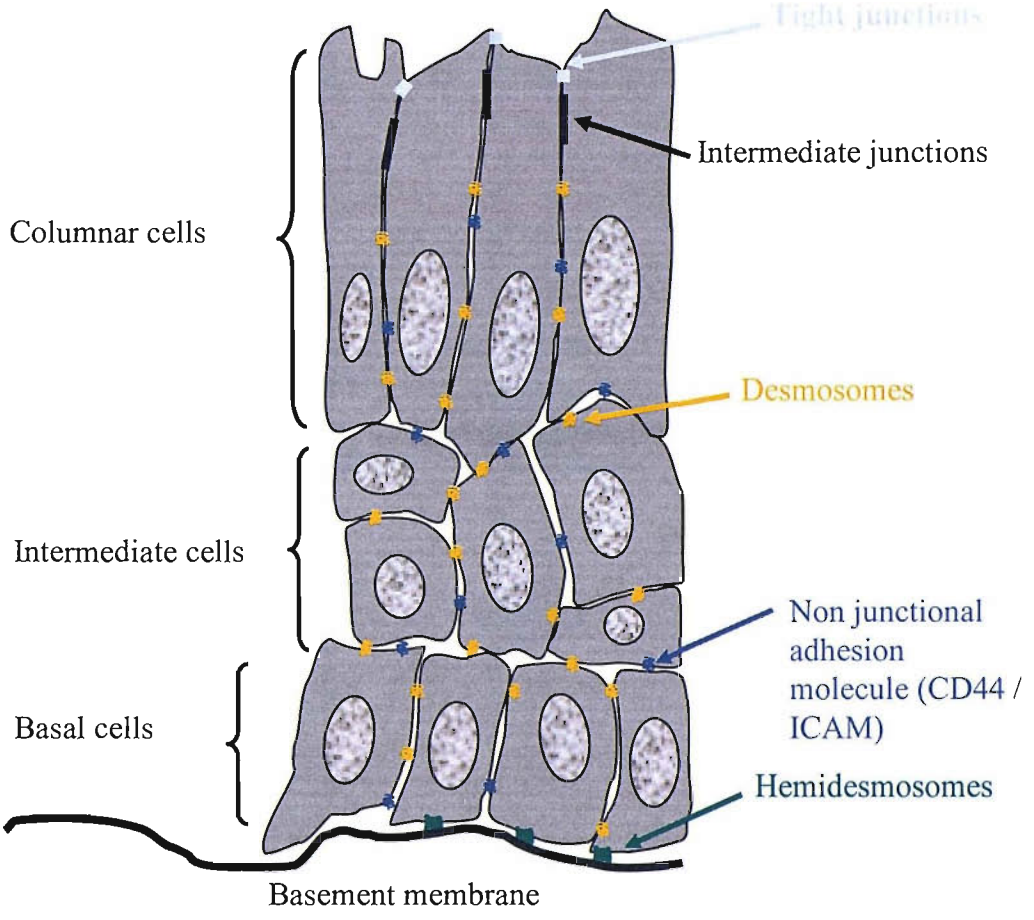


This cartoon represents the conjunctival epithelium showing the layer morphology as well as the junctional and adhesion components of the epithelium of interest within this thesis; the Tight junctional, the Intermediate junction, Desmosome spot junctions, Hemi-desmosomes and Non-junctional adhesion molecules (CD44 and I-CAM 1).

# Figure 1.6 Tight Junction

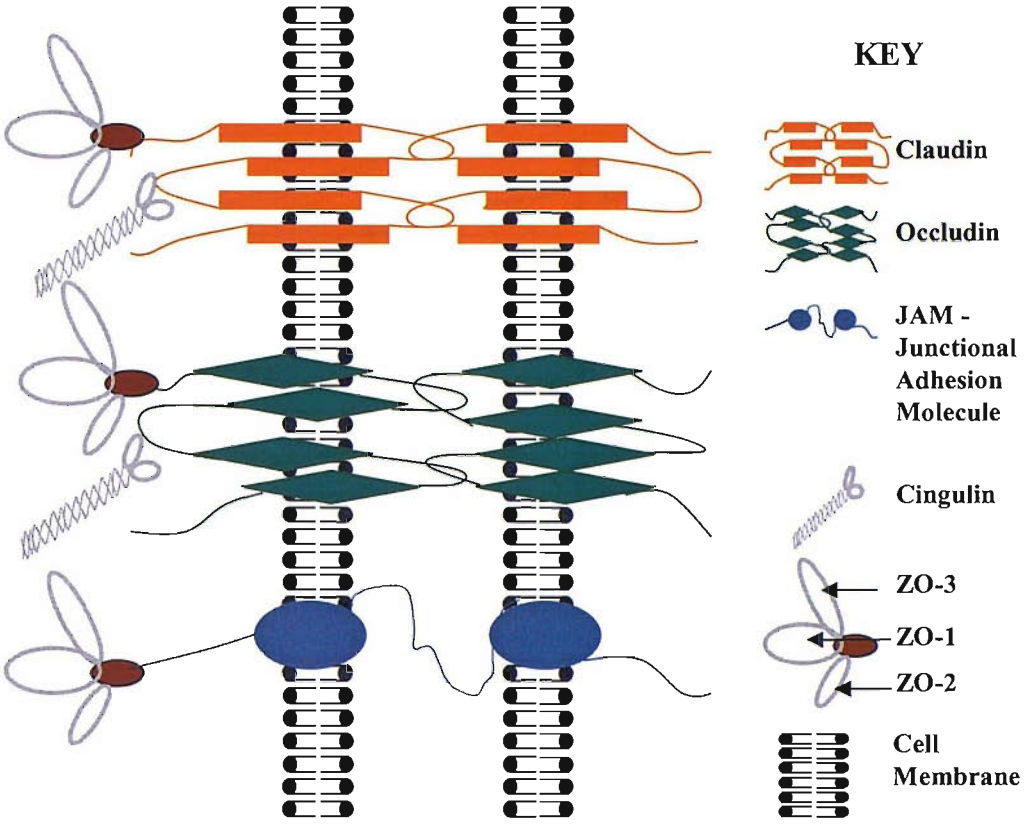


Tight junctions are the first cell-cell junction that is found running apical to basal in an epithelial tissue located exclusively on the superficial cell layer.

Tight junctions can be identified on transmission electron micrographs by the characteristic appearance of two adjacent membranes fusing into one. More than 40 different proteins have been identified within the junction infra-structure. For ease, only a limited number of the major proteins have been represented within the above diagram. Namely the transmembrane proteins – Occludin, Claudin (members of the tetraspan protein family) and JAM (a member of the immunoglobulin superfamily). Also plaque proteins ZO-1, 2, 3 (members of the MAGUK (Membrane Associated Guanylate Kinase homologues) family of PDZ domain containing proteins) and Cingulin (a member of the lacking PDZ domain family of proteins).

The tight junction acts as a physical barrier to the passage ions and molecules through the paracellular pathways, also blocking the free diffusion of lipids and proteins between the apical and basolateral domains. It is the tight junctions function as a barrier that generates and maintains cell polarity.

# Figure 1.7 Intermediate Junction

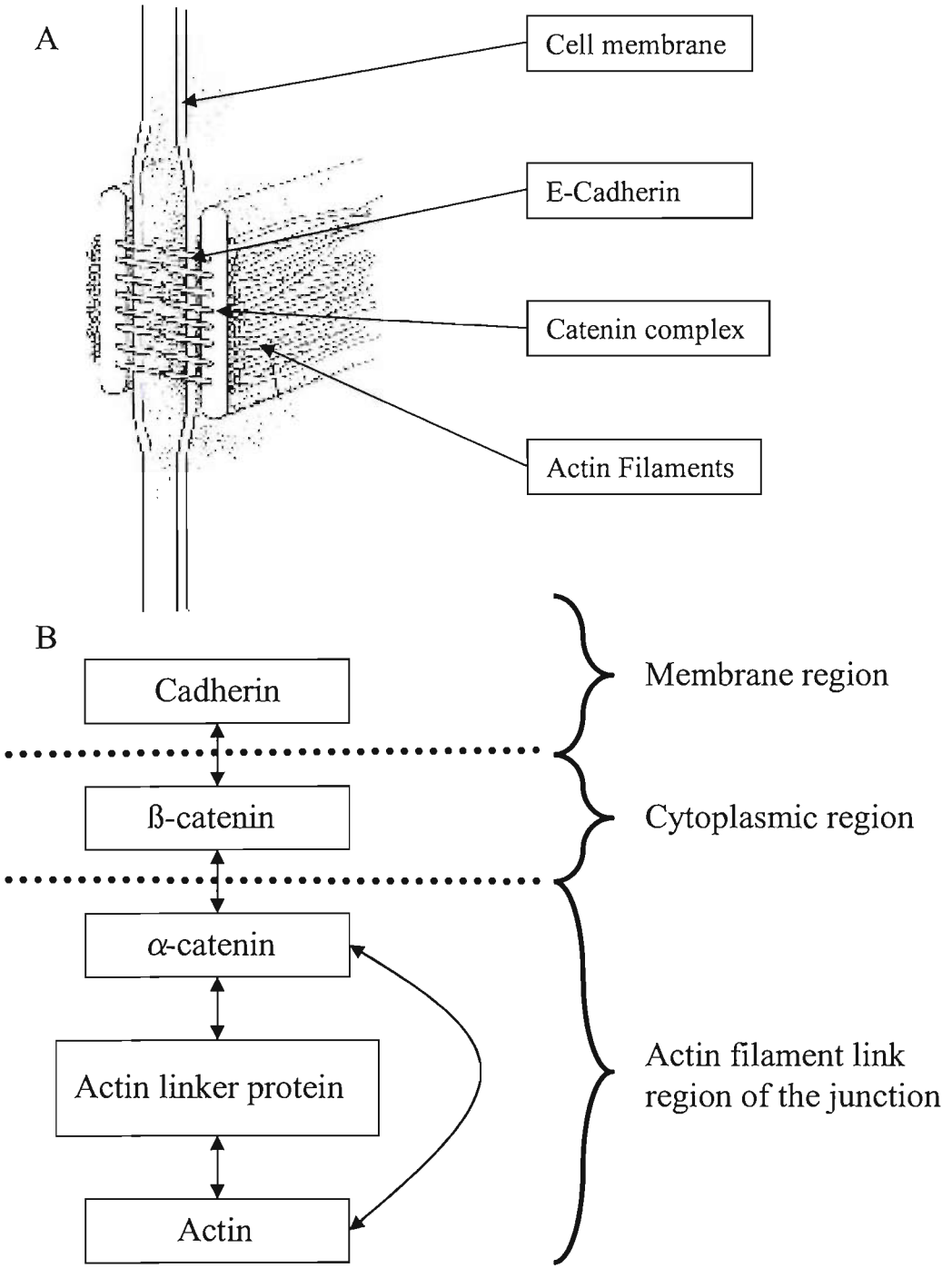


A, shows a schematic representation of the intermediate junction.

B, shows the major proteins found in the intermediate junction.

Intermediate junctions are found immediately below the tight junction on the superficial cell layer. Typically larger and longer in length than the tight junction, they are composed of two trans-membrane domains which span into the extra-cellular space. They are thought to form a zipper-like structure, with the Cadherin molecules cross-linking each other. Within the cytoplasmic region they bind to the actin cytoskeletal network of the cell via the catenin molecules, thus increasing the structural strength of the cell.

# Figure 1.8 E-Cadherin

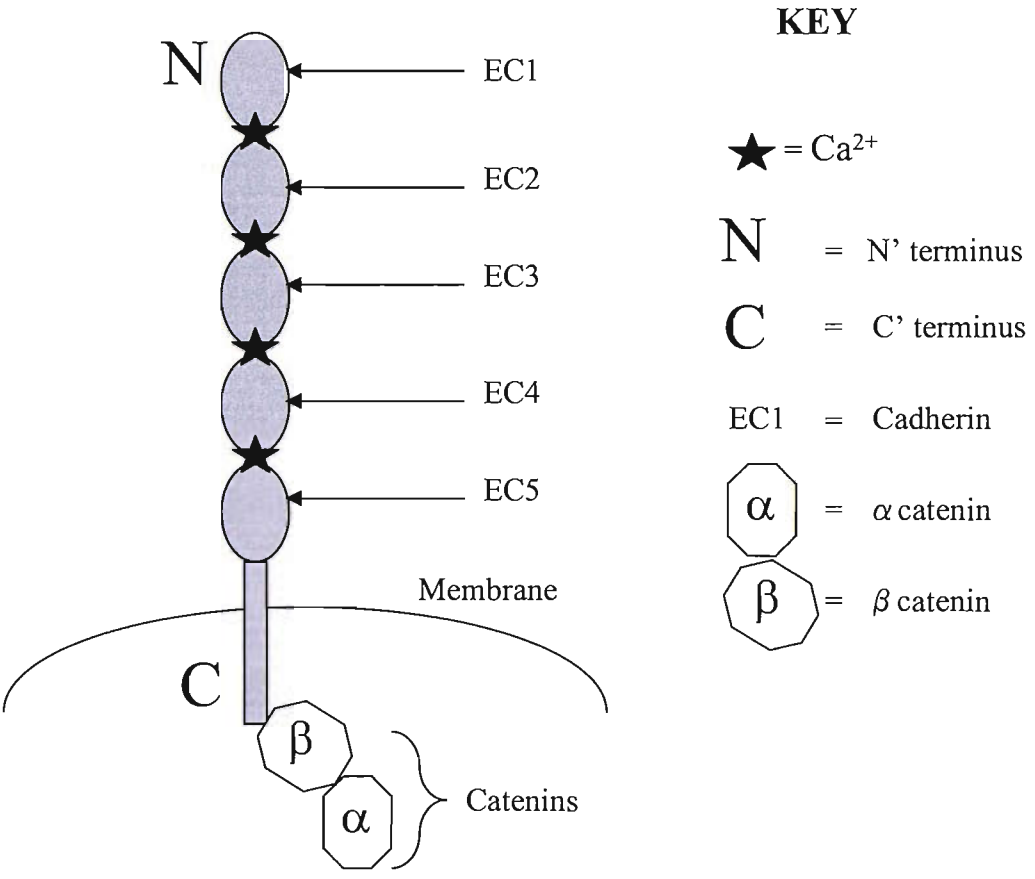


Above is a simplified schematic of one side of the intermediate junction showing the arrangement of the E-Cadherin molecules and some of the other junction accessory proteins. E-Cadherin is found on non-neural epithelial tissues.

The two opposing E-Cadherin containing complexes bind in the extra cellular space in between two opposing cells, forming a zipper-like structure, as seen at high magnification.

E-Cadherin is vital to the $Ca^{2+}$, dependent adhesion between epithelial cells both during periods of generation and / or maintenance. It also fulfills a role in the organisation of cytoplasmic and membrane proteins, therefore influencing the polarity generated by those membranes / epithelial tissue layers.

E-Cadherin is encoded on gene 16 p11-16qter, and its regulation is developmentally dependant.

Diagram taken from Ivanov et al 2001.

# Figure 1.9 Desmosome spot junction

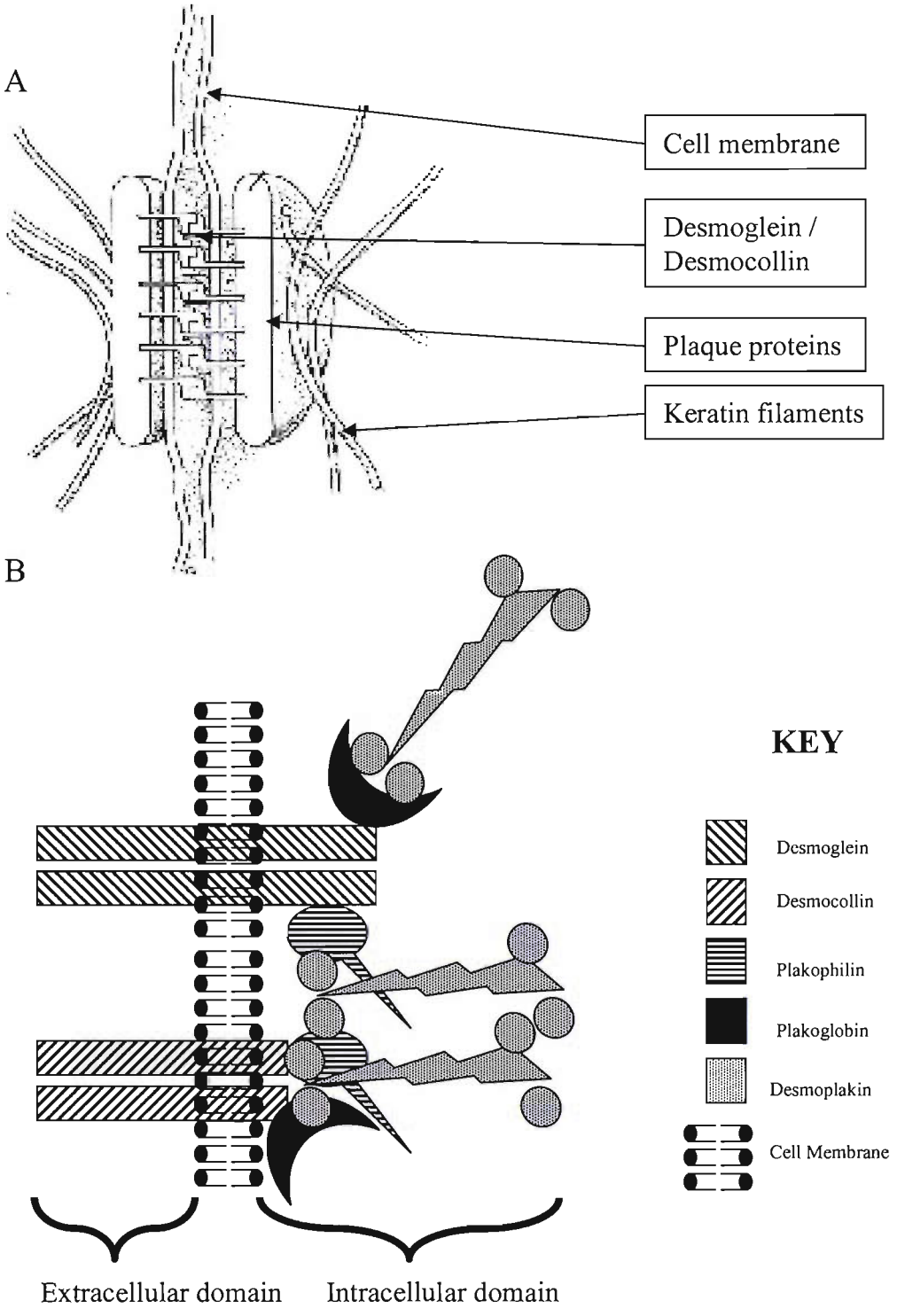


A, shows a diagrammatic representation of a desmosome spot junction.

B, shows the major proteins that constitute the desmosome spot junction.

Desmosome spot junctions can be found on the baso-lateral membranes of epithelial cells. The plaque proteins are linked to keratin filaments that run throughout the cell, providing an anchoring system for the cell's scaffolding.

# Figure 1.10 CD44

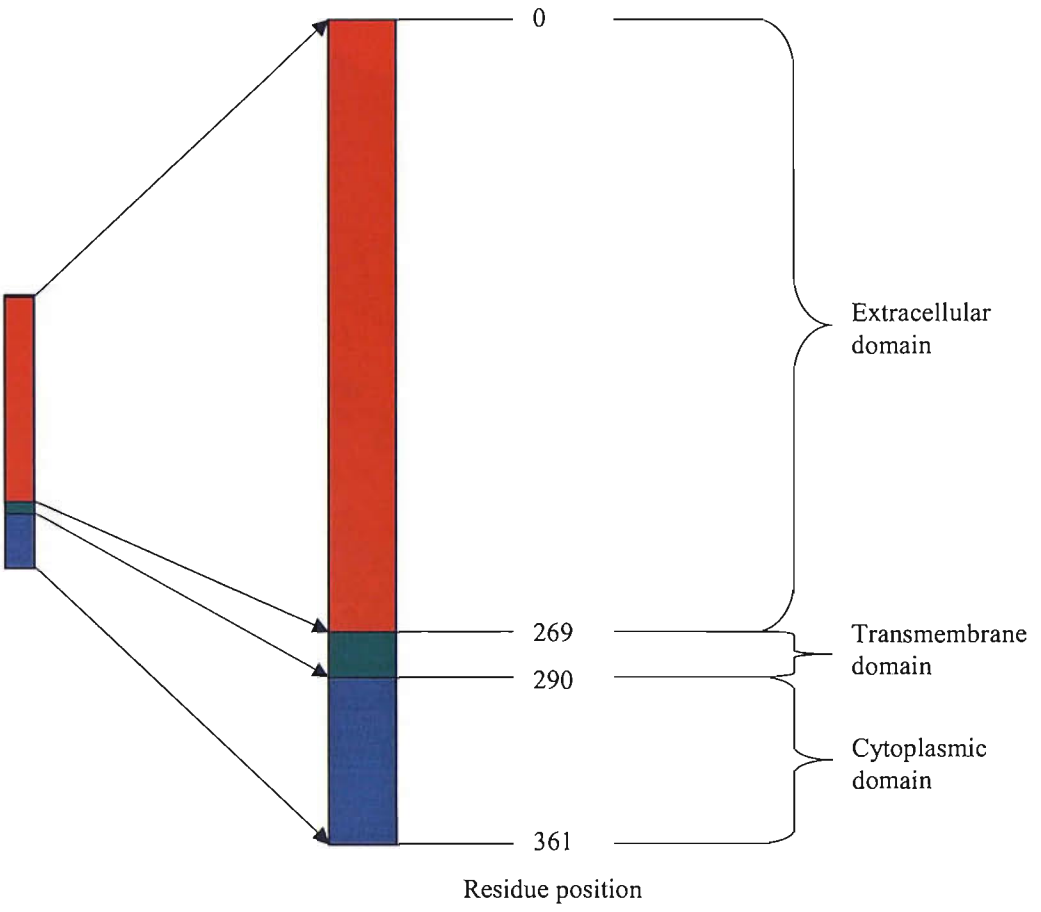


CD44 is a transmembrane protein that is expressed on a multitude of cell types, such as epithelial cells, fibroblasts, myocytes and members of the haematopoietic family of cells.

It has functions that include cell-cell adhesion, cell-matrix adhesion, T-cell activation and lymphocytic adhesion. In its role as a cellular adhesion molecule it is anchored to the cytoskeleton of the cell and then binds directly with hyaluronic acid and other extra cellular matrix components such as collagens.

A number of variants of CD44 can be found, with molecular weights ranging from $M_r$ 85,000 to $M_r$ 250,000 depending on the post-translational modifications that the molecule undergoes.

CD44 in encoded on gene 11p13. Lymphocyte maturation has been implicated the regulation of its expression. Increased expression has also been linked to carcinoma development.

# Figure 1.11 Keratin structure

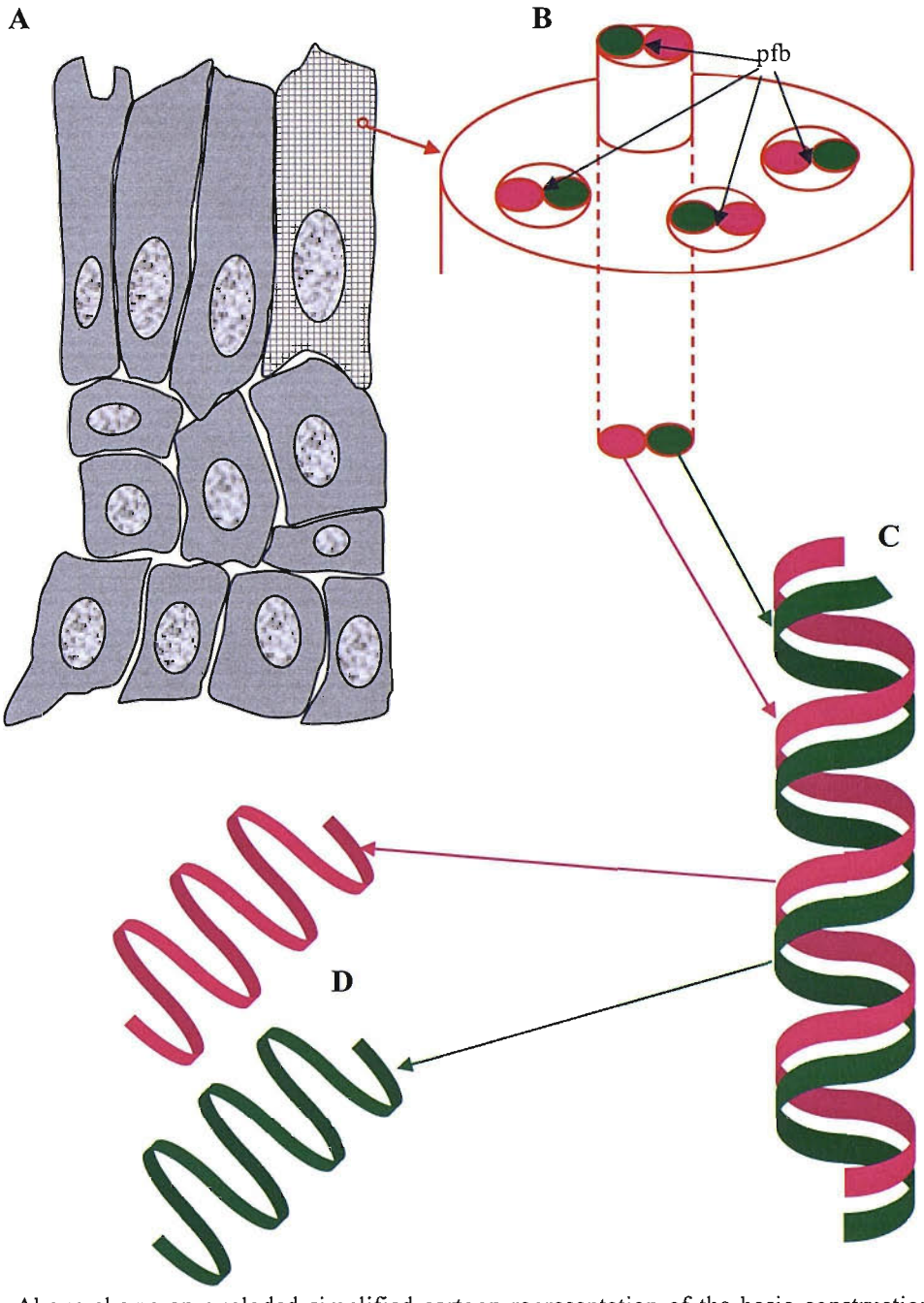


Above shows an exploded simplified cartoon representation of the basic construction of the intermediate filaments.

From A, within the epithelial cell is the cytoskeletal network including the intermediate filaments (red) B. Which are constructed of the 4 left-handed interwined protofibrils (pfb). Within the protofibril are the two coiled protofilaments C. The two paired, acid (bright green) and basic (pink), coiled tetramers make up the protofilament, running in opposite, peptide heterodimer, directions. In terms of size, the intermediate filament (B) is 10nm in diameter, the protofibrils are 4.5-5 nm in diameter and the protofilaments are 2.5-3 nm in diameter.

# 2.1 Materials

### 2.1.1 Cell Culture conditions

Three types of in vitro epithelial cell models were employed for experimental purposes within this thesis;

1% Antibiotics / Antimycotic solution (A/A) (10,000 units of penicillin (base), 10,000μg of streptomycin (base), and 25μg of amphotericin B/ml was added to the culture mediums throughout the project.

1, Chang conjunctival epithelial cell,

Chang conjunctival epithelial cell clone (1-5c-4, (ChWk), American Type Culture Collection, Maryland, USA), were cultured in Medium 199 supplemented with 10% heat inactivated foetal bovine serum (FBS). Passages used throughout the project were P + 1 to P + 15.

2, IOBA-NHC conjunctival epithelial cell,

The spontaneously immortalised conjunctival epithelial cell line IOBA-NHC were a gift from M. Calonge (University Institute of Applied Ophthalmobiology (IOBA), University of Valladolid, Valladolid, Spain). These cells were cultured in Medium 199 supplemented with 10% heat inactivated FBS. Passages used throughout the project were P 72 to P 77.

3, 16HBE 14o- bronchial epithelial cell,

The Simian Virus 40-transformed bronchial epithelial cell line, 16HBE 14o- was a gift from Dr. D. Gruenert (Cardiovascular Research Institute, University of California, USA), was cultured in Minimum Essential Medium (MEM with Eagle's salts) supplemented with 10% heat inactivated FBS and 2 mM L-glutamine. Passages used throughout the project were P + 27 to P + 42.

Ex vivo cell models were established from biopsy material throughout the thesis; the protocol for the harvesting primary cells was devised as part of chapter four, therefore is described therein.

Explant outgrowth were cultured in Medium 199 supplemented with 10% heat inactivated foetal bovine serum (FBS) and 1% Antibiotics / Antimycotic solution.

### 2.1.2 Stratified tissue model (*Ovis aries*)

*Ovis aries* conjunctival epithelial tissue was dissected from healthy specimens. The entire orbit was removed immediately after the specimen had undergone euthanasia, then conjunctival epithelium was micro-dissected away immediately. The protocol used to harvest the stratified fresh tissue was devised by the author as part of chapter four and is detailed therein.

### 2.1.3 Ethics for using patient material

Full approval was granted by the Southampton and South West Hants Local Research Ethics Committee before the collection of biopsy material commenced; ethical reference number 036/02.

### 2.1.4 Patient Details

Patient suitability was assessed pre-operatively by a consultant surgeon and the researcher, full written consent was then taken. Patients included those on day case and in-patient lists. Samples were collected during retinal detachment, cataract, lens replacement, Phaco-oil replacement and corneal graft surgical procedures. A full list of the number, age, sex and date of each biopsy used within this thesis can be found in the appendix.

### 2.1.5 Antibody details

| Name (antigen) | Label | Dilution | | Note / source |
|---|---|---|---|---|
| | | IS | GMA | |
| Primary antibodies | | | | |
| 11-5F (Desmoplakin dp1-2) | None | | 1/8 | † |

| | | | | |
|---|---|---|---|---|
| Human Epithelial Antigen 125 (HEA125) | None | single drop | | Serotec |
| CD44 | None | 1/250 | 1/4 | hybridoma |
| E-cadherin (E-Cad) | None | 1/250 | 1/80 | Takara |
| Keratin (K) 5/6 | None | 1/200 | 1/100 | Sigma |
| K7 | None | 1/200 | 1/100 | Sigma |
| K8 | None | 1/200 | 1/100 | Sigma |
| K13 | None | 1/200 | 1/100 | Sigma |
| K14 | None | 1/200 | 1/100 | Sigma |
| K18 | None | 1/200 | 1/100 | Sigma |
| Pan keratin | None | 1/200 | 1/100 | Sigma |
| Zonula Occludin-1 (ZO-1) | None | 1/100 | | Zymed |
| Timothy Grass extract (Phl p1, 5 and 6) | None | | 1/800 | € |
| *Secondary antibodies* | | | | |
| Rabbit anti-mouse | FITC | 1/80 | | Dako |
| Rabbit anti-mouse | Biotin | | 1/200 | Dako |
| Mouse anit-rabbit | Biotin | | 1/200 | Dako |

*Key*

€ = Gift from R. Valenta, Medical University of Vienna, Austria

† = Gift from D. Garrod.

IS = Immunostaining – indirect immunofluorescence.

GMA = Immunohistochemistry (GMA embedded samples).

### 2.1.5 In vitro allergen challenge (treatments)

Cells were cultured in the usual fashion (section 2.1.1) then seeded on membrane insert chambers (Greiner bio-one ThinCert ™ Tissue culture inserts for multiwell plates, Cat no. 662 640) according to section 2.2.10.1.

Epithelial layer development was visually assessed by light microscopy and also trans-epithelial electrical resistance. Once the mono-layer had reached / surpassed a visually confluent layer and the experiment resistance threshold had

been passed then the specific treatment was added to the medium in the upper chamber.

A control set of wells were run in parallel with any treatment runs.

Treatment used were

Timothy grass pollen extract [1] (ALK),

Protease [2] (added as a positive control),

Timothy grass pollen + protease inhibitor cocktail [3],

Timothy grass pollen + histamine [4].

[1] Timothy grass pollen, Aquagen® SQ, (ALK® Cat no. 1004046, Phl p).

[2] Protease, (Sigma® Cat no. P5147), the pronase E mixture includes five serine proteases, two zinc endopeptidases, two zinc leucine aminopeptidases and one zinc carboxypeptidase.

[3] Protease inhibitor cocktail (Sigma® Cat no. P2714), containing

- 4-(2-Aminoethyl) Benzenesulfonyl Fluoride Hydrochloride (AEBSF), inhibits serine proteases, such as trypsin, chymotrypsin, plasmin and kallikrein.
- EDTA inhibits metalloproteases.
- Bestatin inhibits aminopeptidases, such as leucine aminopeptidase, alanyl aminopeptidase, aminopeptidase B and triamino peptidase.
- trans-Epoxysuccinyl-L-Leucylamindo-(4-Guanidino) Butane (E-64), inhibits cysteine proteases such as calpain, papain, cathepsin B and cathepsin L.
- Leupeptin inhibits both serine and cysteine proteases, such as calpain, trypsin, papain and cathepsin B.
- Aprotinin inhibits serine proteases such as, trypsin, chymotrypsin, plasmin, trysinogen, urokinase, kallikein and human leukocyte elastase.

4 Histamine (Sigma® Cat no. H7125)

# 2.2 Methods

### 2.2.1 In vitro maintenance

All cells were grown in their respective culture medium at 37°C, in a humidified incubator with 5% carbon dioxide ($CO_2$).

Cell stocks were grown in 75cm2 flasks; the medium was changed every 3-4 days. When >90% confluence was established, cells were detached and passaged with the use of trypsin/ethylenediaminetetraacetic acid (EDTA) (0.05% trypsin / 0.02% EDTA in $Ca^{2+}$ and $Mg^{2+}$ free Hank's Balanced Salt Solution (HBSS)). Briefly, the cell monolayer was washed twice with 7ml HBSS for 5 minutes placing the flask in the incubator during the washing time. The HBSS was removed and 2ml of the trypsin/EDTA solution was added then incubated for a further 5 minutes. To stop the activity of the trypsin/EDTA, 8ml of media + 10% FCS was added. The 10ml of cell suspension was centrifuged for 5 minutes at 110 x G, the liquid was discarded and the pellet was fully re-suspended in 1ml of un-supplemented growth medium. Cells were counted using a Nebauer haemocytometer and viability was established by the trypan blue dye exclusion method. Cells were seeded into 75$cm^2$ flasks at approximately 1 x $10^6$/ml. All cell lines used in this project were used within 30 passages from the original frozen stock in order to minimise phenotypic drift associated with long-term culture. ChWk, IOBA-NHC and 16HBE 14 o- cell lines were passaged according to this method.

#### 2.2.1.1 Cell line storage

Cell suspensions were prepared by using the trypsin/EDTA detachment method, 0.8ml of this suspension was placed into a 1.8ml cryo-tube, then 0.1ml FCS and 0.1ml Dimethyl Sulfoxide (DMSO) was added. The tube was then sealed, shaken and immediately placed in a container, insulated with isopropanol, and placed in a -80°C freezer and left overnight. This container was designed to allow the cryotubes to cool at a rate of about 0.5/1°C per minute. The tube was then transferred to the liquid nitrogen storage.

For thawing, the cryo-tube was taken out of the liquid nitrogen tank and placed in a 37°C water-bath and rapidly thawed, within 2 minutes. The cell suspension was added to 2-3 ml of supplemented growth medium and placed in a 25 $cm^2$ flask; the medium was replaced with new after 24 hours then cultured as per section 2.3. Once the monolayer reached 80-90% confluence the cells were detached and seeded into 75 $cm^2$ flasks.

### 2.2.2 Ex vivo maintenance

Description of successful pilot culture technique

Conjunctival bulbar biopsies were collected from all the subject groups. Biopsies were immediately placed in Leibovitz's L-15 medium and kept overnight at 4°C before processing.

Using a dissection microscope under sterile conditions, the sub-mucosal layer below the epithelial layers was removed. The tissue was cut into sections of about 0.5 $mm^2$, using a sterile scalpel. Individual explants were then placed with the superficial epithelial layer up and allowed to attach to the surface of the culture vessel. Once attached, medium was added so that a thin covering of the surface was achieved. After 2 days the explant was flooded with culture medium, and every 3 days approximately 50% of the medium was replaced with fresh medium. If no growth had been observed by 2-3 days of preparation, then it was deemed to have failed and the explant was discarded.

### 2.2.3 Indirect Immunofluorescence

Cells were grown on sterile 13 mm diameter glass coverslips placed an in 24 well plates. Cells were seeded at 2 x $10^5$ cells/ml using 100µl cell suspension which was placed on the central region of the coverslip and incubated for 1 hour to allow for cell attachment to take place. The wells were carefully flooded with medium and incubated further. Once the cells had reached the desired confluence, the coverslips were washed briefly with warm serum free medium. Cells were fixed by using 1 ml of cold methanol (-20°C) which was replaced at 2 minutes, and left for a further 8 minutes before washing twice in PBS for 10 minutes. Coverslips were stored at 4°C and used within one week of fixing. Non-

specific binding was reduced by blocking with 1% Bovine Serum Albumin (BSA) in PBS.

Primary antibodies (1°) were diluted in 0.1% BSA/PBS solution. The coverslip was inverted and placed on 50µl of the 1° on Parafilm and incubated for 60 minutes at room temperature (RT). After three washes in PBS, the coverslips were incubated with a fluorescein isothiocyanate (FITC) conjugated secondary antibody (2°) in 0.1% BSA/PBS for a further 60 minutes at RT. For localisation of the cells, the nuclei were counter stained. The coverslips were washed and incubated in the counter stain for 5 minutes at RT. The coverslips were washed, carefully dried and the non-cell surface careful wiped and dried, then mounted on slides using mowiol containing the anti-fading agent Citifluor (Citifluor, London, UK).

All slides were examined, within 24 hours of the staining procedure, using a Leica DM-RBE fluorescence microscope; digital images were captured using a Hamamatsu digital camera and the WASABI software package from Hamamatsu.

### 2.2.4 Immunohistochemistry (GMA embedded samples)

Specimens were fixed and embedded in Glycol methacrylate (GMA) resin, allowing thin sections (2-4µm) to be cut, thus providing optimal morphology and antigenicity.

Biopsy materials were placed immediately in ice-cold acetone containing 2mM phenyl-methyl-sulphonyl-fluoride (35mg/100ml) and 20mM iodoacetamide (370mg/100ml) and left overnight at –20°C.

The primary fixative solution was replaced with acetone at RT for 15 minutes; this was then replaced with Methyl benzoate at RT for a further 15 minutes. The processing solution containing 5% methyl benzoate in glycol methacrylate (GMA solution A) was made; the material was then infiltrated with this for 2 hours at 4°C, repeated three times. The specimen was then embedded in a solution containing 10ml of GMA solution A, 250µl of GMA solution B and 70mg Benzoyl peroxide. The specimen was then placed at the bottom of a labelled, flat-bottomed Taab capsule and allowed to polymerise overnight at 4°C. Once fully polymerised the blocks were stored in airtight containers at –20°C.

Sectioning

The capsules were trimmed of excess resin and the biopsy block faces were filed to allow optimal cutting. 2μm thick sections were cut using a Leica supercut microtome, sections then pick up and floated out on ammonia water (1ml of ammonia in 500ml of distilled water) allowing antigenicity to be preserved. After 60-90 seconds the sections were collected on labelled poly-L-lysine coated glass slides and air-dried for about an hour. The position of the section were marked on the slide; the slide can either be stained immediately or stored at –20°C for a maximum of one week.

Toludine blue staining was used on the first run of cut sections for orientation of biopsy and assessment of epithelial layer.

Avidin–biotin staining

To aid antibody visualisation, the avidin-biotin method was used, which binds to the biotinylated antibody; the avidin and biotin are in an avidin-biotin-peroxidase complex (figure 2.2).

To reduce background staining. Endogenous peroxidase was inhibited by adding 0.1% sodium azide and 0.3% hydrogen peroxide in Reverse Osmosis for 30 minutes.

Tris Buffered Saline (TBS) were used throughout as the washing solution, after three washes the slides were blocked with the use of a blocking medium Dulbecco's modified Eagles medium (DMEM), 20% FCS and 1% BSA, this reduced non-specific protein binding. The slides were washed then the 1° antibody were applied and incubated at RT overnight. The slides were washed, then the 2° biotinylated antibody applied and the slides incubated at RT for 2 hours. The slides were washed; streptavidin biotin-peroxidase solution in tris-HCl buffer (pH 7.4) was applied and incubated for a further two hours at RT. Slides were washed, then diaminobenzedine (DAB) was applied and incubated for a further 10 minutes, then the slides were washed and placed in running tap water for 5 minutes. Sections were counter stained with Mayer's haematoxylin for 1-2 minutes depending upon the freshness of the counter stain solution, and allowed to blue in running tap water. Slides were drained and crystal mount applied, the slides were then placed in an oven at 80°C for 10 minutes. Slides

were cooled then mounted with DPX mounting solution. After drying the slides they were ready to be viewed/analysed.

Imaging

Slides were viewed using a Leica DM-RBE upright microscope, and captured via a JVC 3CCD, using the Acquis image programme and a 10x or 40x objective. Digital images were then transferred to the ImageJ programme for analysis.

### 2.2.5 ImageJ – computer assisted image analysis programme.

The ImageJ computer assisted analysis package was used to measured and calculate epithelial layer height, cell density, percentage staining and calculate the distribution of staining throughout the epithelium. Image is a free web based analysis software package from http:/rsb.info.nih.gov/ij this analysis package also allows the user to write specific a sub-programme for the individual needs of the user.

2.2.5.1 Epithelial layer thickness.

10 lines were drawn perpendicular to the basement membrane along the epithelial section, at 10 micron intervals. The length of each line was then calculated, and an average length was then generated for the section measured (figure 2.3a).

2.2.5.2 Epithelial layer cell density.

Epithelial cell density was measured by two methods (figure 2.3b).

The first methods involved calculating the mean epithelial cell area within a specific highlighted area of epithelium. The second method involved calculating the number of nuclei against a length of basement membrane (no set length of basement was used, as a set length could not be superimposed over the varied tomography of the basement membranes).

1. Epithelial cell density was calculated by a box being drawn around an area of the epithelium. The box was then highlighted and the nuclei within the box were highlighted. Any nuclei that touched the basal line or right hand line were discounted. The number of nuclei was then divided by the total area of the

highlighted box of epithelium, which gave the mean epithelial cell area or volume of cells and thus the cell density within an area of epithelium.

2. Number of nuclei present per unit area was calculated by highlighting a length of basement membrane, then highlighting the nuclei that lay above this length. The number of nuclei was then divided by the length of basement membrane which gave the number of nuclei, therefore cells, against a unit length of basement membrane.

2.2.5.3 Percentage expression.

The percentage expression was measured by a specifically written programme for calculating the percentage expression and the following protocol (figure 2.3c),

The area of epithelium to be measured is highlighted by a box being drawn around it,

The image is then changed to black and white and the staining is placed above the threshold and given a colour (seen in plate B, figure 2.3c),

The programme would then calculate the percentage of staining seen within the highlighted area.

2.2.5.4 Distribution.

The distribution of the staining throughout the epithelium was achieved by extending the programme used to calculate the percentage staining using the additional protocol (figure 2.3d),

After stage three, the programme shaded the stain pixels according to the distance from the basement membrane (figure 2.3d, plate C), white being the closest to the basement membrane,

Lines were then drawn on over the coloured pixels (by the programme) at 5 micron intervals along the basement membrane line, starting at the left hand side of the highlighted area (figure 2.3d, plate D),

The programme recorded any coloured pixels that were transected by these lines, therefore giving the distance from the basement membrane of any positive staining,

The data from all the lines were normalised to 100% so that the different lengths of the lines would give an accurate depiction of the epithelial layer and the staining pixels at each percentile point from the basement membrane,
Given below is an example of a stain measured across an epithelial layer,

| | | | | | | | | | |
|---|---|---|---|---|---|---|---|---|---|
| 1 | 1.235058 | 21 | 0.798785 | 41 | 1.191721 | 61 | 1.273869 | 81 | 1.195844 |
| 2 | 0.919886 | 22 | 1.003375 | 42 | 1.055782 | 62 | 1.309526 | 82 | 1.132723 |
| 3 | 0.500262 | 23 | 0.77936 | 43 | 1.117684 | 63 | 1.142965 | 83 | 1.094479 |
| 4 | 0.590069 | 24 | 0.775973 | 44 | 1.185516 | 64 | 1.209488 | 84 | 1.052259 |
| 5 | 0.574654 | 25 | 1.279788 | 45 | 1.085457 | 65 | 1.37122 | 85 | 1.140936 |
| 6 | 0.645332 | 26 | 1.067429 | 46 | 1.260083 | 66 | 1.226512 | 86 | 0.982697 |
| 7 | 0.504476 | 27 | 0.804845 | 47 | 1.020617 | 67 | 1.286695 | 87 | 1.12684 |
| 8 | 0.691728 | 28 | 1.055191 | 48 | 1.350666 | 68 | 1.286174 | 88 | 1.147084 |
| 9 | 0.570536 | 29 | 0.959778 | 49 | 0.429426 | 69 | 1.144429 | 89 | 0.762708 |
| 10 | 0.636164 | 30 | 1.085268 | 50 | 1.717776 | 70 | 1.421794 | 90 | 1.173821 |
| 11 | 0.603655 | 31 | 0.970338 | 51 | 1.17628 | 71 | 1.181198 | 91 | 0.841686 |
| 12 | 0.743308 | 32 | 1.11333 | 52 | 1.22143 | 72 | 1.206877 | 92 | 0.821363 |
| 13 | 0.631932 | 33 | 1.000367 | 53 | 1.285046 | 73 | 1.305417 | 93 | 0.95114 |
| 14 | 0.746296 | 34 | 1.136565 | 54 | 1.072072 | 74 | 0.923789 | 94 | 0.587584 |
| 15 | 0.606847 | 35 | 1.032719 | 55 | 1.336425 | 75 | 1.506704 | 95 | 0.717876 |
| 16 | 0.840541 | 36 | 1.089221 | 56 | 1.306419 | 76 | 1.319292 | 96 | 0.707837 |
| 17 | 0.797775 | 37 | 1.164768 | 57 | 1.119028 | 77 | 1.220322 | 97 | 0.440704 |
| 18 | 0.852098 | 38 | 1.145684 | 58 | 1.377187 | 78 | 1.12825 | 98 | 0.388126 |
| 19 | 0.640911 | 39 | 0.733117 | 59 | 1.054471 | 79 | 1.030427 | 99 | 0 |
| 20 | 1.064877 | 40 | 1.428396 | 60 | 1.392472 | 80 | 1.395105 | 100 | 0.267932 |

2.2.5.5 Analysis of distribution.

In order to use the distribution graphs of the percentage staining in the three groups the data has been presented in two different ways. The first methods displays the continuous staining pattern across the entire epithelium starting from the basement membrane to the apical membrane showing the percentage at each percentile point. The second method was to display the percentage staining in each of the three cell layer which make-up the epithelial layer. To display this data accurately the size of each of the layers had to be calculated. 30 random

sections from each subject group were used. The total thickness of the epithelium was measured then the thickness of each of the cell layers was measured and percentage that each cell layer makes of the epithelial layer was calculated (figure 2.3e). Given below is the mean group percentage for each cell layer within the subject groups;

| Cell layer | Basal | Intermediate | Superficial |
|---|---|---|---|
| Control | 20% | 30% | 50% |
| SACq | 30% | 40% | 30% |
| SACa | 15% | 60% | 25%. |

### 2.2.6 Confocal microscopy

Biopsies for Confocal microscopy were immediately placed in plain Leibovitz's L-15 medium in theatre, and then transported on ice, to the laboratory.

Preparation

Using a dissecting microscope under sterile conditions, the underlying sub-mucosal tissue below the epithelium was removed. Biopsies were cut into sections of roughly 1-2 $mm^2$, using a sterile scalpel. Individual pieces were then placed superficial surface up and allowed to attach to the surface of an untreated sterile glass coverslip.

Fixation and staining.

Once attached, before the explant dried out, the coverslip was fully immersed and in 4% paraformaldehyde solution for 60 minutes.

The coverslip was washed in 0.1% BSA/PBS three times for 5 minutes, then permeabilised using cold methanol (kept at -20°C) for 10 minutes, repeating the washing step.

The coverslip was inverted in the 1° antibody on parafilm then incubated for 90 minutes at RT before being washed. Then inverted in a 2° antibody with a FITC label and incubated for a further 90 minutes, before being washed. The coverslip was then placed in a nuclear counter stain (Acridine orange, Sigma® Cat no. A6014) and incubated for 3 minutes, before washing again.

The coverslip was mounted in mowiol containing the anti-fading agent Citifluor onto a glass slide for viewing.

A Leica TC3 SP2 confocal microscope and associated software, was used to capture digital images of optical sections through the epithelial layers.

### 2.2.7 Electron microscopy fixation

Specimens (whether cultured cells or biopsies) were immediately placed in fresh 4% paraformaldehyde, 3% glutaraldehyde in 0.1M PIPES buffer solution for a minimum of 60 minutes and placed on ice. The biopsy was washed in buffer, and then placed in a solution containing ammonium chloride ($NH_4Cl$ – [50 mMol]) for 30 minutes to stop the fixation and quench any remaining free aldehyde groups. Washed in buffer then placed in fresh buffer before further processing for either scanning or transmission electron microscopy.

### 2.2.8 Scanning electron microscopy

The specimens were removed from the main fixative and twice washed for 10 minutes in rinse buffer (0.1M PIPES, pH 7.4). Then placed in post fixative solution (1% osmium tetroxide in 0.1M PIPES) for 60 minutes. The specimens were washed with buffer, then dehydrated using increasing grades of ethanol up to absolute, each stage lasted for 10 minutes except at the absolute stage where the time was increased to 20 minutes. The specimens were then critical point dried, mounted on stubs and sputter coated with gold palladium. The stubs were viewed using a Hitachi S800 scanning electron microscope. After drying each sample was cut into two sections and each section was mounted in different orientations to ensure that the correct desired plane of the sample could be seen.

### 2.2.9 Transmission electron microscopy

Fixed samples were washed twice in buffer (0.1M PIPES, pH 7.4), then placed in 1% osmium tetroxide in 0.1M PIPES for 60 minutes. The sample was washed in buffer then dehydrated, using solutions with increasing ethanol concentrations up to absolute. The sample was then placed in acetonitrile for 10 minutes, and then left overnight in acetonitrile:resin (50:50) (Taab – resin). The sample was placed into resin to allow infiltration, then put into fresh resin for and polymerised at 60°C for 24 hours.

2.2.9.1 Sectioning and staining

The resin blocked was trimmed and ultra-thin sections (70-90nm) were cut and mounted on grids. The grids are then inverted onto drops of uranyl acetate solution under minimal light conditions for 15 minutes, and then gently washed under a stream of fresh distilled water. The grids are then inverted onto drops of the Reynolds lead stain for 5 minutes using NaOH to reduce the presence of $CO^2$, the gently washed again with fresh distilled water and blotted dry. The grid was then viewed using a Hitachi H7000 transmission electron microscope.

**2.2.10 Trans-epithelial electrical resistance (TEER)**

All trans-epithelial electrical resistance experiments were carried out within a sterile environment / conditions.

2.2.10.1 In vitro

Cells were seeded on membrane inserts in a 24-well plate at 1 x $10^5$/ml. Trans-epithelial electrical resistance measurements commenced when the cells reached confluence. Electrical resistance was measured by introducing the STX2 (chopstick) electrodes (World Precision Instruments (WPI) UK) into the well, ensuring that the longer tip is placed in the deeper outer chamber of the well, the shorter tip is placed in the upper chamber above but not touching the cells on the membrane (figure 2.4, plate A). An AC current was used to avoid causing adverse effects on the tissue. For multiple readings the electrodes remained in position, with minimal movement in between each reading. A cable from the chopsticks was plugged into a jack on the epithelial voltohmmeter (EVOM, WPI, UK), the test result were displayed on the LCD display on the front of the voltohmmeter (figure 2.4, plate B). Measurements were taken as required by the design of the experiment.

Before and after each set of test results were taken the electrodes were sterilised by soaking in 70% ethanol.

2.2.10.2 Double inserts

This method was devised to measure the electrical resistance of stratified sheep conjunctiva before the availability of suitable re-circulating Ussing chamber equipment. Pieces of tissue were processed according to section 2.1.2.

Two used 24 well format inserts had their membranes removed and were sterilised overnight in 70% ethanol (figure 2.5, plate A).

Pieces of processed tissue were orientated so that the superficial cell layer was accessible from the top chamber, then the tissue was placed in between the two chambers (figure 2.5, plate B). The two chambers where then pushed together so that one fitted inside the other and in the process trapping the tissue and ensuring a good tight seal with the tissue (figure 2.5, plate C). To test whether a good seal had been established, a small amount (~100µl) of culture medium was added into the top chamber only, to check for leaks. If leaks were detected, possibly due to a tear in the tissue, then the tissue was discarded and the procedure was started afresh. If no leaks were identified then the top chamber was filled with culture medium, and the two inserts with tissue in between were placed in a well with culture medium in. The electrical resistance could then be measured using a pair of modified STX2 chopsticks (figure 2.5, plate D). Readings were taken using the epithelial voltohmmeter used in the previous resistance studies. This method only allowed one set of tests to be carried out on each section of tissue.

2.2.10.3 Ussing chamber

When an appropriate re-circulating Ussing chamber became available, the measuring of the trans-epithelial electrical resistance of sheep conjunctival epithelium was carried out using the method described below instead of the devised double insert method. Pieces of tissue were processed according to section 2.1.2.

Before the experiment was carried out, all the equipment were pieced together and flushed with 70 % ethanol in order to sterilise the equipment and check for potential leakage. The processed tissue was placed over the holding pins of the half of the chamber, the second half of the chamber was lined up against the first half so that the pins slotted into their opposite holes, and the two sections were tightly pushed together. In order to keep the two halves of the chamber firmly together, they were placed in a specialised clamp stand. Tubes from two medium reservoirs were inserted into the chamber and medium was slowly released into the tubes / chamber, so as not to damage the tissue. If no leaks were seen, then the experiment was commenced. The modified chop sticks were placed in the medium reservoirs so that continuous measurements could be taken throughout

the time scale of the experiment without disturbing the piece of tissue (figure 2.6). Readings were taken using the epithelial voltohmmeter used in the previous resistance studies.

### 2.2.11 FITC-Dextran

FITC tagged dextran (Sigma® Cat no. C6884)

FITC-Dextran levels were monitored during the in vitro allergen challenges.

During each time point of the experiment 100µl was removed from the lower chamber, then stored in the dark until the completion of the experiment. Samples where then placed into a 96-well plate and the FITC-Dextran levels were measured by excitation at 485 nm, when read at 530 nm.

Validations of this measurement of FITC-Dextran were carried out using serial dilutions, diluting with PBS and the culture mediums to measure background levels.

These background readings each of the diluents were subtracted from the result.

The final concentration of FITC-Dextran used was 1/1000 in the culture medium.

### 2.2.12 Data analysis

Raw data was transferred and organised within the Microsoft excel programme. Data was then transferred to the Minitab 13 statistical programme. Each data set was then run through the Anderson-Darling (empirical cumulative distribution function) normality test. If the data was found to be normally distributed then a parametric test was applied, if non-normally distributed then a non-parametric test was applied. Statistical significance was taken when the p value was $<0.05$.

# Figure 2.1 Conjunctival biopsy

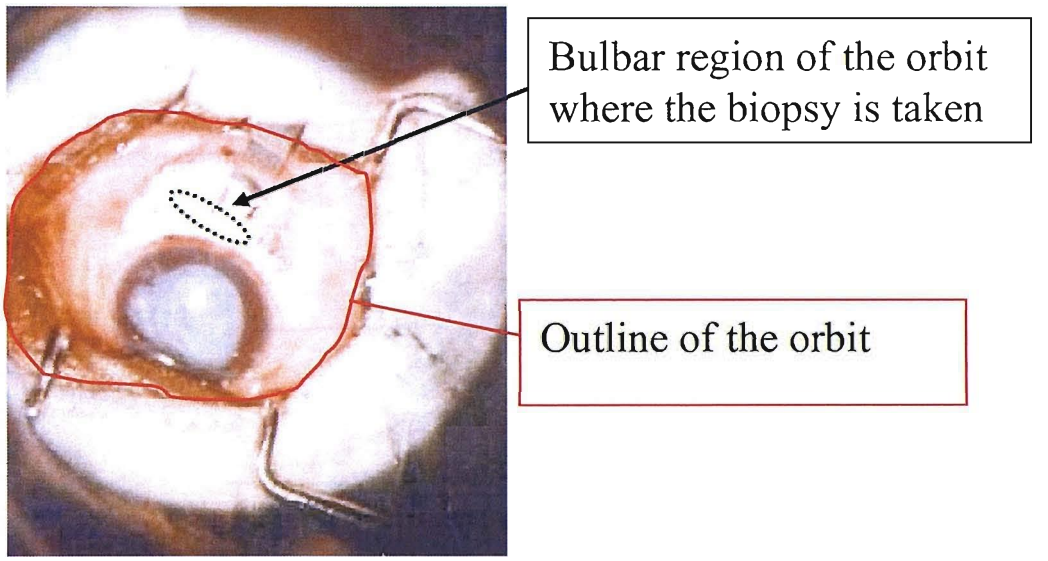


After anaesthesia is applied and allowed a short time to work, prior to the operation, the bulbar conjunctiva was elevated using forceps and using scissors a snip biopsy was taken. Then placed immediately in sterile L-15 transport medium for further processing.

# Figure 2.2 Immunohistochemistry – The Avidin-Biotin peroxidase complex

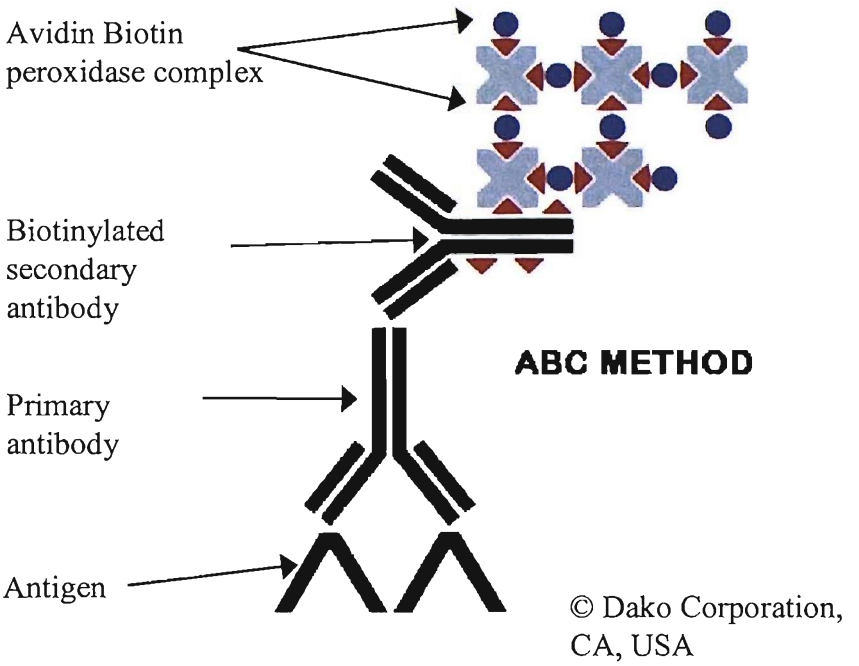


The above diagram represents the avidin-biotin peroxidase complex that is used to amplify and identify the binding of primary antibodies directed against specific antigens. Briefly after the application of the primary antibody, a secondary antibody labelled with biotin. Streptavidin biotin peroxidase complexes are used to amplify the secondary antibodies' signal. The peroxidase complexes are utilised to develop the chromogen, diaminobenzedine (DAB) giving a dark brown colour.

# Figure 2.3a ImageJ – Epithelial thickness

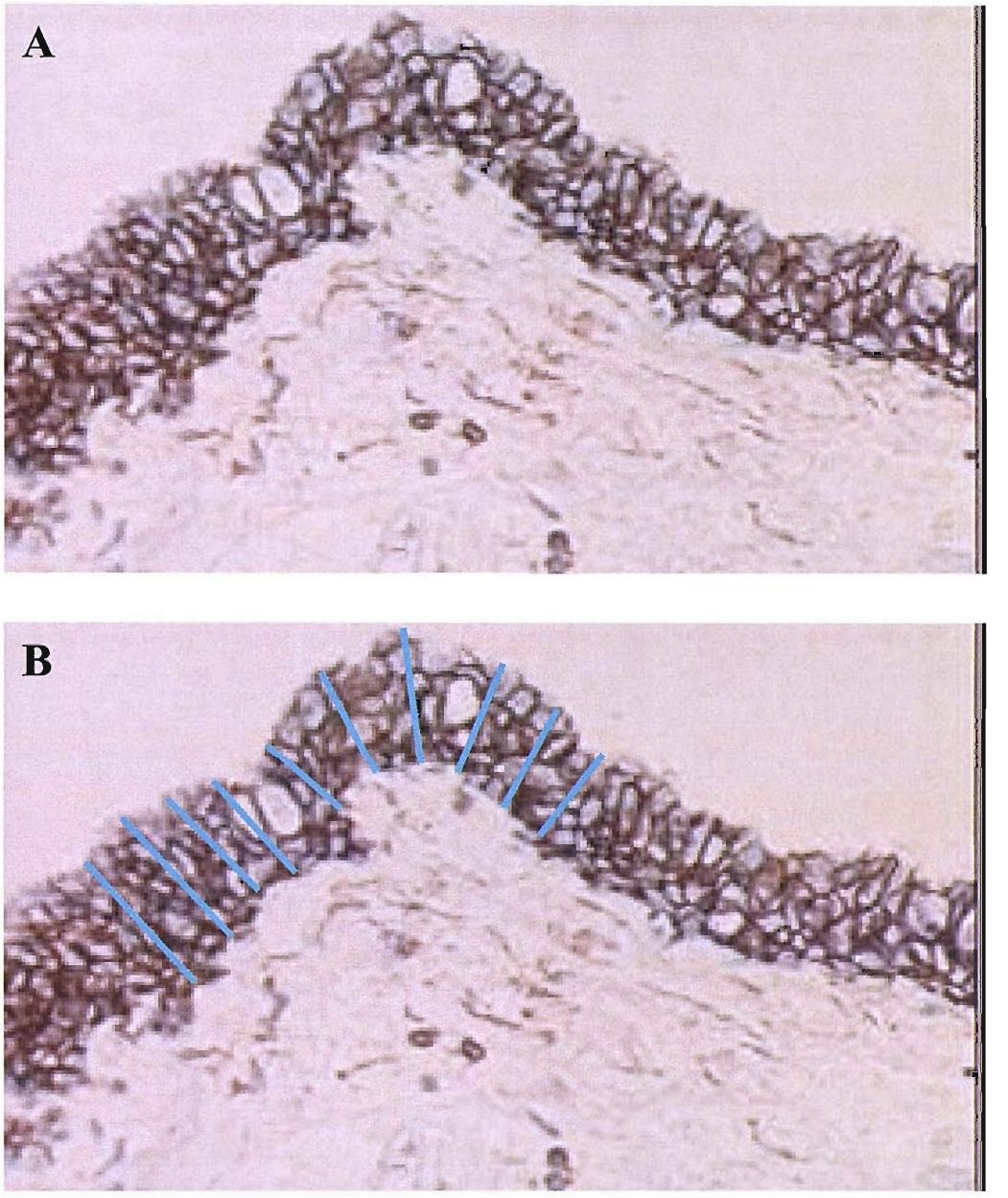


Plate A shows the captured image.

Plate B shows the ten lines drawn over the image.

Briefly, in order to measure the thickness of the conjunctival epithelial layer, firstly an image was captured, then ten, equally spaced, lines were drawn at approximately 90° to the basement membrane. Each of the lines were then measured, the average calculated for each image, then the average for each section was produced. Data was grouped for subject group.

Example shown is control epithelium.

# Figure 2.3b ImageJ – Epithelial cell layer density

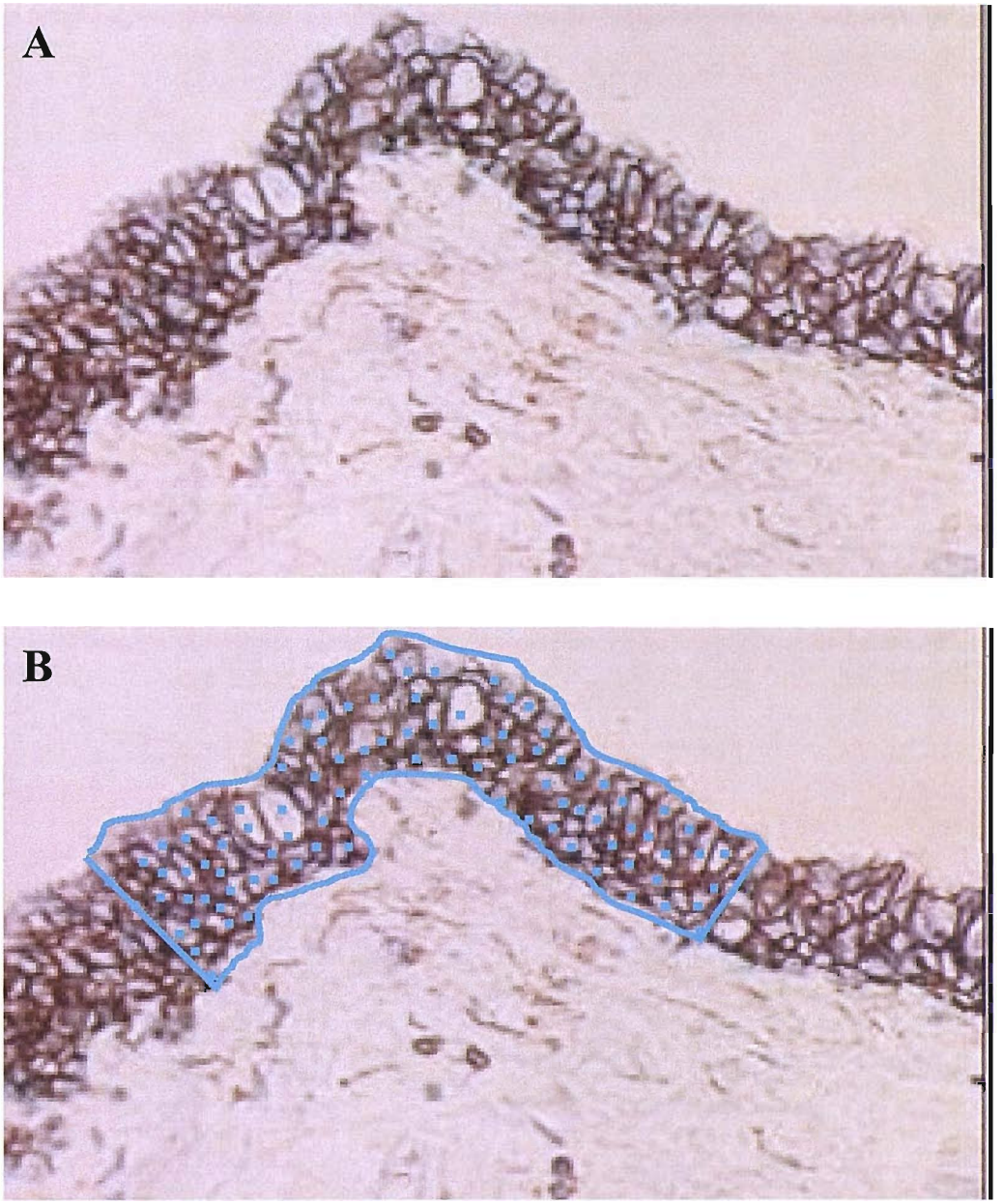


Plate A shows the captured image.

Plate B shows the highlighted area of interest and highlighted positions of cell nucleus'.

Briefly, an image is captured, the area of interest is highlighted by drawing a box, every visible cell nucleus is highlighted, using the rule that if any nucleus touch the boundary line only those touching the left or superficial lines are included, those touching the basal or right line are discounted. The cell layer density is calculated by two methods.

1.The the number of highlighted nuclei are divided by the total area highlighted, or

2. The number of highlighted nuclei are divided by the length of basement membrane, of the highlighted area.

Example shown is control epithelium.

# Figure 2.3c ImageJ – Percentage expression staining

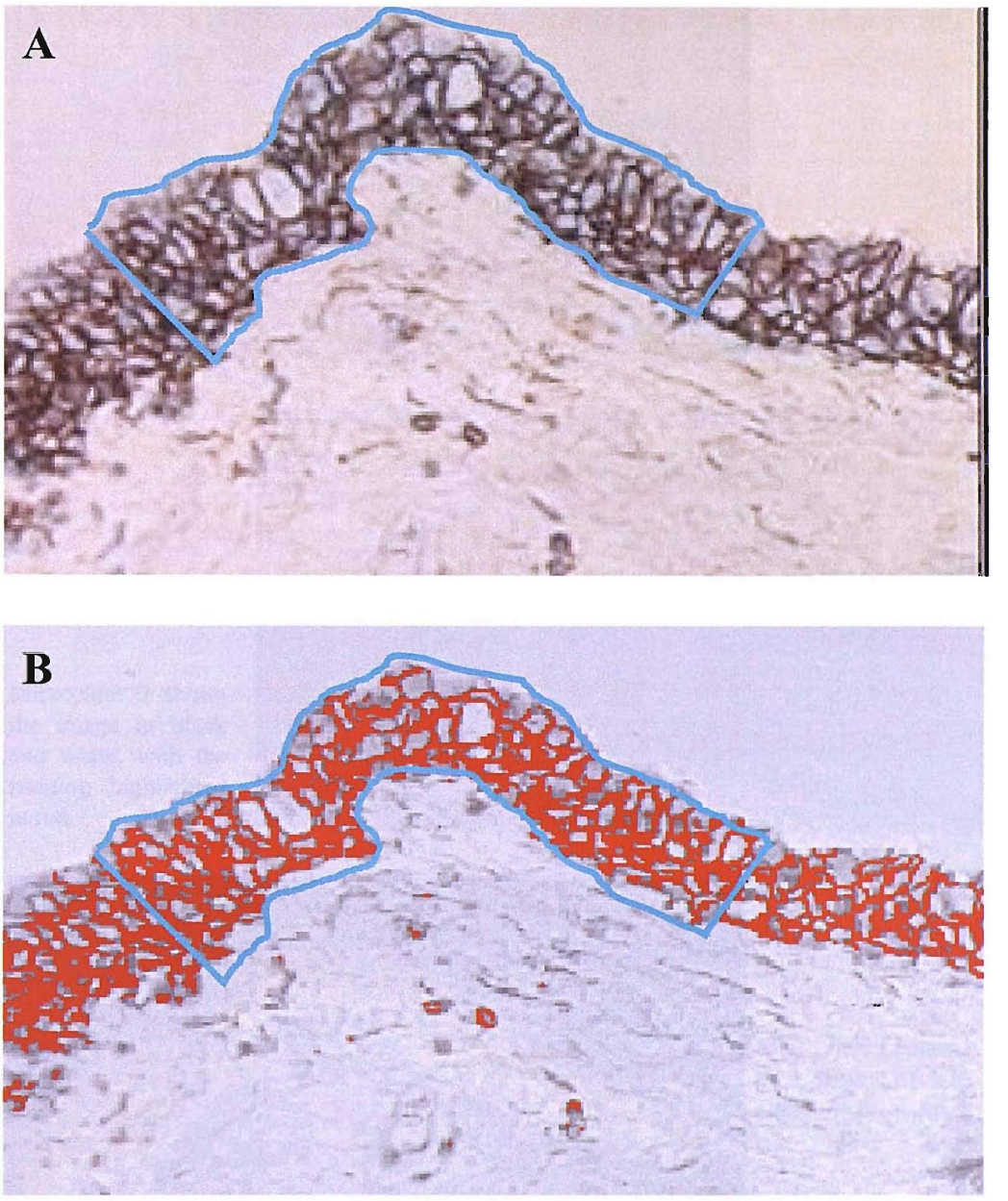


Plate A shows the captured image and highlighted area of interest.

Plate B shows the image in black and white, the highlighted area, and the highlighted areas of staining.

Briefly, to calculate the percentage area of staining, an image is captured, the area of interest is highlighted then the image is changed from its original colour to black and white. The area of staining is then placed above the threshold and given the red colour. The total area of red is then divided by the total area within the highlighted box

Example shown is control epithelium.

# Figure 2.3d ImageJ – Staining distribution

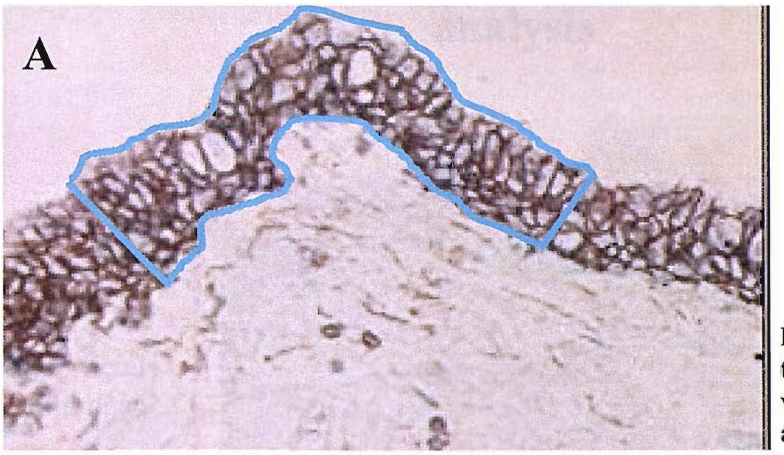


Microplate A shows the original image with highlighted area of interest.

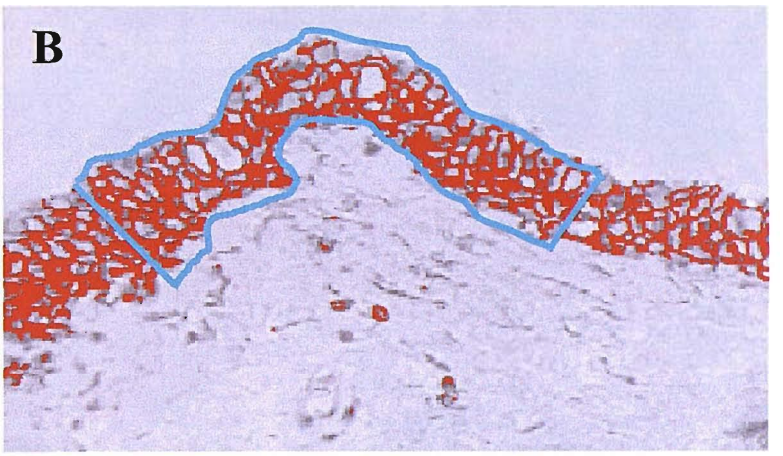


Microplate B shows the image in black and white, with the staining highlighted in red.

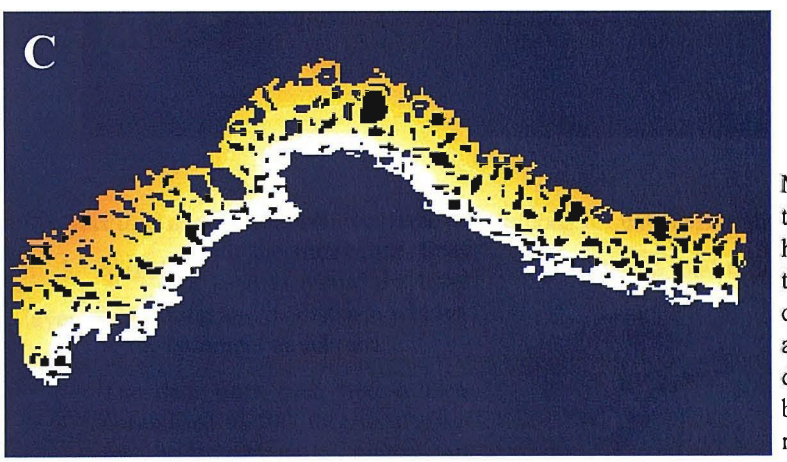


Microplate C shows the pixels of the highlighted staining that have been colour grading according to their distance from the basement membrane.

Microplate D shows the area of staining with the transecting lines that were used to record the level of staining and its distance relative to the basement membrane.

The data from each line is then normalised to 100, to give a value for each percentile point and therefore each pixel along the line.

# Figure 2.3e ImageJ – Staining distribution analysis

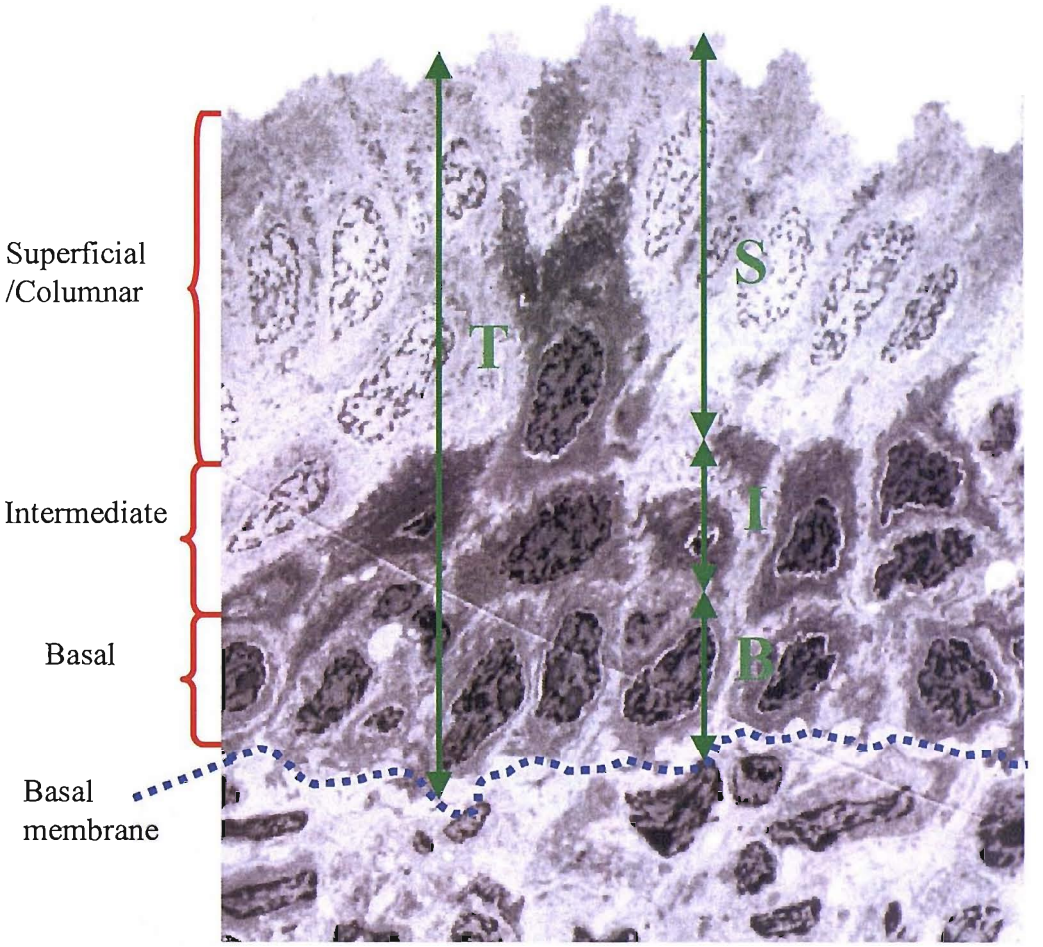


The electron micrograph above shows the methods for calculating the percentage make-up of the epithelial layer and the three cell layers. Briefly, the total thickness of the epithelial layer was measured, then the thickness of each of the cell layers were measured and expressed as a percentage of the total epithelial thickness. These data are displayed in the distribution graphs in section 3.5.4 of chapter three.

An electron micrograph was used as the template in this figure, as it demonstrates clearly the three cell layers that make up the conjunctival epithelium.

# Figure 2.4 TEER method – Chop sticks

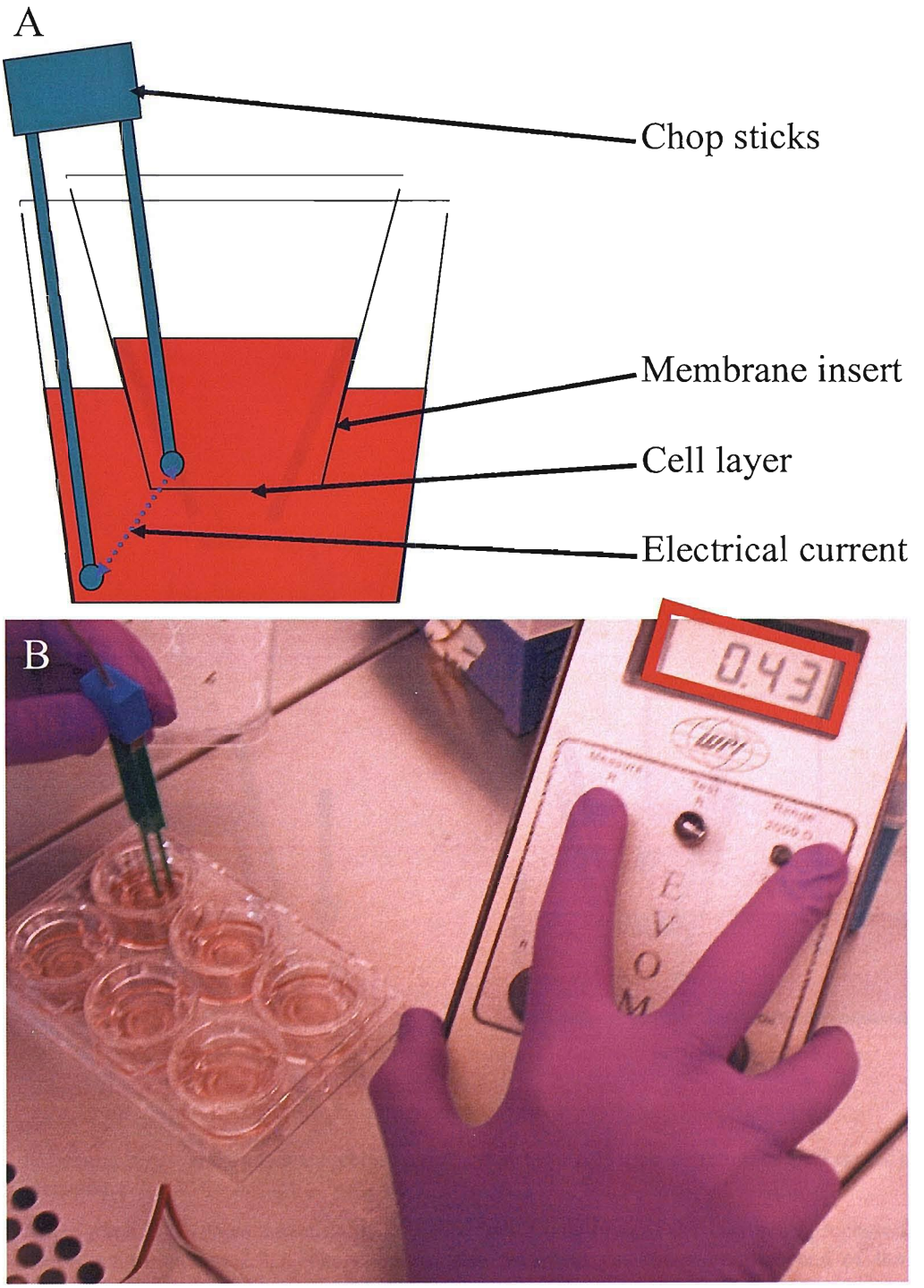


Plate A – shows a cartoon representation of the method of measuring the trans-epithelial electrical resistance via chop sticks (STX-2 Electrode, World Precision Instruments, Inc). One of the electrode ends is introduced into the bottom reservoir of culture medium, the other is carefully introduced into the top chamber and lowered to so not to touch the cell layer but just placed above the cell monolayer. The resistance is then measured using the meter (EVOM Epithelial Voltohmmeter, World Precision Instruments, Inc). At each measuring point during an experiment, four readings are taken and the average is calculated.

Plate B – shows the actual equipment used. The resistance of the cell layer is shown in the red highlighted box.

# Figure 2.5 TEER method – Double insert chamber method

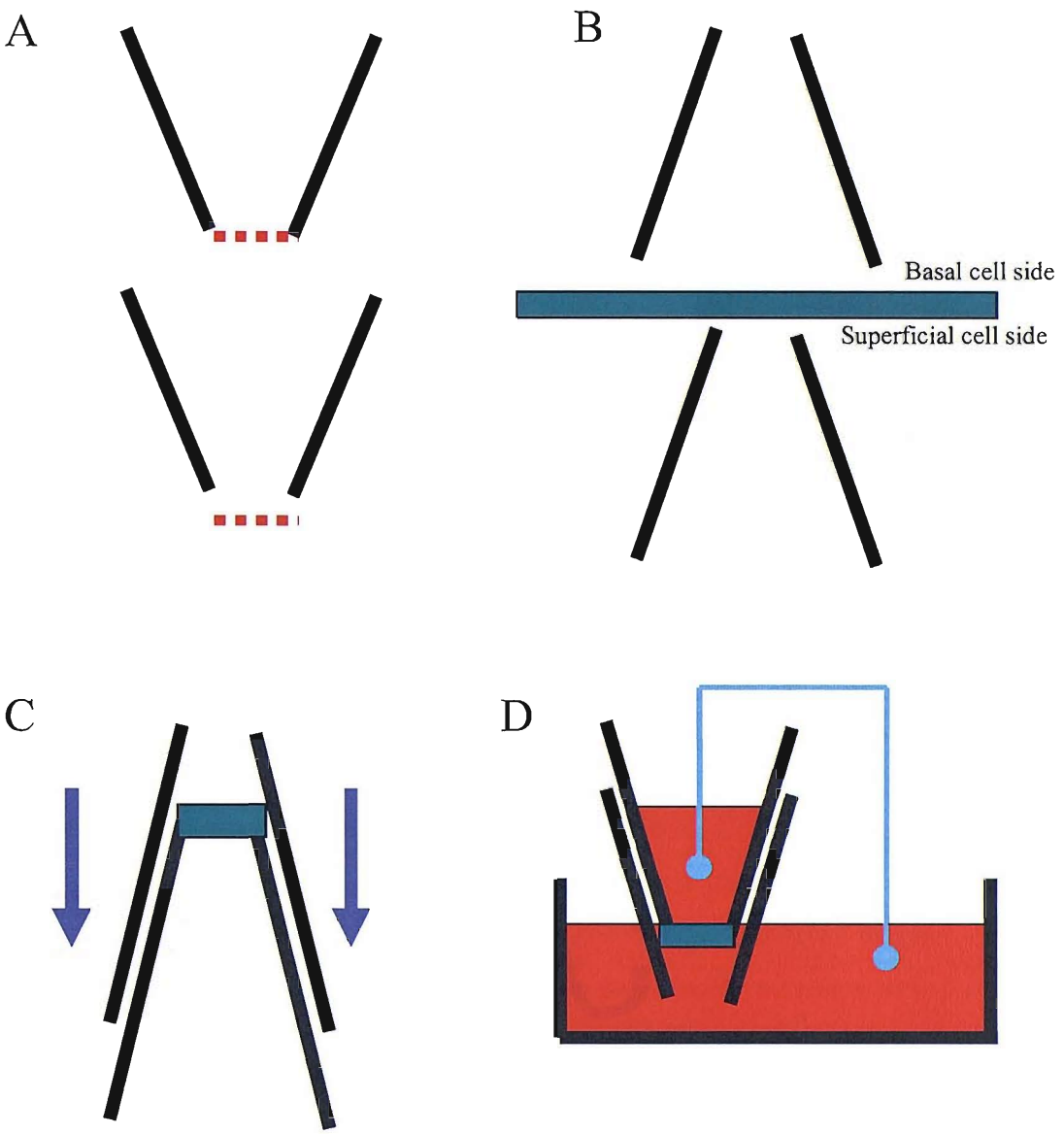


Micrograph A – shows two membrane inserts that have had their membranes (red dotted) removed

Micrograph B – shows a section of the Ovis aries tissue (green) that has been processed according to section 2.1.2. The tissue is then placed across the membrane end of the chamber.

Micrograph C – shows that the second chamber insert that is placed over the tissue and firmly / carefully pushed down in the direction shown by the blue arrows, until the tissue seals the two chambers together.

Micrograph D – shows that once the tissue is sealed in-between the two inserts the lower insert is placed in normal culture medium, then medium is placed above the tissue in the top insert. A probe is then placed in the bottom medium and the top medium so that a measurement can be obtained using a pair of modified STX-2 electrodes (Chop sticks).

# Figure 2.6 TEER Ussing Chamber

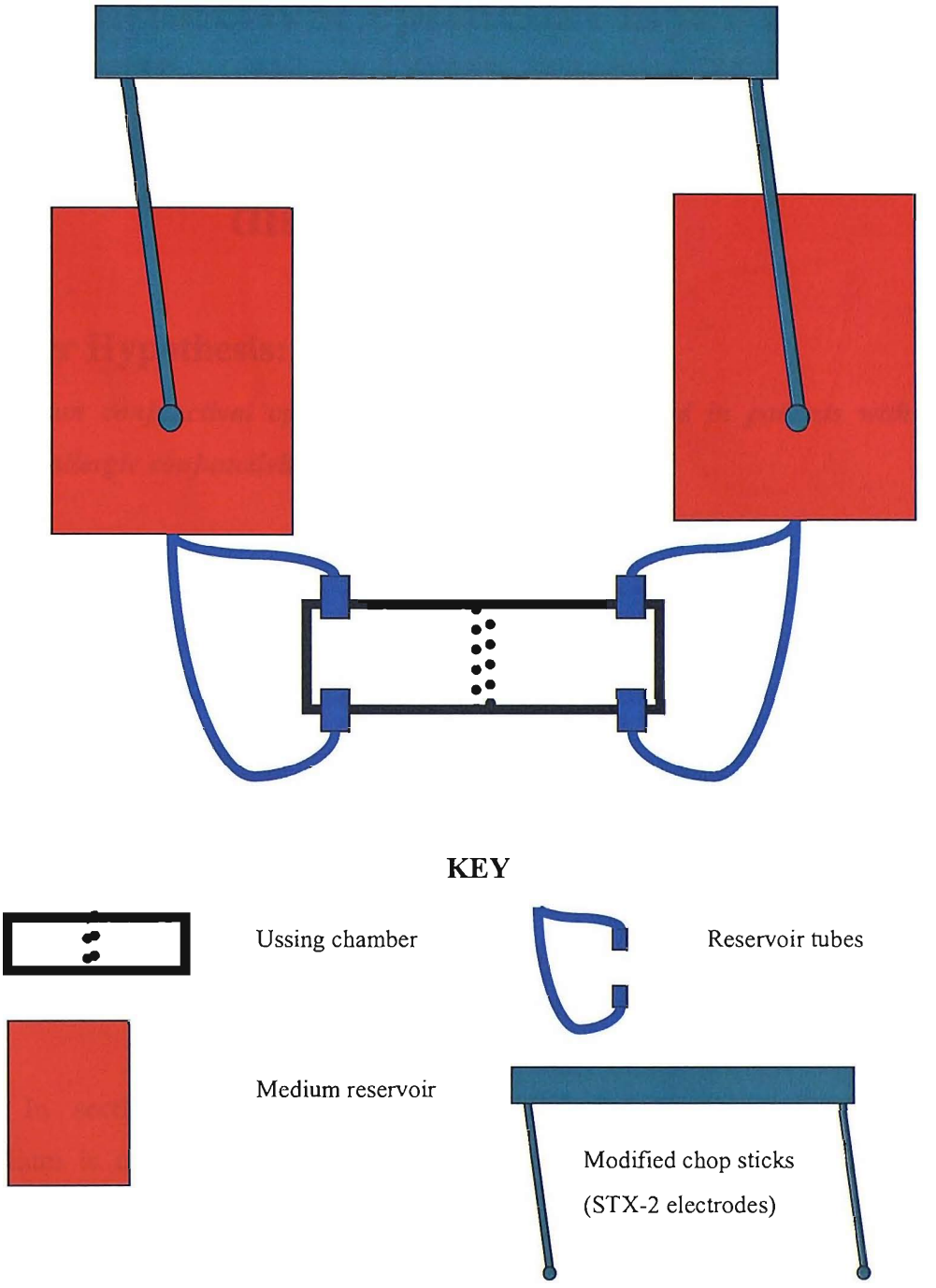


The above cartoon represents the modified Ussing chamber equipment used to measure the trans-epithelial electrical resistance generated by freshly excised pieces of stratified epithelial tissue.

Briefly, tissue was inserted in between the two halves of the chamber, which was then securely fixed together using a specialised clamp stand. Tubes were attached to the chamber to allow the circulation of medium from the reservoirs into the chamber and back to the reservoirs. The modified chop sticks were inserted into the reservoirs, allowing the TEER to be measured constantly without the need to disturb the tissue or chamber during the experiment.

# 3. Characterisation of the human conjunctival epithelial layer in control, patients with active disease (SACa) and patients with quiescent disease (SACq)

## Chapter Hypothesis:

***The human conjunctival epithelium is structurally altered in patients with seasonal allergic conjunctivitis (SAC).***

### 3.1 Introduction

To test the chapter hypothesis, structural components of the conjunctival epithelium were characterised from biopsy material, then compared between patient groups. The patient groups used were control patients, with no history of allergic eye disease, and patients with a positive history of seasonal allergic eye disease. As described in section 1.1 (Seasonal allergic conjunctivitis), seasonal allergic eye disease has two distinct phases, the active phase, during the periods of air-borne pollen allergen release and the quiescent phase, during periods where no air-borne pollen allergens are released. Therefore, the disease patient group was divided according to the date of the biopsy and therefore disease state.

In section 1.5 (Conjunctival epithelium) the human conjunctival epithelium is classified as a non-keratinised non-ciliated stratified columnar epithelium, of 3 to 5 cell layers thick. In the conjunctival epithelium of the patient with SAC, genetic disposition or environmental influence has altered aspects of epithelial architecture through changes in certain cell characteristics, resulting in an epithelium that has a reduced barrier function to exogenous and otherwise inert antigens. These cellular characteristics are proposed to be cell adhesion molecules and the cytoskeleton of the cell (specifically the keratin intermediate filaments), resulting in altered epithelial layer morphology.
The specific targets investigated within this chapter are firstly, the adhesion proteins;

- E-Cadherin,
- CD44 and
- Desmoplakin 1-2.

The target keratin filaments were;

- Keratin (K) 5/6,
- K 7,
- K 8,
- K 13,
- K 14,
- K 18 and
- A pan keratin marker.

The work in this chapter concerning epithelial characterisation was divided into two main sections

1. Ultra-structure (utilising scanning and transmission electron microscopy),
2. Layer morphology, split into (utilising confocal and light microscopy);
    - Descriptive morphology and
    - Quantified morphology.

Using biopsy material, the control epithelium was described and compared to the current opinion and the disease groups.

Ultra-structure was assessed by utilising electron microscopy, both scanning and transmission. The surface features of the epithelial cells were visualised under a scanning electron microscope; micrographs were then taken, assessed and described. Using transmission electron microscopy the intra-cellular structures and junctional complexes could be identified and assessed. Electron microscopy was used because samples could be visualised and scrutinised with greater detail than using other techniques of embedding samples (Bozzola 2002).

Descriptive morphology was undertaken by using biopsy sections embedded in GMA, visualising these sections under light microscopy. Confocal microscopy was used on dissected biopsy material to obtain optical sections through the biopsy to, visualise both general layer morphology and then at higher magnification the individual epithelial cells. Histological damage in the epithelial

layer was assessed by using a minimum of three non-serial sections of each biopsy. Regions of damage were measured; this measurement was then expressed as percentage epithelium undamaged. Damage was classed as regions of supra-basal cell or basement membrane denudation. To determine whether the physical size of the epithelial layer was affected in each of the subject groups, epithelial layer thickness / height was measured from the basement membrane to the apical membrane. Epithelial density was investigated to determine whether changes in the layer thickness / height were attributed to a hyperplasic or hypertrophic process within the tissue. For epithelial density, epithelial cell cross-sectional area was measured, this, was then taken as a reflection of cell volume from each subject group, also the actual number of cell nuclei compared to basement membrane length was measured too.

Quantitative morphology was undertaken in biopsy material, embedded in GMA, stained for the specific adhesion and keratin proteins listed above. The percentage expression in each subject group was calculated, and then the distribution throughout the epithelial layer of this expression was investigated. Changes in protein expression and distribution between the three groups were quantified using digital images, analysed using the ImageJ computer programme.

The results and possible changes in the structure of the conjunctival epithelium, as well as the evaluation of the chapter hypothesis are discussed at the end of the chapter.

## 3.2 Ultra-structure

### 3.2.1 Scanning electron microscopy characterisation of control conjunctival epithelium

The conjunctival epithelium forms a continuous and organised tissue surface constructed from cells with apical membranes that are polygonal in shape. When removed from the conjunctiva the epithelial layer curves to cover the underlying layers of the conjunctival, such as the connective tissue layer, (figure 3.1a microplate A and B and figure 3.2a microplate A). When viewed at higher magnification, valleys can be identified in between the cells of the superficial layer (figure 3.1a microplate C, D and E). The superficial layer is

covered by a dense layer of cellular processes that are microvilli-like that are branched and flattened in appearance (figure 3.1b and c microplate F, G and H). The conjunctival epithelial layer is morphologically different to the connective tissue layer (figure 3.2a microplate B). The connective tissue layer is composed of collagenous fibres with occasional migrating cells present, in appearance the fibres do not form a smooth layer but, are organised (figure 3.2b microplate C). Present within the connective tissue layer are various cell types, red blood cells can be observed in microplate D (figure 3.2b), these were possibly released during the physical damage occurred during the removal of the biopsy material from the patient.

### 3.2.2 Transmission electron microscopy characterisation of control conjunctival epithelium

At low magnification, cross-sectional micrographs of the apical cells show that the microvilli-like cellular processes are uniformly distributed across the superficial membrane (figures 3.3a microplate A and B). This is further highlighted in microplate C (figure 3.3b). The microvilli-like processes may act as a physical support for the tear film layer (figure 3.3b microplate D). The processes appear to branch and no actin filaments were seen in the central core of the processes (figure 3.3c microplate E and F).

The presence of cell-cell junctional complexes located between the apical cell membranes is a feature of an organised epithelium. The junctional complexes are; a tight junction, directly below the apical membrane, followed by an intermediate junction and then a desmosome spot junction (figure 3.4 microplate A). The intermediate junction can be identified, by the electron dense bands that run parallel to the cell membranes in the extra-cellular portion of the junction, and the electron dense plaques which are the intracellular portion of the junction (figure 3.4 microplate A, enlarged section). The tight junction displays the classical expected appearance, where the two opposing plasma membranes coming together to become indistinguishable from each other (figure 3.4 microplate B). The desmosome spot junction is the last junction in the junctional complex, but desmosomes are also located throughout the entire epithelial layer on all cell-cell membrane surfaces (figure 3.5a microplate A and B). It is identified by the two opposing electron dense plaques, where the intracellular

domain of the desmosome junction connects with the intermediate filament proteins of the epithelial cytoskeleton (figure 3.5b, microplate C and D).

The last major junction of an organised epithelial layer is the hemi-desmosome. The hemi-desmosome anchors the basal epithelial cells to the basal lamina and underlying connective tissue layer. The epithelial-connective border is not a static entity, as exo or endo-cytotic vesicles can be identified on the basal surface of the basal cells (figure 3.6 microplate A). As seen in Figure 3.2b microplate C and described in section 3.2.1 the connective tissue layer is morphologically different to the epithelial layer. Its structural components, the collagen fibres are manufactured and deposited by fibroblast cells, then laid in a highly organised distribution pattern, one set runs perpendicular to its neighbouring set (figure 3.6 microplate B). The distinct fibrous banding of the fibres can also be clearly identified.

## 3.3 Descriptive morphology

49 conjunctival biopsies were taken in total from all subject groups (Control = 26, 11 ♂, mean age = 68.77, age range 22 - 91, SACq = 12, 8 ♂, mean age = 41.75, age range 19 - 71, SACa = 11, 7 ♂, mean age = 54, age range 28 - 79). The control epithelium resembled a non-ciliated stratified columnar, comprised of 3 to 5 cell layers. The SACq and SACa epithelium resembled a non-ciliated stratified cubiodal (figure 3.7 Epithelial morphology).

## 3.4 Confocal microscopic analysis of conjunctival epithelium

Control biopsy material was prepared according to section 2.2.6. Entire biopsy pieces were stained with the epithelial markers keratin 18 and HEA125, then counter stained with sytox orange as the nuclear stain.

The epithelium showed positive staining for keratin 18 across the apical membrane of the superficial layer of cells, using the x-y sectional visual plain, and at higher magnification the individual staining pattern can be observed (figure 3.8 microplate A and B).

When using the x-z sectional visual plain, the apical, intermediate and basal layers demonstrated positive staining for HEA125 (figure 3.8, microplate

C). This sectional visual plain also highlights the three layer composition of the conjunctival epithelium.

## 3.5 Quantitative morphology

3.5.1 Regions of undamaged epithelium.

Regions of epithelial damage / remodelling were visually assessed by identifying any areas of damage / remodelling, then measuring the length of these regions, then expressing the percentage of undamaged epithelium.

Damage or remodelling was assessed using the following criteria,

- Areas of total de-epithelialisation,
- Areas of superficial cell layer loss,
- Areas of superficial and intermediate cell layer loss and,
- Areas of substantial irregular cell shape.

No significant regions of damage were seen in the three subject groups (Control - 99.7%, SACq – 100%, SACa 99.8%), (Figure 3.9).

3.5.2 Conjunctival epithelium thickness.

Epithelial thickness was assessed according to section 2.2.5.1.

Control epithelium had a mean thickness of 48.73μm ± 3.12, SACa of 66.13μm ± 4.51 and SACq of 47.19μm ± 7.15 (Figure 3.10). When compared, the SACa epithelium was significantly increased compared to control, (p=0.011), but not statistically compared to SACq, (p=0.075). SACq and control showed no significant difference, p=0.764 (figure 3.10).

3.5.3 Epithelial layer cell density.

Epithelial cell density was measured according to the two methods in section 2.2.5.2.

1. Cell density was expressed as the mean epithelial cell cross-sectional area; this was then compared against the thickness of the sample. The corresponding data points were then plotted on a scatter graph (Figure 3.11, graph A).

Control epithelium had a median cell area of 134.19 $\mu m^2$ (6.25), SACa 156.33 $\mu m^2$ (14.28) and SACq 123.02 $\mu m^2$ (17.27). When compared, SACa was significantly increased to control (p = 0.025) but not significant compared to

SACq ($p = 0.136$). Control and SACq showed no significant difference ($p = 0.585$). To test whether the data correlated together control height and density had a Pearson correlation of 0.791 / $p < 0.001$, SACa had a Pearson value of 0.829 / $p = 0.011$ and SACq had a Pearson value of 0.933 / $p < 0.001$.

2. The cell number per unit length of basement membrane was measured (Figure 3.11 graph B), control measured 9.70, SACq measured 9.79 and SACa measured 10.06, again showing no difference between the subject groups.

3.5.4 Immunohistochemical staining.

In order to quantify the immunostaining, the amount positive staining in each of the sections was measured and then the percentage expression and distribution were calculated according to section 2.2.5.3. and 2.2.5.4.

Examples of the adhesion molecule and keratin staining are shown in figures 3.16 and 3.25 respectively.

For descriptive purposes in terms of the distribution of staining throughout the epithelium, the epithelium was sub-divided into its three cell layers according to section 2.2.5.5. Briefly the epithelium from each subject group were divided as follows;

| | | |
|---|---|---|
| Control = | Basal | 20% |
| | Intermediate | 30% |
| | Superficial | 50% |
| SACq = | Basal | 30% |
| | Intermediate | 40% |
| | Superficial | 30% |
| SACa = | Basal | 15% |
| | Intermediate | 60% |
| | Superficial | 25% |

(The basement membrane represents 0% and the most anterior point on the superficial cell layer represents 100%.)

3.5.4.1 CD44

Control epithelium percentage staining of CD44 was 33.65% (Standard error ± 3.71), SACq was 2.68% (± 1.05) and SACa was 12.92% (± 2.86). The percentage staining in the control was significantly greater, statistically, against the percentage staining in the SACq and SACq subject groups ($p = 0.002$ and $p < 0.001$ respectively). The percentage staining in the SACa groups was significantly greater than the SACq group ($p = 0.005$) (figure 3.12).

In terms of the distribution, when considering the epithelium as a whole, the three subjects groups followed a similar pattern (figure 3.13, graph A).

When the data was sorted into the percentage staining in each of the cell layers, differences can be seen (figure 3.13, graph B).

Control epithelium's distribution of CD44 through the three layers was, 17.89% basal, 43.48% intermediate and 38.63% superficial.

SACq distribution was 31.11% basal, 45.76% intermediate and 23.13% superficial.

SACa distribution was 12.67% basal, 71.82% superficial and 15.51% superficial.

3.5.4.2 E-Cadherin

Control epithelium percentage staining of E-Cadherin was 24.57 (± 3.13), SACq was 1.57 (± 1.81) and SACa was 21.67 (± 1.01). Control epithelium showed a significantly greater staining than SACq, but not than the SACa ($p = 0.0090$ and $p = 0.0807$ respectively). SACa showed a significantly greater staining than SACq ($p = 0.002$) (figure 3.12).

When the distribution of E-Cadherin was viewed across the whole epithelial layer, the pattern of the disease groups appear to have shifted towards the intermediate and superficial layers compared to the pattern of distribution seen in the control epithelium (figure 3.14, graph A).

When this data was transposed into the three cell layers of the epithelium, the percentage breakdown for each layer showed (figure 3.14, graph B),

Control basal percentage staining was 15.65%, intermediate staining was 43.80% and superficial staining was 40.55%.

SACq basal staining was 19.98%, intermediate staining was 47.77% and superficial staining was 32.25%.

SACa basal staining was 4.73%, intermediate staining was 73.89 and superficial staining was 21.38%.

3.5.4.3 Desmoplakin 1-2 (dp 1-2)

Control epithelium percentage staining of dp 1-2 was 18.92% (± 4.32), SACq was 0.052% (± 0.05) and SACa was 17.60% (± 2.61). The percentage staining in the control was significantly greater, statistically, against the percentage staining of the SACq group, but not the SACa group ($p = 0.006$ and $p = 0.702$ respectively). The percentage staining in the SACa groups was significantly greater than the SACq group ($p = 0.006$) (figure 3.12).

The distribution patterns of dp 1-2 across the whole epithelium in each of the three groups showed a similar pattern, with the exception of the disease groups having a more flattened mid-curve (figure 3.15, graph A).

When the data was sorted into the percentage staining in each of the cell layers, differences can be seen (figure 3.13, graph B).

Control epithelium's distribution of dp 1-2 through the three layers was, 16.47% basal, 47.00% intermediate and 36.53% superficial.

SACq distribution was 38.09% basal, 41.31% intermediate and 20.60% superficial.

SACa distribution was 15.52% basal, 66.30% superficial and 18.18% superficial.

3.5.4.4 Keratin 5/6

Control epithelium percentage staining of keratin 5/6 was 44.66 (± 4.70), SACq was 21.03 (± 3.39) and SACa was 39.76 (± 5.09). The percentage staining in the control was significantly greater, statistically, against the percentage staining of the SACq group, but not the SACa group ($p = 0.0016$ and $p = 0.244$

respectively). The percentage staining in the SACa groups was not significantly greater than the SACq group ($p = 0.206$) (figure 3.12).
When the distribution of keratin 5/6 was viewed across the whole epithelial layer, the staining of the three subject groups followed a similar pattern (figure 3.18, graph A).

When the data was sorted into the percentage staining in each of the cell layers, differences can be seen (figure 3.18, graph B).

Control epithelium's distribution of keratin 5/6 through the three layers was, 14.21% basal, 55.52% intermediate and 30.27% superficial.

SACq distribution was 24.04% basal, 50.05% intermediate and 25.91% superficial.

SACa distribution was 12.88% basal, 68.48% superficial and 18.64% superficial.

3.5.4.5 Keratin 7

Control epithelium percentage staining of keratin 7 was 41.86% (± 4.86), SACq was 17.67% (± 3.55) and SACa was 35.32% (± 4.74). The percentage staining in the control was significantly greater, statistically, against the percentage staining of the SACq group, but not the SACa group ($p = 0.001$ and $p = 0.1748$ respectively). The percentage staining in the SACa groups was significantly greater than the SACq group ($p = 0.016$) (figure 3.12).

When the distribution of keratin 7 was viewed across the whole epithelial layer, the staining of the three subject groups followed a very similar pattern (figure 3.19, graph A).

When this data was transposed into the three cell layers of the epithelium, the percentage breakdown for each layer showed (figure 3.19, graph B),

Control basal percentage staining was 13.95%, intermediate staining was 58.99% and superficial staining was 27.06%.

SACq basal staining was 16.37%, intermediate staining was 49.00% and superficial staining was 34.63%.

SACa basal staining was 13.99%, intermediate staining was 64.43% and superficial staining was 21.58%.

3.5.4.6 Keratin 8

Control epithelium percentage staining of keratin 8 was 29.10% (± 2.75), SACq was 7.35% (± 3.80) and SACa was 22.43% (± 1.63). The percentage staining in the control was significantly greater, statistically, against the percentage staining of the SACq group, but not the SACa group ($p = 0.004$ and $p = 0.100$ respectively). The percentage staining in the SACa groups was significantly greater than the SACq group ($p = 0.0137$) (figure 3.12).

When the distribution of keratin 8 was viewed across the whole epithelial layer, the staining of the three subject groups followed a very similar pattern (figure 3.20, graph A).

When this data was transposed into the three cell layers of the epithelium, the percentage breakdown for each layer showed (figure 3.20, graph B),

Control basal percentage staining was 13.88%, intermediate staining was 60.26% and superficial staining was 25.86%.

SACq basal staining was 22.99%, intermediate staining was 42.82% and superficial staining was 34.19%.

SACa basal staining was 11.51%, intermediate staining was 57.97% and superficial staining was 30.52%.

3.5.4.7 Keratin 13

Control epithelium percentage staining of keratin 13 was 50.83% (± 4.24), SACq was 17.21% (± 3.56) and SACa was 44.75% (± 5.05). The percentage staining in the control was significantly greater, statistically, against the percentage staining of the SACq group, but not the SACa group ($p = 0.001$ and $p = 0.331$ respectively). The percentage staining in the SACa groups was significantly greater than the SACq group ($p = 0.002$) (figure 3.12).

When the distribution of keratin 13 was viewed across the whole epithelial layer, the pattern of the disease groups appear to have shifted towards

the intermediate and superficial layers compared to the pattern of distribution seen in the control epithelium (figure 3.21, graph A).

When this data was transposed into the three cell layers of the epithelium, the percentage breakdown for each layer showed (figure 3.21, graph B),

Control basal percentage staining was 19.55%, intermediate staining was 38.77% and superficial staining was 41.68%.

SACq basal staining was 28.94%, intermediate staining was 46.74% and superficial staining was 24.32%.

SACa basal staining was 8.25%, intermediate staining was 69.37% and superficial staining was 22.38%.

3.5.4.8 Keratin 14

Control epithelium percentage staining of keratin 14 was 15.26% (± 3.75), SACq was 2.33% (± 0.58) and SACa was 10.43% (± 2.18). The percentage staining in the control was significantly greater, statistically, against the percentage staining of the SACq group, but not the SACa group ($p = 0.006$ and $p = 0.702$ respectively). The percentage staining in the SACa groups was significantly greater than the SACq group ($p = 0.006$) (figure 3.12).

When the distribution of keratin 14 was viewed across the whole epithelial layer, the pattern of the disease groups was different to the pattern of the control staining. Greater staining was seen in the upper intermediate and superficial cell layers compared to control (figure 3.22, graph A).

When this data was transposed into the three cell layers of the epithelium, the percentage breakdown for each layer showed (figure 3.21, graph B),

Control basal percentage staining was 21.36%, intermediate staining was 36.30% and superficial staining was 42.34%.

SACq basal staining was 32.49%, intermediate staining was 32.60% and superficial staining was 34.91%.

SACa basal staining was 11.96%, intermediate staining was 58.53% and superficial staining was 29.51%.

3.5.4.9 Keratin 18

Control epithelium percentage staining of keratin 14 was 17.65% (± 4.30), SACq was 3.81% (± 1.38) and SACa was 11.67% (± 2.21). The percentage staining in the control was significantly greater, statistically, against the percentage staining of the SACq group, but not the SACa group ($p = 0.001$ and $p = 0.2584$ respectively). The percentage staining in the SACa groups was significantly greater than the SACq group ($p = 0.0115$) (figure 3.12).

When the distribution of keratin 18 was viewed across the whole epithelial layer, the pattern of the SACq disease groups was different to the pattern of the control and SACa staining. The SACq displayed a two peaked pattern with keratin 18 loss in the lower intermediate layer (figure 3.23, graph A).

When this data was transposed into the three cell layers of the epithelium, the percentage breakdown for each layer showed (figure 3.21, graph B),

Control basal percentage staining was 18.02%, intermediate staining was 55.40% and superficial staining was 26.58%.

SACq basal staining was 43.83%, intermediate staining was 38.26% and superficial staining was 17.91%.

SACa basal staining was 12.50%, intermediate staining was 65.23% and superficial staining was 22.27%.

3.5.4.10 Pan keratin

Control epithelium percentage staining of pan keratin was 55.47% (± 3.50), SACq was 27.77% (± 3.57) and SACa was 49.55% (± 3.42). The percentage staining in the control was significantly greater, statistically, against the percentage staining of the SACq group, but not the SACa group ($p = 0.001$ and $p = 0.1331$ respectively). The percentage staining in the SACa groups was significantly greater than the SACq group ($p = 0.0014$) (figure 3.12).

When the distribution of pan keratin was viewed across the whole epithelial layer, the patterns of staining in the three subject groups showed no difference (figure 3.24, graph A).

When this data was transposed into the three cell layers of the epithelium, the percentage breakdown for each layer showed (figure 3.24, graph B),

Control basal percentage staining was 14.21%, intermediate staining was 55.52% and superficial staining was 30.27%.

SACq basal staining was 20.33%, intermediate staining was 49.70% and superficial staining was 29.97%.

SACa basal staining was 10.20%, intermediate staining was 67.17% and superficial staining was 22.63%.

## 3.6 Discussion

The chapter hypothesis states:

***The human conjunctival epithelium is structurally altered in patients with seasonal allergic conjunctivitis (SAC).***

In order to answer this, aspects of the structural component of the conjunctival epithelium of control and subjects with seasonal allergic conjunctivitis were analysed and compared.

**Ultra structure**

Ultrastructure analysis of the conjunctival epithelium were carried out using scanning and transmission electron microscopy, scanning electron microscopy allows precise analysis of epithelial cells and their definitions (Renard *et al* 1980, Yamano *et al* 1979). Pfister (1974) described the surface features of the rabbit conjunctiva as showing 'the monotonous appearance of fine, finger-like cytoplasmic protrusions (microvilli) covering the polygonal cells'. This is in agreement with Weyrauch (1983 (b)), who identified 'microvilli projecting over the uppermost epithelial cells only occasionally containing a filamentous internal structure' on the epithelial cells of domestic ruminants. Nichols (*et al* 1983), described the surface features of guinea pig conjunctival surfaces, identifying regularly, closely spaced surface projection (microvilli) covered epithelial cells. These microvilli had bundles of filaments, which extended down into the superficial cytoplasm. Goller (1993) describes polygonal conjunctiva covered with microvilli. Figures 3.1a, b, c and d demonstrate that the

human conjunctival epithelium has close neighbouring polygonal-shaped cells, that under high magnification are covered in a dense layer of branching microvilli. The epithelial layer has a marked morphology compared to the underlying connective tissue of the epi/sclera, which shows a fibrous appearance, with a more diverse cell population present (figure 3.2 a and b). Figures 3.3a and b show a transmission view of the apical membrane and the microvilli, no bundles of filaments can be identified in the micrographs, but in the cited literature above the presence of bundles of filament was found to be occasional therefore greater investigations would be required to demonstrate their absence / presence in the samples used in this study. An important structural function of the microvilli on conjunctival epithelial cells is to provide a support frame for the glycocalyx / tear film. As touched on in the introduction the glycocalyx is an important barrier between the eye and the external environment. It is postulated that the glycocalyx can be identified in figure 3.3 micrograph D (highlighted with the arrows). Weyrauch (1983 (b)), describes the apical closure of the epithelium with zonulae occludentes (tight junctions) followed by desmosomes, with rarely observed zonulae adherentes (intermediate junctions). Figure 3.4 demonstrates the human conjunctival epithelium has complete junctional complexes, throughout the superficial cell layer, with tight followed by intermediate finishing with desmosome spot junctions. Figures 3.5a and b demonstrate that the epithelial layer is littered with desmosome junctions. The epithelial layer is anchored to the basement membrane via hemidesmosomes as identified in figure 3.6 micrograph A.

Analysis of the ultrastructure of the human conjunctival epithelium demonstrates that it constitutes an epithelial layer with the structural component to form a physical barrier against the environment, and also provides the support for the glycocalyx and tear film fitting with the literature on epithelial layers.

**Embedded sections of tissue / Confocal sections**

Classically the epithelial layer of the bulbar human conjunctival has been classified as a stratified columnar epithelium, with squamous epithelium seen in different regions. This has also been shown in animal tissue (Goller and Weyrauch 1993, Nichols *et al* 1983, Pfister 1974). Through the use of confocal microscopy, and staining, using the epithelial specific epithelial glycoprotein

(HEA125, Simon *et al* 1990), the 3 layer construction of the conjunctival epithelium was demonstrated (figure 3.8). Morphologically the control sections fitted this description displaying a stratified columnar epithelium, but subjects from the disease group resembled a more stratified cubiodal epithelium. This change in appearance could be a result of the increased epithelial activity that the disease groups undergo during times of repeated inflammatory reactions.

**Damage**

At the general morphological level, there were no regions of the epithelial damage / remodeling in GMA embedded sections (figure 3.9). However, Dogru (1998) showed that epithelial damage could be identified in subjects with AKC using impression cytology. These differences in result could be a consequence of the chronic nature of AKC and the more destructive method of impression cytology.

**Thickness**

At the general morphological level, increased thickness was observed in the SACa subject group. Adbel-Khalek (1978) showed that the structure of the conjunctival, patients older than 79 years old showed irregularities in thickness, which consisted of mild superficial stratification, but also seen in samples from younger patients. This finding was also seen in the conjunctival epithelium of canine species (Goller and Weyrauch 1993). The three groups used had average ages of 68.77 for control, 41.75 for SACq and 54 for SACa, well under the age cited above.

**Epithelial density**

At the general morphological level the increase in layer height observed in the SACa group was attributed to hypertrophism (increased cell cross sectional area and therefore theoretically cell volume) and not hyperplasia in the cells.

**Adhesion proteins**

During the development of inflammation, adhesion molecules have been shown to play an important role in localising the inflammatory response (Carreno *et al* 1995, Canonica *et al* 1997).

Morphological techniques were used for analysis, rather than stereological methods, this was due to the size and the extremely limited supply of the biopsy material. If stereological methods had been applied, insufficient serial sections could have been cut from each biopsy to cover the desired number of protein targets of interest.

In the statistical testing of immunohistochemical stained of biopsy material within this chapter. Paired parametric testing were applied and with the number of tests carried out, the author recognises that significant values could be calculated purely in coincidence with the numerous tests be carried out. With this said, using another 'group' style of test would be inappropriate as only ever two values were statistically tested at a time.

The percentage expression of the adhesion proteins CD44, E-Cadherin and desmoplakin 1-2 all showed a general trend of low expression in SACq subjects, this level increased during episodes of inflammation, as seen in the SACa subjects, but this increase was still lower than the expression level measured in the control subjects.

**CD44**

CD44 is an ubiquitous multi-structural, multi-functional cell surface adhesion protein. It is involved in cell-cell and cell-matrix interactions, also in leukocyte trafficking, and cellular signaling pathways. Only slight changes in the expression of CD44 between the control and disease groups was seen with, SACq was basally higher, SACa was intermediately higher and both lower apically. CD44s' proposed function within the context of this project is as an extra-cellular matrix adhesion molecule. The re-distribution of this cell-cell / cell-matrix adhesion molecule could be due to the re-organisation of the cell layer as a direct result of injury from the inflammation reaction.

**E-Cadherin**

The SACa group had lower basal and greater intermediate expression than control.

E-Cadherin has been suggested as having a role in the organisation of the epithelial layer and is found throughout the epithelial layer (Cyr *et al* 1995). In the conjunctival epithelium, E-Cadherin is present in all layers, which agrees with the percentage expression data (Scott *el at* 1997), but this article does not highlight any changes in E-Cadherin distribution intra-layerly. Horiguchi (1994), found a similar result with the lack of E-Cadherin on the basal surface of the basal cells when epithelial cells were challenged with physiological conditions. Kobayashi (1998), reported decreased E-Cadherin expression as a consequence of eosinophil infiltration. During inflammation, it is the basal cells that would be the first contact of any infiltrating immune cells therefore this could lead to a loss of E-Cadherin from these cells and the lower intermediate layer of cells, with the effects reduced through the upper layers. Jang (2002), reported that in the nasal epithelium E-Cadherin expression was up-regulated with the increased severity of epithelial re-modeling; although in the conjunctiva no active areas of re-modeling could be seen morphologically, the increase in expression in the superficial layer could be attributed to these cells being stressed resulting in the change in morphology.

**Dp1-2**

The SACq showed greater basal and lower apical than control, whereas the SACa showed greater intermediate and lower apical expression than control. The re-distribution of the desmosome proteins could be due to the re-organisation of the epithelial layer post inflammation.

**Keratins**

The percentage expression of the keratin proteins all showed a general trend of low expression in SACq subjects, this level increased during episodes of inflammation, as seen in the SACa subjects, but this increase was still lower than the expression level measured in the control subjects.

No significant changes in the expression of K 5/6, 7 or Pan were seen in the subject groups.

**K8**

The SACq showed greater basal expression and lower intermediate expression than the SACa or control groups.

**K13**

The SACq showed higher basal and lower superficial expression, whereas the SACa group showed lower basal, higher intermediate and lower superficial expression than control.

**K14**

The SACq showed higher basal expression, whereas the SACa showed lower basal and higher intermediate expression.

**K18**

The SACq showed greater basal and lower intermediate expression, whereas SACa showed greater intermediate expression than control.

Classically keratin 14 has been termed as a marker of basal epithelial cells (Porter and Lane 2003), which can be seen in its distribution within the control group. It has received a lot of attention through its involvement in epidermolysis bullosa simplex, where its mutation causes blistering of the skin, where the basal epithelial cells display increased fragility to mechanical stress (Porter and Lane 2003). It has also been described in pterygia where abnormal expression causes structural changes in the epithelium leading to abnormal tear formation (Zhang *et al* 2000). Knockout studies with keratin 14 have shown that expressional loss can lead to rupture of stratified epithelial tissues (Galou *et al* 1997). Freedberg (2001) postulated that the expression of K14 is indicative of a healthy epithelium that has returned from an activated state, which could be induced via pro / inflammatory cytokines during inflammatory reactions.

Keratin 18 is expressed with 8 and has been described in simple epithelium tissues and in columnar cell types (Broers *et al* 1989, Ogawa *et al* 2001, Chu and Weiss 2002, Ku *et al* 2002, Porter *et al* 2003). Ogawa reported that keratin 18 was localised throughout the layer, and postulated that it is

involved mainly in cell-cell / cell-matrix contacts. Marceau (2001), cited keratin 18 as a candidate for providing resistance to mechanical or toxic stress.

Studies of keratin filament suspensions have shown that intermediate filament display strong mechanical support to the epithelial sheet, thus retaining cell shape even under repeated episodes of stress in a $Ca^{2+}$ dependent fashion (Ma *et al* 1999, Goebeler *et al* 1995).

The loss of expression of key adhesion proteins and the re-distribution of keratin 14 and 18 could be the markers of a structurally weakened epithelium attempting to rescue its integrity and maintain its organisation due to cycles appropriate inflammatory mediated damage. Toivola (2000), postulated that keratin filament re-organisation is a normal physiological response to direct injury, and an intact filament network is not essential for cellular protection. The gene expression of keratins in response to frictional or immune-mediated mechanisms has been shown to be altered which would have a direct result on their distribution within the epithelia layer (Bloor *et al* 2000). This raises the possibility of other structural elements, or the redistribution of structural elements, compensating for the disruption in the epithelial layer.

## 3.7 Conclusion

*The human conjunctival epithelium is structurally altered in patients with seasonal allergic conjunctivitis (SAC).*

So does the hypothesis hold true?

In summary the conjunctival epithelium from seasonal allergic patients shows to no gross morphological differences to the epithelium from the control group. Immunohistochemical analysis of the epithelial cell layers shows a phenotypic shift, of reduced expression of adhesion proteins and reduced, expression and re-distribution of keratin proteins, predominantly in the SACq group. This may be the result of cycles of inflammatory mediators and mechanical stress affecting the ability of the epithelium to stabilize its environment. With the epithelial layer in a state of flux this weakens the conjunctival, which further extenuates the pathogenesis of seasonal allergic

conjunctivitis, and reduces its ability to form a fully polarised and resistance physical barrier to aeroallergens and other stimuli.

# Figure 3.1a Surface features of the apical membrane


Micrograph A.

This scanning electron micrograph of a conjunctival biopsy which has under-gone fixation immediately after being surgical removed. Once the biopsy was taken, the epithelial layer curled around the connective tissue, fully encasing it.

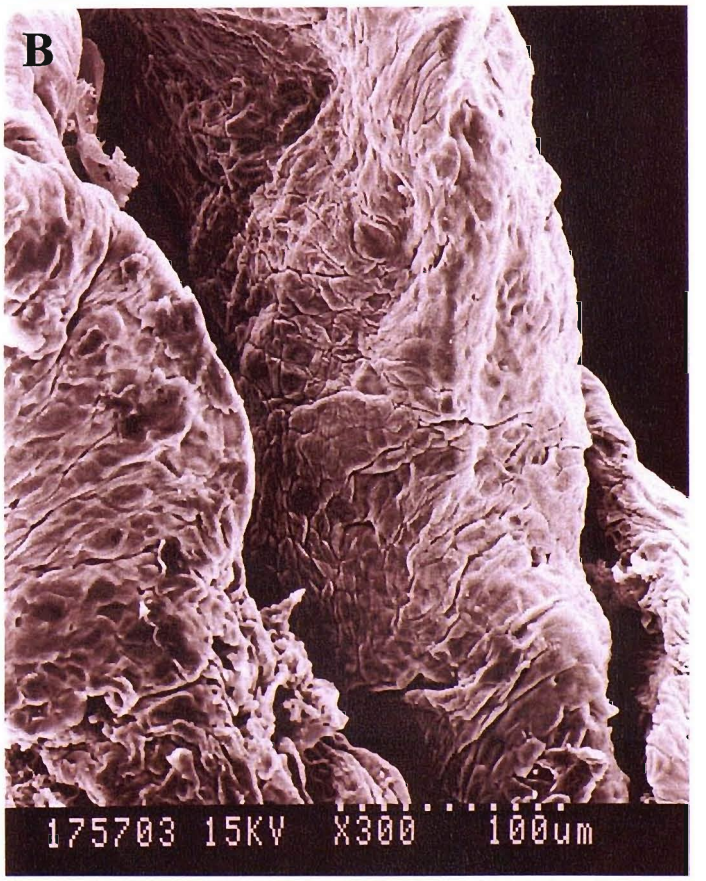


Micrograph B.

This scanning electron micrograph of the biopsy from the previous micrograph, again showing the curling nature of the biopsy.

# Figure 3.1b Surface features of the apical membrane

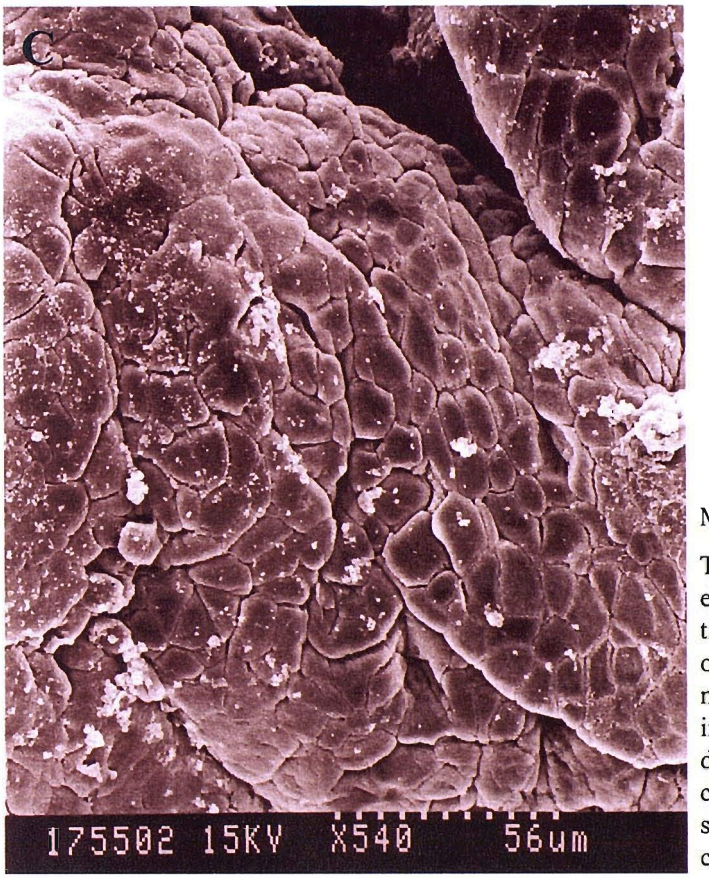


Micrograph C.

This higher power scanning electron micrograph (540 times magnification) in order to identify the apical membranes of the individual epithelial cells, displaying their characteristic polygonal shape with tight cell-cell contacts.


Micrograph D.

This micrograph shows a region of the biopsy at 960 times magnification, clearly showing the shape of the cells.

# Figure 3.1c Surface features of the apical membrane


Micrograph E.

This micrograph shows the highlighted region within micrograph D (white dotted lines). In this micrograph it can be seen that the neighbouring cells are not strictly connected at the extremity of the apical membrane, but in some cases valleys in between the cells can be identified. Observing the edges of the cells (highlighted with white arrows), the surface of the cells appears to be a rough rather than a smooth surface.


Micrograph F.

This micrograph shows that viewed at 5,000 times magnification the epithelial cells have a covering layer of microvili-like processes on the apical membrane surface.

# Figure 3.1d Surface features of the apical membrane

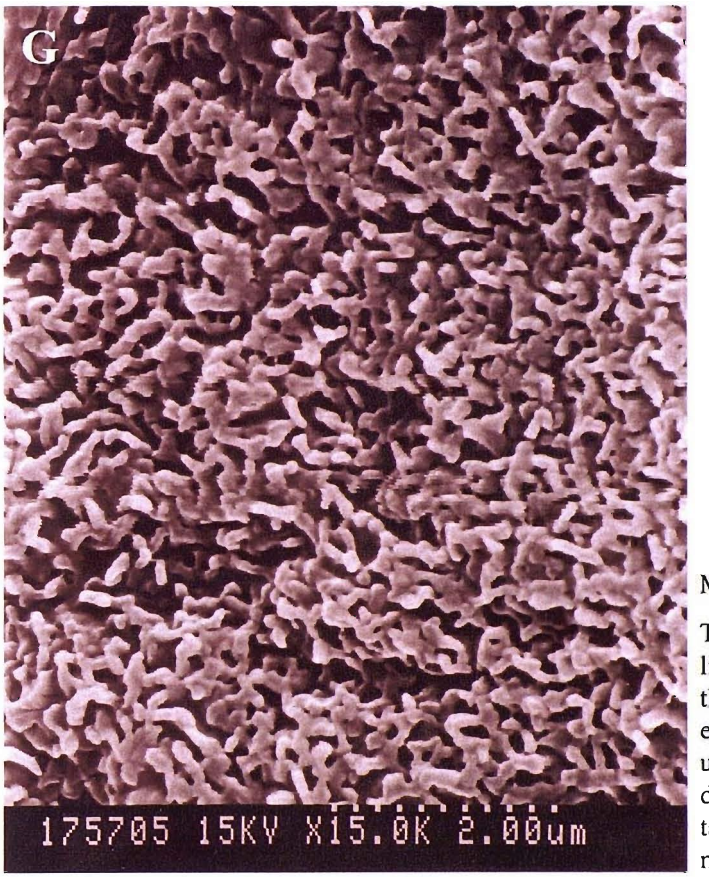


Micrograph G.

This shows the microvili-like processes covering of the apical surface of the epithelial cells, in an uniform but dis-ordered distribution. Micrograph taken at 15,000 times magnification.

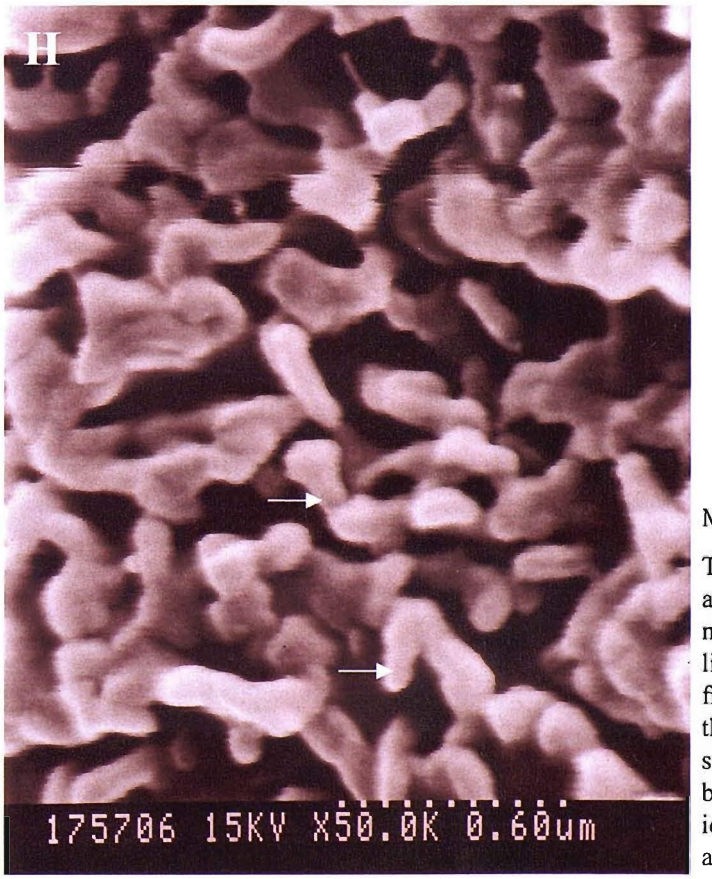


Micrograph H.

This micrograph shows that at 50,000 times magnification the microvili-like processes extending from the apical surface of the epithelial cell can be seen in greater detail, with branching of these processes identified by the white arrows.

# Figure 3.2a Epithelial layer / connective tissue border

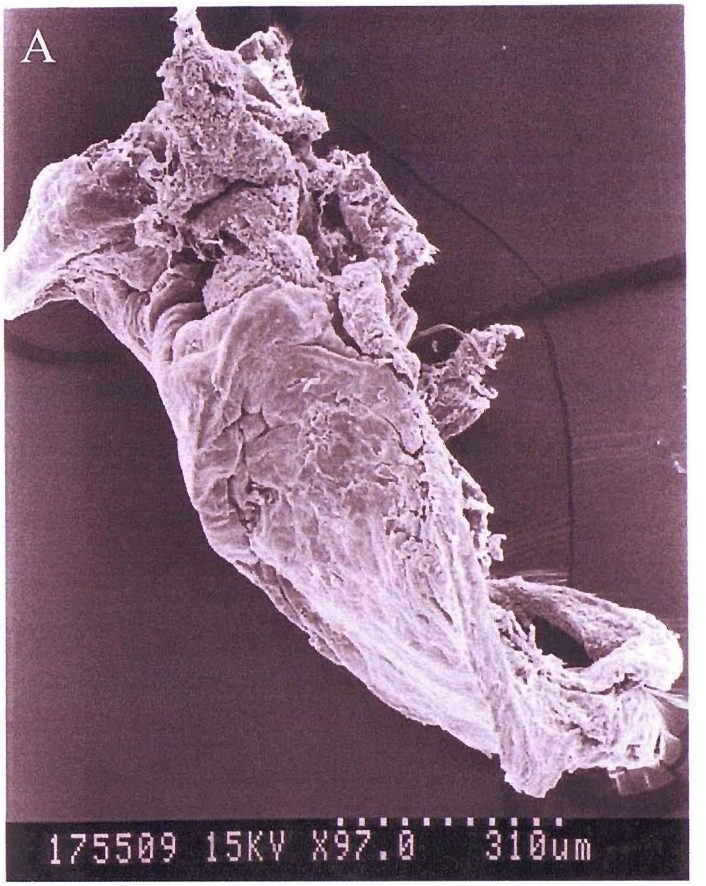


Micrograph A.
This scanning electron micrograph shows the entire conjunctival biopsy (97 times magnification). The curling of the biopsy can clearly be seen, with the epithelial layer outermost. This biopsy was cut into two pieces post fixation to reveal the underlying connective tissue.

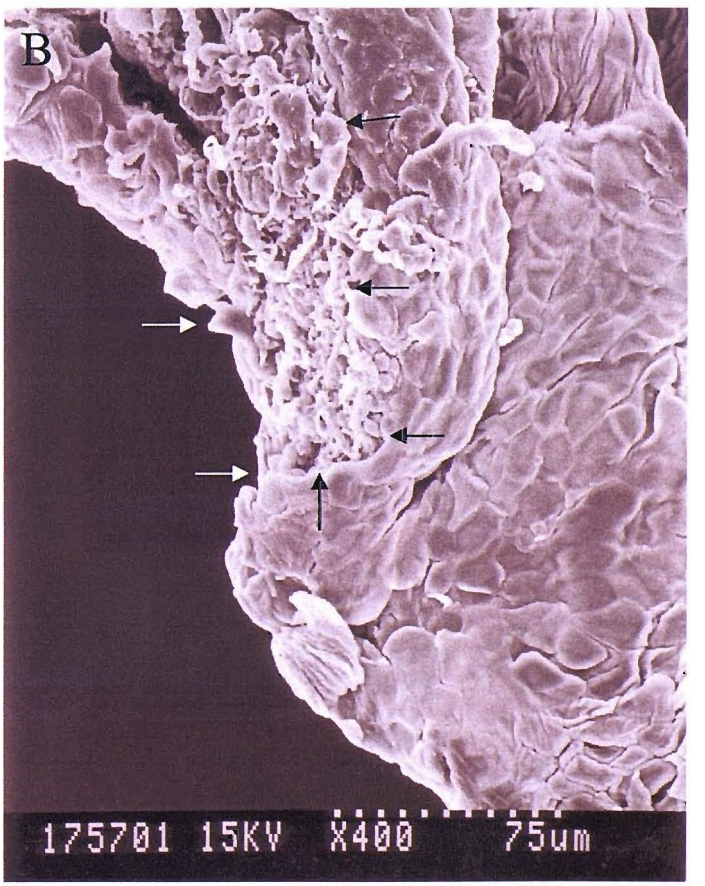


Micrograph B.
This micrograph shows a higher power scan of the region of the epithelium that was cut (highlighted with the black and white arrows).

# Figure 3.2b Epithelial layer / connective tissue border


Micrograph C.
This scanning electron micrograph shows the highlighted region from micrograph B in figure 3.4a (1690 times magnification). Within the lower quarter of the micrograph, the edge of the epithelial cell layer can be seen (highlighted with the white and black arrows). The epithelial cells can be distinguished by their hexagonal shape and their "furry" appearance which are the microvili-like processes seen in figure 3.3c. The remainder of the micrograph shows the underlying connective tissue and some of its components.

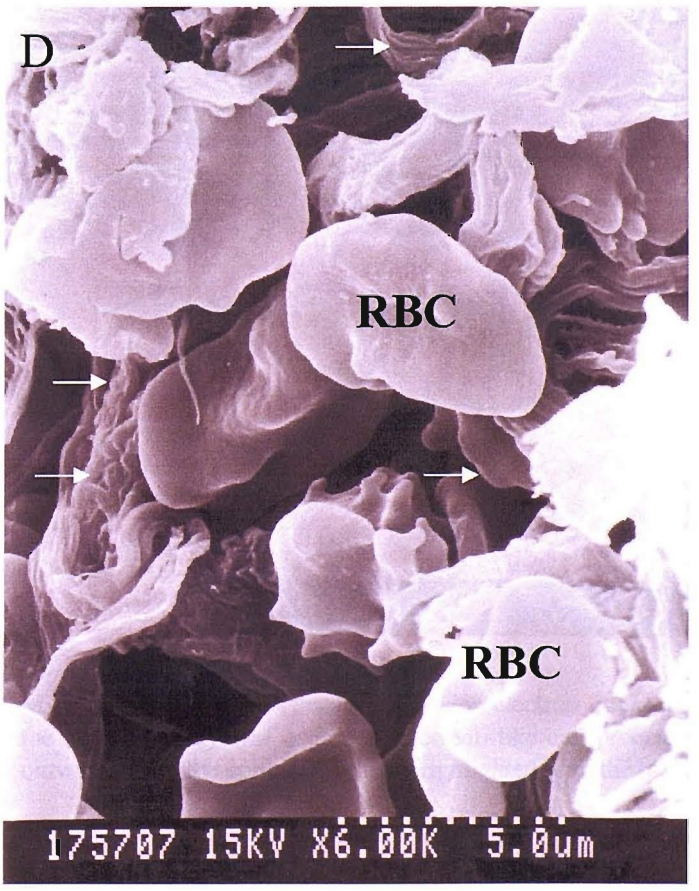


Micrograph D.
This micrograph shows an area of the connective tissue (6000 times magnification). Mostly within the connective tissue the collagenous fibres (highlighted by the white arrows) would be found with the occasional circulating immune cell. In the micrograph shown, red blood cells (highlighted with RBC) can be identified, possibly seen as a result of the surgical / mechanical damage suffered when the biopsy was removed. Other cell types could also be present although not identified.

# 3.3a Apical membrane

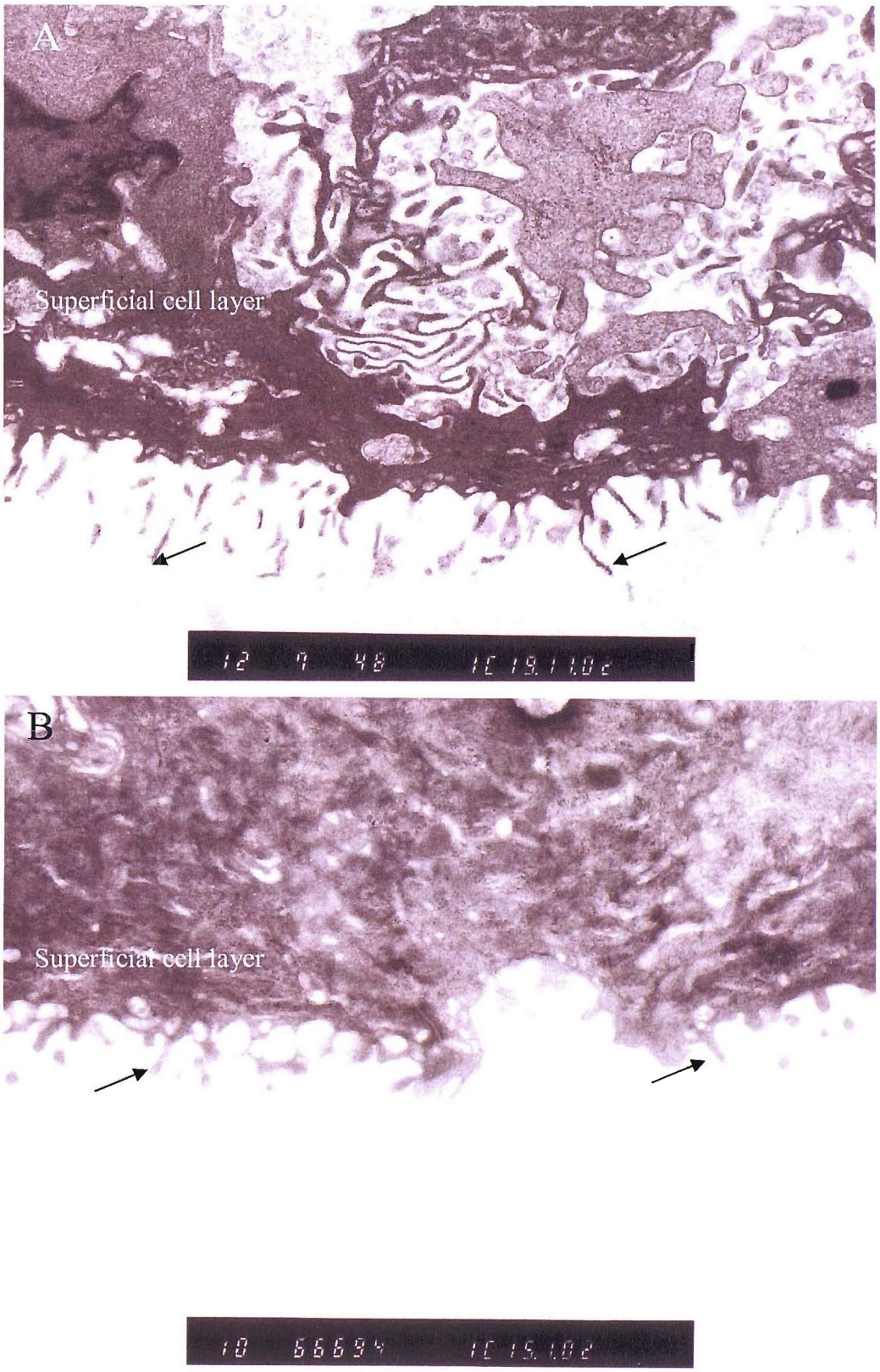


Micrographs A and B. These transmission electron micrograph of the apical membrane of the superficial layer of cells, the microvili-like cell processes can be identified extending outwards from the epithelial tissue (Highlighted with the black arrows).

# 3.3b Apical membrane

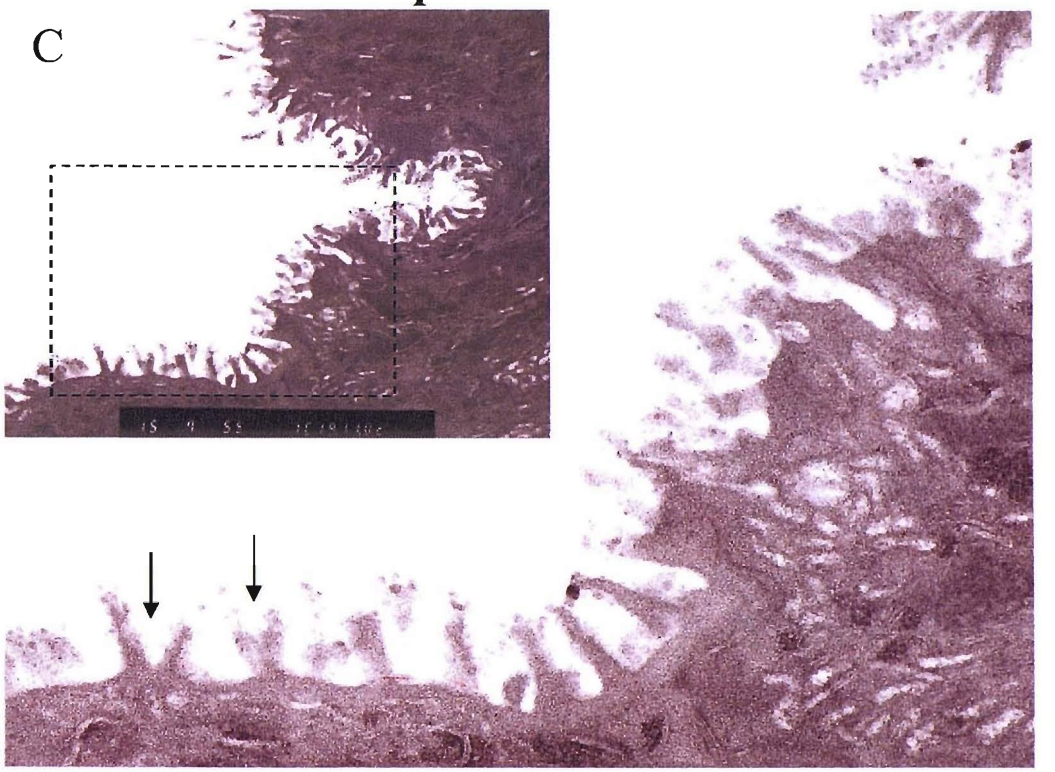


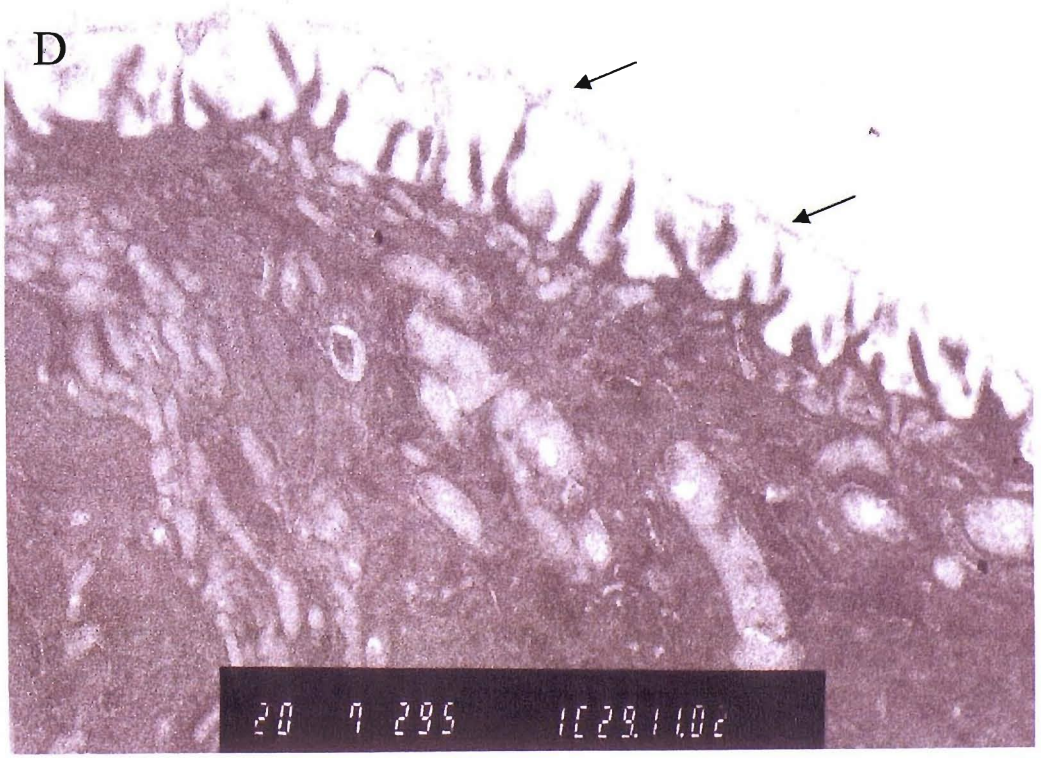


Micrograph C. This micrograph shows the processes at higher magnification and their relative distribution along the apical membrane. Also process branching can be identified (Highlighted with the black arrows).

Micro graph D - shows the processes supporting an electron dense line, that is proposed to be the glycocalyx / tear film layer of the eye. Functioning both, as another physical barrier to the eye and maintaining the wet tissue surface of the orbit (highlighted by the black arrows).

# 3.3c Apical membrane

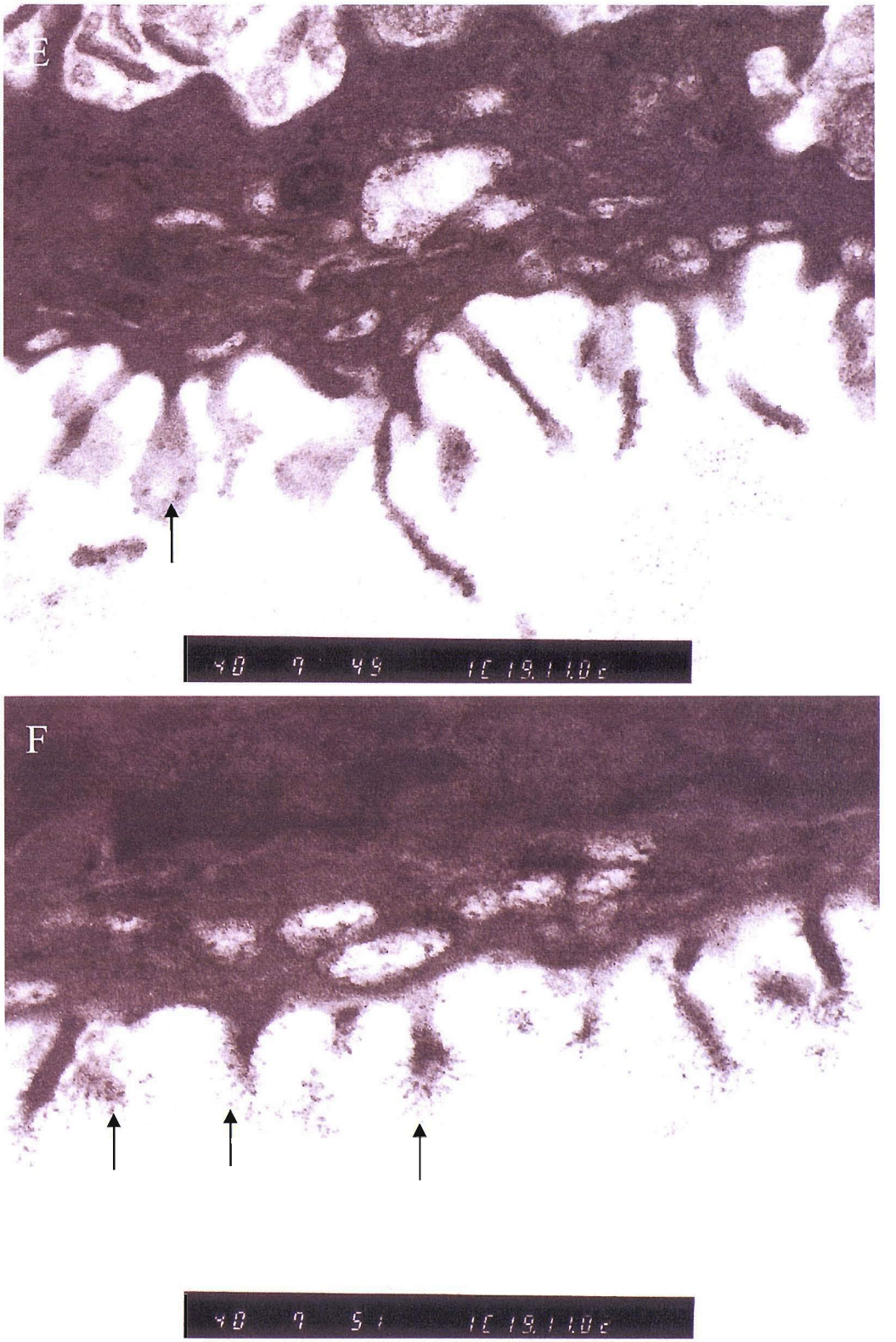


Micrographs E and F. These micrographs show the processes at high magnification, in order to establish whether actin filaments can be identified within the central core. Unfortunately none were seen, but this alone does not mean that the processes are not microvili. These sections were not specifically immuno-stained, so the electron dense spots seen on the micrographs (highlighted with the black arrows), could be residues of the lead stain or uranyl acetate on the glycocalyx from the processing stages.

# Figure 3.4 Junctional complex

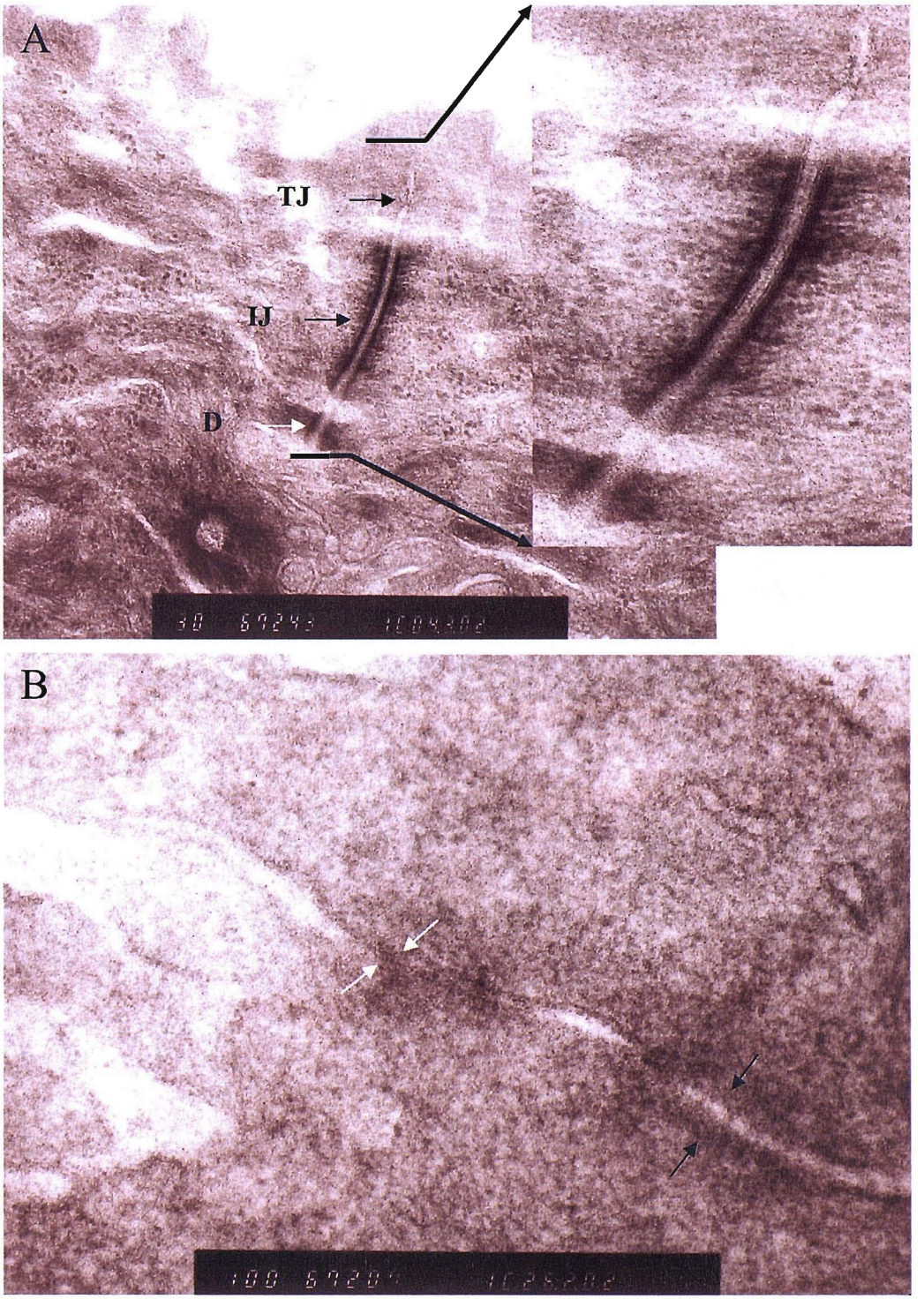


Micrograph A. This transmission electron micrograph shows the junctional complex that is found in between the apical layer of conjunctival epithelial cells. The three junctions that constituent the junctional complex, running from an apical to basal direction, are the tight junction (labelled TJ), the intermediate junction (IJ) and the desmosome spot junction (D). The junctions can be clearly identified in the enlarged section of the microplate.

Micrograph B. This micrograph shows the tight junction (highlighted with the white arrows), in more detail. Running down the cell membrane the start of the intermediate junction can also be identified (highlighted with the black arrows).

# 3.5a Desmosome junctions

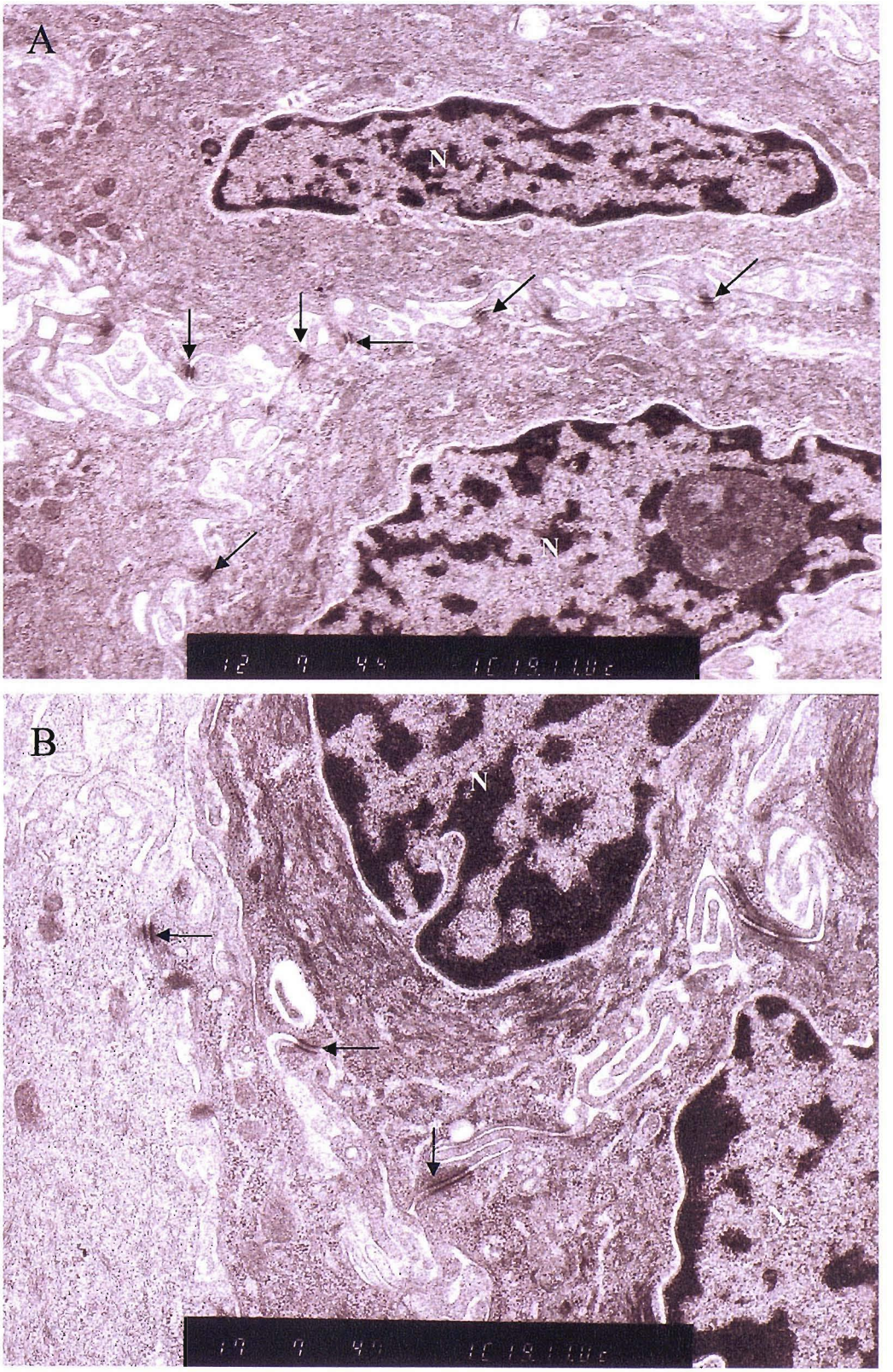


Micrograph A. This micrograph shows the desmosome junctions located between two adjacent epithelial cells (highlighted with the black arrows). Each of the cell's nucleus are highlighted with the letter N. Demonstrating their extensive distribution throughout the epithelial cell layers.

Micrograph B. This micrograph shows again the extensive distribution of desmosomes along the plasma membranes (highlighted with the black arrows).

# 3.5b Desmosome junctions

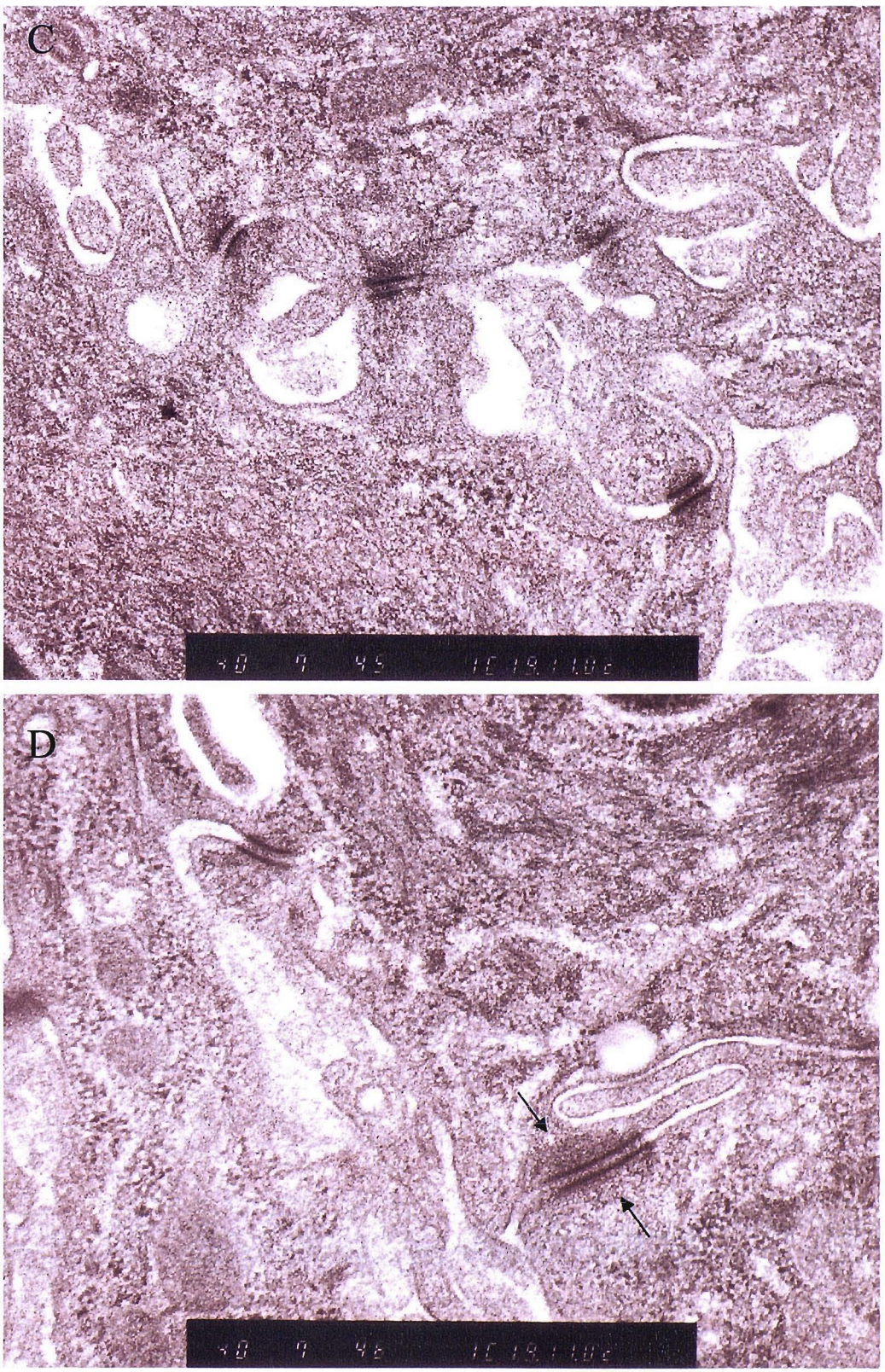


Micrographs C and D. These micrographs show the desmosomes spot junction at a higher magnification, so that the architecture of the desmosome can be observed. The classical construction of the structure can be seen with the electron dense plaques of the intracellular domain where the linker proteins bond with the intermediate filaments of the cytotskeleton (highlighted with the black arrows). The extracellular domains of the junctions can also be identified as they are slightly more electron dense that the surrounding extracellular space.

# 3.6 Basement membrane morphology

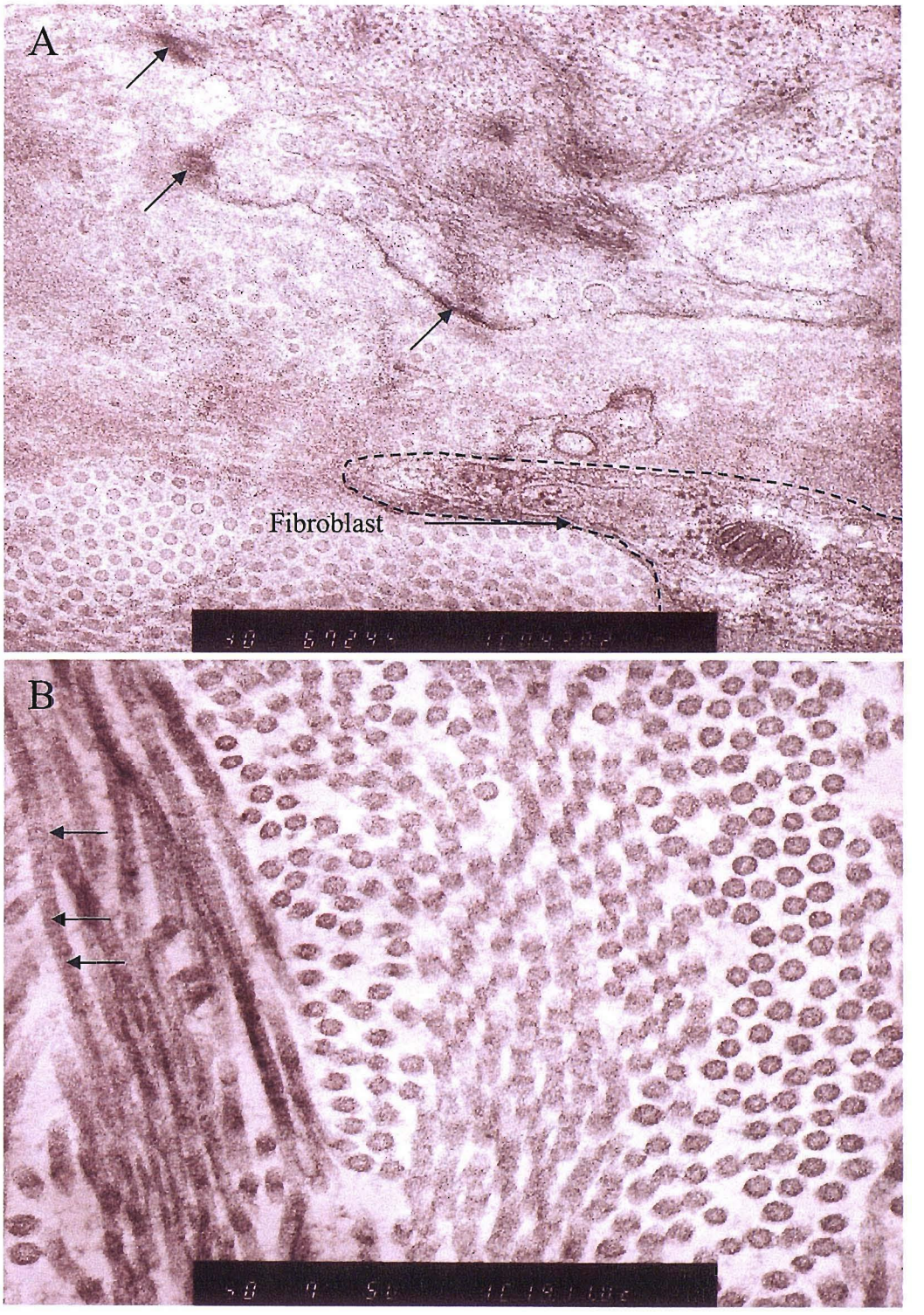


Micrograph A. This transmission electron micrograph shows the basement membrane of the epithelial cell layer and the start of the underlying connective tissue layer. Identified at the epithelial cell/connective border are hemi-desmosomes (highlighted with the black arrows), these ensure that the epithelial layer is anchored to the connective tissue layer. Within the bottom right hand corner a fibroblast can be identified (highlighted with the dotted line), possibly laying down new collagen fibres.

Micrograph B. This micrograph shows the collagen fibres at higher magnification and the orientation that the fibres are constructed / laid within the connective tissue layer. The collagen banding is highlighted with the black arrows.

# Figure 3.7 Epithelial morphology

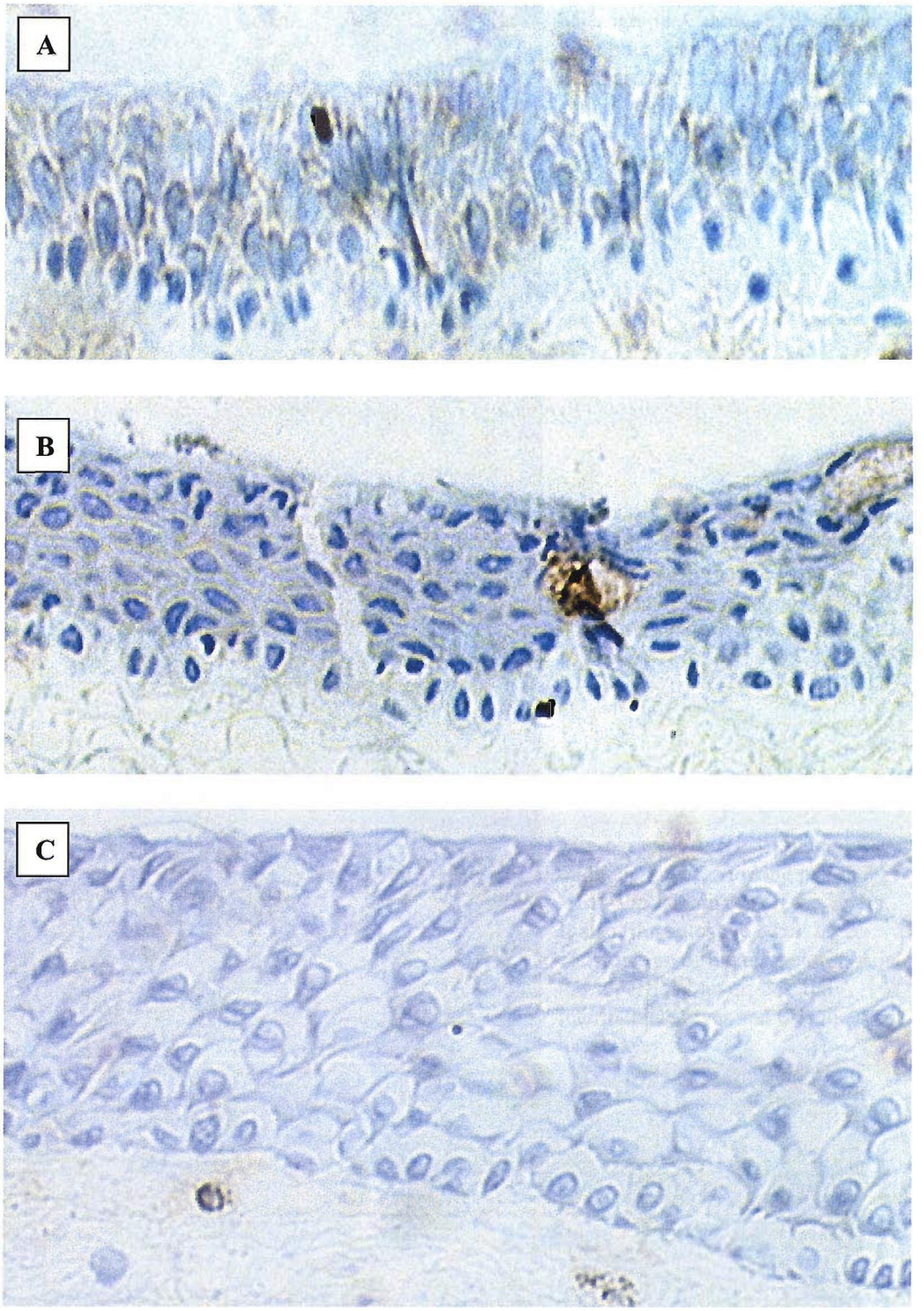


A shows the control epithelium,

B is the SACq epithelium,

C shows the SACa epithelium.

The control epithelium resembles a non-ciliated stratified columnar epithelium, B and C epitheliums resemble a non-ciliated stratified cubiodal layer.

All micrographs are x20 magnification.

# Figure 3.8 Confocal imagery of the human conjunctival epithelium

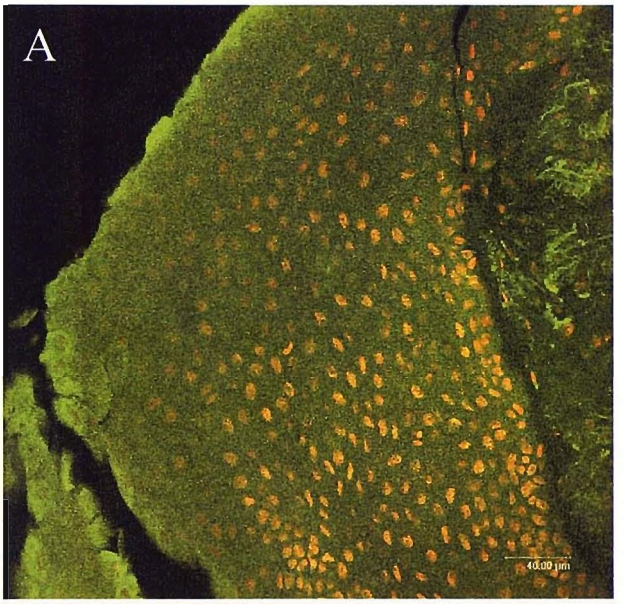


Micrograph A shows a low power x-y optical plane of the epithelium demonstrating positive keratin 18 staining across the entire layer.

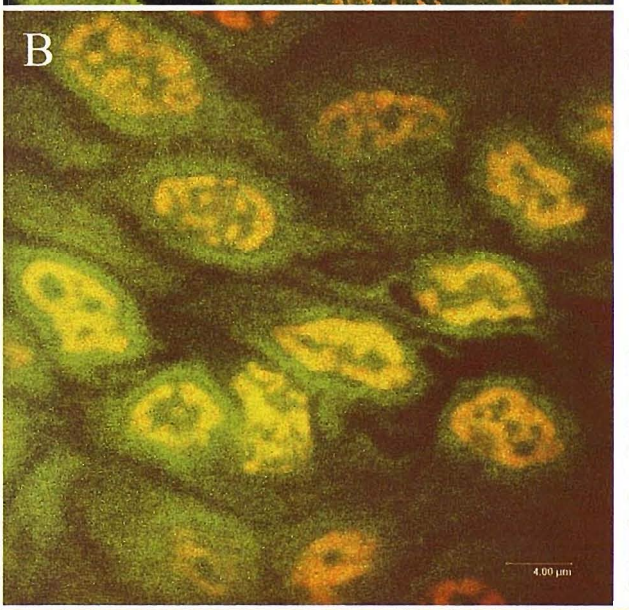


Micrograph B is an optical x-y plane of the epithelial layer taken at a higher magnification, demonstrating positive keratin 18 staining.

Micrograph C is a z-y plane of the epithelial layer, showing positive HEA-125 staining in all the layers. It also illustrates the 3 cell layer construction of the epithelium. A is the superficial layer, B is the intermediate layer and C is the basal layer.

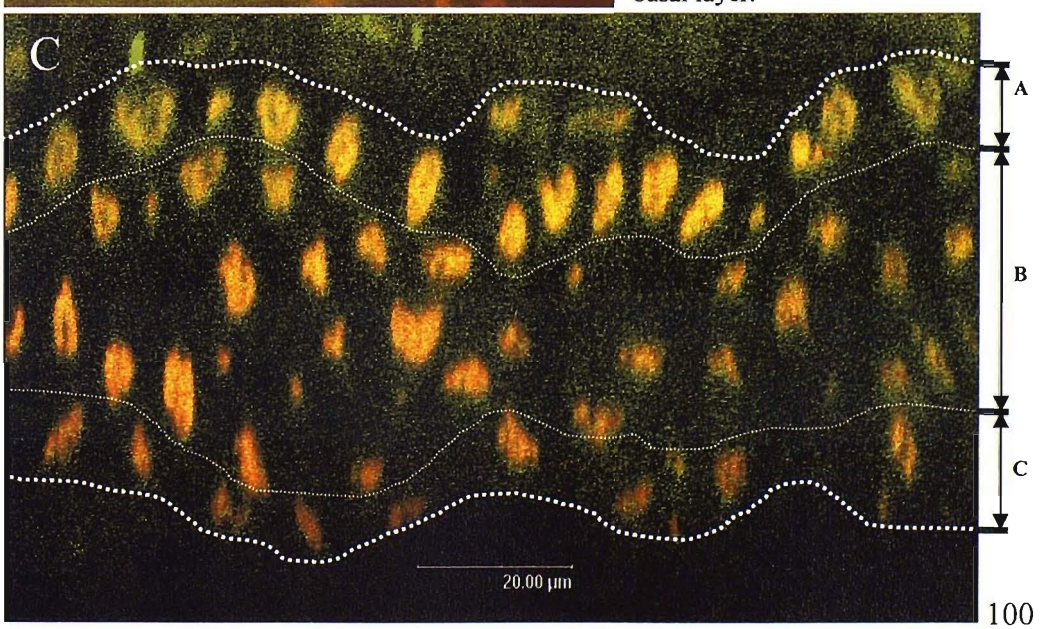

# Figure 3.9 Regions of undamaged epithelium

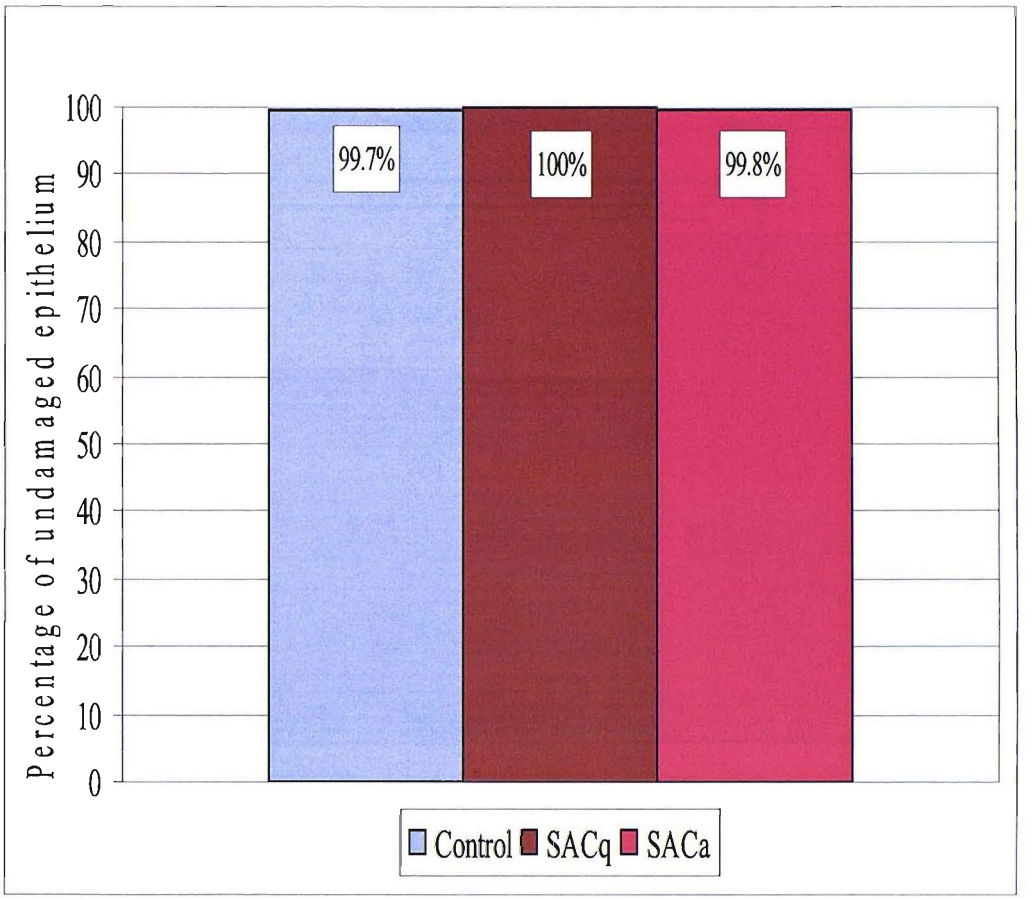


Damage was assessed by identifying regions of de-epithelialisation along the epithelial layer.

When assessed none of the three subject groups showed any significant measurable areas of damage. Regions that were deemed to be damaged, were the areas were physical damage occurred during the surgical removal of the biopsy material.

n = Control 28, SACa 9, SACq 8.

# Figure 3.10 Epithelial layer thickness

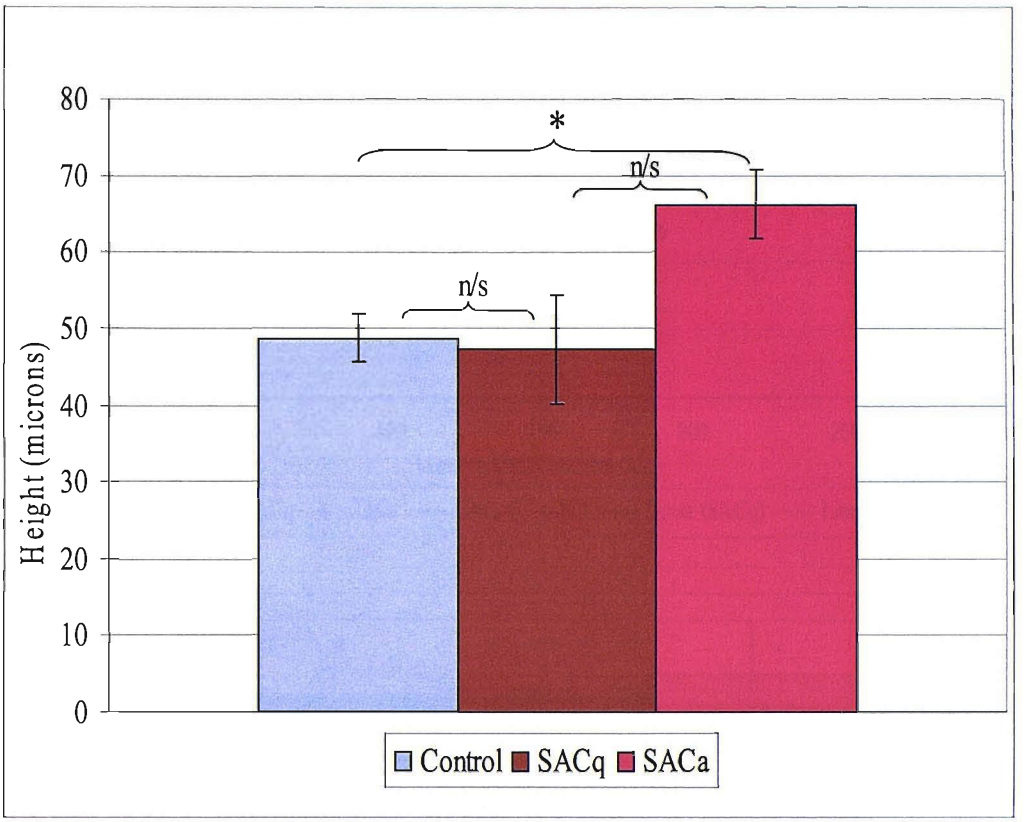


Epithelial layer thickness was calculated according to the method described in section 2.2.5.1, briefly lines were drawn perpendicular to the epithelial layer at regular intervals, the length of these lines were measured and the average taken for each section was calculated.

This graph shows that a significant increase in epithelial thickness was measured in the SACa subject group compared to the control (* = $p<0.05$), although no significant difference was measured when the SACa subject group was compared to the SACq subject group (p = n/s).

n = control 28, SACa 9, SACq 8.

# Figure 3.11 Epithelial layer cell density

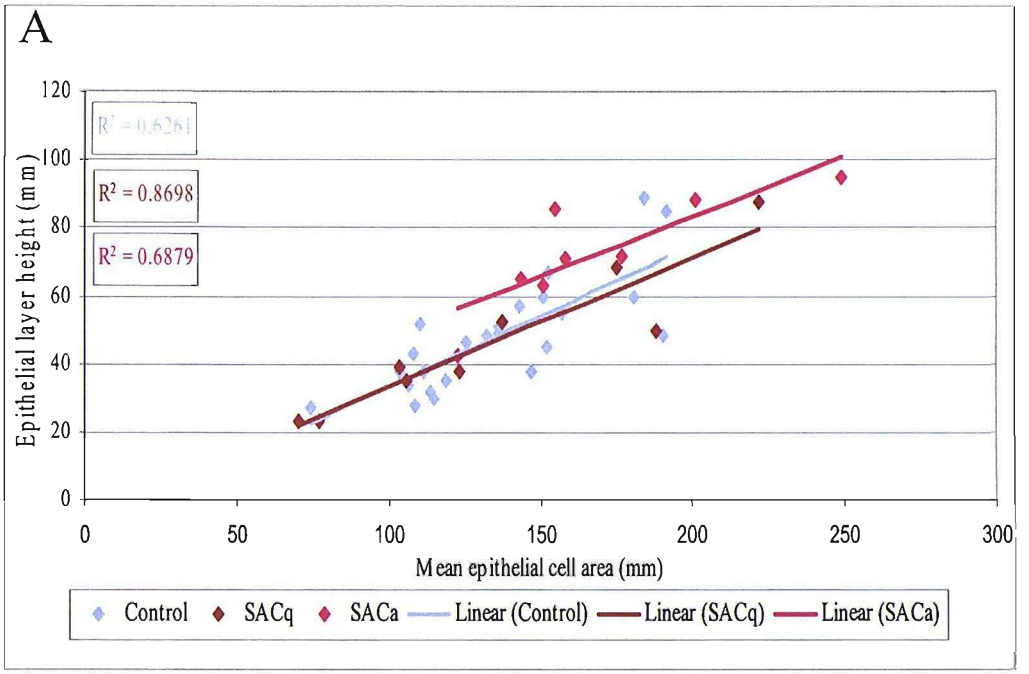


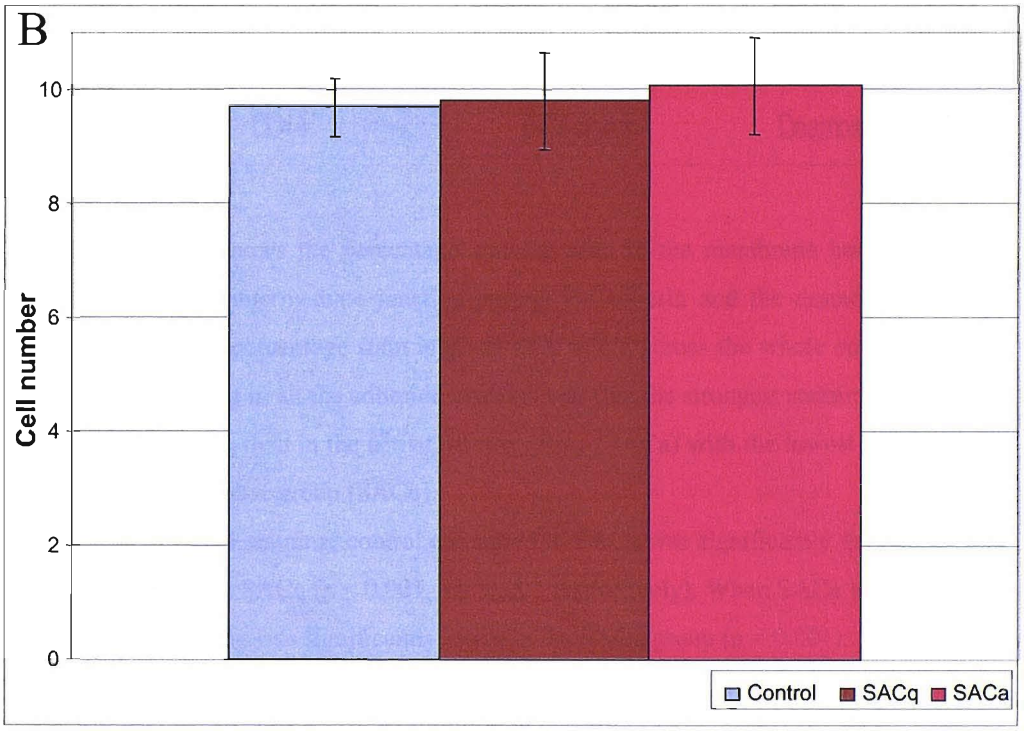


Graph A shows that when the mean epithelial cell area is plotted against the epithelial layer height in each of the groups, they display a similar relationship. As the epithelial layer height increases the average area of the individual epithelial cells increase.

Graph B shows the resulting plot of measuring the cell number per unit length of basement membrane, showing no difference between the subject groups.

Therefore suggesting that the increase in epithelial layer height can be attributed to a hypertrophic cell morphology not a hyperplasic cellular event.

n = Control 28, SACa 9, SACq 8.

# Figure 3.12 Adhesion protein percentage staining

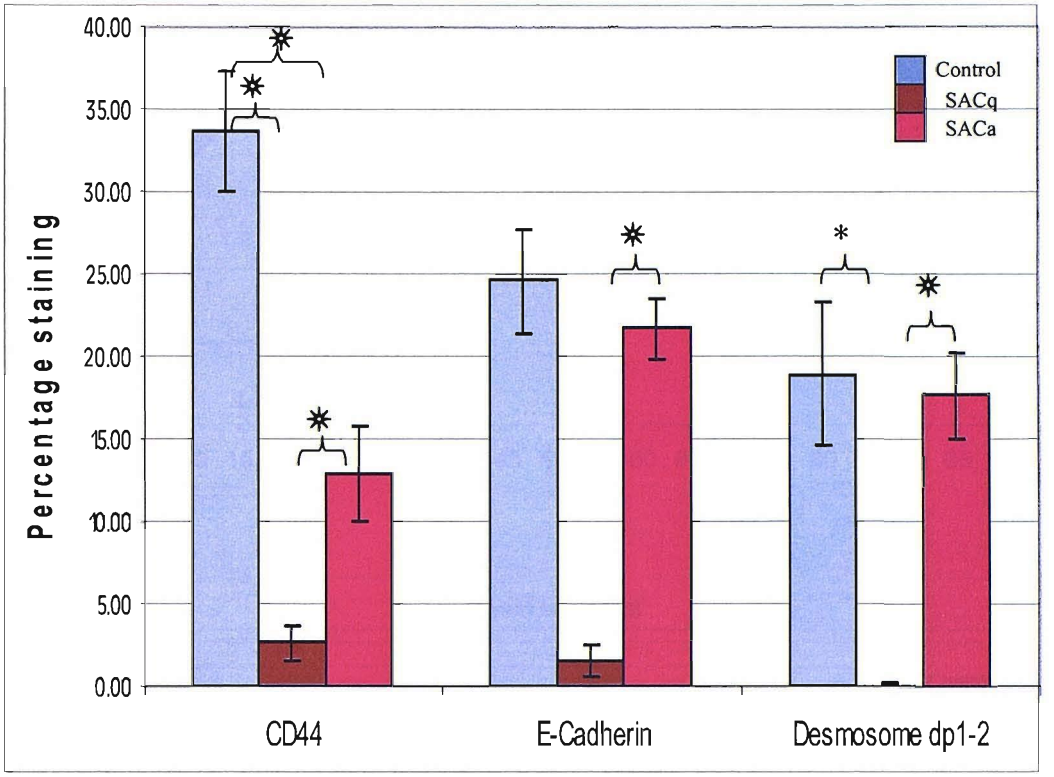


The above graph shows the percentage staining seen in the membrane bound adhesion protein CD44, the intermediate junction protein E-Cadherin and the desmosome plaque protein dp1-2. The percentage stain is given as a whole across the whole epithelial layer. The trend in staining in all the adhesion proteins was that the strongest staining was seen in the control subjects, then in the active disease group (SACa) with the lowest staining seen in the quiescent disease group (SACq).

In the case of CD44 staining, control compared to SACa was significantly greater, as was control compared to SACq ($p < 0.001$, and 0.001 respectively). When SACa was compared to SACq, the staining was significantly lower in the SACq group ($p = 0.001$).

In the case of E-Cadherin staining, control demonstrated significantly greater staining when compared to the SACq group but no difference seen compared to the SACa group ($p < 0.001$ and $p$ = n/s respectively). A significant difference in staining was seen in between the SACa and SACq groups ($p < 0.001$).

In the case of dp1-2 staining, the control group demonstrated greater staining than the SACa group but this wasn't significant, but significantly greater when compared to the SACq group ($p$ = n/s and $p < 0.05$ respectively). The SACa group demonstrated significantly greater staining than the SACq group with a $p < 0.001$).

$p < 0.05$ = * $p < 0.001$ = ✱

All adhesion molecule staining subject numbers are, n = control 17, SACa 7, SACq 7.

# Figure 3.13 CD44 distribution

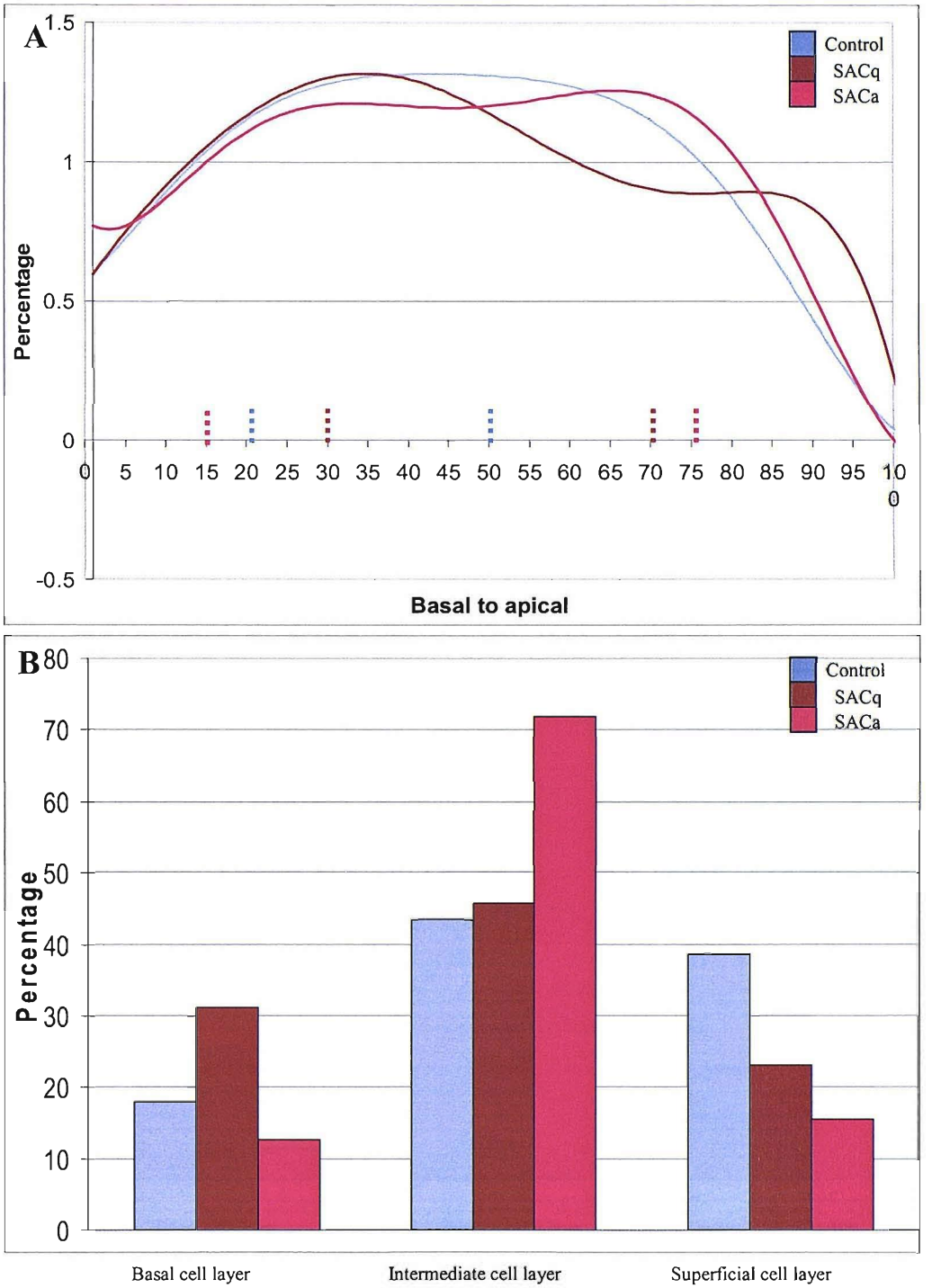


Graph A shows the continuous staining distribution, running from the basement membrane to the apical membrane, for CD44 as seen in the conjunctival epithelium of the three subject groups. The coloured lines on the x axis represent the layer of cells within the epithelium.

Graph B shows the percentage staining seen within the three layers of the epithelium.

Graph A shows that the continuous distribution staining pattern is similar for the three groups, but when the data is put into the three cell layers, SACq shows greater staining in the basal cell layer, whereas SACa shows greater staining in the intermediate cell layer.

# Figure 3.14 E-Cadherin distribution

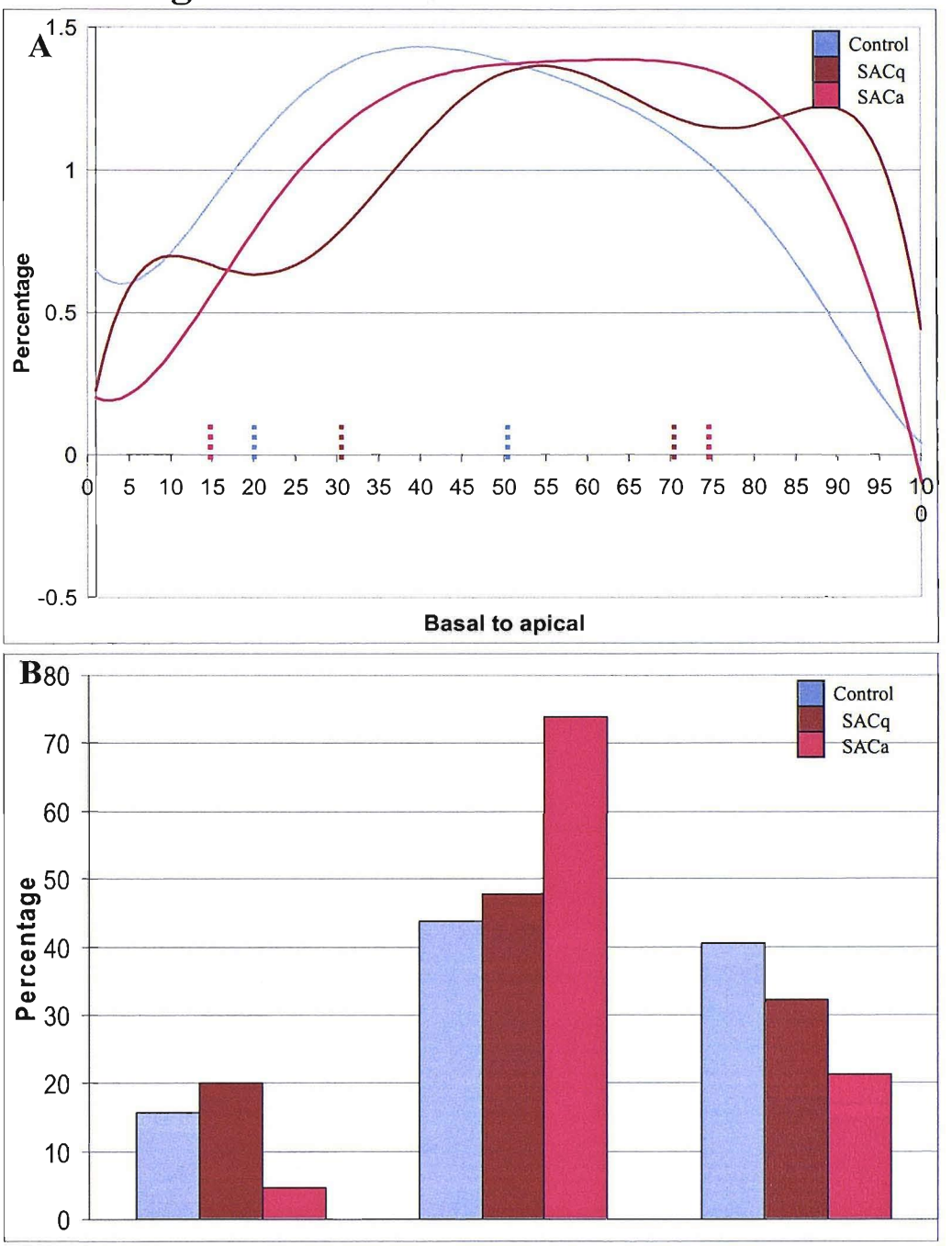


Graph A shows the continuous distribution staining pattern, running from the basement membrane to the apical membrane, of E-Cadherin in the conjunctival epithelium of the three subject groups. The coloured lines on the x axis represent the layer of cells within the epithelium.

Graph B shows the percentage staining seen within the three layers of the epithelium.

From the above graphs the control and SACq distribution of E-Cadherin follow similar staining patterns. The distribution of E-Cadherin staining seen in the SACa shows a greater staining in the intermediate cell layer and lower staining in the basal cell layer than the staining levels seen in the control and SACq.

# Figure 3.15 Desmoplakin 1-2 distribution

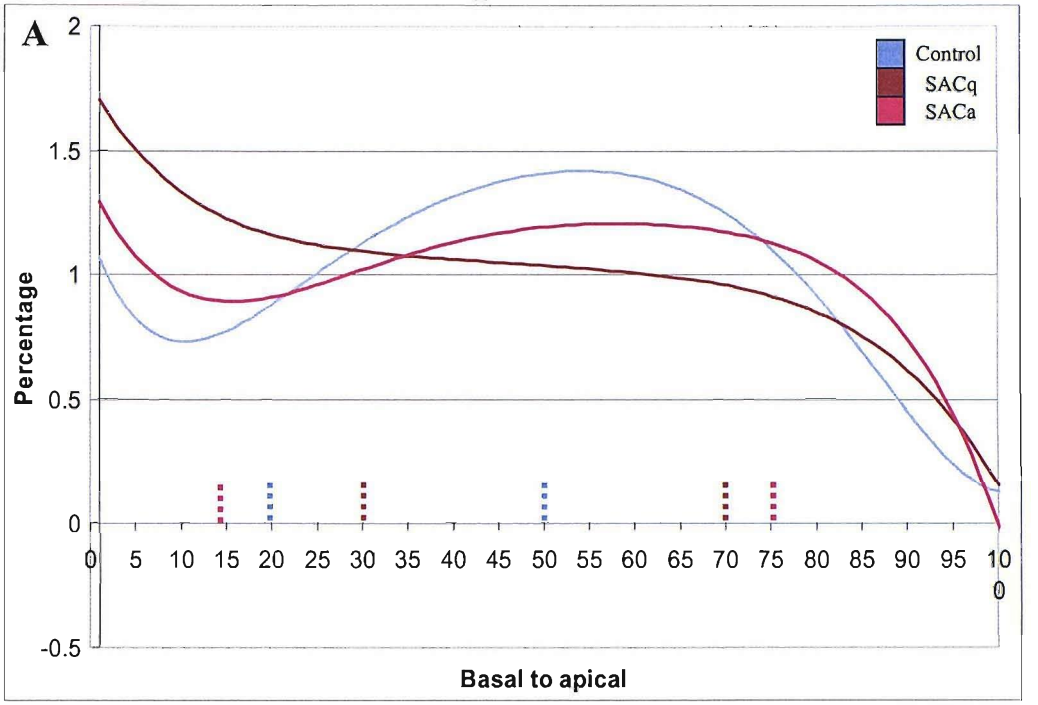


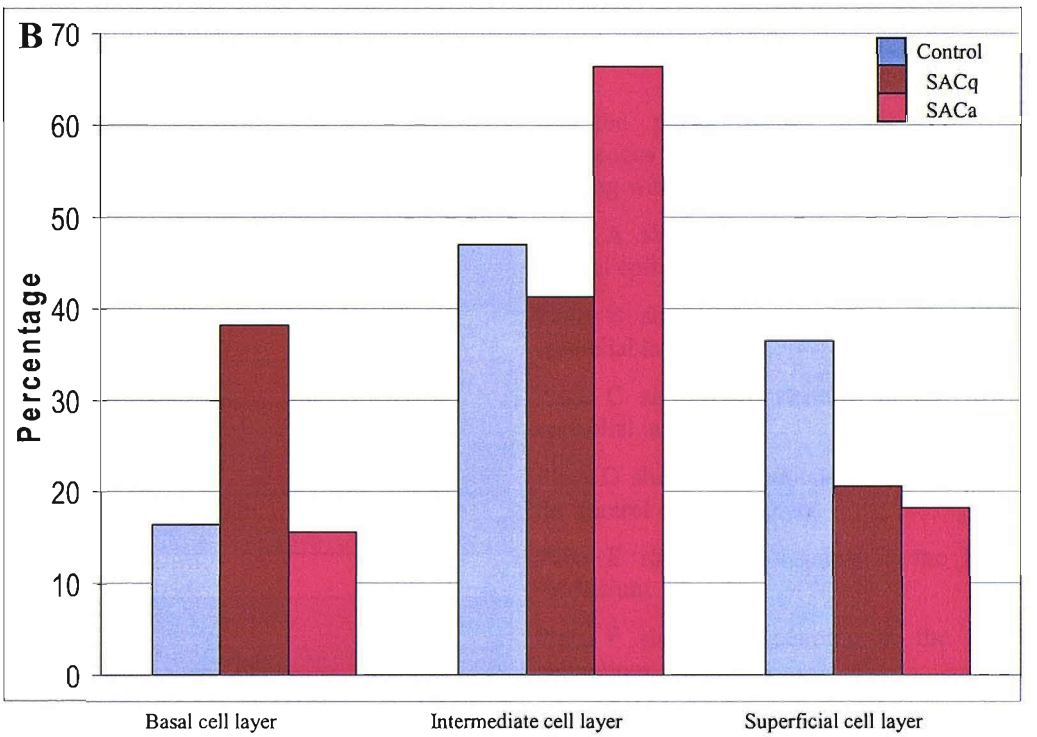


Graph A shows the continuous staining distribution, running from the basement membrane to the apical membrane, for Desmoplakin 1-2 in the conjunctival epithelium of the three subject groups. The coloured lines on the x axis represent the cell layer divisions of the epithelium.

Graph B shows the percentage staining seen within the three layers of the epithelium.

From graph A each of the groups show a similar staining distribution pattern, but when the data is displayed according to staining level in each cell layer, it can be seen that the SACq group has higher staining in the basal cell layer than seen in the other groups.

# Figure 3.16 Adhesion molecule immunostaining

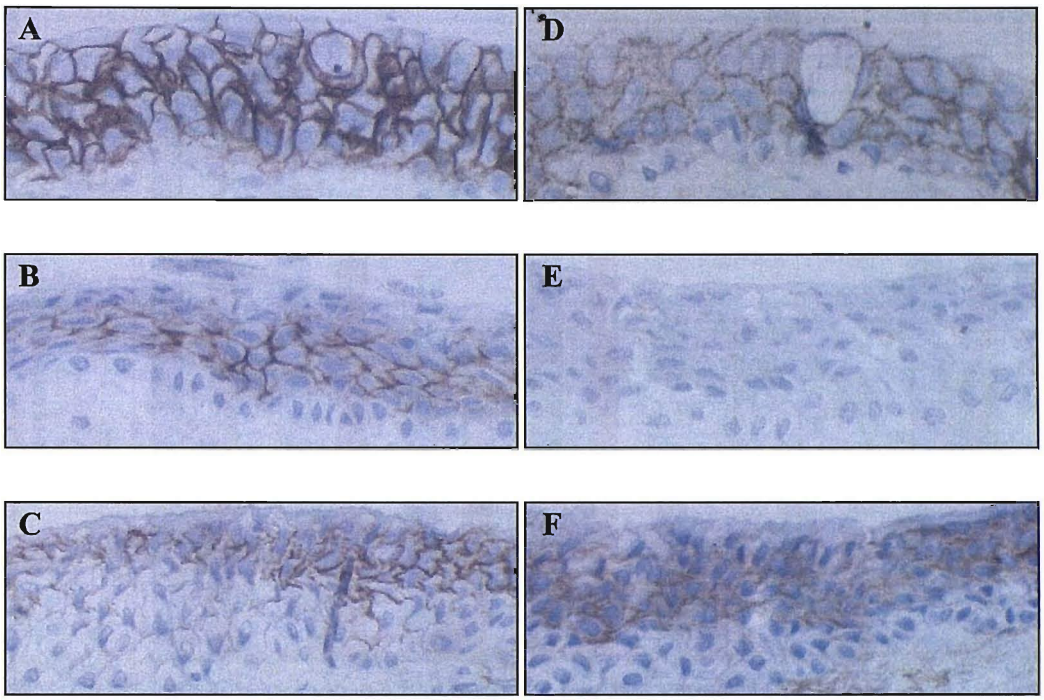




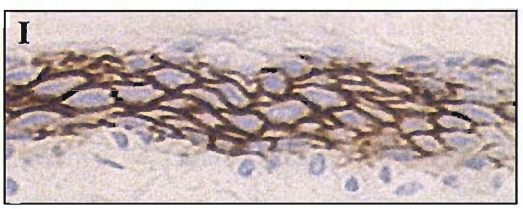


All the plates shown demonstrate the differences seen in adhesion molecule staining within the three subject groups.

Plate A shows E-cadherin staining in the control epithelial layer.

Plate B shows the staining in the SACq epithelial layer.

Plate C shows the staining in the SACa epithelial layer.

Plate D shows Desmoplakin 1-2 staining in the control epithelial layer.

Plate E shows the staining in the SACq epithelium.

Plate F shows the staining in the SACa epithelium.

Plate G shows CD44 staining in the control epithelial layer.

Plate H shows the staining in the SACq epithelium.

Plate I shows the staining in the SACa epithelium.

All images are at x20 magnification.

# Figure 3.17 Percentage staining of keratins

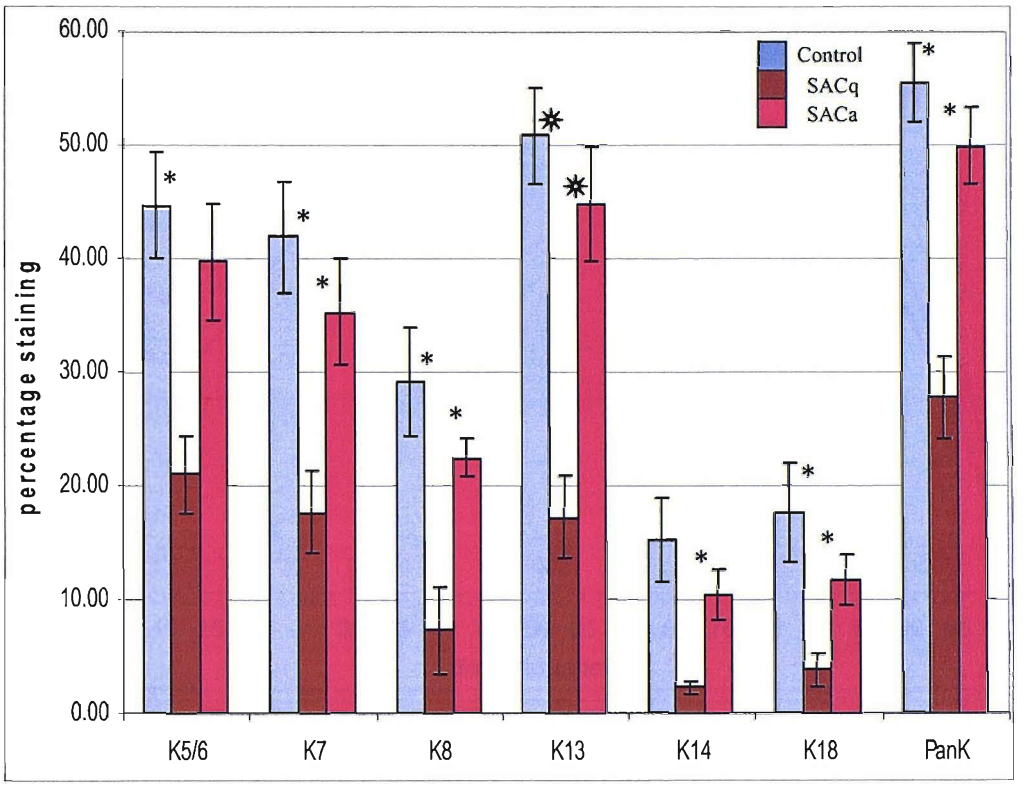


The graph above shows the percentage staining of the intermediate filaments, keratin 5/6, 7, 8, 13, 14, 18 and a broad keratin marker (Pan), within the three subject groups. The greatest staining was demonstrated in the control group, then the active disease subject group (SACa) and the lowest staining seen in the quiescent disease subject group (SACq).

When staining was compared between the three groups with each keratin staining, significant differences were seen in;

•Keratin 5/6, control versus SACq ($p < 0.05$),

•Keratin 7, Control versus SACq and SACa versus SACq (both $p < 0.05$),

•Keratin 8, Control versus SACq and SACa versus SACq (both $p < 0.05$),

•Keratin 13, Control versus SACq and SACa versus SACq (both $p < 0.001$),

•Keratin 14, Control versus SACq and SACa versus SACq ($p < 0.05$),

•Keratin 18, Control versus SACq and SACa versus SACq (both $p < 0.05$),

•Pan Keratin, Control versus SACq and SACa versus SACq (both $p < 0.05$).

$p < 0.05$ = * $p < 0.001$ = ✲

The remaining combinations all produced no statistical significant differences in staining.

All keratin staining subject numbers are n = control 17, SACa 7, SACq 7.

# Figure 3.18 Keratin 5/6 distribution

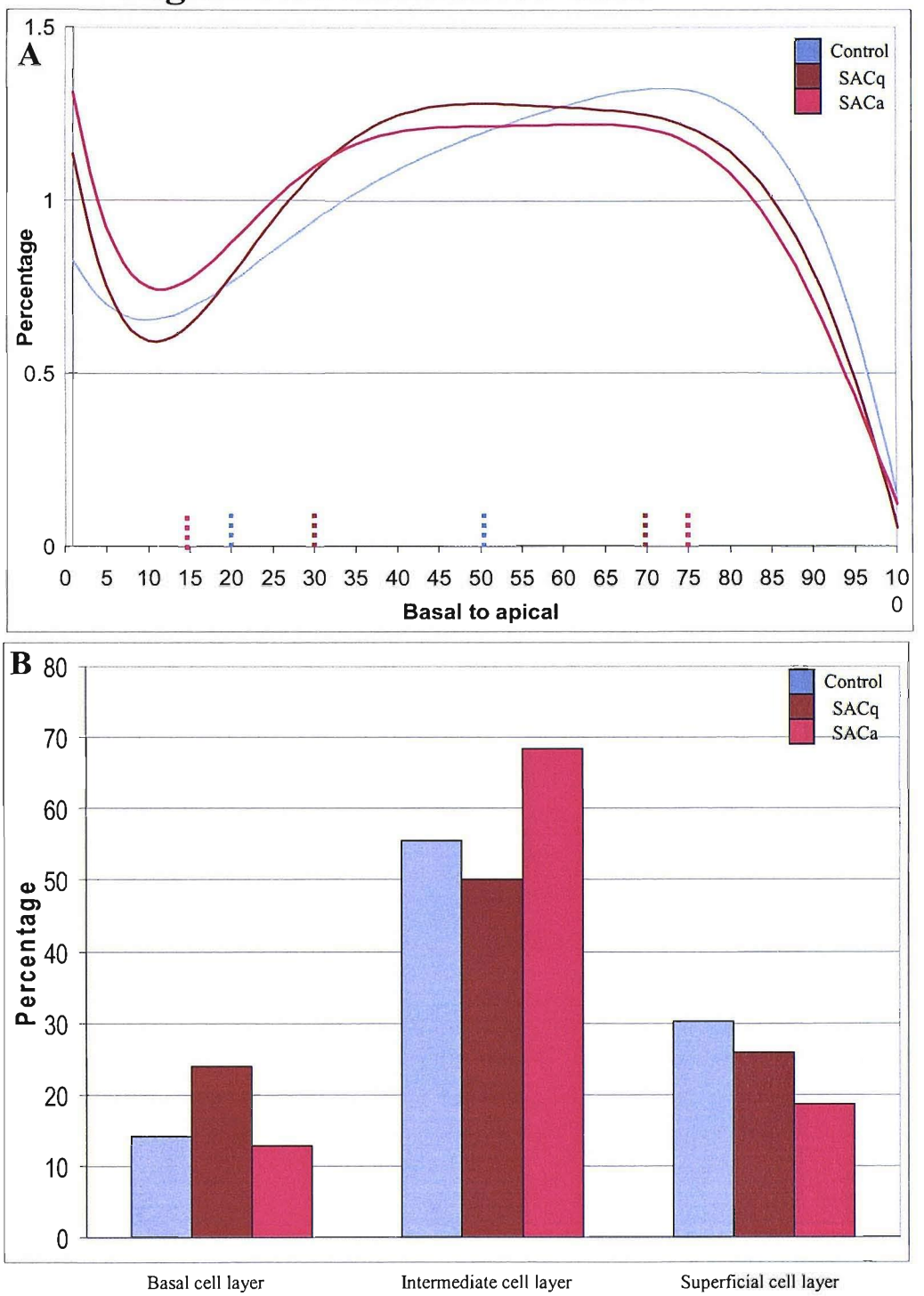


Graph A shows the continuous staining distribution, running from the basement membrane to the apical membrane, for keratin 5/6 in the conjunctival epithelium of the three subject groups. The coloured lines on the x axis represent the layer of cells within the epithelium.

Graph B shows the percentage staining seen within the three layers of the epithelium.

The above graphs show that the staining distribution pattern for keratin 5/6 is similar in the three subject groups.

# Figure 3.19 Keratin 7 distribution

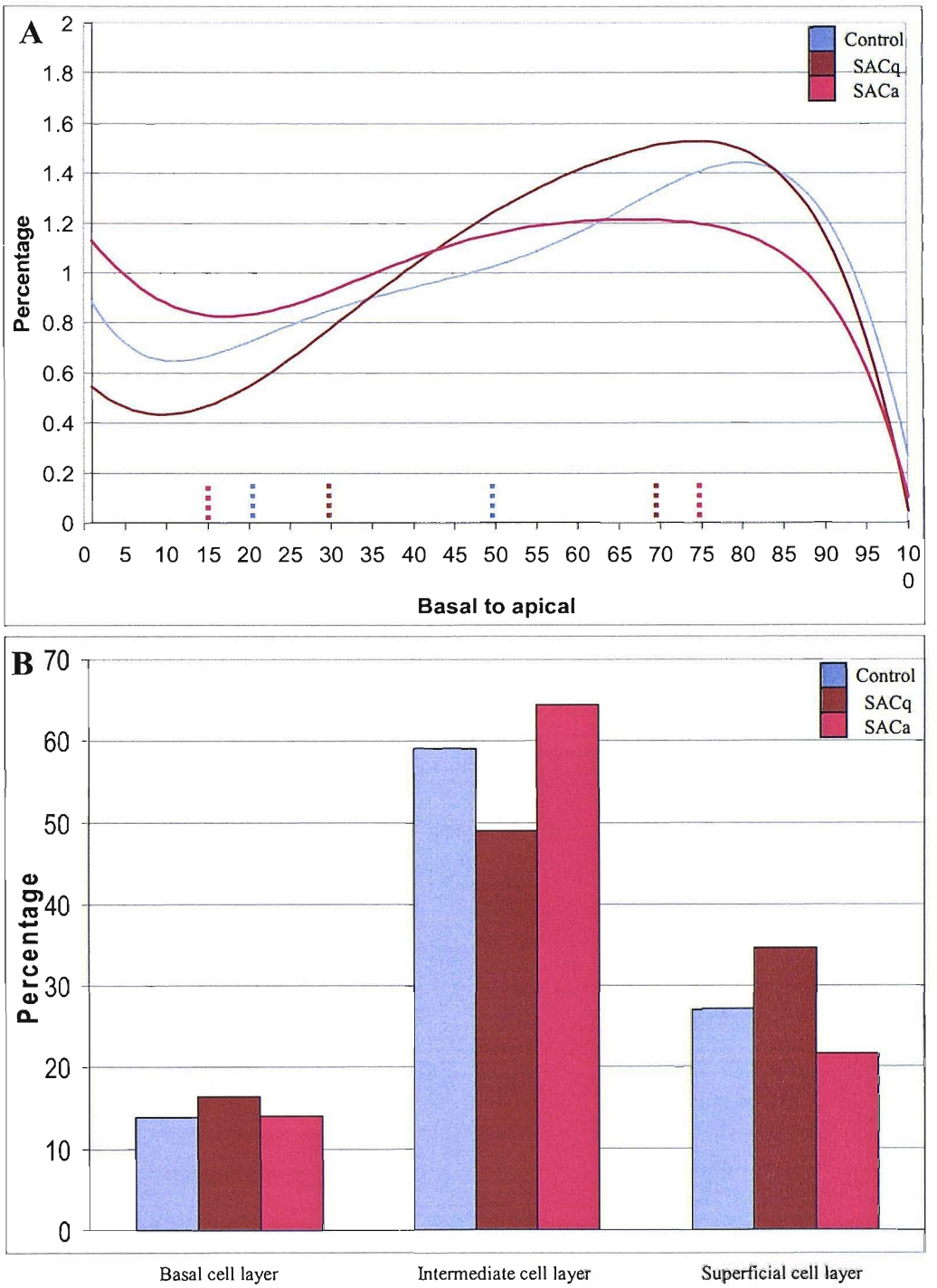


Graph A shows the continuous staining distribution, running from the basement membrane to the apical membrane, for keratin 7 as seen in the conjunctival epithelium of the three subject groups. The coloured lines on the x axis represent the layer of cells within the epithelium.

Graph B shows the percentage staining seen within the three layers of the epithelium.

The graphs above show that the distribution of keratin 7 staining seen in the three subject groups follow a similar pattern.

# Figure 3.20 Keratin 8 distribution

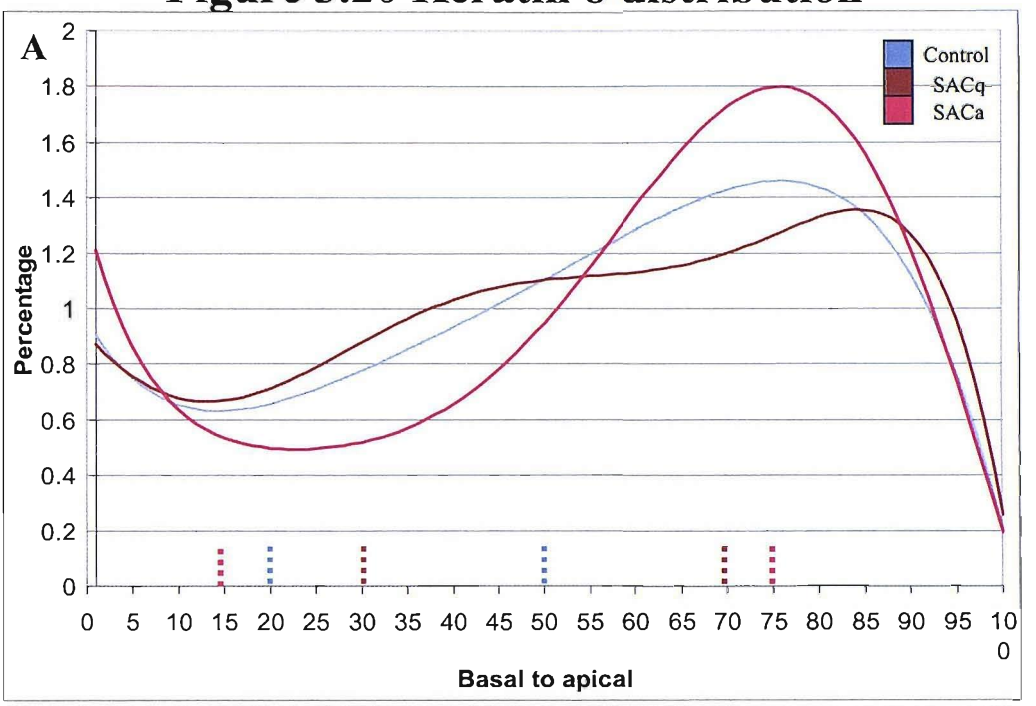


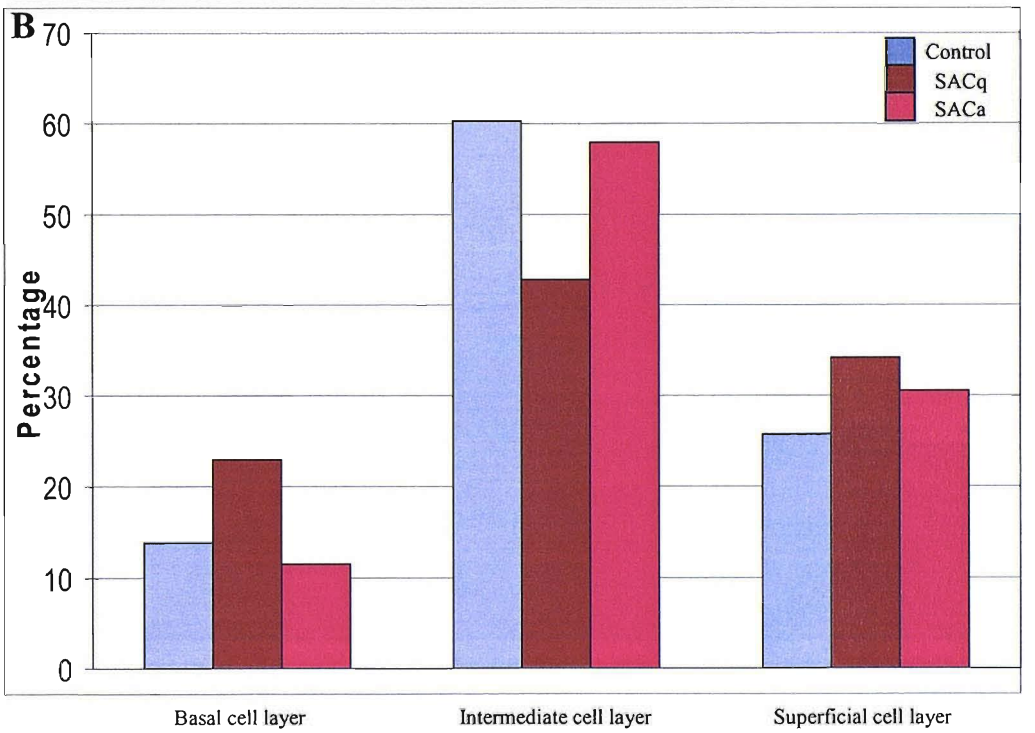


Graph A shows the continuous staining distribution, running from the basement membrane to the apical membrane, for keratin 8 in the conjunctival epithelium of the three subject groups. The coloured lines on the x axis represent the layer of cells within the epithelium.

Graph B shows the percentage staining seen within the three layers of the epithelium.

Graph A shows that the three groups have a similar staining distribution pattern, when he data is presented in terms of staining within the cell layers, the SACq shows greater staining in the basal cell layer and lower staining in the intermediate cell layer.

# Figure 3.21 Keratin 13 distribution

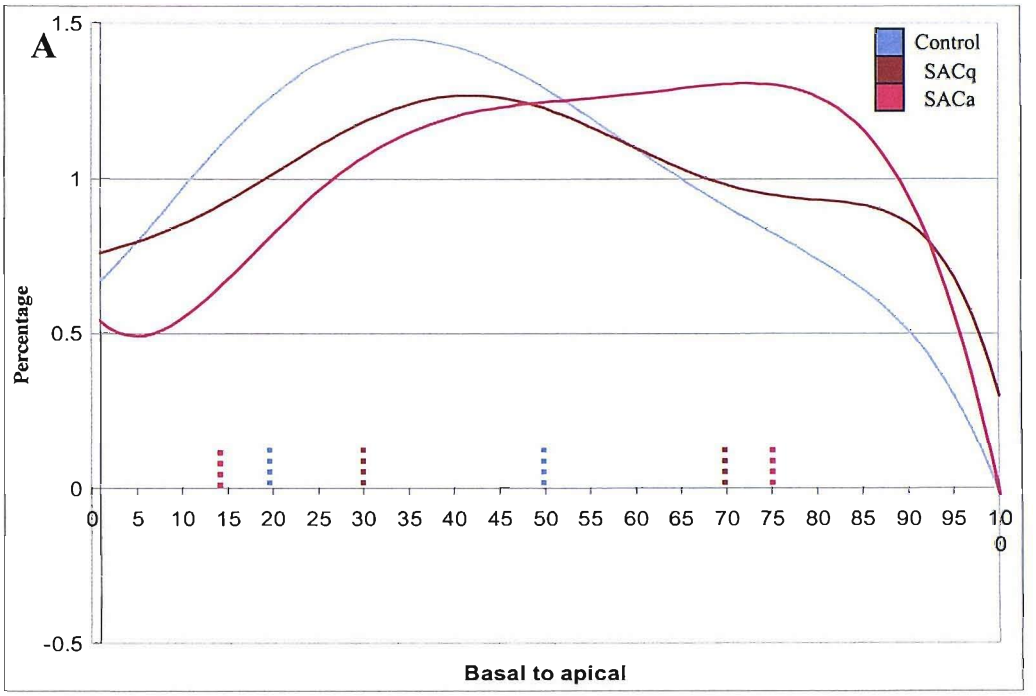


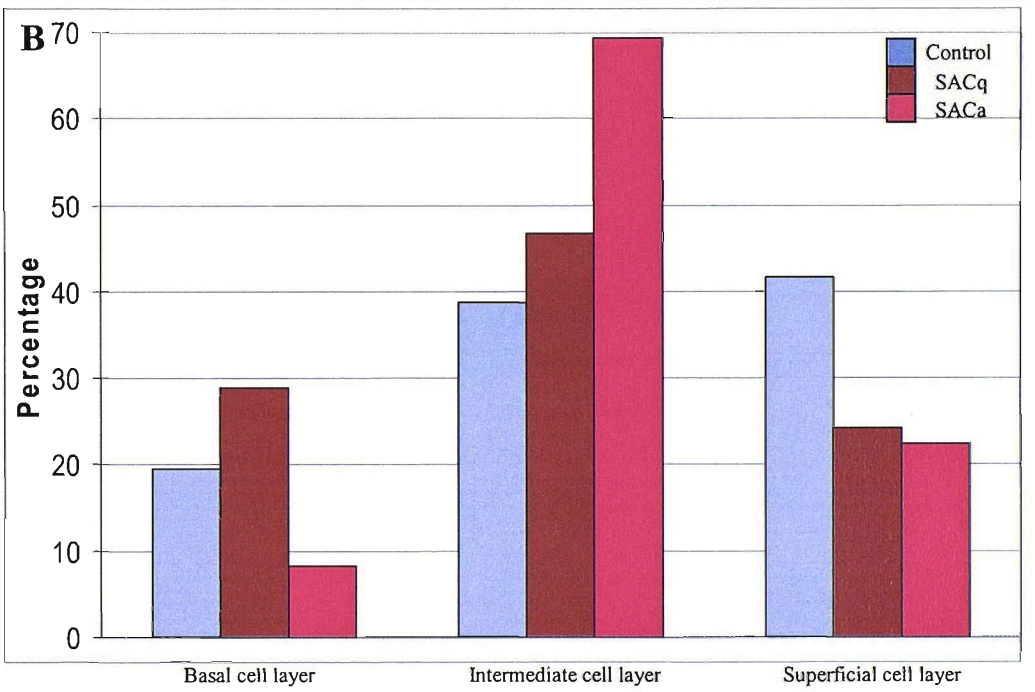


Graph A shows the continuous staining distribution, running from the basement membrane to the apical membrane, for keratin 13 in the conjunctival epithelium of the three subject groups. The coloured lines on the x axis represent the layer of cells within the epithelium.

Graph B shows the percentage staining seen within the three layers of the epithelium.

Graph A shows that the disease groups SACq and SACa display a different staining pattern to the pattern seen in control. This is highlighted in graph B where SACa keratin 13 shows lower staining in the basal cell layer and greater staining in the intermediate cell layer. Both SACa and SACq show lower staining in the superficial cell layer.

# Figure 3.22 Keratin 14 distribution

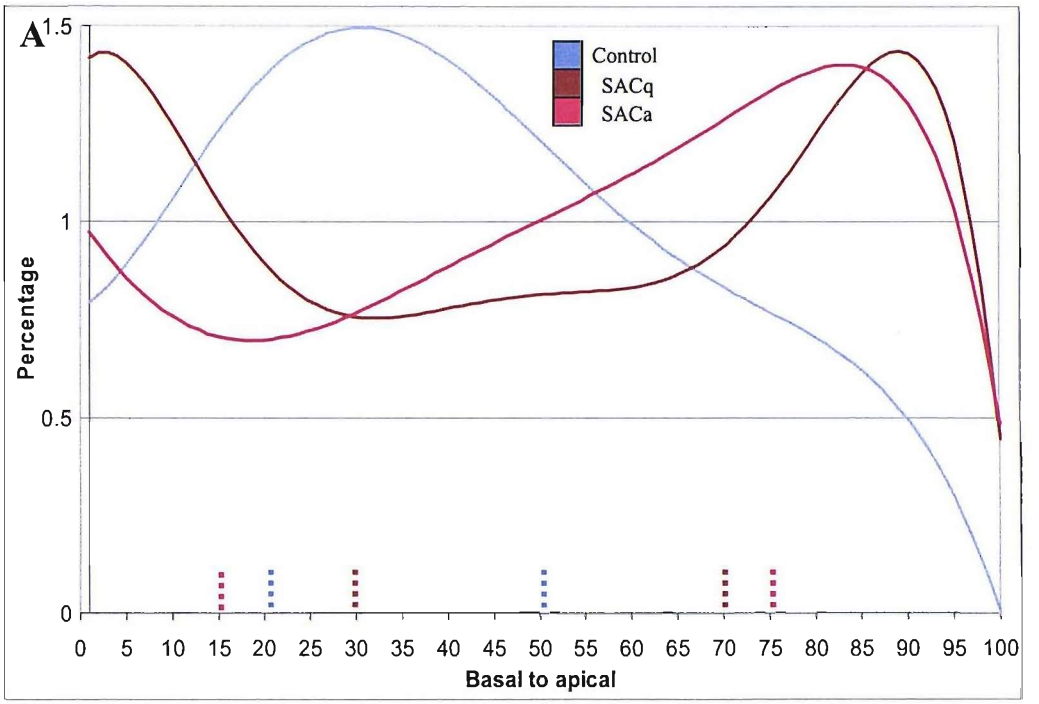


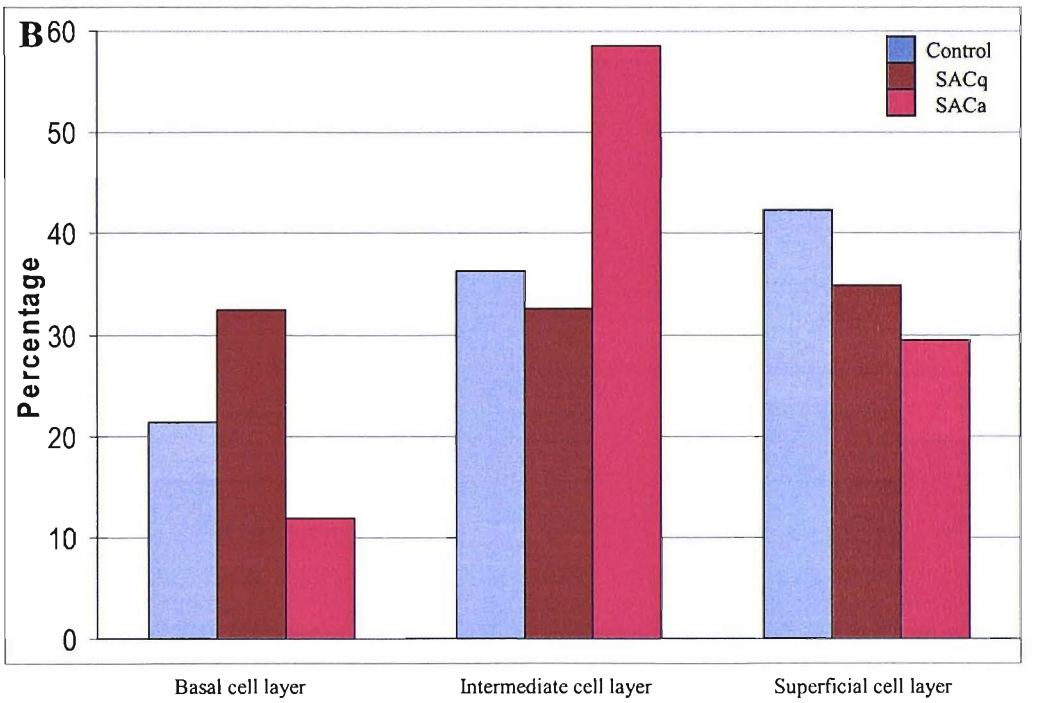


Graph A shows the continuous distribution of staining, running from the basement membrane to the apical membrane, for keratin 14 in the conjunctival epithelium of the three subject groups. The coloured lines on the x axis represent the layer of cells within the epithelium.

Graph B shows the percentage staining seen within the three layers of the epithelium.

From the above graphs, the staining distribution seen in the disease groups shows a different pattern to that in the control subjects. This is highlighted in graph A, and the differences in the staining in each cell layer can be seen in graph B.

# Figure 3.23 Keratin 18 distribution

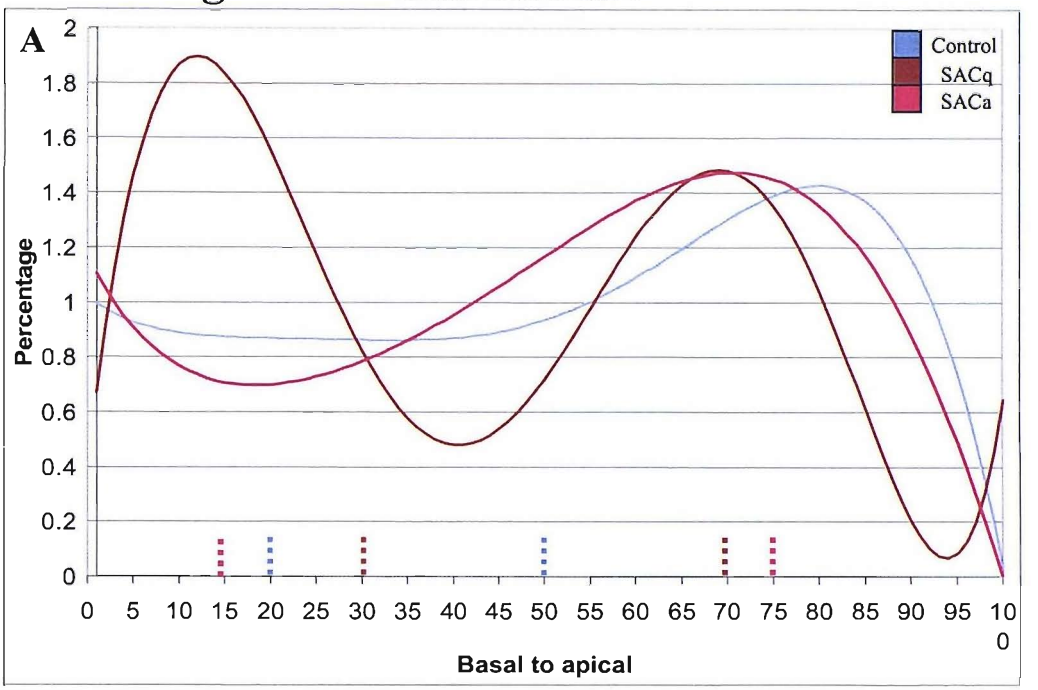


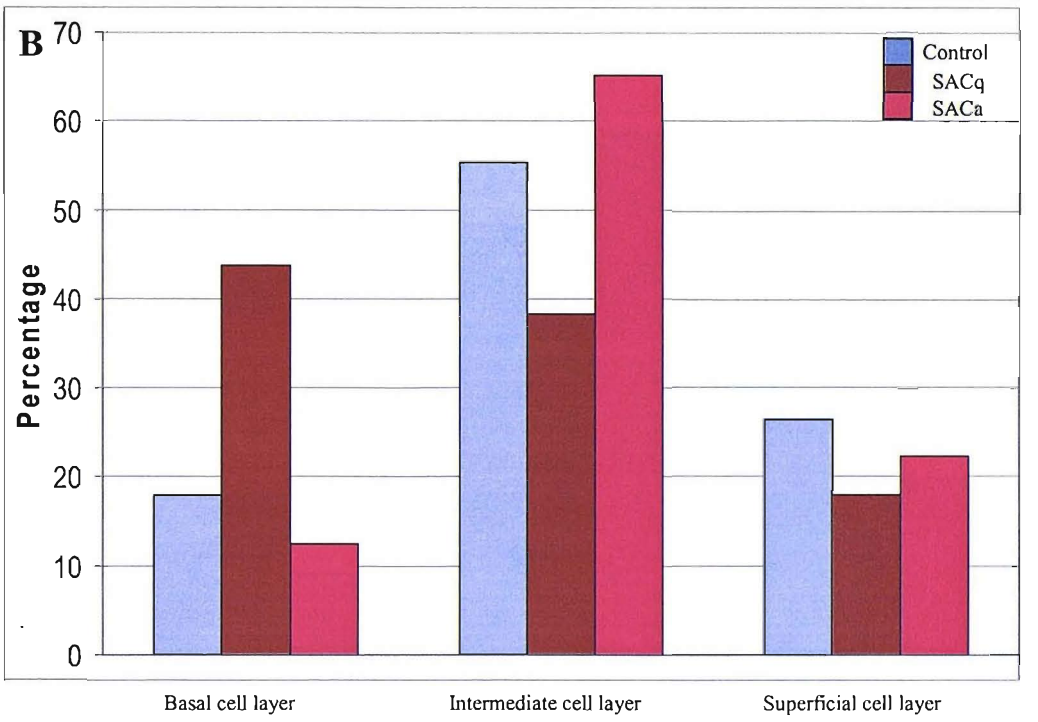


Graph A shows the continuous staining distribution, running from the basement membrane to the apical membrane, for keratin 18 in the conjunctival epithelium of the three subject groups. The coloured lines on the x axis represent the layer of cells within the epithelium.

Graph B shows the percentage staining seen within the three layers of the epithelium.

The pattern of staining of keratin 18 in the SACq group, shows a re-distribution, with a higher level of staining in the basal cell layer also lower staining in the intermediate cell layer, than the staining patterns in the other two groups.

# Figure 3.24 Pan Keratin distribution

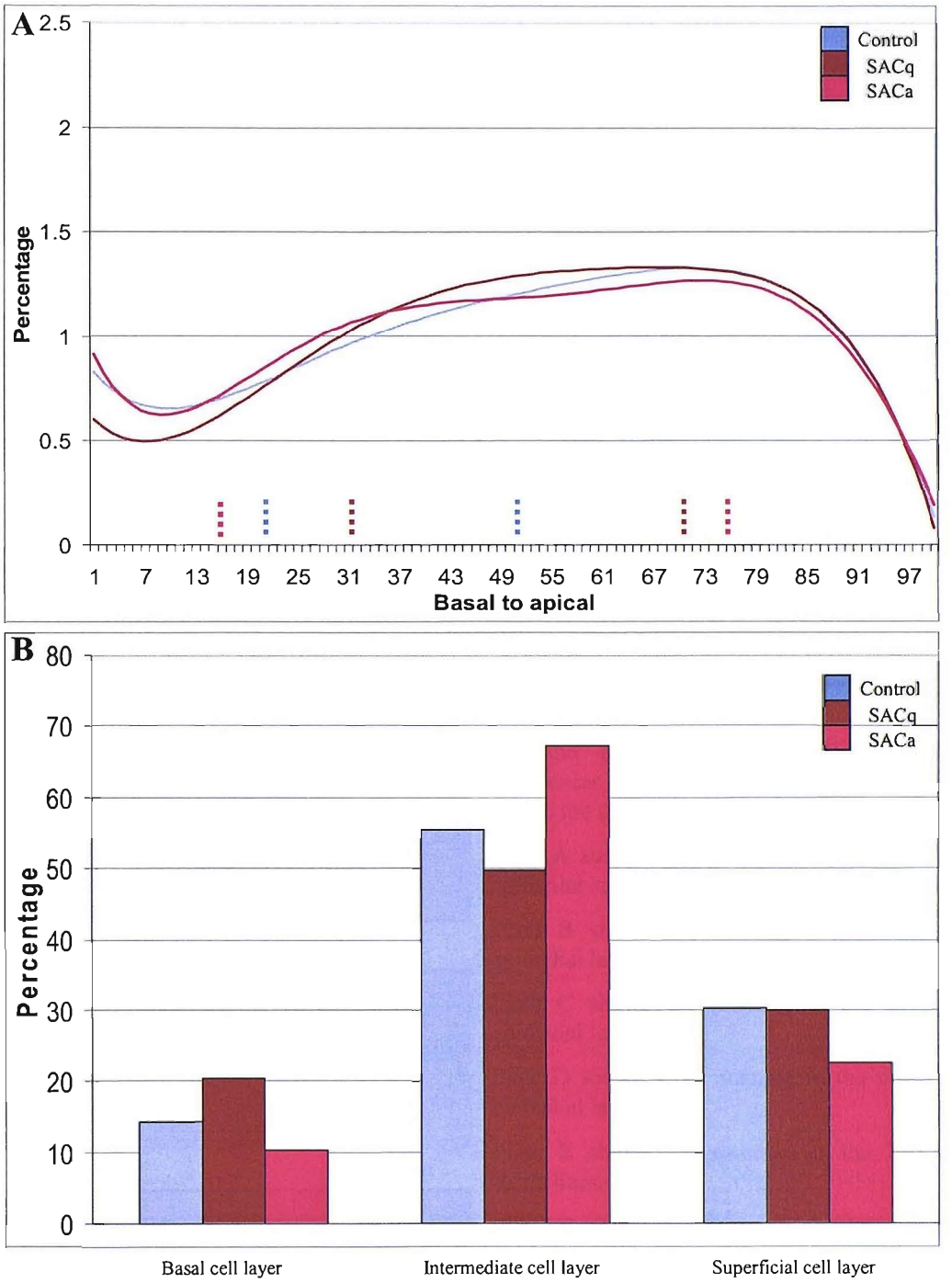


Graph A shows the continuous staining distribution, running from the basement membrane to the apical membrane, of pan keratin in the conjunctival epithelium of the three subject groups. The coloured lines on the x axis represent the layer of cells within the epithelium.

Graph B shows the percentage staining seen within the three layers of the epithelium.

Both the above graphs show no difference in the distribution of pan keratin staining in the three groups.

# Figure 3.25 Keratin immunostaining

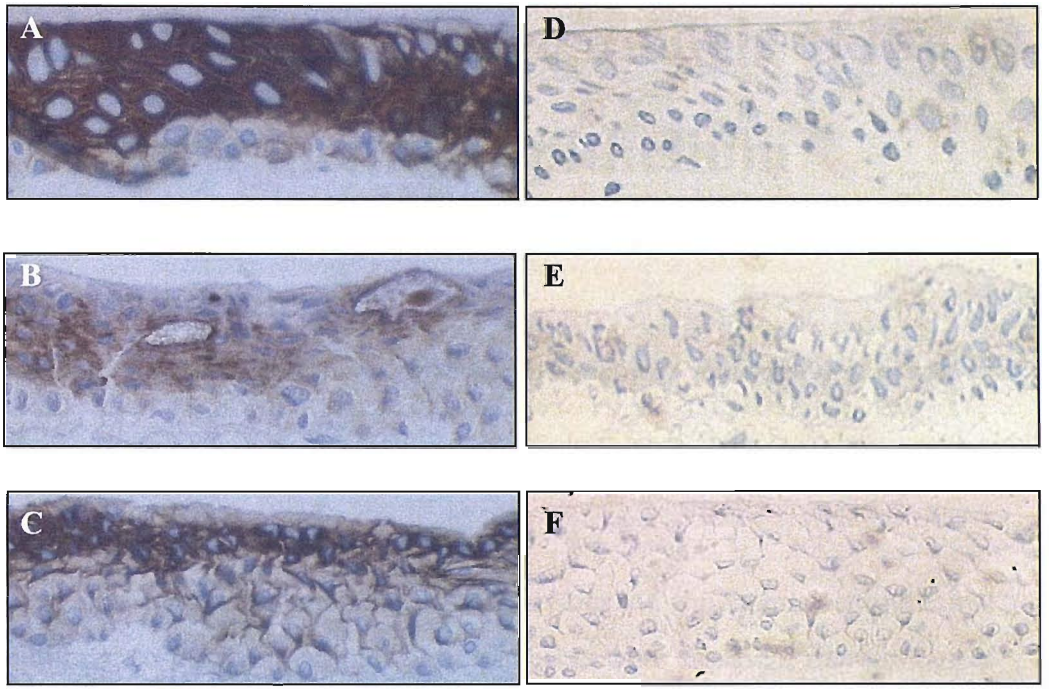



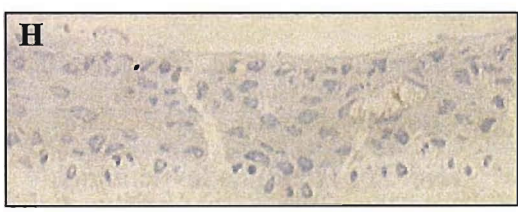


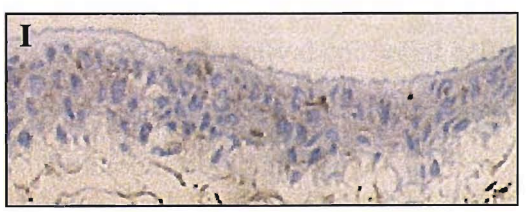


All the plates shown demonstrate the differences seen in Keratin (K) staining within the three subject groups.

Plate A shows K 13 staining in the control epithelial layer.

Plate B shows the staining in the SACq epithelial layer.

Plate C shows the staining in the SACa epithelial layer.

Plate D shows K 14 staining in the control epithelial layer.

Plate E shows the staining in the SACq epithelium.

Plate F shows the staining in the SACa epithelium.

Plate G shows K 18 staining in the control epithelial layer.

Plate H shows the staining in the SACq epithelium.

Plate I shows the staining in the SACa epithelium.

All images are at x20 magnification.

# 4. Development and characterisation of *in vitro* and *ex vivo* models of the conjunctival epithelium

## Chapter Hypothesis:

***Conjunctival epithelial cell models provide an accurate experimental model of the human conjunctival epithelium.***

### 4.1 Introduction

In chapter 3, the epithelial characteristics of the human conjunctival epithelium taken from non-atopic control subjects were assessed; morphological aspects of those characteristics were then compared against tissue from the SACa and SACq subject groups. To further investigate the epithelial associated mechanisms that are involved within the pathogenesis of seasonal allergic conjunctivitis, an experimental model system of the conjunctival epithelium for *in vitro* cellular response testing is required.

In this chapter, three different approaches were undertaken to develop an epithelial cell model of the conjunctiva,

- firstly, the characterisation of existing and newly established conjunctival epithelial cell lines,
- secondly, the development and characterisation of human biopsy derived conjunctival epithelial cells (primary cultures) and
- thirdly, the development and characterisation of a stratified conjunctival epithelial tissue model.

1. *In vitro* epithelial cell models.

*In vitro* model systems, such as cell lines, should resemble as closely as possible the tissue of interest, and offer a means of studying cellular responses *in vitro* under strictly controlled culture conditions producing repeatable and standardised results. Cell lines offer subcultures of phenotypically similar cells

with the ability to bulk store each passage for repeat testing, they also offer an alternative to the less controlled conditions of *in vivo* experiments and are increasingly seen as a method to fulfill the 3R's principle (Reduction, refinement, and replacement of tests using animal subjects). The continuous cell lines used in this chapter were the Clone 1-5c-4, Wong-Kilbourne derivative (D) of Chang conjunctiva (ATCC CCL20.2) (ChWk), IOBA-NHC and 16HBE 14o- all of which from knowledge to date, are not Hayflick limited (Stacey G 2001).

The ChWk cell line has been used in many studies including, viral, bacterial, cytokine production and therapeutic work, but has had little work on its structural characteristics (De Saint Jean M. *et al* 1999, 2000. Diebold *et al* 1998. Trejdosiewicz *et al* 1979. Zhan *et al* 2003) and is the only commercially available conjunctival epithelial cell line.

The IOBA-NHC cell line is a spontaneously immortalised conjunctival epithelial cell line (Diebold *et al* 2003).

The 16HBE 14o- cell line is a human bronchial epithelial cell line; it was produced by SV40 large-T antigen transformation and found to retain its differentiated epithelial morphology and functions (Cozens *et al* 1994).

2. *Ex vivo* epithelial cell models.

Primary cell cultures provide cells for experimental purposes that display characteristics very close to the tissue of origin, closer than cell lines that have been passaged multiple times and have possibly undergone slight phenotypic drift as a result.

The ex vivo cell model utilised in this chapter were obtained with informed consent from patients attending the eye unit for routine surgical procedures.

3. Stratified epithelial cell model.

The stratified epithelial cell model was obtained from the species *Ovis aries* as a gift. Whole organs were removed and the conjunctival epitheliums were micro-dissected away from the orbit. Due to the infancy of this model, in relation to the point within the project that it was introduced, only limited characterisation studies were performed.

This chapter is concerned with the development and characterising of conjunctival epithelial cell models for the use in investigating the pathology of seasonal allergic conjunctivitis.

The *in vitro* cell lines used in this chapter required no developmental steps for their inclusion, the *ex vivo* and stratified models however, needed to be developed solely for the purposes of this PhD thesis.

Development steps included the initialisation of a protocol for the micro-dissection of epithelial cells from whole tissue samples and in the case of the ex vivo model the successful culture of epithelial cells from explant material. Once these objectives were achieved, all the models underwent characterisation to identify the ideal candidate for use, as the tissue model of the human conjunctival epithelium, within the context of pathological experiments investigating aspects of seasonal allergic conjunctivitis.

Cell model morphology was assessed by conventional and phase contrast light microscopy.

Ultra-structure was assessed by scanning electron microscopy.

Protein expression was assessed by indirect immunofluorescence, which offers increased sensitivity and versatility, and immunostaining of GMA embedded sections (Fritschy and Härtig 2002).

The protein targets in this chapter were;

- the tight junction protein ZO-1,
- E-Cadherin,
- CD44,
- Keratin 13 and
- Keratin 18.

Epithelial barrier function assessment was carried out by measuring the trans-epithelial electrical resistance generated by the models.

The results of the development and characterisation of the cell models of the conjunctival epithelium as well as the chapter hypothesis were evaluated and are discussed at the end of the chapter.

## 4.2 In vitro cell line models

### 4.2.1 Morphology (Phase contrast microscopy)

Chang conjunctival cells clone (ChWk), (section 2.1.1.), adhered to the basal surface of the culture vessel and flattened out. They took a fibroblastic appearance, elongated in shape and cell-cell contacts were seen between the extremities of the cells (figure 4.1a micrograph A). Cells grew out forming colonies in a net-like pattern branching towards each other across the surface of the culture vessel (figure 4.1a micrograph B and C). Cells continued to divide until a confluent layer was achieved cells in the confluent layer then were more polygonal in shape (no shown). When in the confluent layer cells measured approximately 10-15μm in diameter.

IOBA-NHC cells (section 2.1.1), when plated down adhered to the surface of the culture were as individual cells and flattened out. They took a slight fibroblastic / elongated look as they grew (figure 4.1b micrograph A). Cell-cell contacts were made and colonies grew across the culture vessel in a net-like pattern (figure 4.1b micrograph B). Colonies continued to cover the surface of the culture vessel until confluent. A polygonal cell shape was seen when a fully confluent layer was achieved. The growth of the IOBA-NHC was observed to be slower than both the ChWk and 16HBE 14o- cell lines.

16HBE 14o- cells (section 2.1.1) settled individually on the culture surface adhered down and flattened out (figure 4.1c micrograph A). Once adhered, the cells took a polygonal shape in their colonies; these divided filling the gaps on the vessel surface (figure 4.1c micrograph B). A fully confluent layer was achieved (post 4-5 days of plating down) and the cells within their colonies were polygonal (figure 4.1c micrograph C).

### 4.2.2 Surface-morphology (Scanning Electron Microscopy)

ChWk – SEM revealed the surface features of the growing cell layer. The general layer morphology is ruffled and uneven. Gaps between the cell colonies

can also be identified (figure 4.2 micrograph A). Cells demonstrate their elongated shape when growing; also present on their surface are cellular processes extending outwards facilitating cell-cell contact (figure 4.2 micrograph B). At high magnification, the microvilli can be identified, and on the leading edge of the cells cellular processes can be identified extending across the surface of the culture vessel from the cell (figure 4.2 micrograph C).

IOBA-NHC – SEM reveals shows that the confluent cell layer has a smooth surface appearance with continuous cell-cell contacts (figure 4.3a micrograph A and B). At higher magnification the apical surface membrane of the cells were seen to be fully covered by microvilli (figure 4.3b micrograph C), the microvilli can be estimated to be greater than 3 μm in length when viewed on figure 4.3b micrograph D.

16HBE 14o- SEM reveals the leading edge of the 16HBE 14o- cell layer and the smooth surface features of the cells behind the leading edge (figure 4.4a micrograph A). At higher magnification of the leading edge, microvilli can be identified on the apical membrane of the cells (figure 4.4a micrograph B). The cells behind the leading edge have microvilli present on the apical membrane (figure 4.4b micrograph C), these microvilli are approximately 0.5 – 1 μm in length (figure 4.4b micrograph D).

### 4.2.3 ZO-1 immunostaining

Immunostaining against ZO-1 (a MAGUK plaque protein of the tight junction, figure 1.7), was undertaken in the three cell line models. ChWk cell cultures demonstrated positive pattern staining around the cells (>60% of the cells, author observation, figure 4.5 micrograph A). IOBA-NHC cell cultures demonstrated a diffuse positive staining for ZO-1, surrounding approximately 50-60% of the cells (author observation, figure 4.5 micrograph B). 16HBE 14o- cell cultures demonstrated positive staining identified surrounding the majority of the cells (>70%, author observation, figure 4.5 micrograph C).

### 4.2.4 E-Cadherin immunostaining

Immunostaining against E-Cadherin (an integral part of the adherens junction), was undertaken in the three cell line models, ChWk cell cultures demonstrated staining across the majority of the cells (~ 90%, author

observation, figure 4.6 micrograph A). IOBA-NHC cell cultures stained for E-Cadherin demonstrated immunostaining across the entire cell layer (figure 4.6 micrograph B); 16HBE 14o- cell cultures stained for E-Cadherin demonstrated staining across the entire cell layer (figure 4.6 micrograph C).

### 4.2.5 CD44 immunostaining

Immunostaining for CD44 (a transmembrane acidic glycoprotein), was undertaken in the three cell line models. ChWk cell cultures showed diffuse positive staining across the cell layer (figure 4.7 micrograph A). IOBA-NHC cell cultures showed positive staining across the entire cell layer (figure 4.7 micrograph B and C). 16HBE 14o- cell cultures showed positive staining across the entire cell layer (figure 4.7 micrograph D and E).

### 4.2.6 Keratin 13 (figure 4.8)

Immunostaining against Keratin 13 (an acidic type I keratin found predominantly in stratified squamous epithelium), was undertaken in the ChWk and 16HBE 14o- cell line models. ChWk cell cultures demonstrated positive staining in 100% of the cells viewed (figure 4.8 micrograph A, B and C). 16HBE 14o- cell cultures demonstrated positive staining in 100% of the cell viewed (figure 4.8 micrograph D, E and F).

### 4.2.7 Keratin 18 (figure 4.9)

Immunostaining against Keratin 18 (an acidic type I keratin found in simple epithelia tissues), was undertaken in the ChWk and 16HBE 14o- cell line models. ChWk cell cultures demonstrated positive staining in 100% of the cells viewed (figure 4.9 micrograph A, B and C), 16HBE 14o- cell cultures demonstrated positive staining in 100% of the cells viewed (figure 4.9 micrograph D, E and F).

### 4.2.8 Trans-epithelial electrical resistance

All three cell lines had their trans-epithelial electrical resistance measured to test whether tight junctions were formed. Once a visible confluent monolayer was formed the readings were taken. The ChWk cell line model produced a resistance of 43.54 $\Omega.cm^2$, when corrected for control and area, after the first

hour of incubation. This value maintained a plateau for the remainder of the experimental timescale, finishing with a value of 43.08 $\Omega.cm^2$ at the end time point (8 hours post plating). The IOBA-NHC cell line model produced a resistance of 40.85 $\Omega.cm^2$ after the first hour of incubation. It too maintained a plateau throughout the experimental timescale, finishing at the 8 hour mark with a resistance of 40.96 $\Omega.cm^2$. The 16HBE 14o- cell line model produced a resistance of 3110.5 $\Omega.cm^2$ after one hour of incubation. The resistance steadily rose throughout the experiment to an end point of 4123 $\Omega.cm^2$ (figure 4.10).

## 4.3 *Ex vivo* cell culture

### 4.3.1 Micro-dissection of human biopsy material

A technique for the harvesting of primary human conjunctival epithelial cells was devised to develop and characterise an *ex vivo* experimental epithelial cell model.

Briefly, during routine surgical procedures such as cataract and retinal detachment surgery, a small (<3mm²) piece of human conjunctival was removed, placed in 3 ml of Leibovitz's medium L-15 and stored overnight at +4°C.
The biopsy was processed according to the following protocol:

Firstly, the biopsy and medium were placed in a sterile Petri-dish and the orientation of the biopsy was established (figure 4.11a micrograph i). A sterile scalpel was used to remove large pieces of the episclera (underlying connective tissue) away from the epithelial layer avoiding the epithelial-connective tissue region (figure 4.11a micrograph ii). The remaining connective tissue was carefully removed using the extreme tip of a fine gage hypodermic needle (figure 4.11a micrograph iii). The connective tissue was then removed from the Petri-dish and discarded leaving only the epithelial layer (figure 4.11b micrograph iv). The orientation of the epithelial layer was established again, then placed basal side down on the surface of the Petri-dish and flattened out as much as possible without damaging the integrity of the layer (figure 4.11b micrograph v). The biopsy was divided into small pieces using the sterile scalpel, firstly along its long axis (figure 4.11b micrograph vi). The biopsy was then further divided perpendicular to the first axial cut into as many equally size pieces as possible (figure 4.11c micrograph vii). A flattened spatula was carefully introduced into

the dissecting medium in order to lift each section of biopsy from the surface of the Petri-dish, also using the non-cutting edge of a hypodermic needle, using the spatula the piece can be moved to the desired culture vessel (figure 4.11c viii). The section of biopsy was then allowed to slip off the end of the spatula on to the surface of the culture vessel (figure 4.11c ix). The section of biopsy was then finally orientated, basal side down then gently spread out and allowed to adhere to the surface of the culture vessel (figure 4.11c micrograph x). When the edge of the meniscus of the medium that the explant was in starts to show shows of slightly drying (approximately 60 mins, author observation), fresh culture medium was added extremely slowly so not to disturb the biopsy. If added too quickly the physical force of flow generated by the newly introduced medium can lift the explant from the surface of the culture vessel (not shown). The explant was incubated overnight, then the 50% of the medium was changed for fresh then the explant was incubated for 3-5 days at which point the success of the culture was assessed and the appropriate action was taken.

### 4.3.2 Pilot primary culture

Prior to the successful primary cell culture protocol being devised and honed, several avenues of cell culturing methods were undertaken with limited success.

In the first instance steps involved with the handling and storage of the freshly cut tissue were investigated.

Explant material was stored on ice, micro-dissection was then carried out and the biopsy was plated down within 2 hours of removal from the donor. In the first instance half the explant material were cultured using Medium 199 (M199) supplemented with 10% heat inactivated FBS and 1% A/A solution and F-12 supplemented with 10% heat inactivated FBS and 1% A/A solution. After approximately three days, individual cell migrated from the biopsy material, but upon visual inspection showed no signs of survival displaying a round shape and a dull appearance under phase contrast microscopy (figure 4.12a plates A and B, 4.12b plate A). After 5 days under the culturing conditions no cells were cultured from material that under went this protocol. The original pieces of processed conjunctival epithelium were then lifted from the culture plate and processed for scanning electron microscopy to investigate the surface features

and if any clues as to the failure to culture cells could be gained. The epithelium had lost its characteristic surface features as seen in the freshly processed / not cultured biopsy material from the previous chapter (figure 4.13a micrograph A) displaying a smoother cell surface. The distinction between epithelial tissue and connective tissue was less apparent. The faint outline of the polygonal cells could be identified although less defined in the cultured explant material (figure 4.13a micrograph B). When viewed at higher magnifications the lost of epithelial surface features was greatly evident (figure 4.13b micrographs C and D). Also observed was the uneven appearance of the cell layer and the loss of the finer surface features such as microvilli-like cellular processes (figure 4.13c micrographs E and F). Unfortunately microscopic investigations offered no clues as to the failure to culture primary cells from conjunctival biopsy material using this protocol of micro-dissecting the epithelial layer away from the underlying connective tissue layer immediately following biopsy removal from the patient. The protocol for storing the biopsy overnight at +4°C arose due to an omission of two samples during the micro-dissection steps of the unsuccessful pilot protocol. On inspection of the processed samples the next morning, the unprocessed biopsy pieces that were missed were discovered at the back of the fridge. The biopsies had lost their clean cut edges giving the appearance of decreased structural integrity. Due to the importance of the samples, they underwent micro-dissection and were plated down on culture plates. On continued daily inspection the immediately processed samples followed the similar pattern of cells migrating from the explant material and no further growth. The samples left overnight showed less defined edges to the material and after three days of culture small areas of epithelial outgrowth were identified, but not surrounding the entire explant just confined to the edges that showed the greatest level of physical damage. The outgrowth survived for a further two days, before the cells lifted from the surface of the culture plate and died, after this no further outgrowths were seen from the explant. The procedure of leaving the biopsy material at +4°C overnight was repeated a further three times with varying success, with growth identified in 3 of 10 explants cultured.

In order to increase the percentage of successful explant culture, attempts to optimise the culture medium used, were undertaken.

Basic culture mediums utilized were;

- M199,
- LHC-9,
- MEM,
- Ham's,
- F-12.

Each basic medium was firstly used singularly with the one following additives then using a mixture;

- FBS or Ultra-ser G,
- Epidermal Growth Factor (EGF).

Each culture run was also carried out using medium with 1% antibiotic / antimycotic solution.

Finally with the success of bronchial primary cultures within the department, using Bronchial Epithelial Growth Medium (BEGM) as the medium, culture runs were carried out using BEGM. (BEGM consists of, bovine pituitary extract (BPE) (52$\mu$g/ml), insulin (5$\mu$g/ml), transferrin (10$\mu$g/ml), retinotic acid (0.1ng/ml), human EGF (0.5ng/ml), epinephrine (0.5$\mu$g/ml), hydrocortisone (0.5$\mu$g/ml), tri-iodothyronine (6.5$\mu$g/ml), and GA-100 (gentamicin sulfate and amphotericin) (1$\mu$/ml)).

Culture runs were attempted using a substrate to assist in the adhering of cells to the culture vessel's surface. Petri dish surfaces were coated with the substance FVB (Fibronectin at mg / 100 ml, Collagen (I/II) 1 ml and BSA 1 mg / ml).

Due to the importance and precious nature of each biopsy, a maximum of two biopsies were used for evaluation in the studies of each primary culture medium combination.

In total 68 samples were used in the primary culture studies (43 ♂, mean age = 68.41, age range 27 - 91).

22 samples were used in the initial (pre overnight storage at +4°C) (11 ♂, mean age = 69.14, age range 27 - 85), 40 in the medium studies (24 ♂, mean age = 68.15, age range 34 - 91), and 6 using the BEGM (3 ♂, mean age = 67.5, age range 42 - 77).

The combination of M199 supplemented with 10% heat inactivated FBS and 1% A/A solution, yielded the best percentage success, of 60% outgrowth (60% represents observed outgrowth, not outgrowth survival as culture runs were lost due to unexplained occurrences and bacterial infections due to the un-sterile and un-documented environment of the origin of the sample).

### 4.3.3 Successful primary culture

The culture protocol that resulted in successful epithelial out growth, involved micro-dissecting the biopsy according to the above section. The culture medium added to the explant was Medium 199 supplemented with 10% heat inactivated FBS and 1% A/A solution. The success of the culture was assessed by the morphological characteristic of a tight cobble stone / pavement appearance of polygonal shaped cells which appeared approximately two to four days after plating down the explant. At each feeding time point 50% of the medium was removed and replaced with the same amount of fresh medium, the medium that was removed was stored in sterile containers. The cultures grew out forming a monolayer from the explant across the culture vessel (figure 4.14 micrograph A, B, C and D). Cultures were incubated for 9 days before cell growth arrested, growing to a maximum radius of ≤15mm (author observation, explant not shown and not all explant material produced reproduced, maximum growth).

In total 20 samples were used (15 ♂, mean age = 64.25, age range 44 - 87).

Attempts to chemically passage cells (using several grades of trypsin), from the primary culture vessel onto secondary culture vessel using the protocol in section 2.2.1 resulting in cells not plating down and cultures were lost (n=3).

Attempts to generate a second outgrowth from explant material involved removed explant material from the primary culture vessel being placed basal side

down in a secondary culture vessel and with the addition of conditioned medium saved and stored from the original primary cell culture vessel. No further cellular out-growth was observed using this method (n=3).

Attempts were also made to measure the TEER generated by primary cells by encouraging growth from explants in membrane chamber inserts. Difficulties were experienced in establishing explant material adherence to the insert membrane, therefore measurements were unable to be taken. This also resulted in the inability to analyse primary cell surface features using scanning electron microscopy (n=4).

### 4.3.4 Primary epithelial cell immunostaining

Primary cells were immunostained, *in situ* on the primary culture vessel, according to section 2.2.3 for keratin 13 and 18. Primary cell cultures stained positively for keratin 13 (figure 4.15 micrographs A, B and C). Positive staining for keratin 18 was also seen in the primary cell cultures (figure 4.16 micrographs A, B and C). Black and white images were included to show the specific keratin staining, as no nuclear counter stain was used. Of the primary cell populations stained within the petri-dish less than 90% were keratin negative.

## 4.4 Stratified conjunctiva epithelial model

### 4.4.1 Dissection of *Ovis aries* material.

Sheep material was provided as a gift material to the author and the project.

The animal species chosen for the model conjunctival epithelial system was the sheep (*Ovis aries*). This model system offered large pieces of tissue material to work with (500mm x 250mm), for experimental purposes. The dissection protocol for harvesting of pieces of tissue was formulated and perfected by the author.

Once the animal had undergone euthanasia, the head was removed from the body and secured in a clamp, where eyelids were taped closed to reduce the chance of damage occurring during the procedure to remove the orbits.

The skin and underlying tissue, approximately 600mm from the eye, was cut and removed from the skull leaving a skin gap of approximately 50mm from the around the eyelid margin (figure 4.17a schematics A and B). This skin and connective tissue gap was then lifted from the skull bone until reaching the edge of the orbital bone. Then the skin was gently cut from the bone, the only connections left were on the eye itself. A slight lifting pressure was applied to the eyelids and scissors were used to cut the orbit muscles and optic nerve so that the whole orbit and the eyelids could be removed as one. The eyelid's skin was removed at the skin/conjunctival border. Then the conjunctiva was cut away from the cornea/conjunctival border, removing 1mm of the conjunctival edge in order to ensure that the epithelial tissue was purely conjunctival. The underlying tissue was micro-dissected away from the basal side of the epithelium. The epithelium was then flattened out in its ring-like shape. A small piece of cartilage that ran from the cornea to the extremity of the conjunctiva was removed, thus opening up the ring of conjunctiva, at which point the tissue was divided into smaller pieces as required.

### 4.4.2. Ultra-structure (Scanning electron microscopy)

Scanning electron microscopic ultra-structural analysis of the surface features of the conjunctival epithelium was undertaken and of the underlying layer of connective tissue. The surface features of the epithelial layer show distinct morphological differences between the epithelial and connective tissues. The epithelial layer shows a smooth and continuous layer of cells covering the underlying connective tissue (figure 4.18a micrograph 1 and 2, with white arrows highlighting the epithelial/connective border). At higher magnification the surface features of the layer can be clearly identified, the layer is undulating in appearance (figure 4.18a micrograph 3). The epithelial cells display the polygonal apical membrane shape with tight cell-cell borders forming the characteristic cobblestone surface appearance (figure 4.18b micrograph 4). The apical membranes are covered in microvili that are extensively distributed across the cell's membrane (figure 4.18b micrographs 5 and 6).

The morphological differences between the epithelial and connective tissue layers can be clearly identified the connective tissue is constructed of long

string-like fibres and other un-identifiable bodies (figure 4.19 micrographs 1 and 2).

### 4.4.3. Tissue morphology

The conjunctival epithelium was also assessed by using toludine blue morphological staining according to the protocol from section 2.2.4. (figure 4.20 micrographs A, B and C). The epithelium displayed characteristics of a non-ciliated stratified cubiodal tissue, composed of three layers the basal, intermediate and superficial. The epithelium is 3 to 5 cells in thickness (figure 4.20 micrographs D and E).

### 4.4.4. Control immunostaining

The epithelium was immunostained using a primary and secondary negative antibody to test for non-specific antibody binding according to the protocol of section 2.2.4. All sections showed no endogenous peroxidase staining was seen (figure 4.21 micrographs A, B, C and D).

### 4.4.5. Secondary and Pan Keratin immunostaining (figure 4.22)

The epithelium was immunostained using a IgG isotype antibody and using a Pan keratin antibody according to the protocol from section 2.2.4. The secondary control IgG control showed no staining within the epithelial layer (figure 4.22 micrographs A and B). Section stained with the Pan keratin antibody showed positive staining within the epithelial layer mainly confined within the upper intermediate and superficial layers (figure 4.22 micrographs C, D and E).

### 4.4.6. Trans-epithelial electrical resistance (TEER)

Measurements of the trans-epithelial electrical resistance generated by the freshly excised tissue were recorded to identify the presence of tight junctions in the stratified epithelial model. Two methods were used in order to measure these values. The first method involved placing the tissue in between two insert chambers that had had their membranes removed, according to section 2.2.10.2. This method was devised and implemented due to the unavailability of an Ussing chamber and due to its nature only one time point was recorded using this

method. The mean average resistance recorded using this method was 1196.75 Ohms using four samples (figure 4.23).

When the appropriate Ussing chamber became available, the method of measuring the TEER of the stratified epithelial model transferred to this method (as described in section 2.2.10.3). The mean average resistance value recorded from freshly excised material was 14,557.5 Ohms. Pieces of material were then incubated in culture medium M199 supplemented with 10% heat inactivated foetal bovine serum (FBS) with 1% Antibiotics / Antimycotic solution, for 24 hours. Resistance levels were taken at 1, 2, 3, 4, 5, 6, 12 and 24 hours at which point the material was discarded. Readings taken at 1 hour to 5 hours rose to a plateau above 16,000 Ohms. At the 6 hour time point the value dropped to 12,925 Ohms. From this point until the end of the experiment at 24 hours the values remained around the 13,000 ohms mark, finishing on 13,547.5 (10 pieces of stratified model tissue were utilised) (figure 4.23).

In order to discount the physical effect that the multi-layer tissue would have on the TEER readings, pieces of material were incubated in either $Ca^{2+}$ and $Mg^{2+}$ free Hank's Balanced Salt Solution (HBSS) or sterile distilled water. The HBSS would allow the cells to survive the incubation period, but the lack of $Ca^{2+}$ and $Mg^{2+}$ would restrict the re-cycling and forming of tight junctions within the tissue, therefore giving the 'background resistance' generated by the tissue. The sterile distilled water would induce cell death while maintaining the structural integrity of the tissue therefore providing the 'inert resistance' of dead tissue. Resistance levels recorded with the incubation of HBSS were 6093.75 Ohms at the 12 hour time point and 6844.75 Ohms at the end time point. Tissue incubated in sterile distilled water had a resistance of 859.25 Ohms after 12 hours and 556.5 Ohms at the end point (10 pieces of stratified model tissue were utilised in the HBSS set of incubations, 4 pieces were used in the sterile distilled water set of incubations) (figure 4.23).

These values could be then taken away from the initial experiment values recorded when tissues were incubated in cell culture medium M199.

Therefore, using this Ussing chamber method for measuring and recording the trans-epithelial electrical resistance of the *Ovis aries* stratified model of the conjunctival epithelium gave an initial experimental reading of 14,557.5 Ohms at time point zero. This dropped to 12842.5 Ohms after 12 hours and 13547.5 Ohms at the end time point. If corrected with the 'background resistance' values it is proposed that the tight junctions produced a resistance of 6748.75 Ohms when measured at the 12 hour time point a decrease of 52.5% from the initial resistance. At the end time point this corrected value was 6702.75 Ohms a decrease of 52.1% from the initial resistance. If the 'inert resistance' is then taken into account, the final epithelial junctional resistance figures are 5889.5 Ohms at 12 hours and 6146.25 Ohms at the end time point.

## 4.5 Discussion

The chapter hypothesis states:

*Conjunctival epithelial cell models provide an accurate experimental model of the human conjunctival epithelium.*

In order to answer this, the epithelial characteristics of three different models were analysed and assessed. The three different approaches were,

1. *In vitro* models,
2. *Ex vivo* model and,
3. Stratified model.

In vitro model.

The Clone 1-5c-4, Wong-Kilbourne derivative (D) of Chang conjunctiva (ChWk), displayed a fibroblastic appearance when first plated down, but showed epithelial characteristics when in a confluent layer, when assessed by phase contrast. When assessed scanning electron microscopy, the microvilli present on the cells appeared to be less dense than the microvilli seen on the control epithelial biopsies of figure 4.2 micrograph C. When stained for the adhesion proteins, ZO-1 (tight junctions), E-Cadherin (intermediate junctions), CD44 (non-junctional) and the keratin filaments 13 and 18, suggestive positive staining was observed, which, in terms of the keratin immunostaining is in agreement with Zhan (2003). Tight junction transepithelial electrical resistance functional

data suggests that ChWk do express tight junctions, but the level of resistance was only a maximum of 43.54 $\Omega.cm^2$ above control (figure 4.10).

This is in agreement with De Saint Jean (2004), who described some of the above morphological aspects of the ChWk cell line (phase contrast morphology, expression of E-cadherin and CD44), apart from the expression of E-Cadherin. Negative staining was seen in ChWk cells in basal conditions, whereas positive staining can be identified in figure 4.6. Zhan (2003) also described the phase contrast and keratin expression of the ChWk cell line which is in agreement with the results in this chapter.

The IOBA-NHC cells displayed epithelial characteristics when viewed under phase contrast and electron microscopy. Positive staining was identified for CD44, E-Cadherin, ZO-1 and a trans-epithelial resistance was measured. The IOBA-NHC cell is one of the newest conjunctival epithelial cell lines to be reported. It was reported in 2003, by researchers at the University Institute of Applied Ophthalmobiology, University of Valladolid, Spain. Cells used in this chapter were given to the author by collaborators at University College London, U.K., who received the cells from Spain. To date IOBA-NHC has only been used in four published articles, Diebold *et al* 2003, Michelini *et al* 2004, Enriquez de Salamanca *et al* 2005, 2006. The morphological data presented in this chapter is in agreement with those published by Diebold (2003), the original IOBA-NHC descriptive article. In addition the work in this chapter was the first time that the tight junctions of the IOBA-NHC cells, using ZO-1 immunostaining and transepithelial electrical resistance of the IOBA-NHC data was measured, suggestive staining of ZO-1 was identified (figure 4.7) and in terms of tight junction functional data the TEER reached a maximum of 40.96 $\Omega.cm^2$ above control (figure 4.10).

When the ultrastructure of the IOBA-NHC was compared to the non-cultured epithelial cells on biopsy material, the most noticeable difference was the length of the microvilli, those present on the IOBA-NHC (figure 4.3b micrograph C), were greater in length, but their distribution was lower on the apical membrane than the biopsy epithelium (figure 3.1b, micrograph G).

16HBE 14o-, the SV-40 T antigen transformed epithelial cell line, is a bronchial epithelial cell line but was included in this work as, a cell line that has been extensively studied (Polosa *et al* 1999, Howat *et al* and Leir *et al* 2003, to name a few). SV-40 T antigen transformed epithelial cell lines retain their structural properties and are accepted as a good epithelial cell line for in vitro experimental purposes (Cozens *et al* 1992). Morphologically epithelial characteristics were seen in phase contrast and electron microscopy. Positive immunostaining was seen for CD44, E-Cadherin, ZO-1 and the keratin proteins 13 and 18. It produced the greatest electrical resistance with a value of 4123 $\Omega.cm^2$ above control (figure 4.10), suggesting the formations of 'tight' tight junctions, making them a valuable inclusion in later structural experiments. This is in agreement with Wan (2000), who reported the tight junction properties of this cell line.

Ex vivo model

In order to attain the highest success rate for culturing primary epithelial cells from the human conjunctival epithelium several processing and culturing methodologies were used. Primary cells offer an invaluable tool in investigating a target tissue, over *in vitro* cell lines, mainly due to the fact that primary cells will retain a phenotype, in their first pre-passage culture, that is much more closely related to the tissue of their origin (Sun and Green 1977). The main draw backs with primary cell culture is that post passage cells will display a more cultured cell phenotype, cultures have finite passages (mostly <3) before they stop growing and the preparation and logistics of their culture is greatly demanding over *in vitro* cells.

Different groups investigating the practicalities of primary cell culture have used different originators and different techniques. My definition of originators is the types and sizes of epithelial tissue used.

When compared to some published material on primary cell culture, the technique developed in this project is relatively simple in methodology and equipment needed. Niiya (1997) reported positive results when culturing rabbit bulbar conjunctiva on type I collagen gel, with cells forming well-developed cell junction structures and surface features. But they did not mention the sizes of tissue they had to plate down, or more importantly, the percentage of successful

culturing runs which would greatly enhance the meaningfulness of their data and thus the primary cell culture technique that they are advocating. Gukasyan (2002) described the disintegration of the epithelial tissue to obtain individual cell for culturing, but this method destroys the important structural elements of the epithelial layer. Other groups have stated that the use of amniotic membranes enhances epithelial growth and the retention of the primary phenotype of the cells, using rabbit epithelial tissue (Meller and Tseng 1999, Meller *et al* 2002). Meller (1999) also reported findings of promoted epithelial stratification and cell polarity, on culturing at the air-liquid interface. Another widely utilised technique is using a seeding/feeder layer, although this technique has shown limited use (Meller and Tseng 1999, Cho *et al* 1999, Tsai *et al* 1994). Studies on human tissue have shown differences in culturing techniques and source material, historically, some with limited success (Koizumi *et al* 2002, Chen *et al* 2001, Shen *et al* 2001, Diebold *et al* 1999, Diebold *et al* 1998, Hicks *et al* 1997, Ebato *et al* 1986). Girolamo (1999) presented a simple primary technique, which is very similar to the one presented in this thesis (without the tissue preparation work), using human pterygia conjunctival, with the cells cultured displaying strong epithelial characteristics. Human pterygia is characterised by the encroachment of a wing of altered conjunctival tissue over the cornea, suggesting that these cells have altered growth behaviour and therefore could survive, with greater success, the *in vitro* culturing conditions.

No literature exists for the micro-dissection of epithelial tissue, the protocol used in this thesis, was a development of a protocol that had been used in respiratory tissue samples. The finer stages of the dissection were honed by careful trial and error.

The preliminary pilot cultures represent a large set of experiments using large amounts of patient material with little return. Phase contrast of these failures showed no epithelial cell survival, although migrating cells were seen, these could possibly be motile tissue cells such as the circulating APC immune cells. Analysis of the surface features of the explant material by scanning electron microscopy showed no clues to the lack of epithelial outgrowth. The epithelial cell layer showed that the polygonal shape seen with healthy epithelial cells had been lost and that the apical membrane of these cells had lost definition

too (comparing micrographs from figure 4.13 against micrographs from figure 3.1).

For the assessment of the successful culturing of primary cells, the important step highlighted in this thesis was the overnight incubation at 4°C. This step was included in the protocol used by Risse Marsh (2002). Of the successful cultures phase contrast microscopy showed polygonal shaped cells extending from the original explant. Immunostaining showed that 90%, by visual estimate, of the primary cell grown from the explant material were keratin 13 and 18 positive, suggesting good epithelial outgrowth. The polygonal shaped cell and keratin positivity findings of cultured conjunctival epithelium are in agreement with Diebold (1997), Risse Marsh (2002), Zhan (2003) and De Saint Jean (2004), unfortunately no data were presented on growing success rates.

So why did the pilot attempts fail to grow? One explanation could be with the site of the biopsy. Kinoshita (1982), described the different characteristics of the limbal regions of the conjunctival epithelium compared to the bulbar and corneal epithelium. Ebato (1987), also demonstrated the different growth characteristics of the central and peripheral corneal, showing that peripheral grew better than central corneal, concluding that the location of the original tissue is critical to epithelial outgrowth, pointing to growth rich areas of epithelial tissue. This theory was further advocated by Wei (1995), whose data showed that the fornical epithelium may be a zone enriched in conjunctival epithelial stem cells, which is important in epithelial development and relevant in wound healing. This process of re-epithelialisation across de-epithelialised areas in wound healing could be the process by which epithelial cells grow out *in vitro* to cover culture vessels, thinking these areas to be physical wounds in the epithelial layer. This theory could be further accepted by the studies that show promoted epithelial cell growth on culture vessel coated with components commonly found in the extracellular matrix and underlying connective tissue such as fibronectin, laminin and collagen (Mackay *et al* 1999, Sanderson and Bernfield 1998). This would imply also that not only the site of the biopsy is important is calculating the chances of epithelial outgrowth, but also the age of the donor and any 'conjunctival' history that could be obtained relating to injury or disease that indirectly affects the epithelium.

Stratified model

Currently there is no sheep model of allergic conjunctivitis, presently the preferred species used for investigating the immunological model of allergic disease is the murine, possibly due to several logistical reasons (Groneberg *et al* 2003). This stratified model was used to investigate the trans-epithelial electrical resistance that a multi-layer tissue generates, which is unfeasible currently in the human eye. The sheep model offered advantages as a candidate as, the orbit of the sheep is large enough to provide conjunctival that could be used in a piece of specialised equipment for the accurate measuring TEER, the circulating Ussing chamber technique (Martin J. Hug, The European Working Group on CTFR Expression, 2002 Unpublished, Lee *et al* 1997). Another important advantage of this model was the freely available amounts of tissue. No literature currently exists in the denudation of the eye, the preparation of conjunctival tissue and the trans-epithelial electrical resistance of this type of tissue.

The procedure for the removal of the orbits was developed solely by the author. The preparation of sheep conjunctival tissue for measuring its TEER was mirrored on the protocol used in the preparation of human conjunctival tissue. Scanning electron microscopy showed that the conjunctival was covered by polygonal shaped cells in a continuous layer, which is morphologically different from the underlying connective tissue, in agreement with Weyrauch (1984). When the surface morphology is compared to human conjunctival epithelium (figure 3.1), the two samples have similarly shaped cells, at higher magnification the apical membrane was covered by microvilli-like cellular protrusions, although they appeared to be shorter in length than those found on human tissue. The underlying connective tissue layer also contained greater levels of fibrous tissue compared to the episclera of the human eye.

Briefly, the immunostaining showed that the tissue is suitable for GMA embedded investigations with the retention of antigenicity. Morphological analysis showed that the *ovis aries* conjunctival is a stratified epithelial tissue mirroring the human conjunctival epithelium. This is in agreement with Weyrauch (1983), who described the conjunctiva of domestic ruminants as Stratified cubiodal, also present are stratified non-keratinsed squamous epithelium, stratified mixed.

The stratified model tissue generated a TEER that was multiple times greater than that of the *in vitro* models. Possibly indicating that the conjunctival epithelium generates a high resistance.

## 4.6 Conclusion

*Conjunctival epithelial cell models provide an accurate experimental model of the human conjunctival epithelium.*

So does the hypothesis hold true?

In summary all the conjunctival epithelial cell models have shown epithelial characteristics in their morphology. The *in vitro* models all stained positively for tight junctions, intermediate junctions and keratin filaments. In terms of keratin filaments the primary cells also displayed positive staining. The stratified models also had suggestive positive staining for the pan keratin antibody. One vital piece of data was the functional TEER data to determine the strength of their polarised barrier; the conjunctival cell lines produced weak resistance, suggesting leaky tight junctions, whereas the stratified conjunctival models produced an extremely high resistance, even when subtracting the inert and background resistance of the tissue. Without any data from primary cell cultures or direct resistance measurements from human tissue, the determination of whether the resistance of the cell lines is a true reflection of the conjunctival epithelium cannot be made. Therefore, the hypothesis, in part, can be accepted, but until this specific issue is resolved, the models should therefore be, within reason, used in parallel with each other when further testing the conjunctival epithelium.

# Figure 4.1a Phase contrast microscopy of the ChWk cell line model

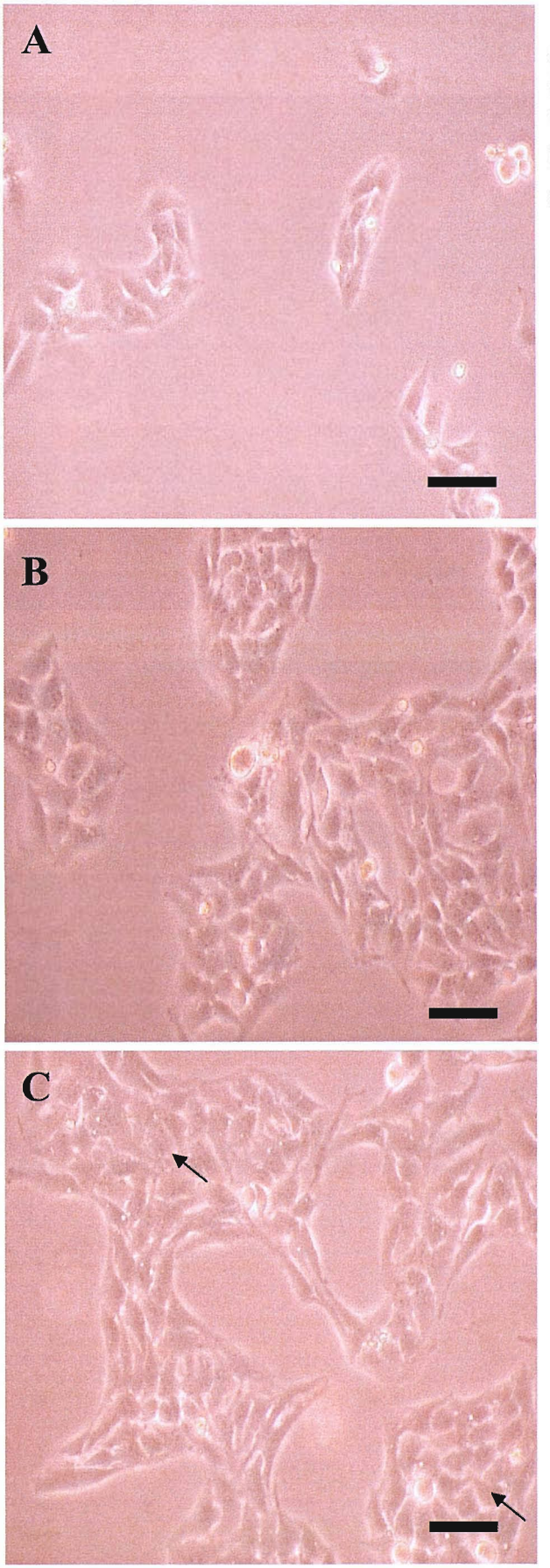


Micrographs A, B and C show the cell morphology of the ChWk cells after plating down in a new culture vessel at 1x $10^6$ml.

Micrograph A.

Once adhered, cells flatten out and started to grow out across the surface. At first their appearance was fibroblastic and elongated in shape, with cell-cell contacts seen in between cell extremities

Micrograph B.

Colonies formed a net-like pattern and continued to divide joining until a confluent layer was formed.

Micrograph C.

The cells resembled a more polygonal shape when present in the larger colonies (shown by the arrows).

Bar = 20 μm

# Figure 4.1b Phase contrast microscopy of the IOBA-NHC cell line model

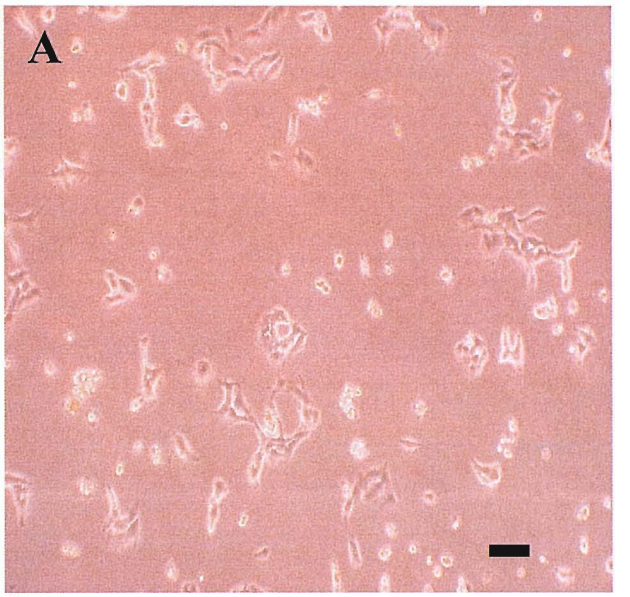


Micrographs A, B and C show the cell morphology of the IOBA-NHC cells after plating down in a new culture vessel at 1x $10^6$ml.

Micrograph A.

Individual IOBA-NHC cells plated down and flattened out. They took a slightly fibroblastic / elongated look.

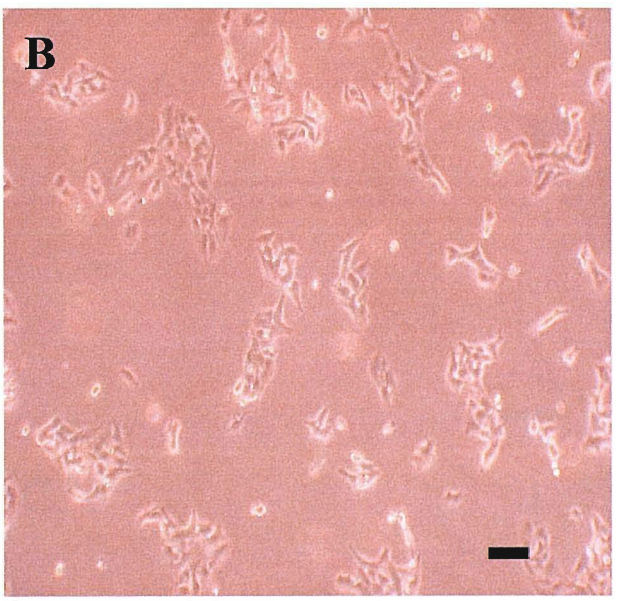


Micrograph B.

Cell-cell contacts were made when colonies divided across the culture vessel forming a net-like pattern

Bar = 20 μm

# Figure 4.1c Phase contrast microscopy of the 16HBE 14o- cell line model

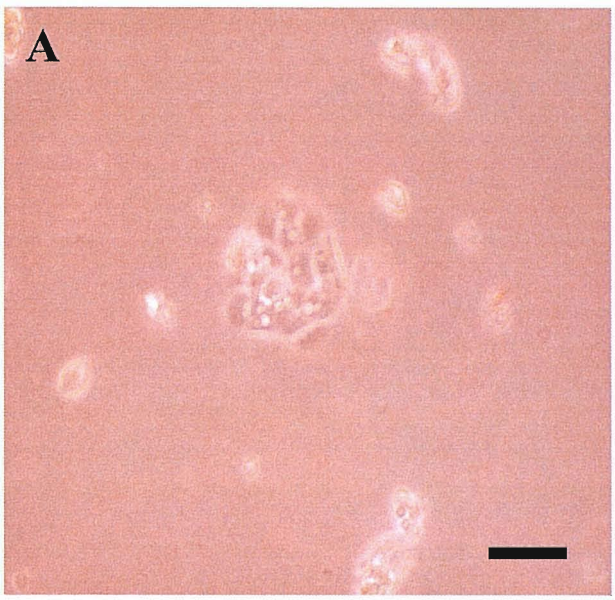


Micrographs A, B and C show the cell morphology of the 16HBE 14o- cells after plating down in a new culture vessel at 1x $10^6$ml.

Micrograph A.

16HBE 14o- cells settled individually, adhered down, flattened out and proceeded to divide.

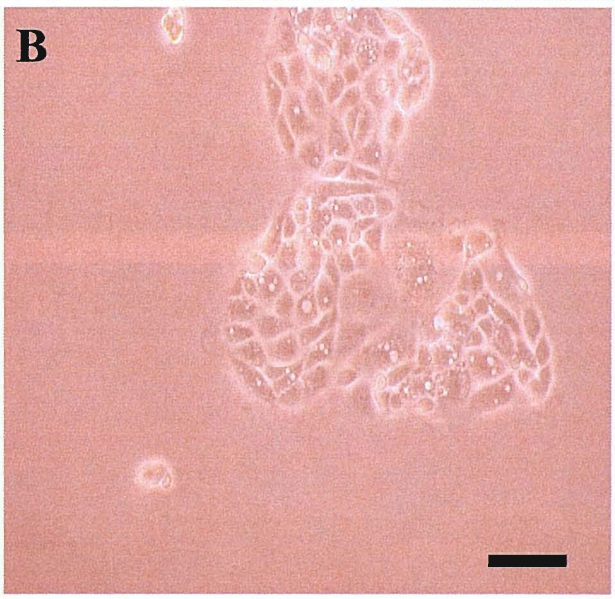


Micrograph B.

Cells took a polygonal shape in their colonies. Colonies divided across the gaps on the culture vessel surface towards each other.

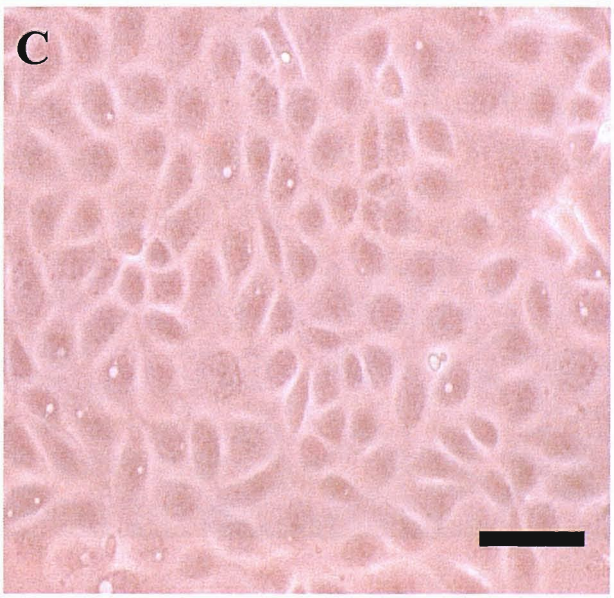


Micrograph C.

A fully confluent layer was achieved (post 4-5 days of plating down) and the cells within their colonies were classically polygonal.

Bar = 20 μm

# Figure 4.2a ChWk surface morphology

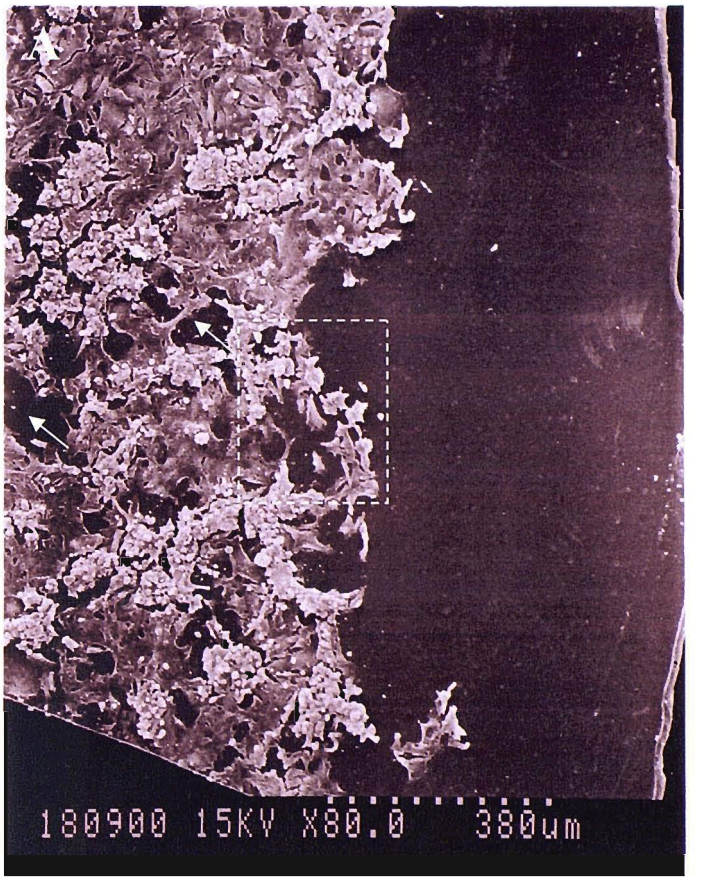


Micrograph A. This micrograph shows the general surface morphology of the ChWk cells. Gaps can be identified within the layer (highlighted with the white arrows). The field shown in micrograph B is shown by the highlighted box.

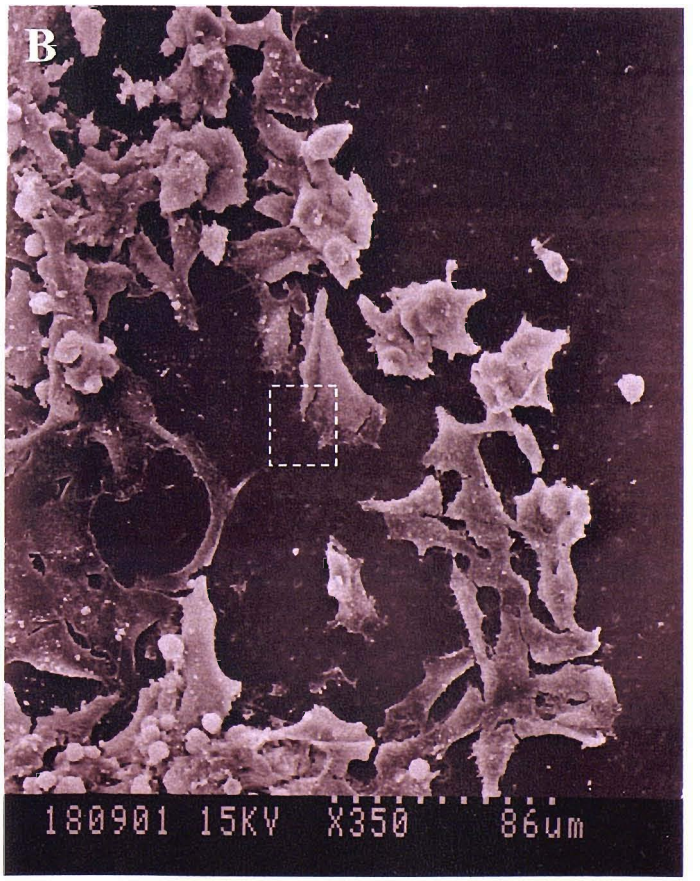


Micrograph B. This shows the rough surface features of the individual ChWk cells with their elongated and flattened shape. The field shown in micrograph C is shown by the highlighted box.

# Figure 4.2b ChWk surface morphology


Micrograph C. This shows the distribution of cellular processes and the microvilli. On the edge of the cells, cellular processes can be identified extending from the migrating cell (highlighted with the white arrows).

# Figure 4.3a IOBA-NHC surface morphology

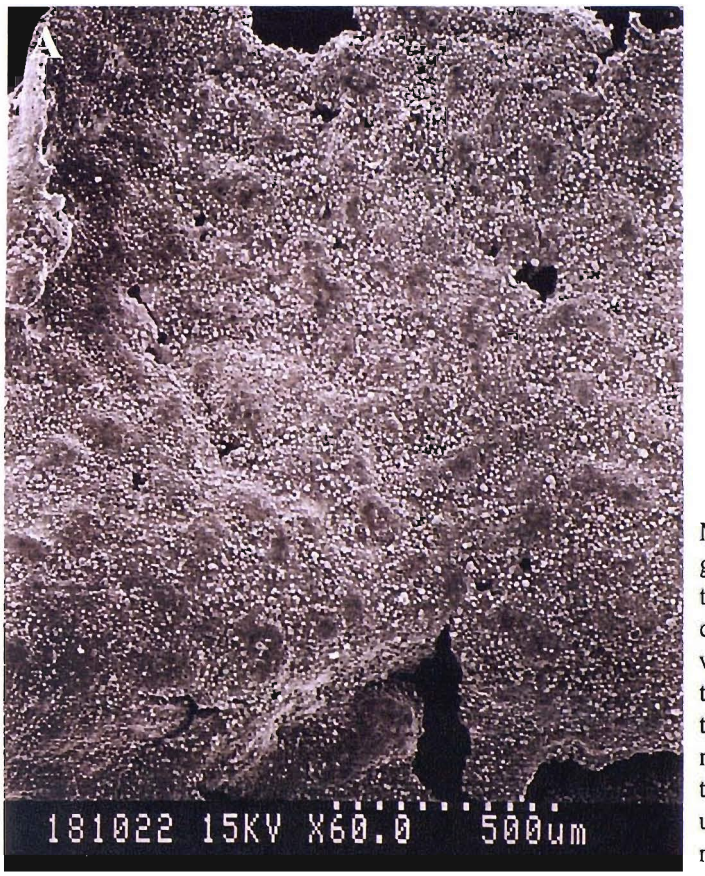


Micrograph A – shows the general surface features of the IOBA-NHC cells. The cells form a confluent layer with tight cell-cell contacts, the gaps in between the cells that can be seen in the micrograph could be due to the processing stages undertaken for electron microscopy.

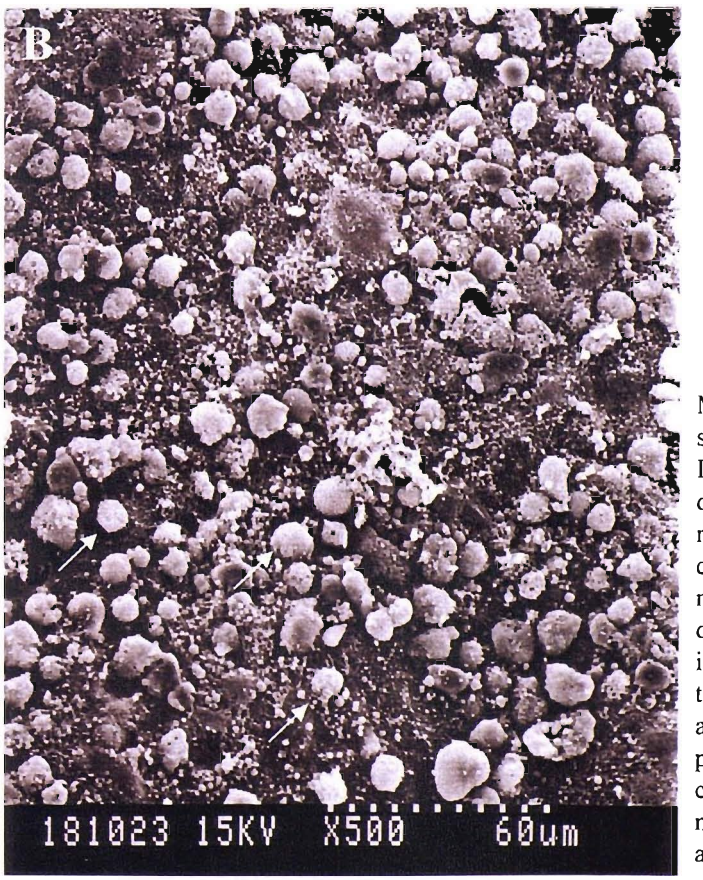


Micrograph B – shows the surface features of the IOBA-NHC cells in greater detail. Once the cell layer reaches a confluent state, cell start to stack up on the mono-layer these non-dividing cells can be identified (highlighted with the white arrows). The amount of these cells present could be due to culture conditions being maintained pass the point of a confluent epithelial layer.

# Figure 4.3b IOBA-NHC surface morphology

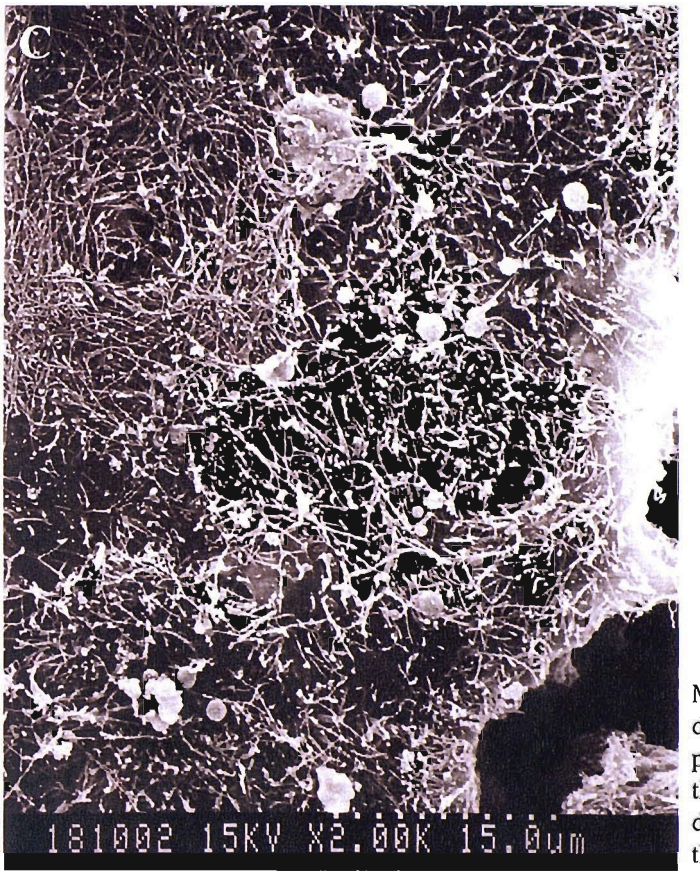


Micrograph C – shows the distribution of cellular processes on the surface of the cells as well as some dead cells (highlighted with the white arrow).

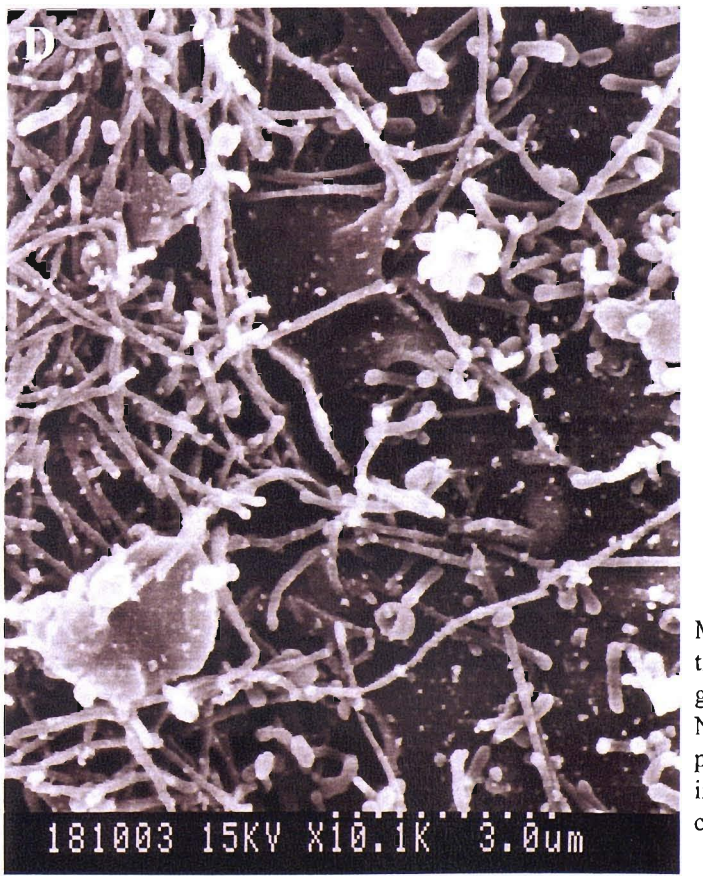


Micrograph D – shows the that the cellular processes, in greater detail, on the IOBA-NHC. These cellular processes show an incomplete coverage of the cell surface.

# Figure 4.4a 16HBE 14o- surface morphology

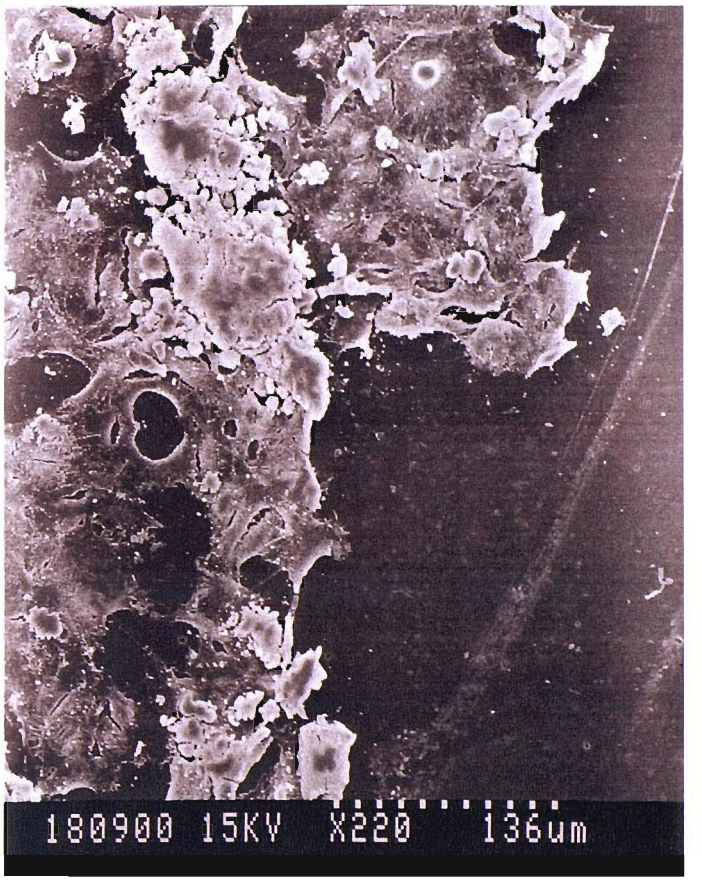


Micrograph A – shows the general surface features of the 16HBE 14o- cell layer.


Micrograph B – shows the edge of the cell layer. The microvilli on the cell surface can also be identified.

# Figure 4.4b 16HBE 14o- surface morphology


Micrograph C – shows the microvilli on the cell surface in greater detail.

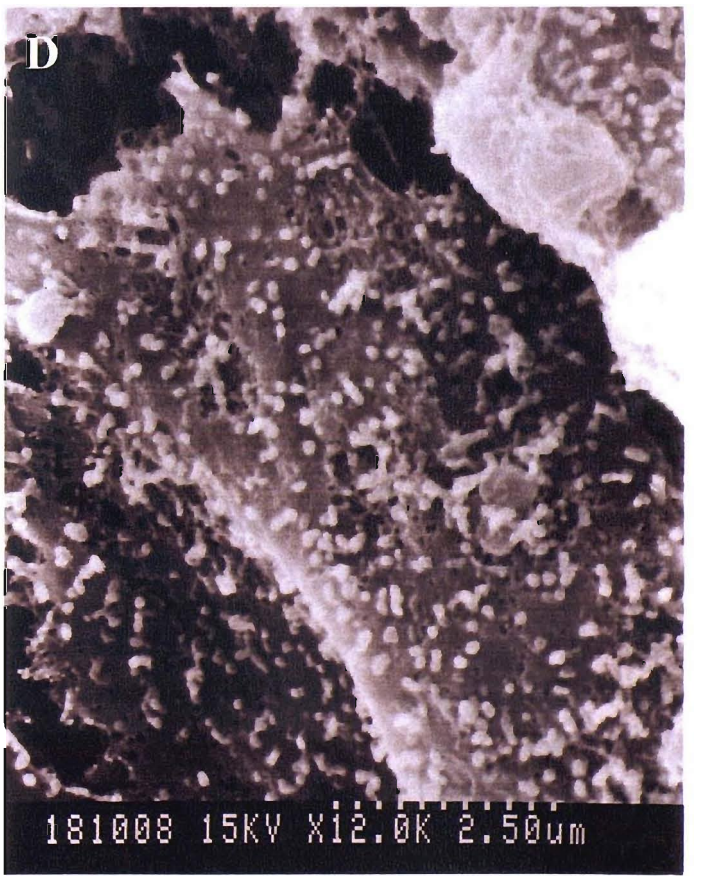


Micrograph D – shows the a high resolution image of the microvilli.

# Figure 4.5 ZO-1 immunostaining of the cell line models

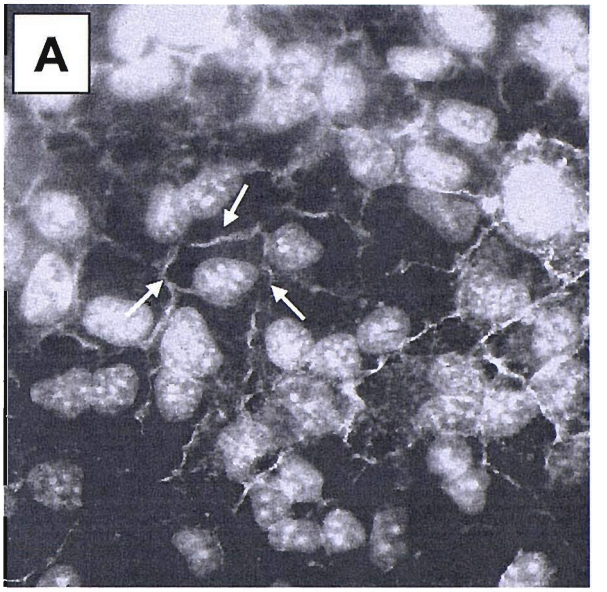


Micrograph A. This micrograph shows the continuous ring ZO-1 staining pattern of the ChWk cell line (highlighted with the white arrow). All cells stained for ZO-1, suggesting the formation of tight junctions.

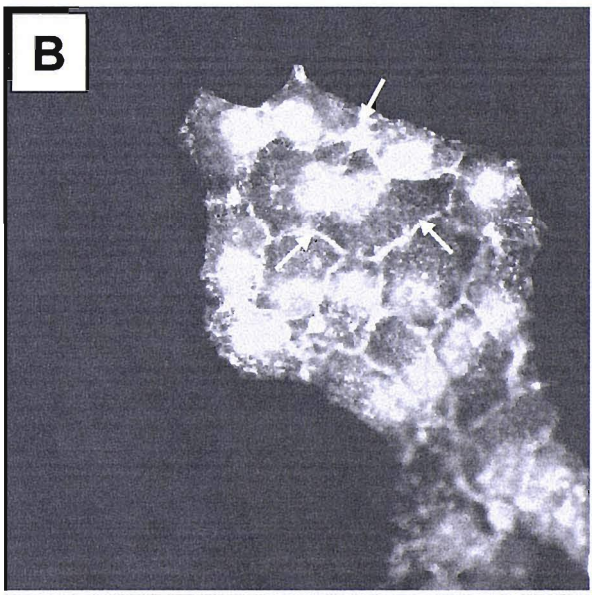


Micrograph B. This micrograph shows the continuous ring ZO-1 staining pattern of the IOBA-NHC cell line (highlighted with the white arrow). All cells showed staining for ZO-1, suggesting the formation of tight junctions.

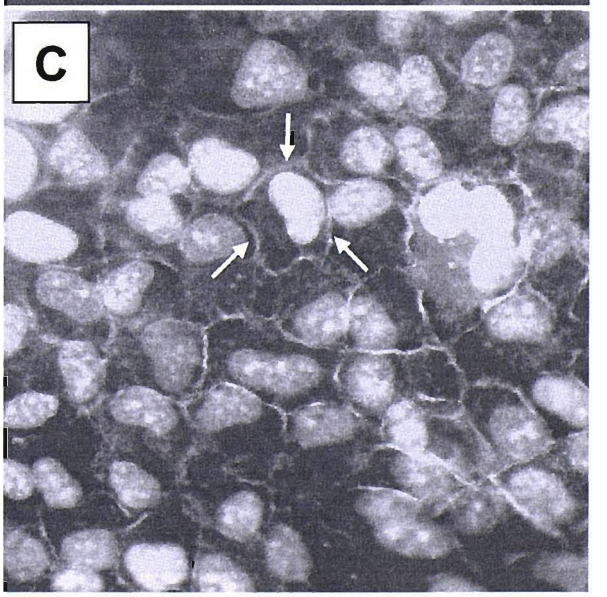


Micrograph C. This micrograph shows the continuous ring ZO-1 staining pattern of the 16HBE 14o- cell line (highlighted with the white arrow). All cells showed staining for ZO-1, suggesting the formation of tight junctions.

# Figure 4.6 E-Cadherin immunostaining of the cell line models

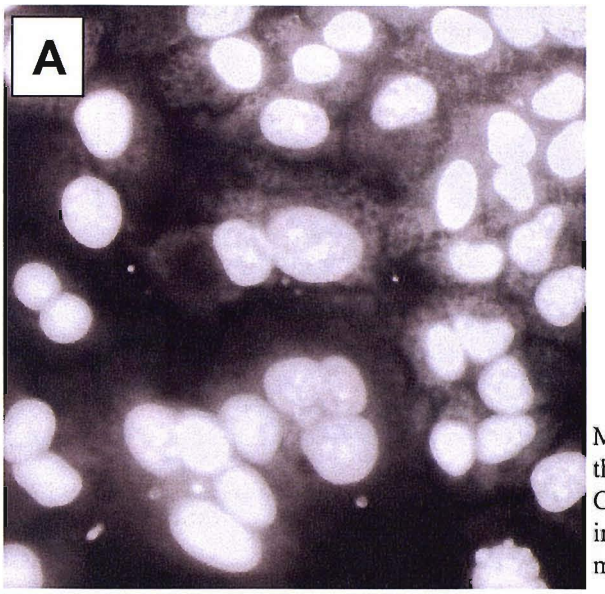


Micrograph A. this micrograph shows the E-Cadherin staining pattern of the ChWk cell line. The ChWk showed an inconsistent staining pattern with the majority of cells positively stained.

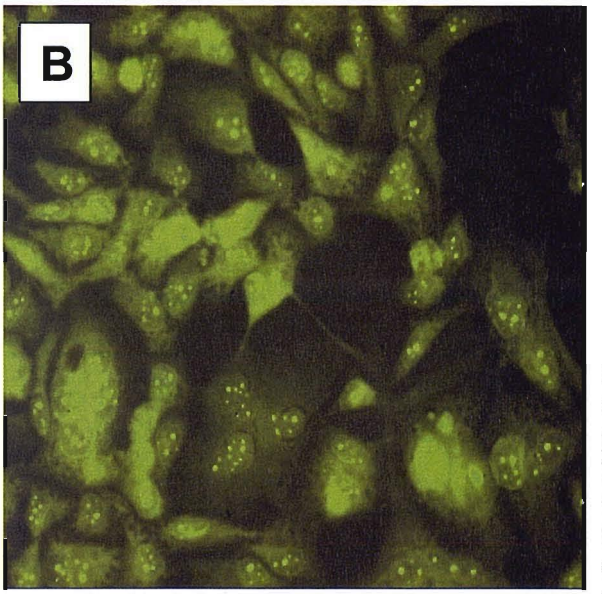


Micrograph B. This micrograph shows the E-Cadherin staining pattern of the IOBA-NHC cell line. The IOBA-NHC showed a more consistent positive stain throughout the epithelial layer although intra-cellular and some nuclear staining was observed.

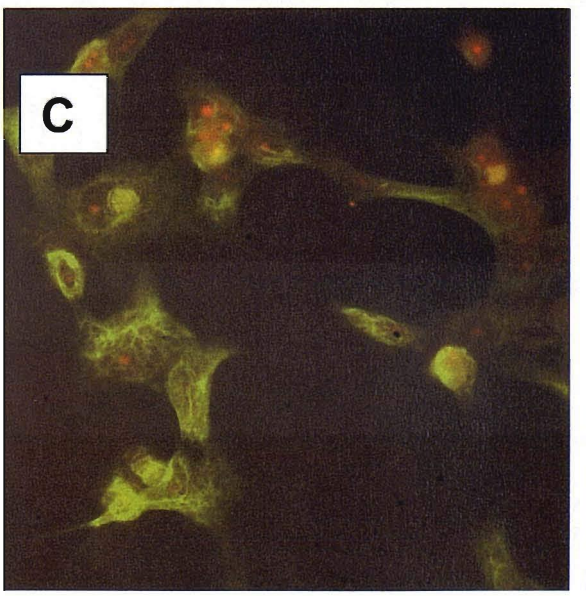


Micrograph C. This micrograph shows the E-Cadherin staining pattern of the 16HBE 14o- cell line. The 16HBE 14o- displayed staining throughout the epithelial layer suggesting the presence of E-Cadherin.

# Figure 4.7 CD44 immunostaining

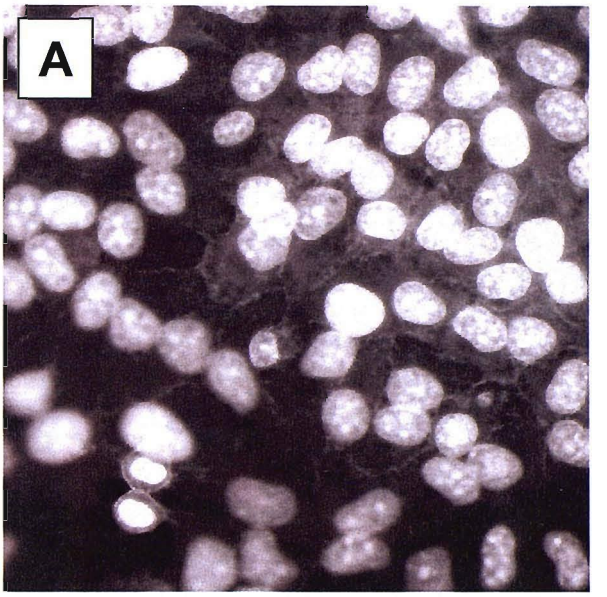


Micrograph A. This micrograph shows the CD44 staining pattern found in the ChWk epithelial cell line model. Its pattern is diffuse across the entire layer, not just confined to the membrane-membrane border regions.

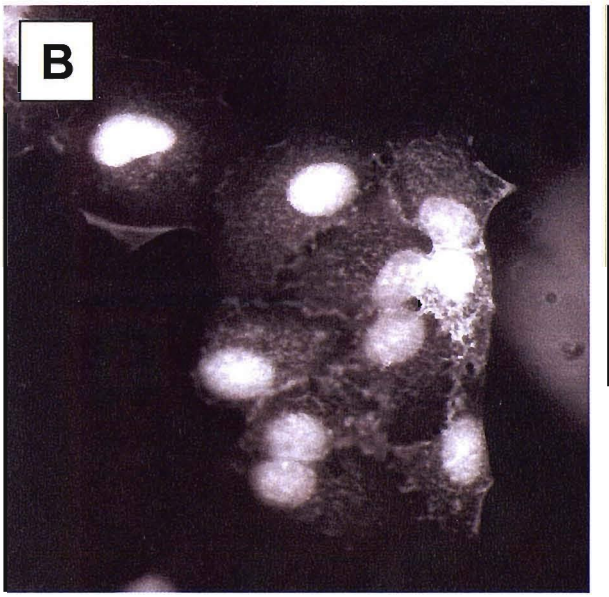


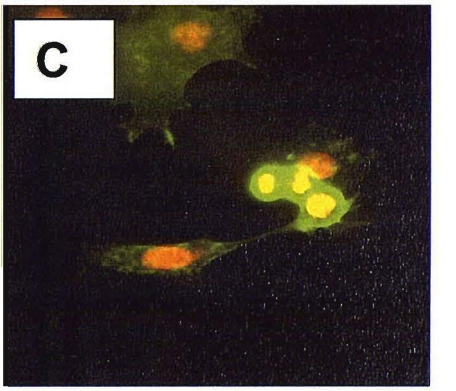


Micrographs B and C. These micrographs shows the CD44 staining pattern found in the IOBA-NHC epithelial cell line model. All cells showed a diffuse staining pattern across their membranes.

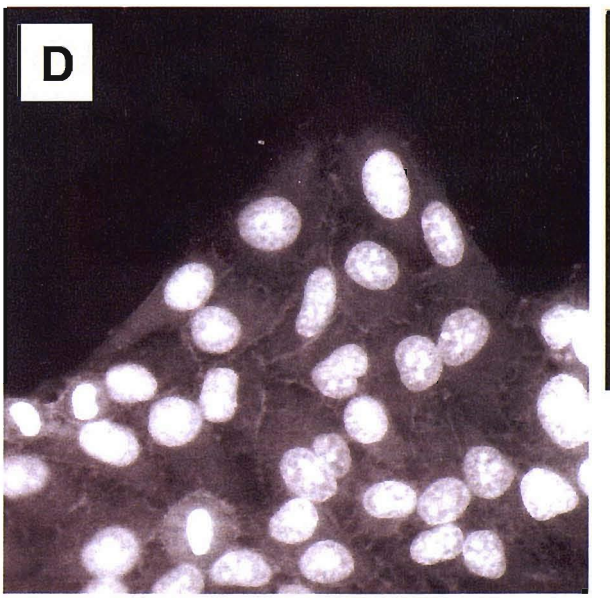


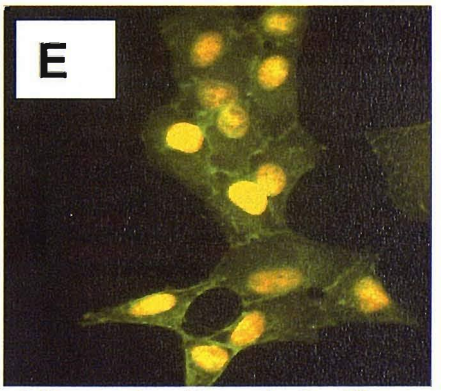


Micrographs D and E. These micrographs shows the CD44 staining pattern found in the 16 HBE 14o- epithelial cell line model. The epithelial showed diffuse staining across cell membranes.

# Figure 4.8 Keratin 13 immunostaining

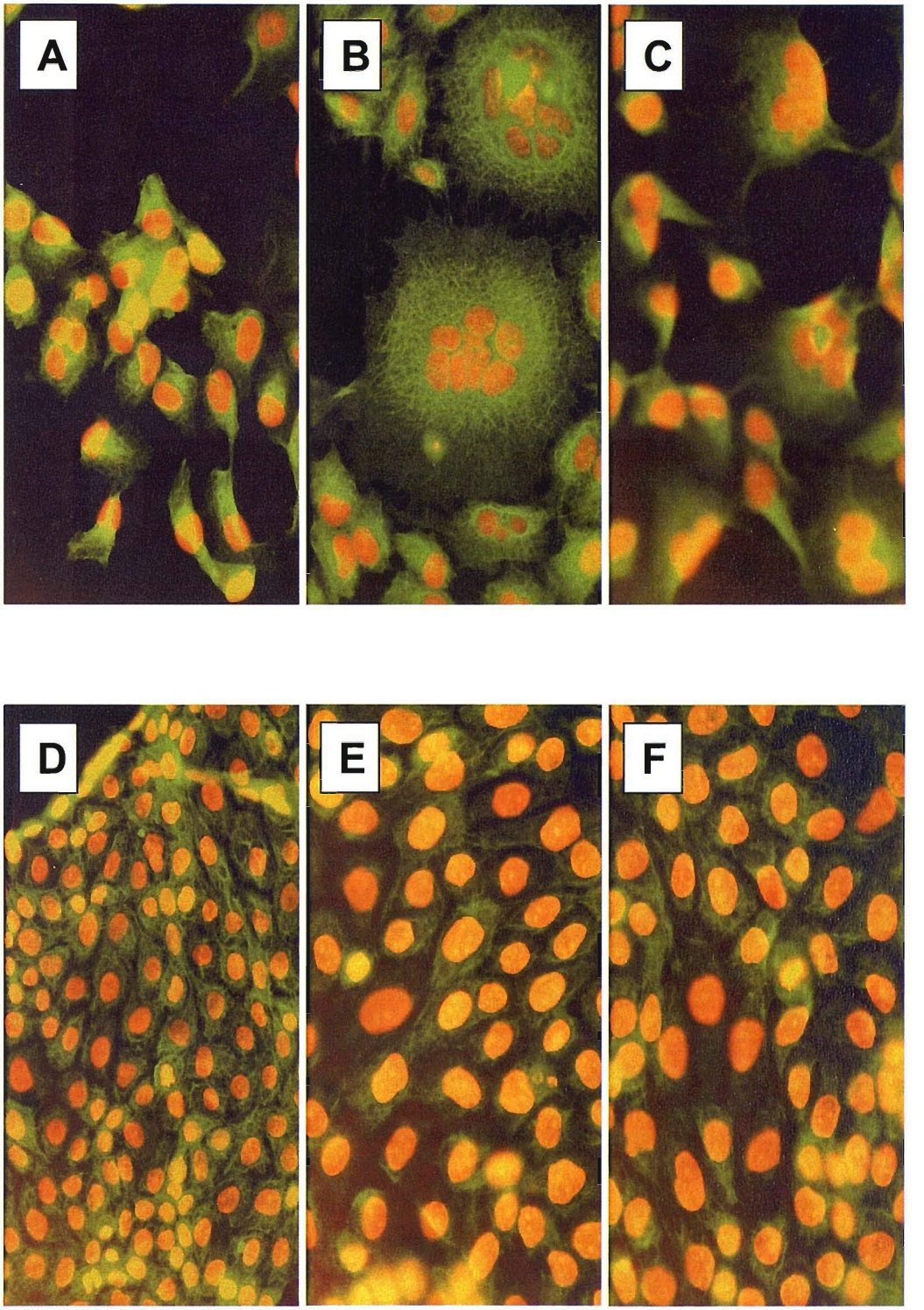


Micrographs A, B and C. These micrographs show the staining pattern of keratin 13 in the ChWk epithelial cell line model. All ChWk cell stained positively for keratin 13 across the entire cell layer, multiple-nuclear giant cells were also present within the epithelial layer (as shown in micrograph B.

Micrographs D, E and F. These micrographs show the staining pattern of keratin 13 in the 16HBE 14o- epithelial cell line model. 100% of the cells stained showed positive staining.

# Figure 4.9 Keratin 18 immunostaining

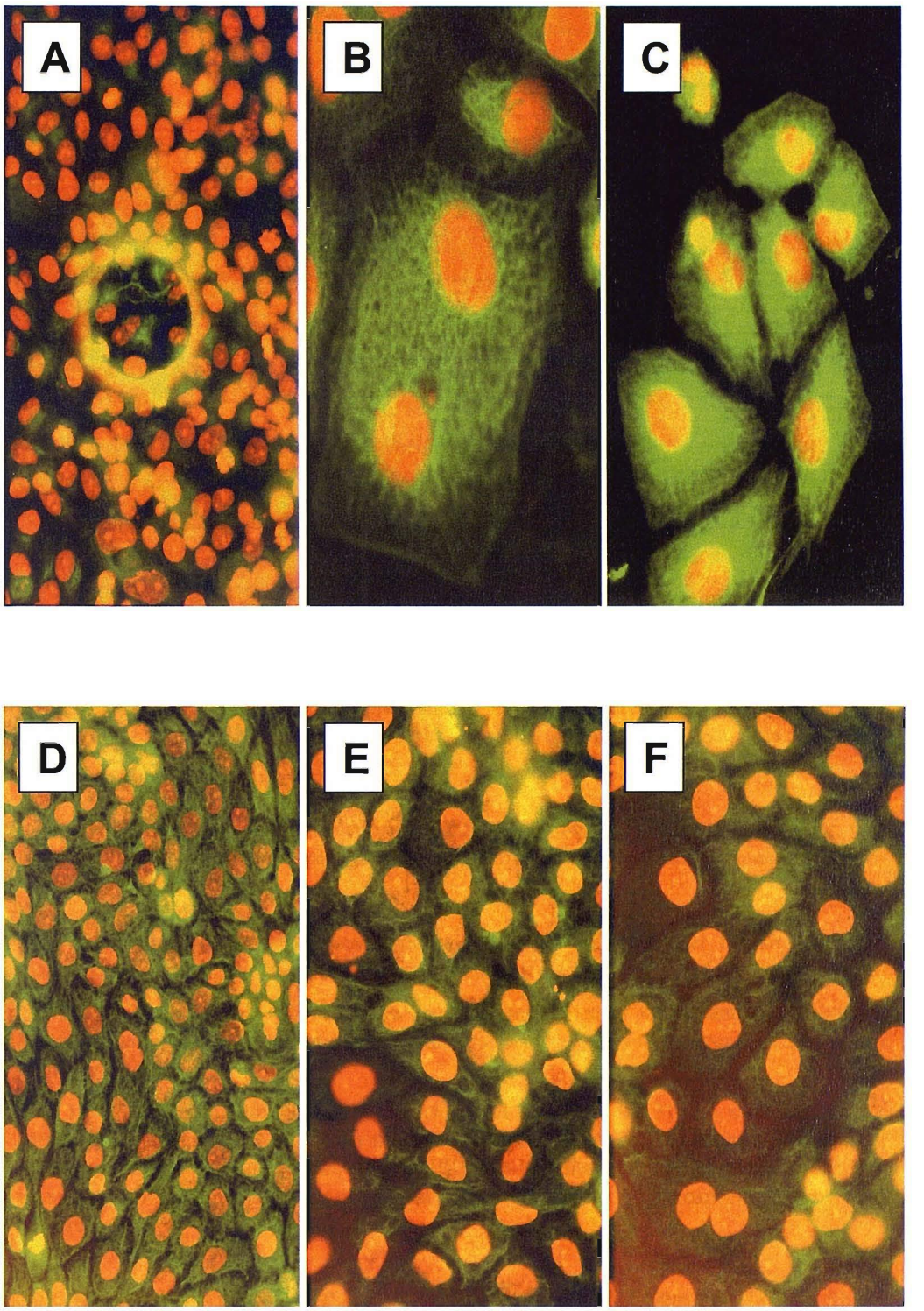


Micrographs A, B and C. These micrographs show the staining pattern of keratin 18 in the ChWk epithelial cell line model. All cells stained showed positive staining.

Micrographs D, E and F. These micrographs show the staining pattern of keratin 18 in the 16HBE 14o- epithelial cell line model. All cells stained showed positive staining.

# 4.10 Trans-epithelial electrical resistance of cell line models

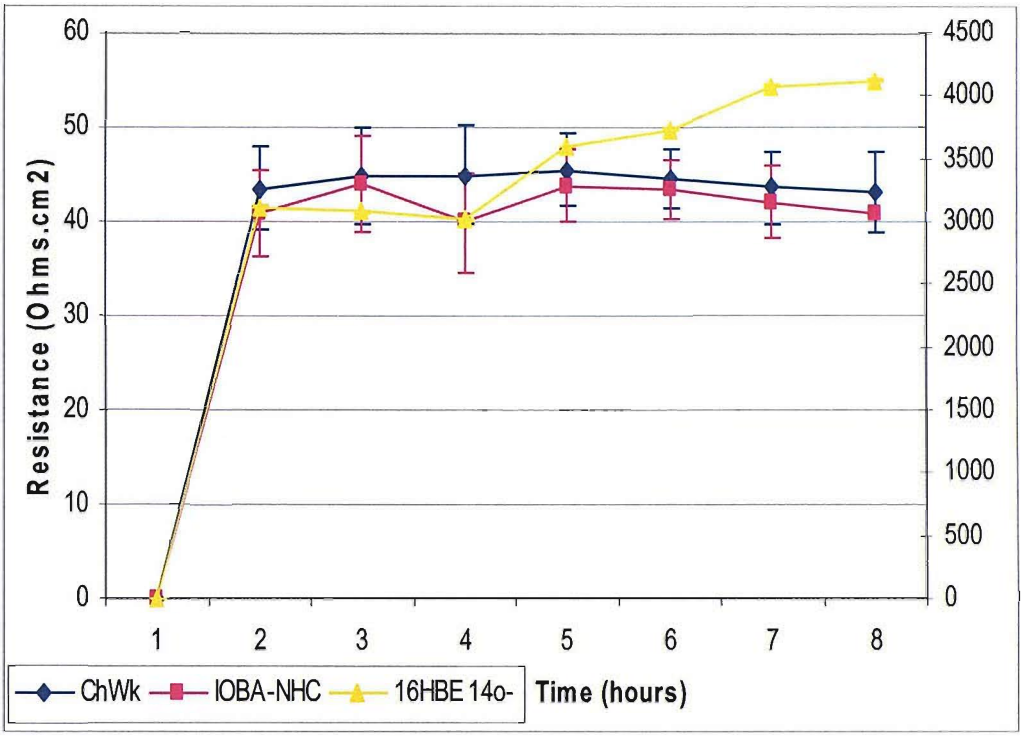


The above graphs shows the trans-epithelial electrical resistance generated by the three in vitro cell line models. The final values shown have been calculated, also corrected for control and surface area of the membrane that the cells were grown on, using the equation,

$$(Re\text{-}Rc)\ \pi r^2 = R\ (Ohms.cm^2),$$

where Re is the experimental measurement, Rc is the control value measured, $\pi$ is pi, $r^2$ is the radius of the culture membrane squared and R is the final electrical resistance.

The ChWk cell line generated an electrical resistance of 43.5 after the first hour of incubation, after this, the values reached and maintained a plateau (n = 16).

The IOBA-NHC cell line generated an electrical resistance of 40.85, and again like the other conjunctival cell line reached and maintained a plateau in values after the first hour of incubation (n = 16).

The 16HBE 14o- cell line generated an electrical resistance of 3110.5 after one hour's incubation. This values rose steadily throughout the duration of the experiment, reaching a plateau of above 4000 at the end. The 16HBE 14o-'s values were plotted on a secondary axis so that all cell lines could be plotted on the same graph and their respective values read (n = 16).

The experimental threshold is the point at which the electrical resistance produced is by the cells indicates that a confluent monolayer has been formed. The threshold is taken when the resistance value is greater than the control insert, therefore the cells have formed a confluent, polarised monolayer on the membrane.

The cells were plated down at 1 x $10^6$ml.

As can be seen by the results, the 16HBE 14o- formed 'tighter' tight junctions, indicated with the higher resistance value than both the ChWk and IOBA-NHC cell lines. These also formed tight junctions but recorded much lower levels of electrical resistance.

# Figure 4.11a Dissection of the human biopsy

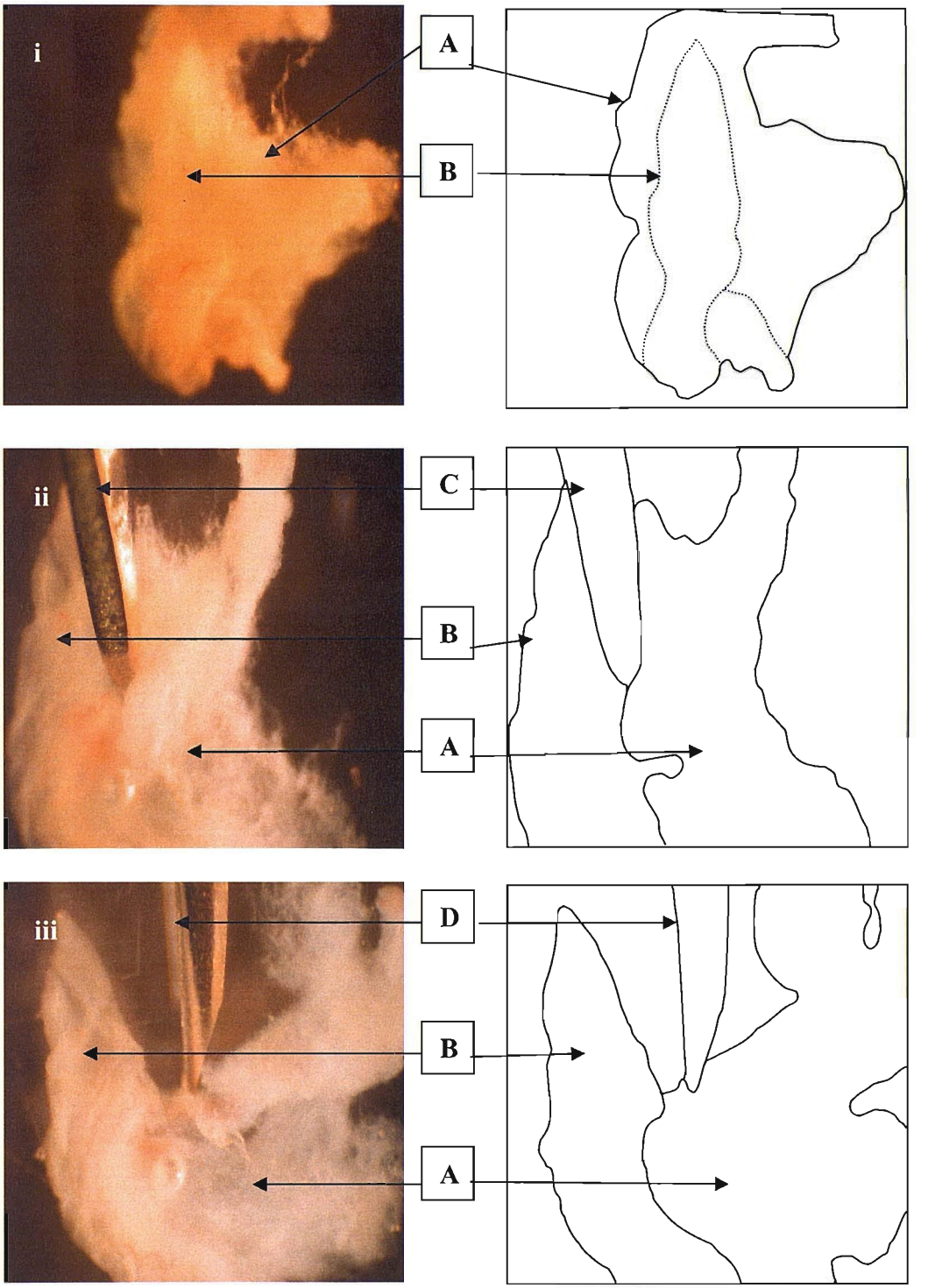


i - The biopsy and medium is placed in a sterile petri-dish, using the dissecting microscope the sample is orientated so that the epithelial layer and the underlying connective tissue can be identified (A is the connective tissue and B is the epithelial tissue).

ii - The connective tissue is then removed extremely carefully so not to damage the epithelial cell layer (C is a sterile scalpel).

iii – The remaining pieces of connective tissue is removed using the tip of a hypodermic needle (D).

# Figure 4.11b Dissection of the human biopsy

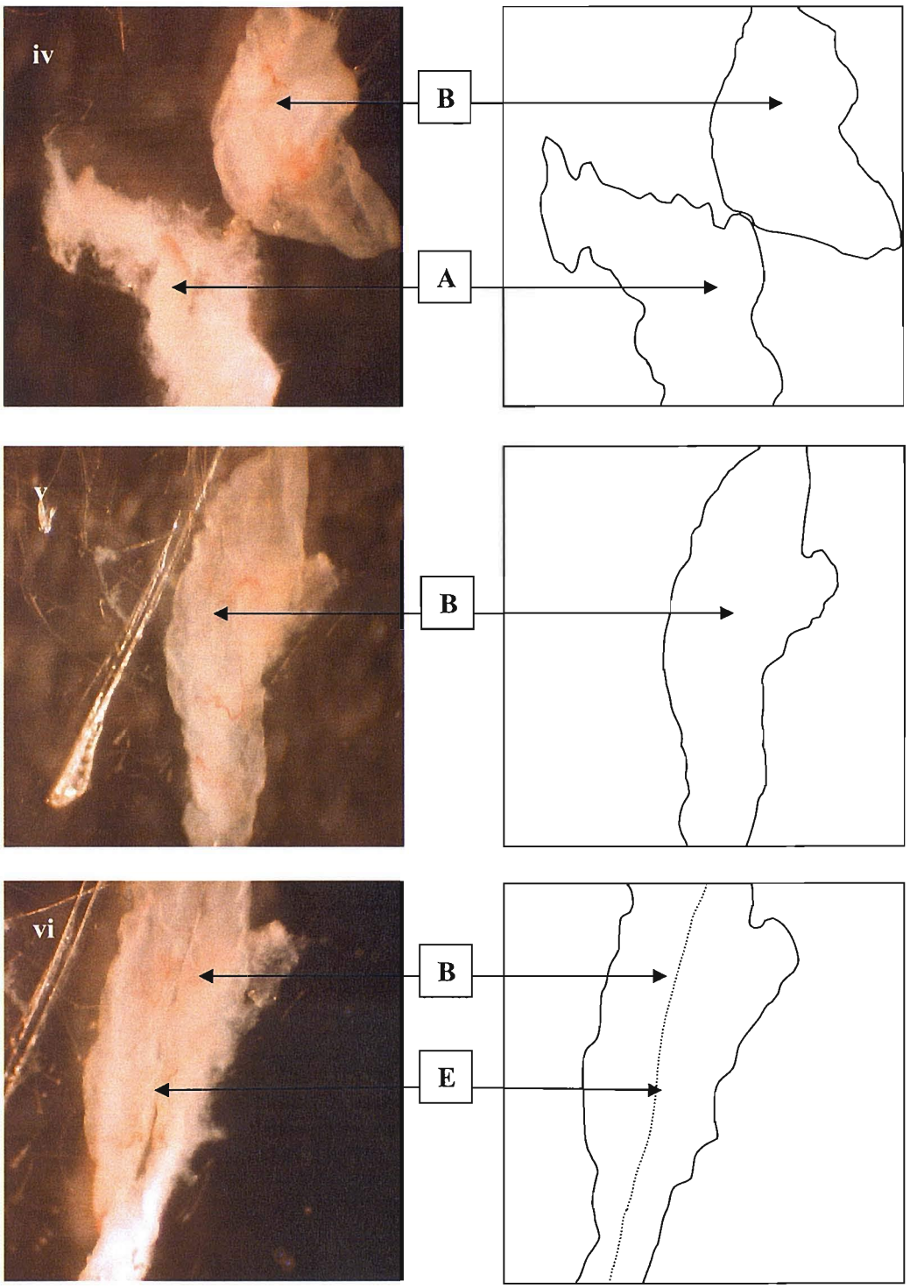


iv – The connective tissue ( A) is removed from the petri-dish and discarded.
v – The epithelial tissue (B) is orientated basal cell layer down and then flattened out.
vi – Once fully flattened the tissue can be sub-divided by scalpel dissecting along the biopsy material as shown by (E).

# Figure 4.11c Dissection of the human biopsy

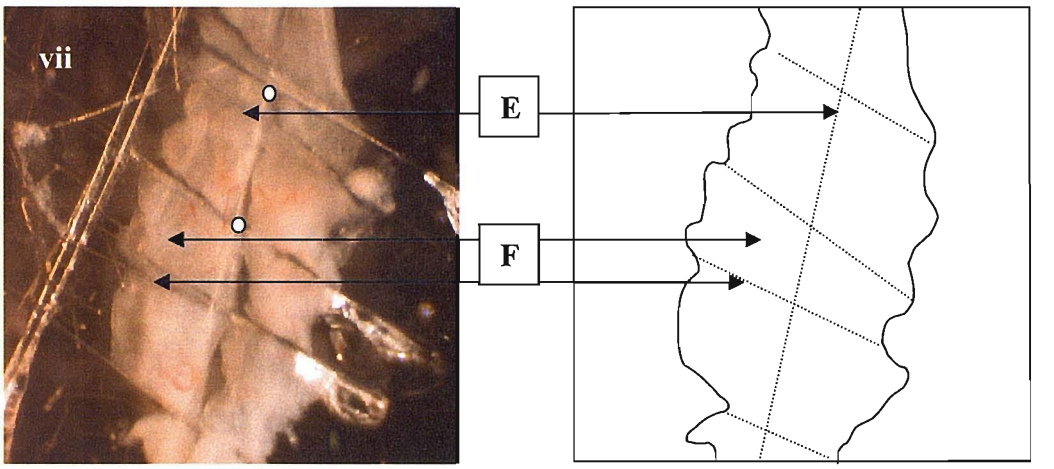


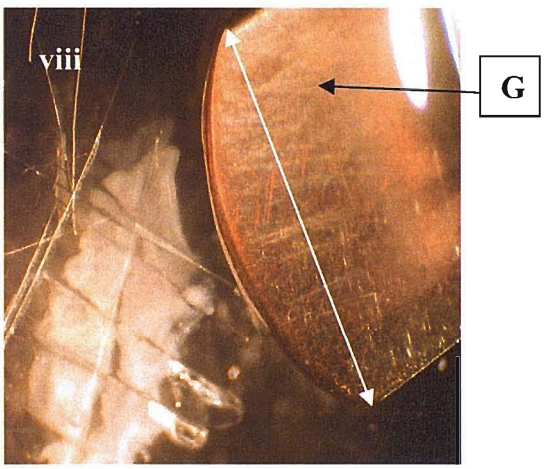


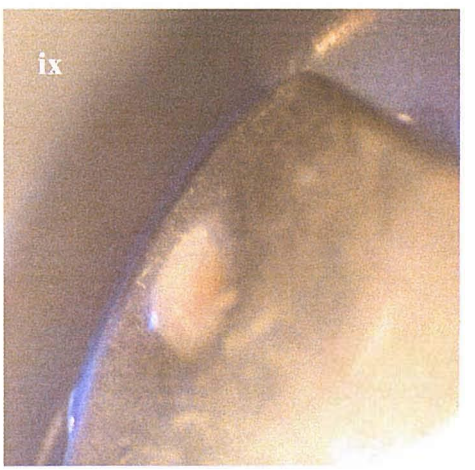



vii – The flattened the tissue can be further sub-divided by scalpel dissecting into smaller pieces (F). For scale from white point to white point is 1mm.
viii – A flat face spatula (G) is introduced so that the individual explants can be lifted and then transfer to the desired culture vessel. The end of the spatula is 4mm across (highlighted with the white line), so that an estimation of scale can be made.
ix – The explant is carefully allowed to 'slip' onto the surface of the culture vessel.
x – The explant is then flattened out to increase the surface area for maximal cell growth.

# Figure 4.12a Phase contrast of pilot primary epithelial culture

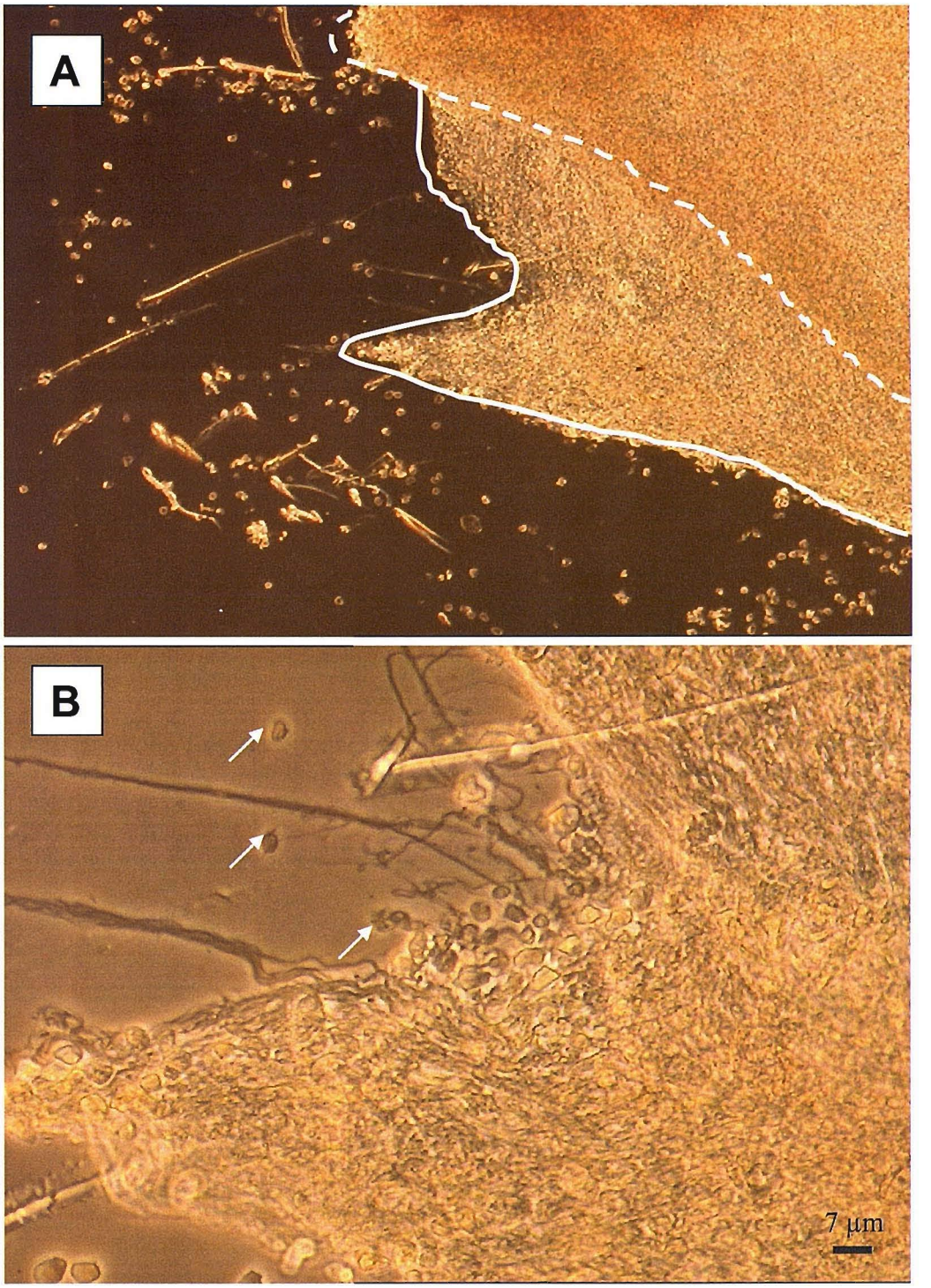


Micrograph A. This micrograph shows the edge of the epithelial layer on the explant material (highlighted with the white dotted line). The edge of the underlying connective tissue layer is highlighted with the white continuous line.

Micrograph B. This micrograph shows the same explant culture. Individual cells that have migrated from the biopsy material (highlighted with the white arrows) move out but do adhere onto the surface of the culture vessel and show no signs of surviving in the submerged culture conditions.

# Figure 4.12b Phase contrast of pilot primary epithelial culture

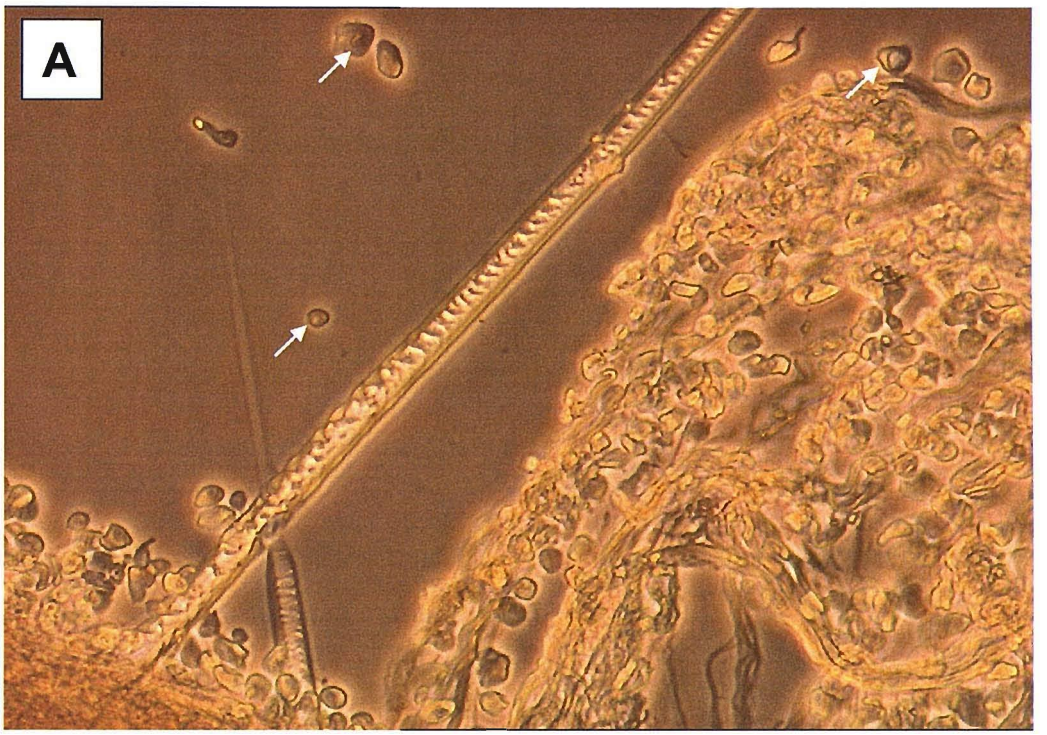


Micrograph A. This micrograph shows the cell that have migrated from the explant material (highlighted with the white arrows). These display appearance of cells that are undergoing or have undergone cellular death. Their round shape and size, with no cellular processes spiking from their surface suggest cell death, also they appear dull under the light of the microscope further suggesting poor cell health.

# Figure 4.13a Pilot primary epithelial culture

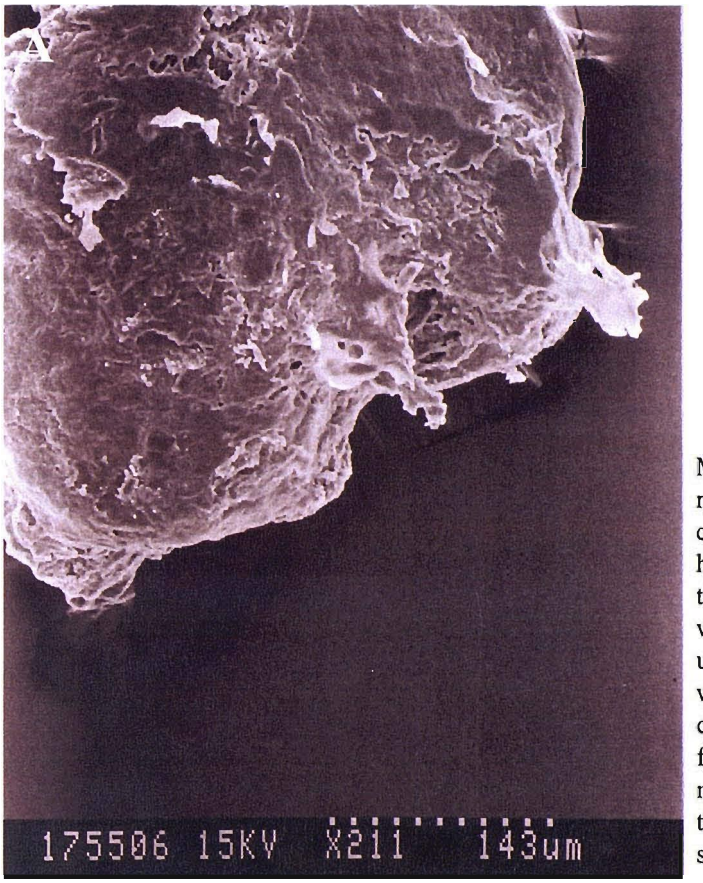


Micrograph A. This micrograph shows a conjunctival biopsy which has undergone the primary tissue culturing method and was deemed to have been unsuccessful. The biopsy was removed from the culture vessel and processed for analysis. The biopsy material seems to have lost the defined apical membrane surface features.

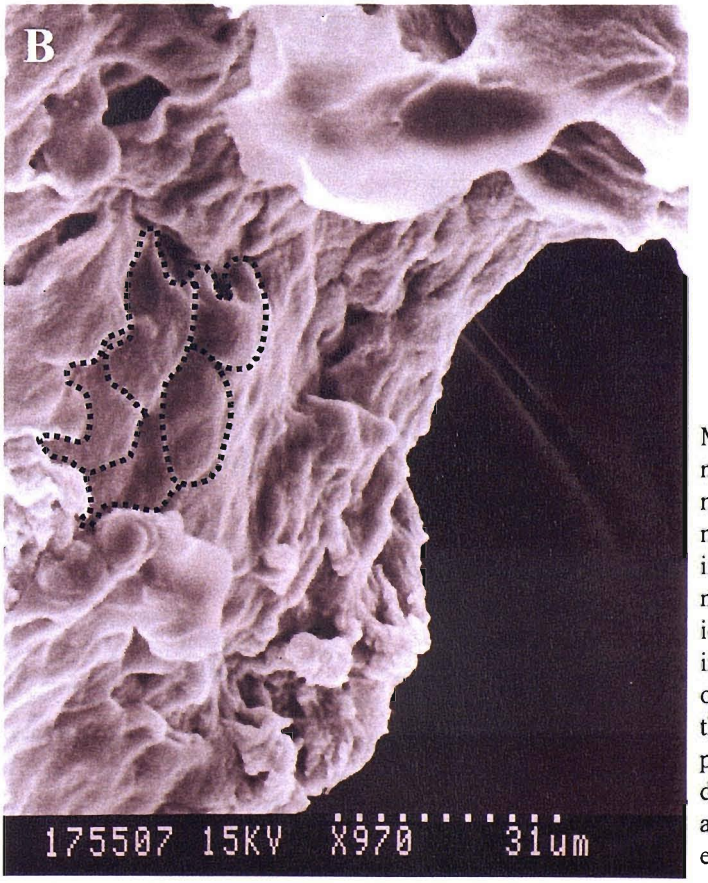


Micrograph B. This micrograph shows the same material at higher magnification. The individual apical cell membranes should be identifiable, instead the individual cells can be observed (highlighted with the dotted line), but their polygonal shape is less defined and their surface appears to be smoother than expected.

# Figure 4.13b Pilot primary epithelial culture

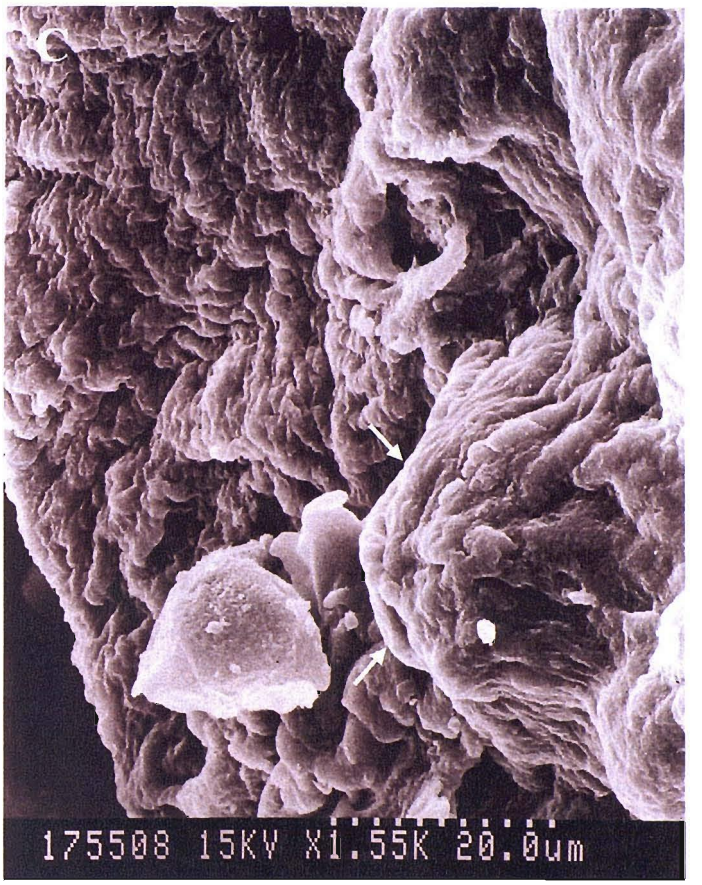


Micrograph C. This micrograph shows loss of apical membrane surface features (highlighted with the white arrows).

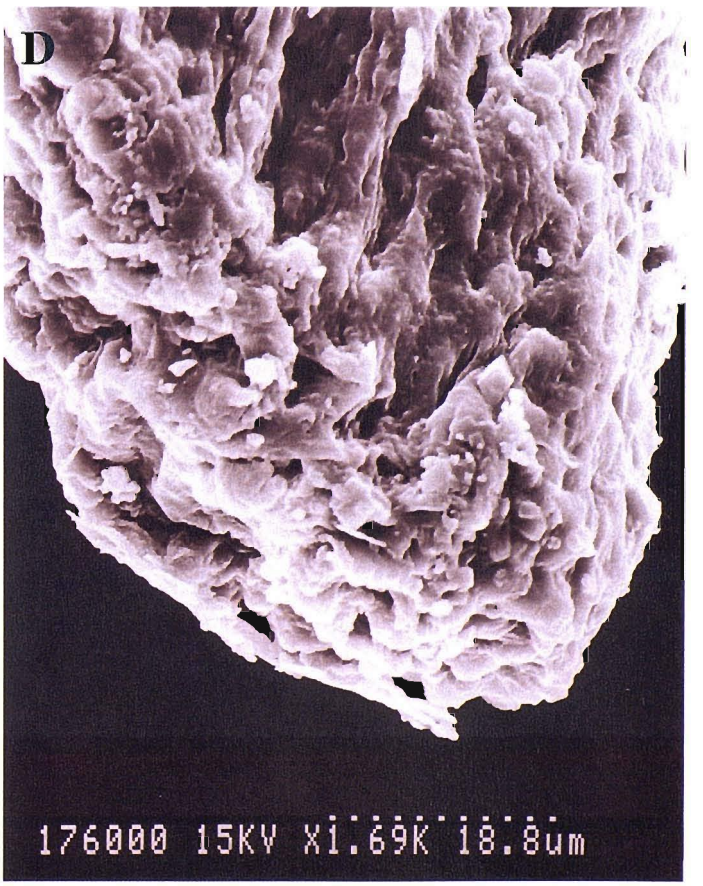


Micrograph D. In this micrograph the superficial epithelial layer of cells have lost their polygonal shape and the rough surface texture. The valleys / gaps in between the cells have also disappeared.

# Figure 4.13c Pilot primary epithelial culture


Micrograph E. In this micrograph the microvilli-like processes should be observed covering the entire apical membrane. This micrograph demonstrates that on this cultured explant no processes can be identified. The smooth surface feature observed at the lower magnification is uneven and the shape of the cells are unrecognisable as the classic epithelial polygonal shape expected.

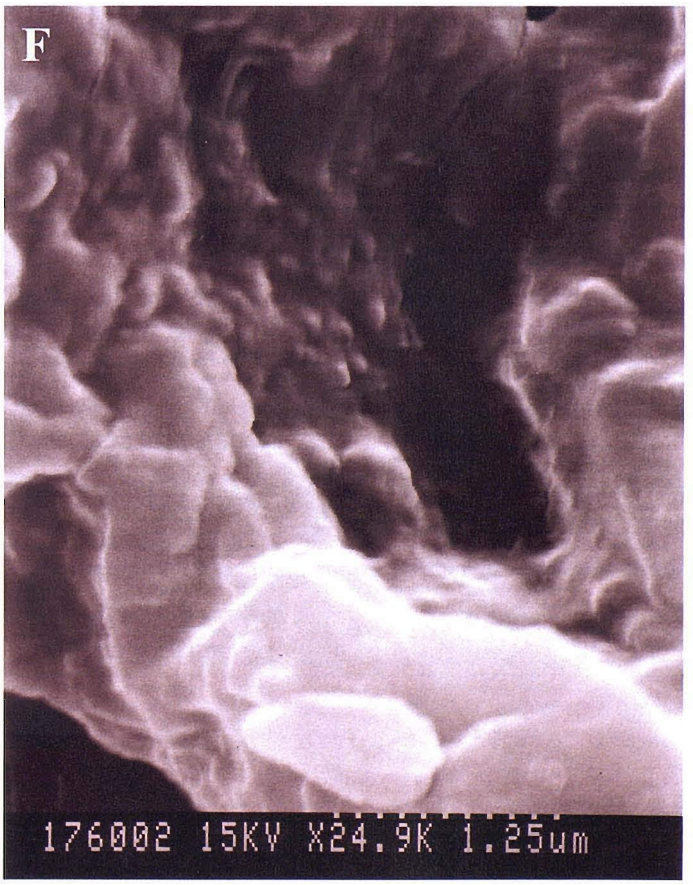


Micrograph F - this microplate shows that the explant has total cellular process loss and total cell shape loss, possibly due to internal structural integrity loss caused by cell death.

# Figure 4.14 Phase contrast of successful primary conjunctival epithelial culture

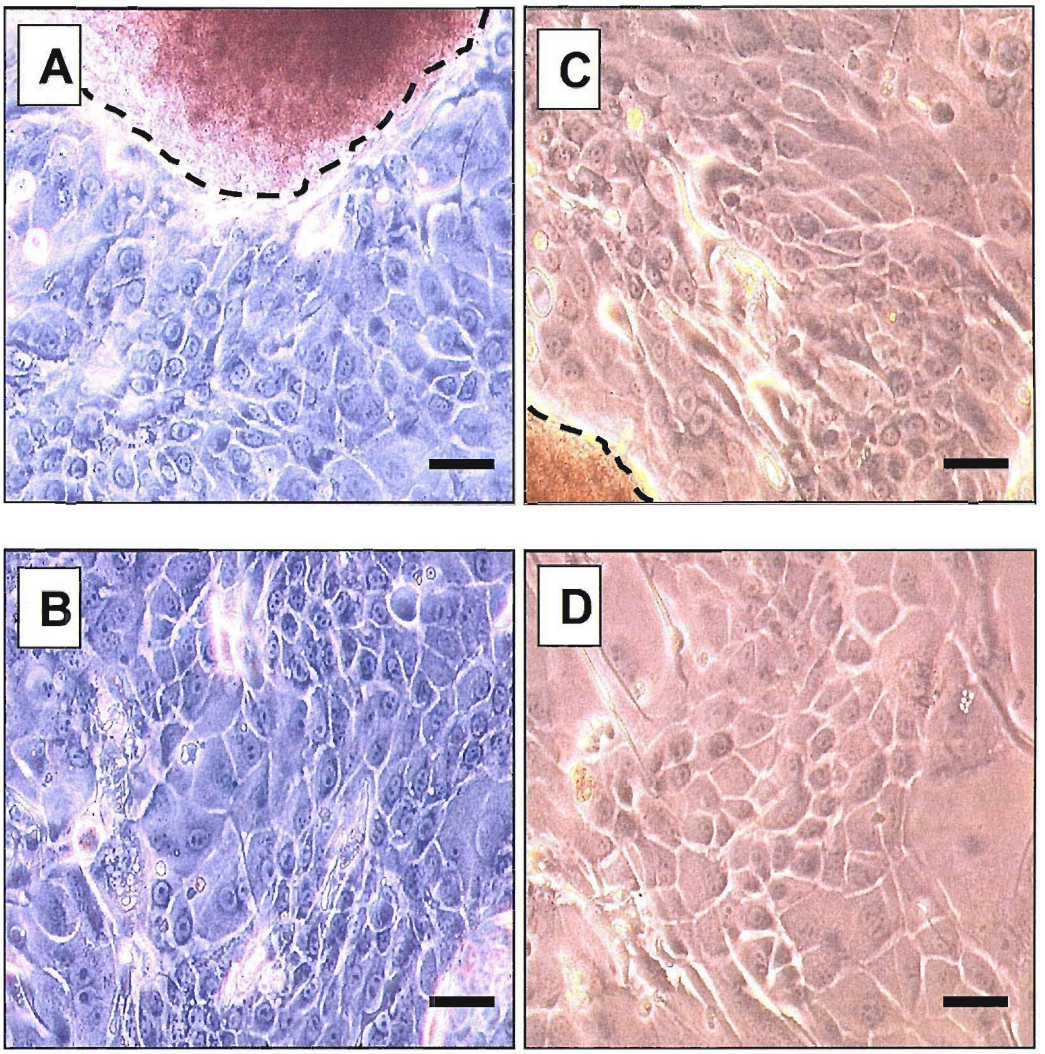


Micrograph A. This plate shows the epithelial outgrowth, from the original explant material (highlighted by the dotted line), forming a dense and compact monolayer of small polygonal shaped cells.

Micrograph B. This plate shows another field of cellular growth from the same explant sample as in micrograph A.

Micrograph C. This plate shows the epithelial outgrowth from the original piece of explant material (highlighted with the dotted line) in a different run of primary cultures.

Micrograph D. This plate shows another field of cells from the same explant sample as in micrograph C.

Scale bar = 10 μm

# Figure 4.15 Keratin 13 Immunostaining of primary conjunctival epithelium

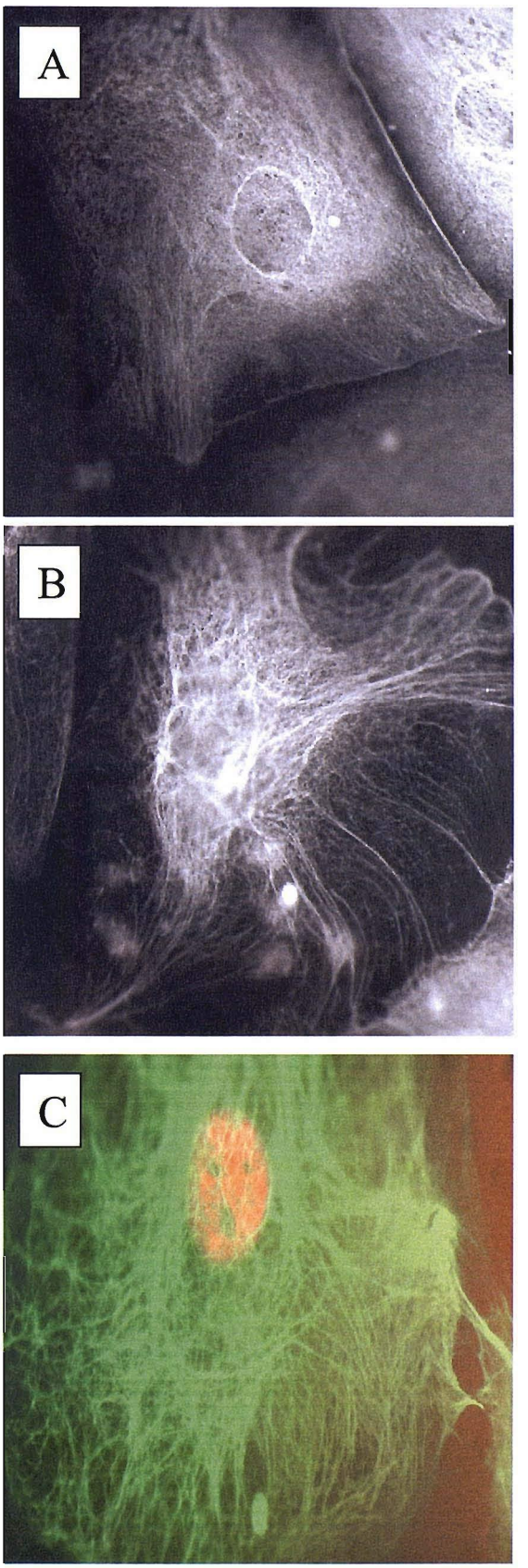


Micrograph A, B and C. These plates show the positive staining for keratin 13 of the primary cells cultured from explant biopsy material. In plate C the nuclear counter stain used was Propidium iodide.

Cultures of primary conjunctival epithelial cells were processed according to section 2.2.3. with the exception that cells were stained *in situ* on the petri-dishes.

Unfortunately scale measurements were not recorded when these micrographs were captured.

# Figure 4.16 Keratin 18 Immunostaining of primary conjunctival epithelium

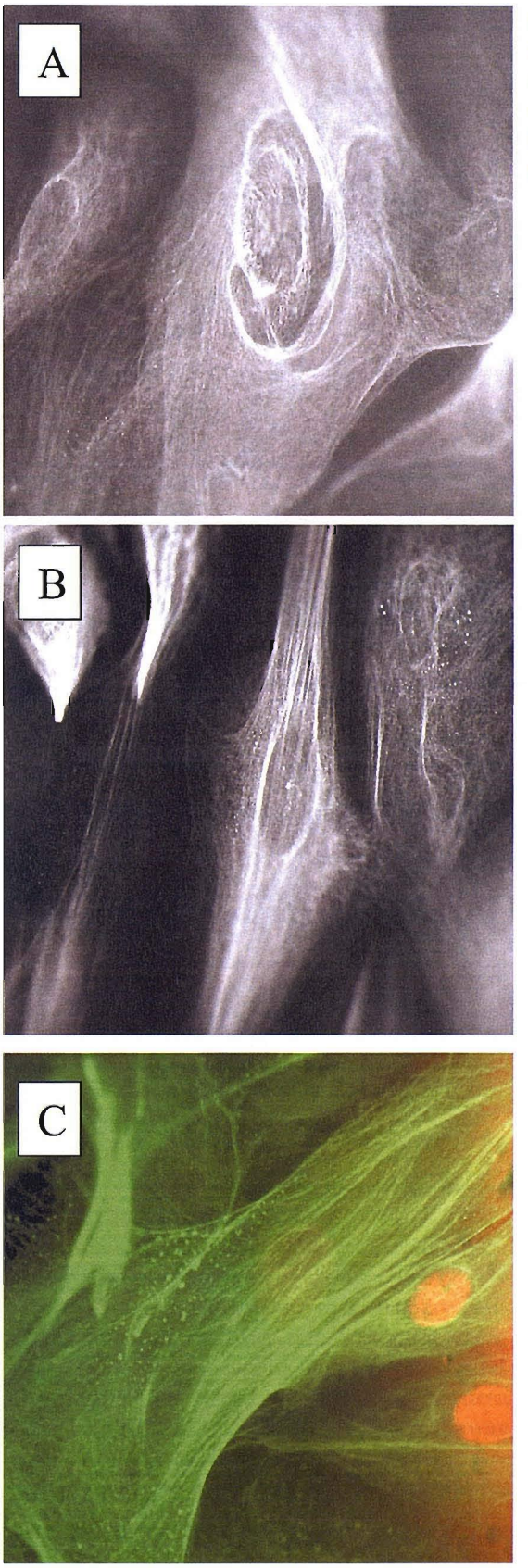


Micrograph A, B and C. These micrographs show the positive staining for keratin 18 of the primary cells cultured from explant biopsy material. In plate C, the nuclear counter stain used was Propidium iodide.

Cultures of primary conjunctival epithelial cells were processed according to section 2.2.3. With the exception that cells were stained *in situ* on the petri-dishes.

Unfortunately scale measurements were not recorded when these micrographs were captured.

# Figure 4.17a Dissection of model conjunctival tissue

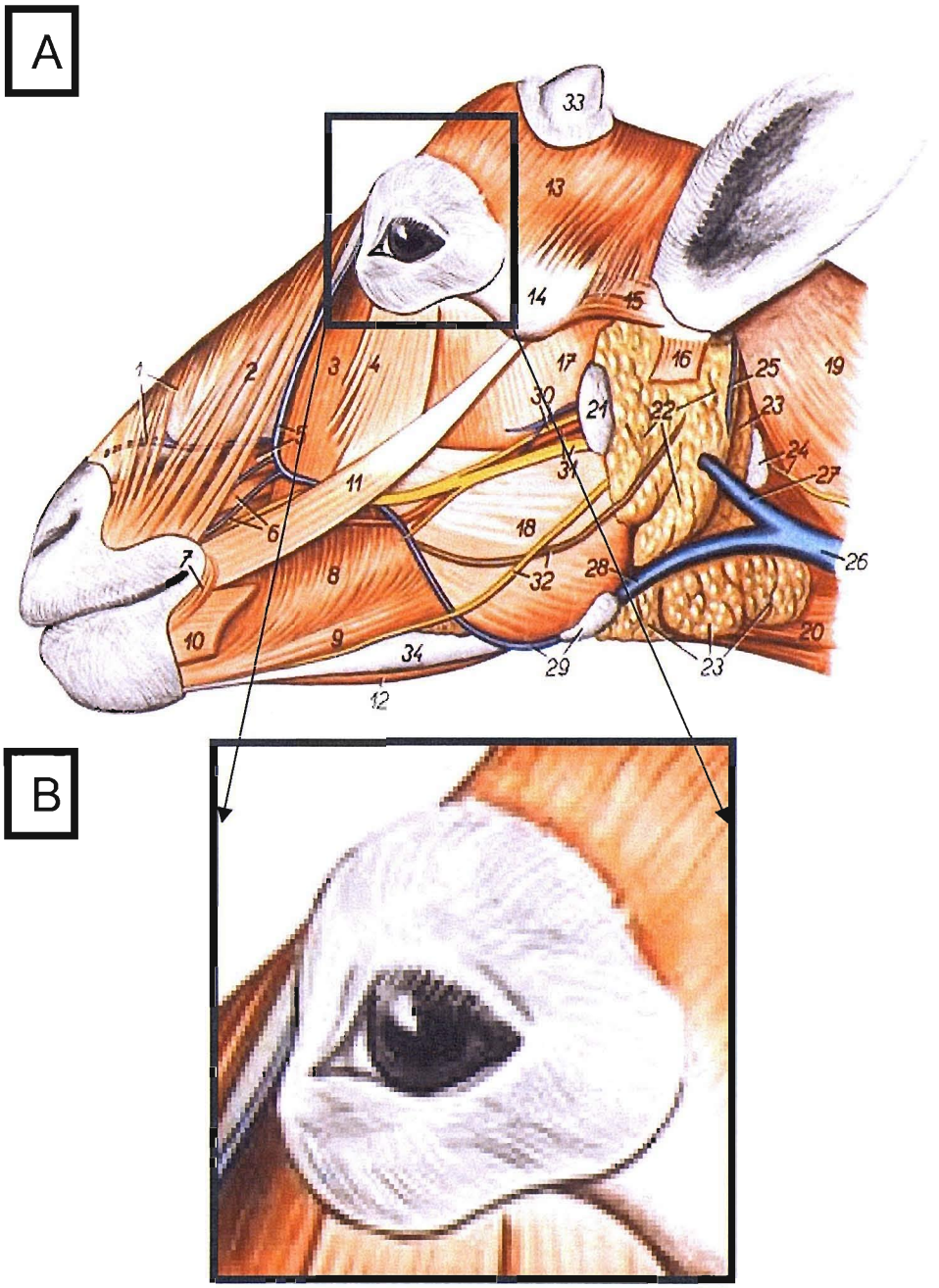


Plates A and B shows the gross anatomy of the head and orbit region. The entire, bilateral conjunctival tissue was removed from each donor animal. Briefly the skin, underlying connective tissue including muscles, vessels and nerve fibres were cut from the skull leaving an inch around the eyelid margin (B). The external portion of skin was left uncut, instead the connective tissue was gently lifted and cut away from the bone until the bone of the orbit. The eye lids were closed, then gently applying pressure the eye was drawn from its socket, the optic muscles and nerve were cut and the orbit was removed as a whole organ.

Source material from the Royal Veterinary College.

# Figure 4.17b Dissection of model conjunctival tissue

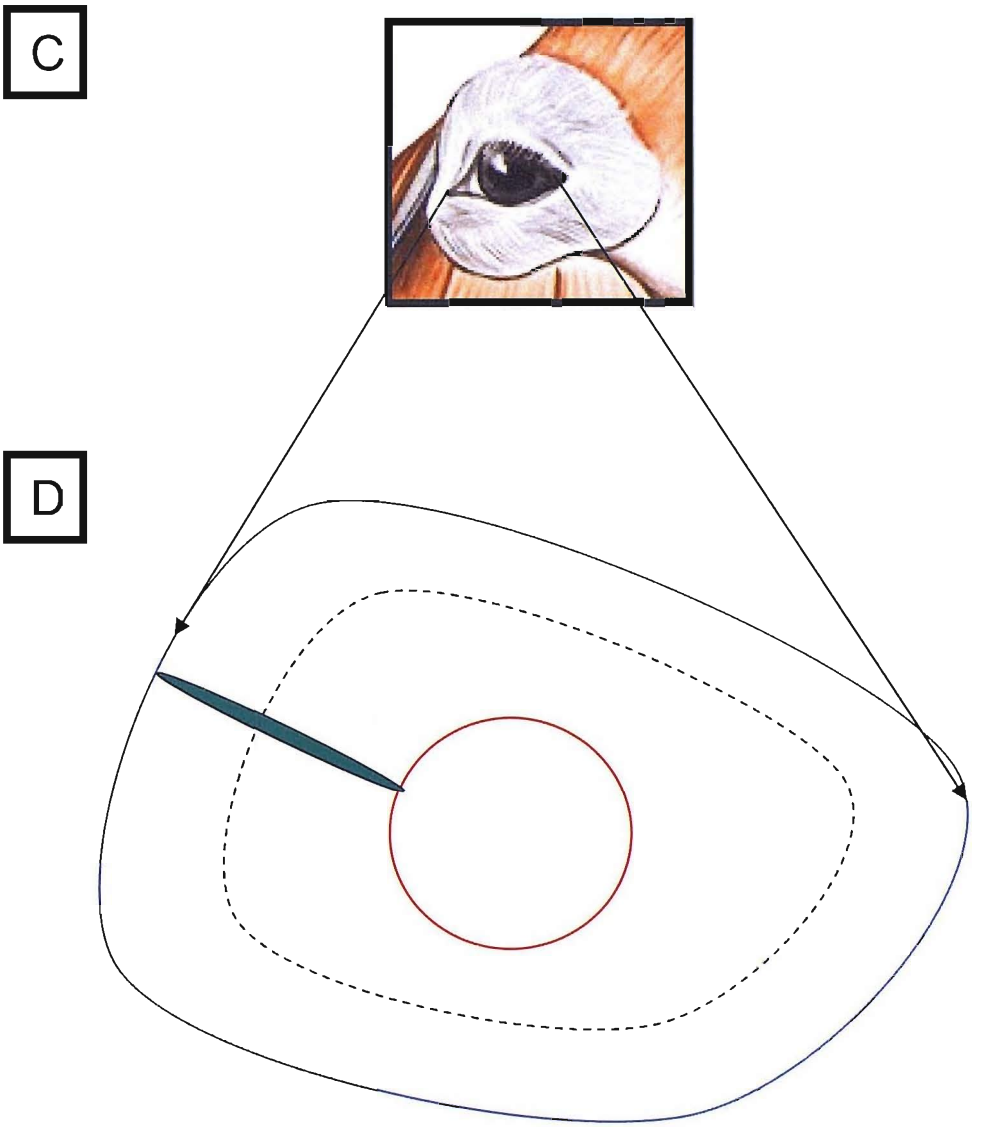


Plate C shows the orbit in situ. Once the whole eye is removed, then the epithelium around the cornea is cut following the cornea/conjunctival border, forming a pineapple ring-like shape, then 1mm is removed from this edge in order to discard any cornea epithelial cells that might be still present. The underlying connective tissue is stripped away from the conjunctival epithelial layer.

Plate D shows a rough diagrammatic outline of the conjunctiva when removed from the orbit. The red line is the inner edge (cornea) of the conjunctiva, the blue is the outer edge (eyelid) of the conjunctiva, the green oval is a piece of cartilage that runs from the cornea border to the eyelid margin. The piece of cartilage is removed thus opening the ring of conjunctiva. The conjunctival epithelium is then ready to be sub-divided as required.

# 4.18a *Ovis aries* conjunctival ultra-structure


Micrographs 1 to 6 show the surface ultra-morphology of the *ovis aries* conjunctival, at increasing powers of magnification. The morphological difference between the epithelial layer and the underlying connective tissue layer can clearly be seen in micrographs 1, and 2 (highlighted with the arrows).

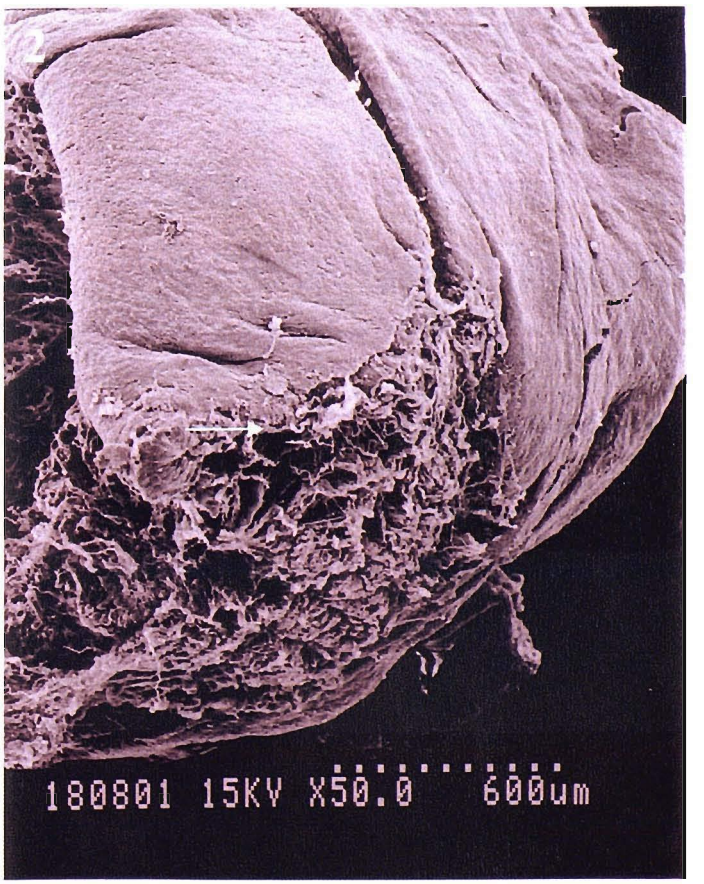

# 4.18b *Ovis aries* conjunctival ultra-structure

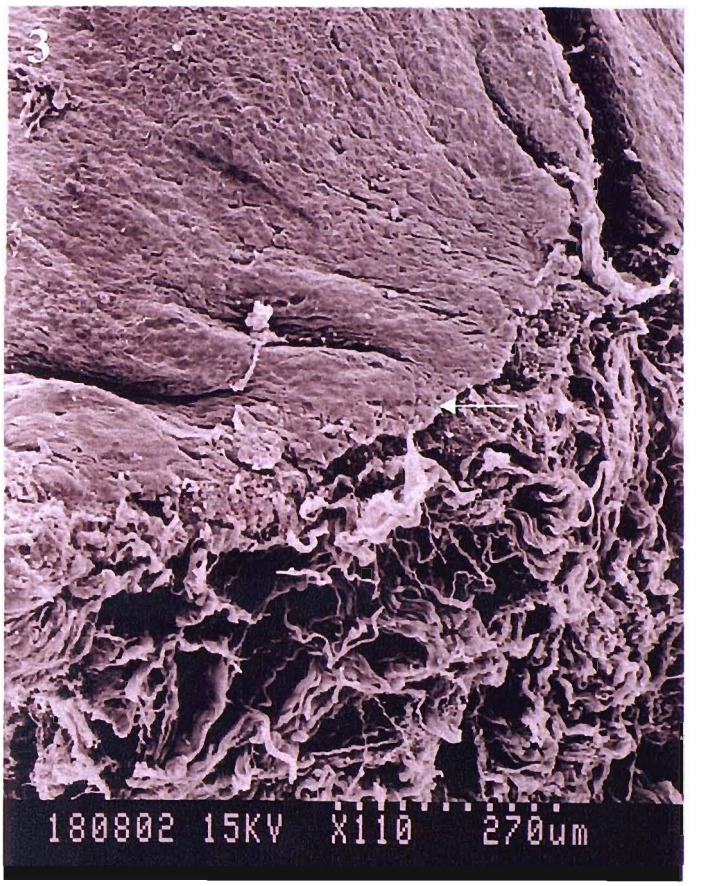


Micrograph 3 shows the edge of the epithelial tissue layer covering the connective tissue layer (highlighted with the white arrow).


Micrograph 4 shows the apical epithelial layer in the bottom half of the picture, characteristic cobblestone cell membrane patterns can be seen (highlighted with the white arrows).

# 4.18c *Ovis aries* conjunctival ultra-structure

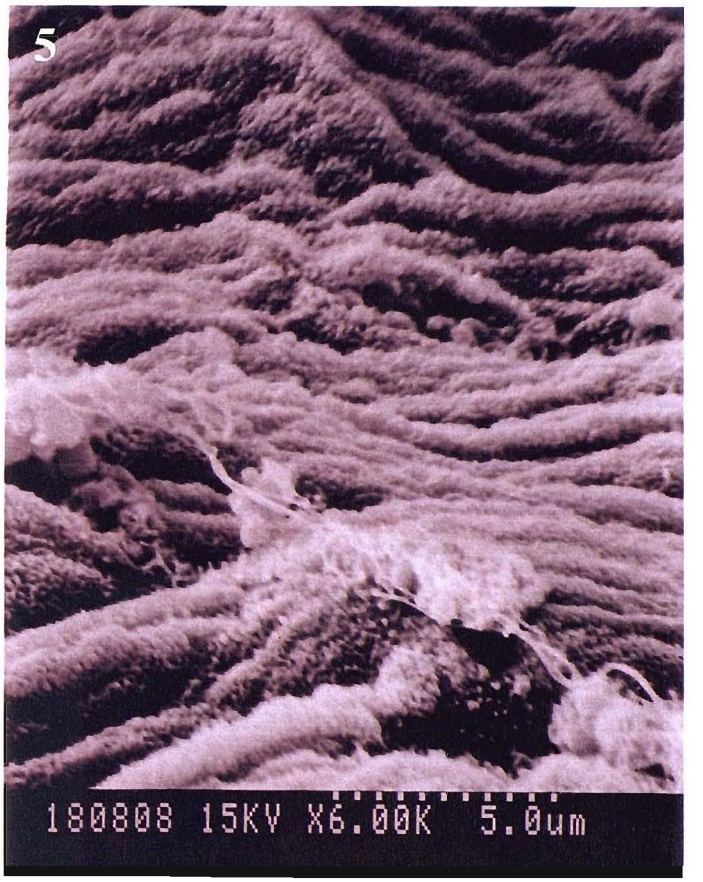


Micrograph 5 and 6 demonstrate that the apical surface of the epithelial cell layer is covered with microvilli-like cell processes.

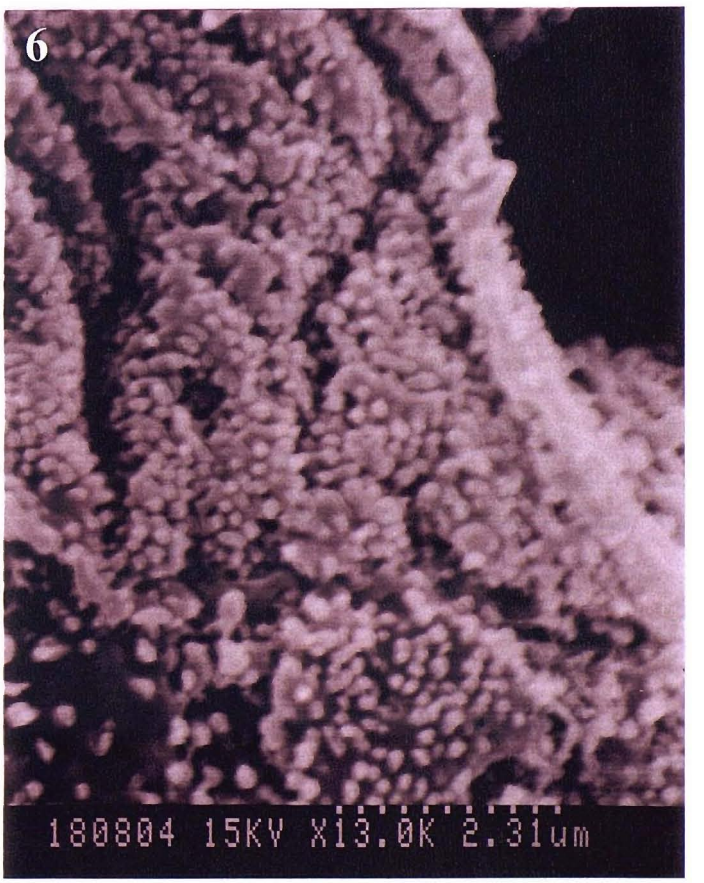

# 4.19 *Ovis aries* connective tissue

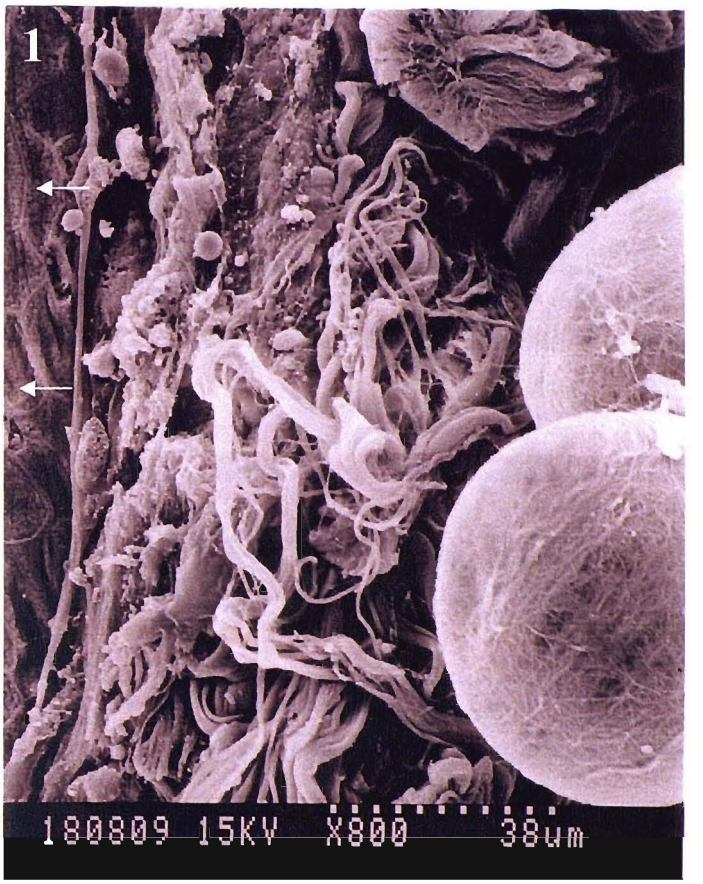


Micrographs 1 and 2 have been included to demonstrate the different morphological between the epithelial and underlying connective tissue layer morphologies.

In micrograph 1 the white arrows show the edge of the epithelial layer, as seen by their microvilli-like processes and their 'furry' appearance and this magnification.

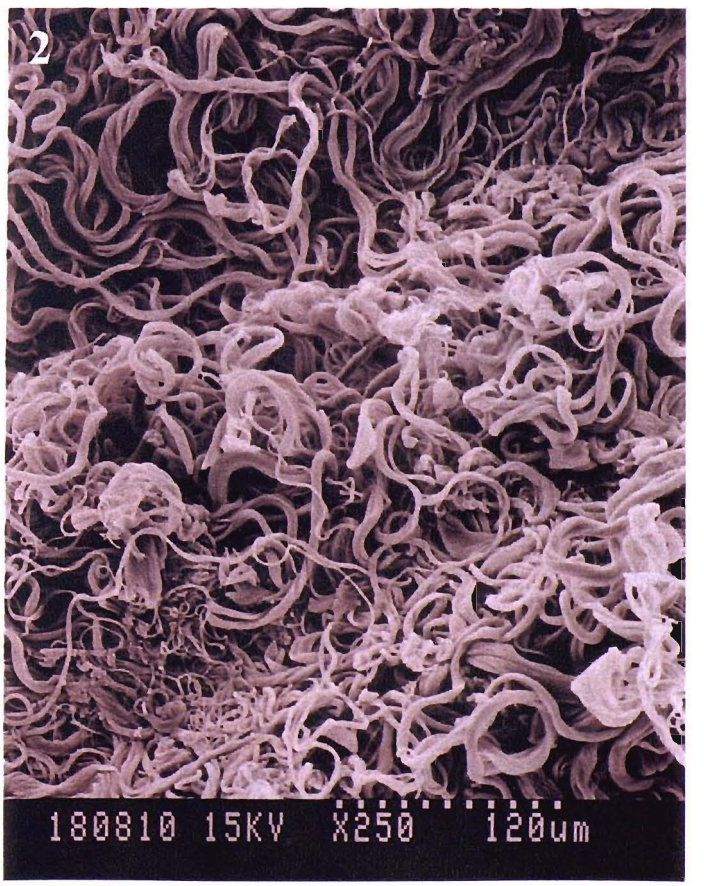


Micrograph 2 demonstrates the string-like nature of connective tissue.

Personal observation - the orbit had a considerable amount of connective tissue around the conjunctiva compared to that around the human orbit.

# 4.20 *Ovis aries* toludine blue morphological staining

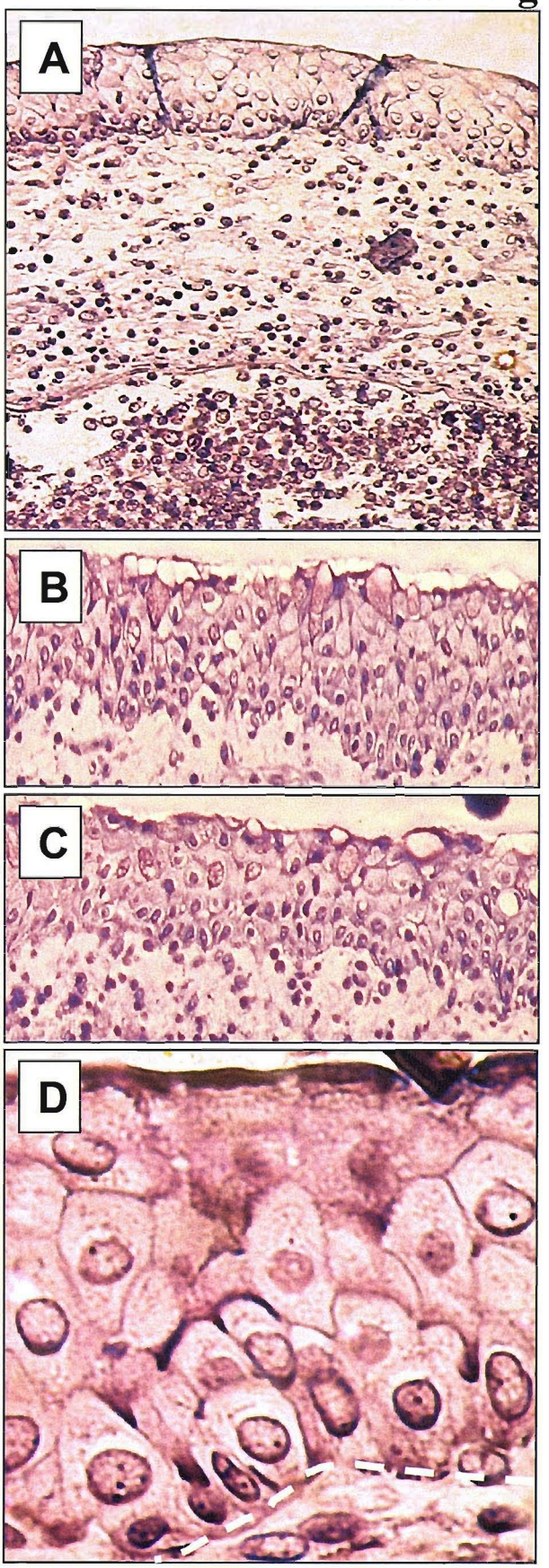


Micrographs A, B, C, D and E show the morphological staining of *Ovis aries* with toludine blue stain.

Plates A, B and C show the epithelial layer and the underlying tissue layers of the orbit.

Plate D shows specifically the epithelial layer, the basement membrane is marked with the dotted white line.

The epithelium of the *Ovis aries* model resembles a non-ciliated stratified cubiodal layer, constructed of 3-5 cells from 3 definable cell layers, the basal, intermediate and superficial layers.

# 4.21 *Ovis aries* primary control immunostaining

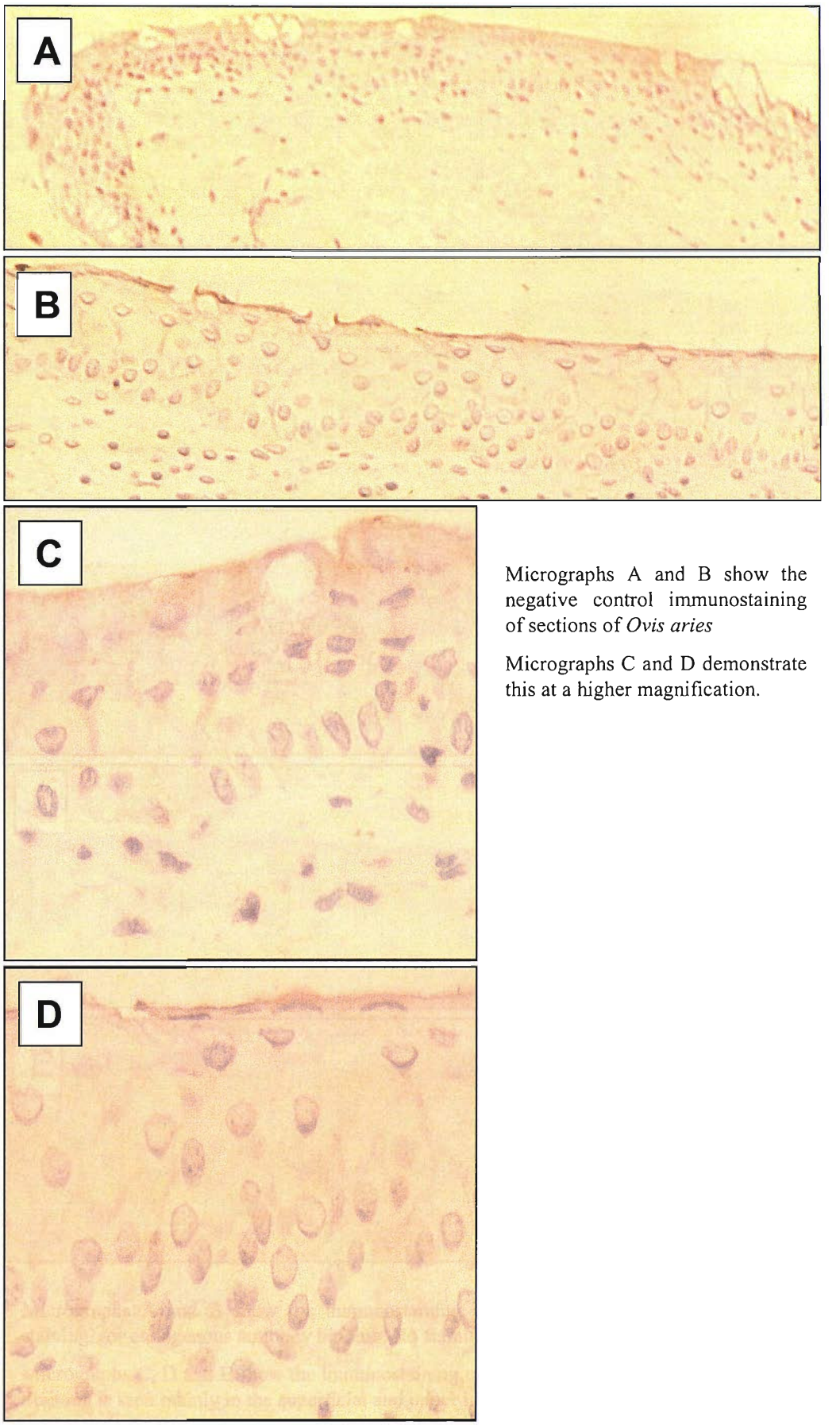


Micrographs A and B show the negative control immunostaining of sections of *Ovis aries*

Micrographs C and D demonstrate this at a higher magnification.

# 4.22 *Ovis aries* immunostaining

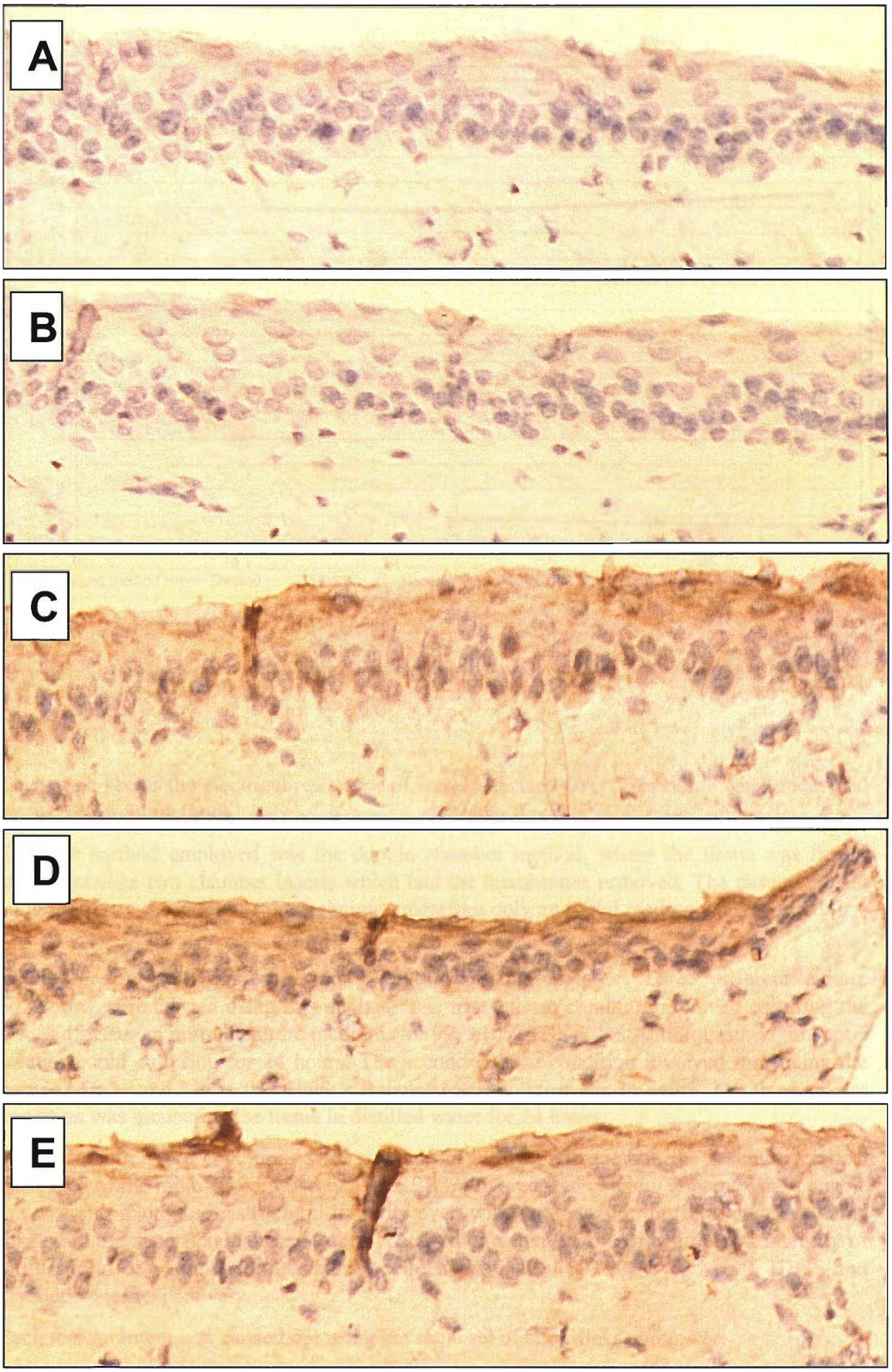


Micrographs A and B show the immunostaining against a secondary negative control staining, for endogenous antibody binding. No staining can be identified.

Micrographs C, D and E show the immunostaining of *Ovis aries* tissue against pan keratin. Staining is seen mainly in the superficial and upper intermediate layers.

# 4.23 TEER data on *Ovis aries* tissue

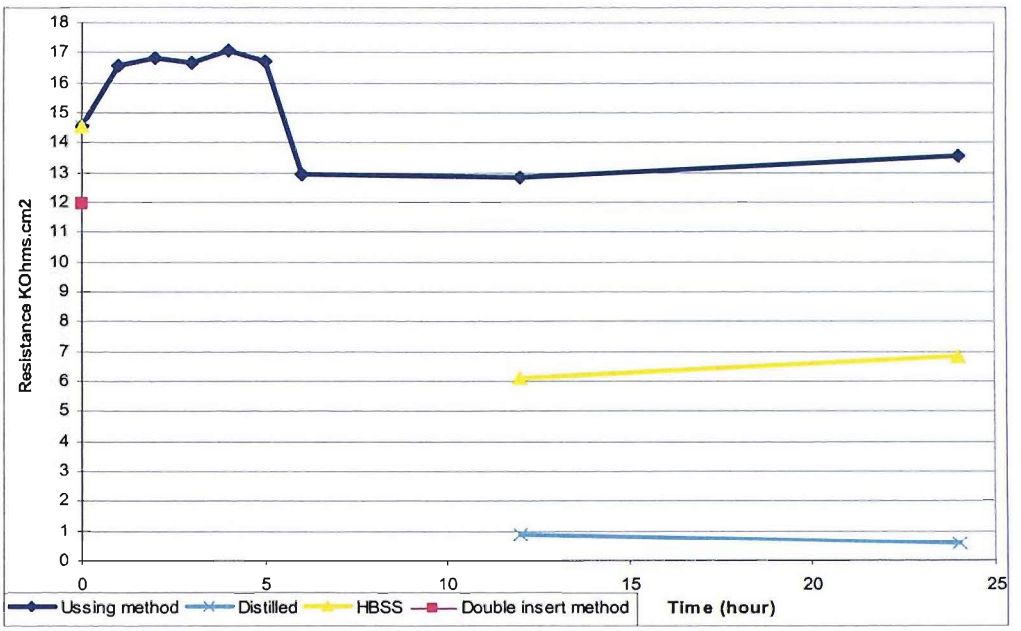


This graph shows the electrical resistance of freshly excised *Ovis aries* tissue when measured by two different methods.

The first method employed was the double chamber method, where the tissue was firmly sealed between two chamber inserts which had the membranes removed. The tissue was not cultured due to the nature of the technique, therefore only an initial reading was recorded (n = 4).

The second method employed was using an Ussing chamber. Three different culture conditions were carried using this method. The first culture condition involved culturing the pieces of tissue in normal culture medium (M199, +10% FBS + 1% Antibiotics / Antimycotic solution), and culturing for 24 hours. The second culture condition involved incubating the tissue in Ca2+ and Mg2+ free Hank's Balanced Salt Solution for 24 hours. The third culture condition was incubating the tissue in distilled water for 24 hours.

The different culture conditions were carried out in order to ascertain the residue electrical resistance of the multi-layered tissue. The HBSS, it its reduced calcium content would enable the tissue to maintain its structural integrity even with the reduction in tight junctions being formed in the superficial layer of cells. The distilled water enables the structural integrity of the tissue to be maintained but induces cellular death. n = 10, 10, 4 for M199, HBSS and distilled water respectively.

Each measurement was carried out using the same set of chopsticks and meter.

# 5. Experimental investigations of *in vitro* allergen challenges

## Chapter hypothesis:

***Phleum pratense (Timothy grass) facilitate paracellular movement of non-indigenous molecules via tight junction disruption.***

## 5.1 Introduction

It is proposed that when allergen containing pollen cytoplasmic granules released from the pollen grain, subsequently come into contact with a hydrating environment such as the tear film, release their allergens and these gain access through mucosal tissue in order to initiate the immune reaction. There are several barriers for the allergens to overcome before they can bind to their corresponding IgE molecules on the tissue population of mast cells or other circulating immuno-regulatory cells. Epithelial tissues have a specific function in regulating the paracellular movement of molecules and providing a structurally sound barrier, to the otherwise harmful, external environment. One current proposed theory is that the group 1 allergens act as proteases, and as a direct result of allergen exposure, they can increase the permeability of epithelial tissue, therefore enhancing the mobility of these allergens and increasing the accessibility of the allergen to immune cells (Herbert *et al* 1995). This mode of action has been implicated in the case of the group 1 Timothy grass pollen allergen Phl p 1, but is not fully understood or globally accepted (Grobe *et al* 1999 & 2002, Li & Cosgrove 2001).

Using the conjunctival epithelial cell models, developed and validated in chapter 4, the effects that Timothy grass pollen extract has on epithelial tight junctions and the architecture of epithelial cells was investigated in this chapter.

*Phleum pratense* allergen extract was added to cultures of the epithelial cell line models ChWk, IOBA-NHC and 16HBE 14o-, to mimic the in vivo reaction that occurs when naturally released pollen comes into contact with the human eye, the cultures were run for a period of 24 hours. The 16HBE 14o- cell line was used in parallel with the conjunctival epithelial cell lines due to its use in previous studies connected with assessing the effects of allergens on epithelial permeability, also due to its tight

junctional properties as discussed in the previous chapter (Winton *et al* 1998, Wan *et al* 2000).

The effect that the introduction of the allergen has on epithelial tight junctions was assessed by measuring and recording the trans-epithelial electrical resistance throughout the experiment time period. Also a FITC tagged dextran molecule was introduced into the culture medium to investigate the paracellular movement of exogenous molecules during the period of epithelial barrier attack.

Morphological changes that occurred to the cells were assessed, by analysing the surface features of the cultured cells, using scanning electron microscopy.

To further investigate several mechanisms, a mixture of the timothy grass pollen allergen and a cocktail protease inhibitor was added to several repeats of the experiment in order to try and deduce the proposed protease action of the allergen extract.

In order to recreate a physiological reaction that occurs within the hypersensitivity reaction upon the contact of allergen and the pre-programmed mast cells is the release of histamine. So in several repeats of the in vitro allergen challenge histamine was introduced in order to investigate and record the effects.

The results of the *in vitro* allergen challenge of the cell models of the conjunctival epithelium were evaluated as well as the chapter hypothesis are discussed at the end of the chapter.

## 5.2 16HBE 14o- allergen challenge

To assess the action that Timothy grass pollen (*Phleum pratense*) has on epithelial tight junctions, the epithelial cell line model, 16HBE 14o-, was challenged in culture for 24 hours.

Briefly, 16HBE 14o- cells were cultured on insert membranes according to section 2.2.10.1 then treated according to section 2.1.6. During the experiment time frame (24 hrs), trans-epithelial electrical resistance was measured using the chop stick method according to section 2.2.10.1 at 1, 2, 3, 4, 6, 12 and 24 hours post allergen introduction, also using the same time point the lower medium reservoirs were sampled and the level of FITC-Dextran was measured according to section 2.2.11. Once the experiment had been run to its conclusion (24 hours post treatment), membranes were either fixed for IHC staining or for scanning electron microscopy according to sections

2.2.4 or 2.2.7 respectively. The membrane embedded in GMA for immunostaining will be dealt with in the next chapter.

### 5.2.1 Trans-epithelial electrical resistance (figure 5.1)

The threshold for the 16HBE 14o- cells was set at 3000Ω, once this was reached / passed then the experiment commenced. Full statistical figures are in appendix C.

The tables of figures below show the trans-epithelial electrical resistance readings taken throughout the in vitro allergen challenge experiment. The first column shows the times at which the measurements were taken. The next column shows the raw TEER readings of the treatment / control. In the treatment tables the third column shows the resistance reading when compared against the control and corrected for area, using the equation (Re - Rc) $\pi r^2$ = R (Ohms.cm$^2$).

The control insert values (cell + / treatment -)

| | |
|---|---|
| 1 | 3462.5 |
| 2 | 3430 |
| 3 | 3372.5 |
| 4 | 3950 |
| 6 | 4090 |
| 12 | 4432.5 |
| 24 | 4475 |

The table on the left shows the raw control trans-epithelial electrical figures for control. Over the 24 hour period, the control value rose from 3462.5 to 4475, an increase of 1012.5.

Phl p values,

| | | |
|---|---|---|
| 1 | 4050.83 | 166.35 |
| 2 | 3245.83 | -52.07 |
| 3 | 3020 | -99.67 |
| 4 | 2971.67 | -276.62 |
| 6 | 3691.08 | -112.79 |
| 12 | 3153.33 | -361.67 |
| 24 | 3662.5 | -229.73 |

The Phl p treatment dropped, from a starting value of 388.33, over the 24 hours, to 3662.5. When compared to control the TEER dropped 229.73 at the end of the experiment (p = n/s).

Protease values

| | | |
|---|---|---|
| 1 | 4098.75 | 179.90 |
| 2 | 607.5 | -798.04 |
| 3 | 375.13 | -847.49 |
| 4 | 346.88 | -1018.76 |
| 6 | 327.75 | -1063.75 |
| 12 | 332.88 | -1159.14 |
| 24 | 345.13 | -1167.69 |

The protease treatment dropped the TEER of the cells by 85.16% after the first hour of incubation to 607.5. At the second measurement the TEER had dropped to the background value. This drop is clearly shown in the corrected values. No recovery

in TEER was seen.

Phl p + protease inhibitor values

| | | |
|---|---|---|
| 1 | 4066.25 | 170.71 |
| 2 | 3790 | 101.79 |
| 3 | 3600 | 64.32 |
| 4 | 3833.75 | -32.87 |
| 6 | 3775 | -89.06 |
| 12 | 4406.25 | -7.42 |
| 24 | 3793.75 | -192.62 |

The Phl p + protease inhibitor treatment dropped the TEER readings throughout the 24 hour period, finishing -192.62 from the control value (p = n/s).

Phl p + histamine values

| | | |
|---|---|---|
| 1 | 3920 | 129.36 |
| 2 | 3740 | 87.65 |
| 3 | 3536.25 | 46.30 |
| 4 | 3568.75 | -107.80 |
| 6 | 2985 | -312.43 |
| 12 | 2460 | -557.71 |
| 24 | 1978.75 | -705.80 |

The Phl p + histamine treatment TEER readings continually dropped throughout the time period of the experiment.

**5.2.2 FITC-Dextran movement (figure 5.2)**

FITC-Dextran movement was calculated by sampling the lower chamber at the same time points that the TEER readings were taken as described in section 2.2.11. The level of FITC-Dextran within each sample was measured at 490nm.

The tables of figures below show the FITC-Dextran readings taken throughout the in vitro allergen challenge experiment. The first column shows the times at which the measurements were taken. The next column shows the raw FITC-Dextran unit readings of the treatment / control. In the treatment tables the third column shows the Corrected reading when the value is corrected for the control value at the same time point.

The control insert values (cell + / but treatment -),

| | |
|---|---|
| 0 | 245 |
| 1 | 221 |
| 2 | 222.33 |
| 4 | 224.67 |
| 6 | 226 |
| 12 | 238 |
| 24 | 248 |

Over the 24 hour period the movement of FITC-Dextran in the control, was absolutely minimal, ending with a reading of 248, a rise of only 3 units.

Phl p values,

| | | |
|---|---|---|
| 0 | 248 | 3 |
| 1 | 232.67 | 11.67 |
| 2 | 227.33 | 5 |
| 4 | 238 | 13.33 |
| 6 | 232 | 6 |
| 12 | 242.33 | 4.33 |
| 24 | 296.33 | 48.33 |

Over the 24 hour period the amount of FITC-Dextran movement remained low until the end reading point. When an increase of 48.33 over the control reading.

Protease values

| | | |
|---|---|---|
| 0 | 237.67 | -7.33 |
| 1 | 227 | 6 |
| 2 | 289.33 | 67 |
| 4 | 384.67 | 160 |
| 6 | 428 | 202 |
| 12 | 743.33 | 505.33 |
| 24 | 1098 | 850 |

The protease treatment produced a constant movement of FITC-Dextran through the epithelial layer finishing with a reading of 850 units.

Phl p + protease inhibitor values

| | | |
|---|---|---|
| 0 | 247 | 2 |
| 1 | 225.67 | 4.67 |
| 2 | 226.33 | 4 |
| 4 | 232.33 | 7.67 |
| 6 | 226.67 | 0.67 |
| 12 | 232.33 | -5.67 |
| 24 | 244.33 | -3.67 |

The Phl p + protease inhibitors showed a level set of FITC-Dextran readings throughout the experiment and did not show any difference in FITC-Dextran movement from the control.

Phl p + histamine values

| | | |
|---|---|---|
| 0 | 242.67 | -2.33 |
| 1 | 226.33 | 5.33 |
| 2 | 217.33 | -5 |
| 4 | 236 | 11.33 |
| 6 | 237.33 | 11.33 |
| 12 | 238.67 | 0.67 |
| 24 | 246.33 | -1.67 |

The Phl p + histamine showed a level set of FITC-Dextran readings throughout the experiment and did not show any difference in FITC-dextran levels compared to control.

### 5.2.3 Scanning electron microscopy - Phl p treatment

When challenged with the Phl p extract the changes in epithelial layer architecture was striking, with large gaps forming in between the cells (figure 5.3a, micrograph A). At higher magnification these gaps can be seen to be to run through the full mono-layer in terms of thickness suggesting cell-cell contact loss. Microvilli can be identified upon the surface of the cells (figure 5.3a, micrograph B). When viewed in more detail the microvilli are still present on the cell surface but appear to be shortened in length and lack any branching (figure 5.3b, micrographs C and D).

### 5.2.4 Scanning electron microscopy - Protease treatment

When treated with the protease, the membrane was stripped of its epithelial layer (figure 5.4, micrograph A). At higher magnification the level of cell debris or cell destruction can be seen (figure 5.4, micrograph B).

### 5.2.5 Scanning electron microscopy - Phl p + protease inhibitors treatment

When challenged with the Phl p + protease inhibitor mixture the cell mono-layer showed large gaps had been formed in between clumps of cells rather than in between the individual cells (figure 5.5a, micrographs A and B). When the surface of the cells was viewed at higher magnification, the surface features of the cells remain in place, but an increase in cellular debris is seen deposited on the apical membrane. Also cell-cell contacts remain (figure 5.5b, micrograph C). The microvilli seem to be shortened and degraded; also the fibrous deposits can be seen covering a proportion of the cell surface (figure 5.5b, micrograph D).

### 5.2.6 Scanning electron microscopy - Phl p + histamine treatment

When the 16HBE 14o- mono-layer was challenged with the Phl p + histamine mixture, large gaps formed in between the cells, this is highlighted in greater detail at higher magnification. At greater magnification the surface features of the cells can be identified, especially the microvilli, which appear to have been shortened, also present is cellular / fibrous debris (figure 5.6a, micrographs A and B). Cellular processes extending from the cells can also be identified suggesting that cell-cell contact was not totally lost due to the Phl p + histamine treatment. Intact cell-cell contacts may have been lost during the fixation and processing of samples for electron microscopy.

## 5.3 ChWk allergen challenge

To assess the action that Timothy grass pollen (*Phleum pratense*) has on epithelial tight junctions, the epithelial cell line model, ChWk, was challenged in culture for 24 hours.

Briefly, ChWk cells were cultured on insert membranes according to section 2.2.10.1 then treated according to section 2.1.6. During the experiment time frame (24 hrs), trans-epithelial electrical resistance was measured using the chop stick method according to section 2.2.10.1 at 1, 2, 3, 4, 6, 12 and 24 hours post treatment, also using the same time point the lower medium reservoirs were sampled and the level of FITC-Dextran was measured according to section 2.2.11. Once the experiment had been run to its conclusion (24 hours post treatment), membranes were either fixed for IHC staining or fixed for scanning electron microscopy according to sections 2.2.4 or 2.2.7 respectively. The membrane embedded in GMA for immunostaining will be dealt with in the next chapter.

### 5.3.1 Trans-epithelial electrical resistance (figure 5.7)

The threshold for the ChWk cells was set at 330Ω, once this was reached then the experiment commenced.

The tables of figures below show the trans-epithelial electrical resistance readings taken throughout the in vitro allergen challenge experiment. The first column shows the times at which the measurements were taken. The next column shows the raw TEER readings of the treatment / control. In the treatment tables the third column shows the resistance reading when compared against the control and corrected for area, using the equation $(Re - Rc)\ \pi r^2 = R$ (Ohms.cm$^2$).

Control insert values (Cell + / treatment -)

| | |
|---|---|
| 0 | 383 |
| 1 | 387.63 |
| 2 | 388 |
| 4 | 390.13 |
| 6 | 386.75 |
| 12 | 383.25 |
| 24 | 381.38 |

The table on the left shows the raw control trans-epithelial electrical figures for control. Over the 24 hour period, the control value remained level, starting at 383 and finishing at 381.38.

Phl p

| | | |
|---|---|---|
| 0 | 371.69 | -3.20 |
| 1 | 359.19 | -8.04 |
| 2 | 347.63 | -11.42 |
| 4 | 341.44 | -13.77 |
| 6 | 333.13 | -15.16 |
| 12 | 352.06 | -8.82 |
| 24 | 334.06 | -13.38 |

The Phl p treatment dropped, from a starting value of 371.69, over the 24 hours, to 334.06. When compared to control the TEER dropped 13.38 at the end of the experiment ($p > 0.001$).

Protease

| | | |
|---|---|---|
| 0 | 367.88 | -4.28 |
| 1 | 322 | -18.56 |
| 2 | 300.75 | -24.67 |
| 4 | 318 | -20.40 |
| 6 | 302.25 | -23.89 |
| 12 | 325.13 | -16.44 |
| 24 | 307.13 | -20.99 |

The protease treatment dropped the TEER of the cells after the first hour of incubation, showing no recovery in TEER through the remainder of the experiment. Finishing 20.99 lower than control after 24 hours.

Phl p + protease inhibitor

| | | |
|---|---|---|
| 0 | 371.38 | -3.27 |
| 1 | 390.63 | 0.85 |
| 2 | 373.25 | -4.17 |
| 4 | 409.63 | 5.51 |
| 6 | 389.13 | 0.67 |
| 12 | 380.13 | -0.88 |
| 24 | 360.63 | -5.87 |

The Phl p + protease inhibitor treatment produced no sustained effect on the TEER of the cells, with the readings lower than control but remaining constant, not dropping as the experiment ran its course.

Phl p + histamine

| | | |
|---|---|---|
| 0 | 378.13 | -1.38 |
| 1 | 371.63 | -4.52 |
| 2 | 351.63 | -10.29 |
| 4 | 357.25 | -9.30 |
| 6 | 340.13 | -13.18 |
| 12 | 360.88 | -6.33 |
| 24 | 372.13 | -2.62 |

The Phl p + histamine treatment TEER readings initially dropped until the 6 hour time point, when a gradual recovery in TEER was observed rises to just 2.62 below control from 13.18 below control at the 6 hour mark.

### 5.3.2 FITC-Dextran movement (figure 5.8)

FITC-Dextran movement was calculated by sampling the lower chamber at the same time points that the TEER readings were taken as described in section 2.2.11. The level of FITC-Dextran within each sample was measured at 490nm.

The tables of figures below show the FITC-Dextran readings taken throughout the in vitro allergen challenge experiment. The first column shows the times at which the measurements were taken. The next column shows the raw FITC-Dextran unit readings of the treatment / control. In the treatment tables the third column shows the Corrected reading when the value is corrected for the control value at the same time point.

Control insert values (Cell + / treatment -)

| | |
|---|---|
| 0 | 122 |
| 1 | 149.33 |
| 2 | 163.67 |
| 4 | 204.33 |
| 6 | 215.33 |
| 12 | 349.33 |
| 24 | 514.67 |

Over the 24 hour period the movement of FITC-Dextran in the control constantly increased from 122 units to 514.67 units at 24 hours.

Phl p

| | | |
|---|---|---|
| 0 | 120.67 | -1.33 |
| 1 | 148.33 | -1 |
| 2 | 160.33 | -3.33 |
| 4 | 206.67 | 2.33 |
| 6 | 224.33 | 9 |
| 12 | 352 | 2.67 |
| 24 | 525.67 | 11 |

Over the 24 hour period the amount of FITC-Dextran movement remained low throughout the experiment finishing at 11 units above control.

Protease

| | | |
|---|---|---|
| 0 | 121.67 | -0.33 |
| 1 | 166 | 16.67 |
| 2 | 187.67 | 24 |
| 4 | 258.33 | 54 |
| 6 | 287 | 71.67 |
| 12 | 486.67 | 137.33 |
| 24 | 761.67 | 247 |

The protease treatment produced a constant movement of FITC-Dextran through the epithelial layer finishing with a reading of 247 units more than control.

Phl p + protease inhibitor

| | | |
|---|---|---|
| 0 | 123 | 1 |
| 1 | 148.67 | -0.67 |
| 2 | 162 | -1.67 |
| 4 | 191.67 | -12.67 |
| 6 | 211.67 | -3.67 |
| 12 | 368.33 | 19 |
| 24 | 609 | 94.33 |

The Phl p + protease inhibitors showed a level set of FITC-Dextran readings until the 12 hour time point, at which the movement increased finishing at 94.33 units above control.

Phl p + histamine

| | | |
|---|---|---|
| 0 | 126.33 | 4.33 |
| 1 | 145.33 | -4 |
| 2 | 162.67 | -1 |
| 4 | 190.33 | -14 |
| 6 | 216.33 | 1 |
| 12 | 334 | -15.33 |
| 24 | 479 | -35.67 |

The Phl p + histamine showed a level set of FITC-Dextran readings throughout the experiment until the 12 hour point, at which the movement of FITC-Dextran was inhibited finishing with a reading of 35.67 units below control.

### 5.3.3 Scanning electron microscopy - Phl p treatment

Treatment with Phl p showed no gross morphological changes in the cell mono-layer (figure 5.9a, micrograph A). At higher magnification large uniform cracks in the mono-layer can be identified, possibly due to the processing stages for electron microscopy (figure 5.9a, micrograph B). When viewed at higher magnification degradation of cell-cell contact can be seen, but the cells still have some cellular processes contacting each other (figure 5.9b, micrograph C). The surface features of the ChWk seem to have been flattened with the Phl p treatment (figure 5.9b, micrograph D).

### 5.3.4 Scanning electron microscopy - Protease treatment

With the treatment of protease, total epithelial denudation can be observed from the culture membrane (figure 5.10a, micrograph A and B). At higher magnification the effect of the protease on the cells can be seen, cells detaching off the membrane, few cells can be identified remaining, with the last of their adhesion processes in contact with the culture membrane and their loss of surface features (figure 5.10b, micrographs C and D).

### 5.3.5 Scanning electron microscopy - Phl p + protease inhibitors treatment

No gross morphological changes in the cell mono-layer can be identified at low magnification (figure 5.11, micrograph A). At higher magnification large cracks can be identified in the cell layer, again possibly due to some of the processing stages of electron microscopy.

### 5.3.6 Scanning electron microscopy - Phl p + histamine treatment

Cells treated with the Phl p + histamine mixture showed no gross morphological changes to the mono-layer (figure 5.12a, micrograph A). At higher magnification the surfaces of the cells seem to have been flattened, and large cracks can be identified (figure 5.12a, micrograph B). This flattening of the surface features of the cells is clearly seen in greater detail at higher magnification (figure 5.12b, micrographs C and D).

## 5.4 IOBA-NHC allergen challenge

To assess the action of the Timothy grass pollen (*Phleum pratense*) has on epithelial tight junctions the epithelial cell line model, IOBA-NHC, was challenged in culture for 24 hours. Briefly, IOBA-NHC cells were cultured on insert membranes according to section 2.2.10.1 then treated according to section 2.1.6. During the experiment time frame (24 hrs), trans-epithelial electrical resistance was measured using the chop stick method according to section 2.2.10.1 at 1, 2, 3, 4, 6, 12 and 24 hours post treatment, also using the same time point the lower medium reservoirs were sampled and the level of FITC-Dextran was measured according to section 2.2.11. Once the experiment had been run to its conclusion (24 hours post treatment), membranes were either fixed for IHC staining or fixed for scanning electron microscopy according to sections 2.2.4 or 2.2.7 respectively. The membrane embedded in GMA for immunostaining will be dealt with in the next chapter.

### 5.4.1 Trans-epithelial electrical resistance (figure 5.13)

The threshold for the IOBA-NHC cells was set at 300Ω, once this was reached then the experiment commenced.

The tables of figures below show the trans-epithelial electrical resistance readings taken throughout the in vitro allergen challenge experiment. The first column shows the times at which the measurements were taken. The next column shows the raw TEER readings of the treatment / control. In the treatment tables the third column shows the resistance reading when compared against the control and corrected for area, using the equation $(Re - Rc)\ \pi r^2 = R\ (Ohms.cm^2)$.

Control insert values (cell + / treatment -)

| | |
|---|---|
| 0 | 384.5 |
| 1 | 396 |
| 2 | 381.25 |
| 4 | 395 |
| 6 | 393.5 |
| 12 | 388.88 |
| 24 | 384.88 |

The table on the left shows the raw control trans-epithelial electrical figures for control. Over the 24 hour period, the control remained level starting at 384.5, then finishing at 384.88.

Phl p

| | | |
|---|---|---|
| 0 | 384.25 | -0.07 |
| 1 | 387.19 | -2.49 |
| 2 | 369.69 | -3.27 |
| 4 | 345.19 | -14.08 |
| 6 | 349.5 | -12.44 |
| 12 | 384.19 | -1.33 |
| 24 | 369 | -4.49 |

The Phl p treatment dropped, from a starting value of 384.25, until the 6 hour time point, when a recovery in TEER was observed up to 369 at the 24 hour point ($p > 0.01$).

Protease

| | | |
|---|---|---|
| 0 | 384.75 | 0.07 |
| 1 | 364.13 | -9.01 |
| 2 | 369.5 | -3.32 |
| 4 | 334.5 | -17.11 |
| 6 | 360.5 | -9.33 |
| 12 | 384.5 | -1.24 |
| 24 | 365.5 | -5.48 |

The protease treatment dropped the TEER until the 4 hour time point to 334.5, at which point a steady recovery in TEER was observed finishing at 365.5 at 24 hours.

Phl p + protease inhibitor

| | | |
|---|---|---|
| 0 | 400.13 | 4.42 |
| 1 | 399.5 | 0.99 |
| 2 | 401.63 | 5.76 |
| 4 | 376.88 | -5.13 |
| 6 | 407 | 3.82 |
| 12 | 399.63 | 3.04 |
| 24 | 395.25 | 2.93 |

The Phl p + protease inhibitor treatment TEER readings stayed within a range of 407 – 376.88 throughout the 24 hour period. Showing little different compared to control.

Phl p + histamine

| | | |
|---|---|---|
| 0 | 391.63 | 2.01 |
| 1 | 381.88 | -3.99 |
| 2 | 374.38 | -1.94 |
| 4 | 351.88 | -12.19 |
| 6 | 349 | -12.58 |
| 12 | 383.88 | -1.41 |
| 24 | 392.38 | 2.12 |

The Phl p + histamine treatment dropped TEER readings until the 4 – 6 hour mark, after which a steady recovery was observed back to the level at the first reading 392.38

**5.4.2 FITC-Dextran movement (figure 5.14)**

FITC-Dextran movement was calculated by sampling the lower chamber at the same time points that the TEER readings were taken as described in section 2.2.11. The level of FITC-Dextran within each sample was measured at 490nm.

The tables of figures below show the FITC-Dextran readings taken throughout the in vitro allergen challenge experiment. The first column shows the times at which the measurements were taken. The next column shows the raw FITC-Dextran unit readings of the treatment / control. In the treatment tables the third column shows the Corrected reading when the value is corrected for the control value at the same time point.

Control insert values (Cell + / treatment -)

| | |
|---|---|
| 0 | 119.67 |
| 1 | 159.33 |
| 2 | 186 |
| 4 | 227.67 |
| 6 | 264.67 |
| 12 | 447.67 |
| | |

Over the 24 hour period the movement of FITC-Dextran in the control constantly increased from 119.67 units to 671.67 units at 24 hours.

Phl p

| | | |
|---|---|---|
| 0 | 125 | 5.33 |
| 1 | 148 | -11.3 |
| 2 | 165.33 | -20.67 |
| 4 | 219.67 | -8 |
| 6 | 245.67 | -19 |
| 12 | 413.67 | -34 |
| 24 | 616.67 | -55 |

The FITC-Dextran movement in the Phl p treatment initially was lowered than control, then fell further until the 24 hour time point to 55 below the control value.

Protease

| | | |
|---|---|---|
| 0 | 125.33 | 5.67 |
| 1 | 151.67 | -7.67 |
| 2 | 174.33 | -11.67 |
| 4 | 237 | 9.33 |
| 6 | 274 | 9.33 |
| 12 | 479.67 | 32 |
| 24 | 744.67 | 73 |

The FITC-Dextran in the protease treatment initially showed little movement until the 12 hour mark, at which point it increased up until the end point finishing at a level of 73 above control.

Phl p + protease inhibitor

| | | |
|---|---|---|
| 0 | 125.33 | 5.67 |
| 1 | 147.67 | -11.67 |
| 2 | 181 | -5 |
| 4 | 210.33 | -17.33 |
| 6 | 235 | -29.67 |
| 12 | 407 | -40.67 |
| 24 | 640.33 | -31.33 |

Phl p + protease inhibitor showed an inhibition in FITC-Dextran movement throughout the entire experiment time frame.

Phl p + histamine

| | | |
|---|---|---|
| 0 | 124 | 4.33 |
| 1 | 151.33 | -8 |
| 2 | 167.67 | -18.33 |
| 4 | 218.33 | -9.33 |
| 6 | 262.33 | -2.33 |
| 12 | 447.33 | -0.33 |
| 24 | 576 | -95.67 |

The Phl p + histamine showed inhibition of FITC-Dextran movement throughout the entire experiment finishing with a reading of 95.67 units below that of control.

### 5.4.3 Scanning electron microscopy - Phl p treatment

The epithelial mono-layer showed no gross morphological changes due to the Phl p treatment, with large cracks appearing possibly due to the processing of the membrane (figure 5.15a, micrograph A). Although at higher magnification, cells can be identified becoming detached from the layer, displaying a rounded appearance not the flattened appearance that would be expected (figure 5.15a, micrograph B). Examination of the finer surface features of the cells shows good microvilli retention, that do not appear to have been effected by the treatment (figure 5.15b, micrograph C and D).

### 5.4.4 Scanning electron microscopy - Protease treatment

Protease treatment of the IOBA-NHC cells shows denudation of the epithelial layer at low magnification (figure 5.16, micrograph A). At higher magnification the cells / cellular debris present on the membrane show loss of surface features and few remaining adhesion processes left (figure 5.16, micrograph B).

### 5.4.5 Scanning electron microscopy - Phl p + protease inhibitors treatment

The Phl p + protease inhibitor treatment shows small regions of epithelial cells with gaps being formed in between them (figure 5.17a, micrograph A). At higher magnifications, fibrous material is seen covering the surface of the cells, making the identification and analysis of cell surface features impossible (figure 5.17a, micrograph B and figure 5.17b, micrographs C and D).

### 5.4.6 Scanning electron microscopy - Phl p + histamine treatment

Treatment with Phl p + histamine produces small gaps to be formed in between cells, and possible cell detachment, with cells displaying rounded shapes (figure 5.18a, micrographs A and B). At higher magnification, deposits of fibrous cellular debris make further identification and analysis of surface features impossible (figure 5.18b, micrographs C and D).

## 5.6 Discussion

The chapter hypothesis states:

*Phleum pratense (Timothy grass) facilitate paracellular movement of non-indigenous molecules via tight junction disruption.*

In order to answer this, cell models described in the previous chapter were used in, *in vitro* allergen challenge experiments where cultures were challenged with Timothy grass pollen extract. Throughout the experiment, TEER was measured and the movement of FITC-Dextran across the layer was also monitored. Scanning electron microscopy was used to assess cell layer morphology and cell surface features.

Trans-epithelial electrical resistance was used a direct measure of the polarity of the epithelial barrier, and therefore tight junction integrity. TEER correlates with permeability of tight junctions (Mine and Zhang 2003).

The Dextran molecule was utilised as an insert molecule that could be tracked, via its FITC tag, through the epithelial monolayer and has been used by previous studies to test conjunctival paracellular permeability (Huang *et al* 1989)

Firstly, the protease treatment in each of the allergen models destroyed the tight junctions, cell-cell contacts and the cell layer; this was clearly demonstrated with the immediate and dramatic reduction in trans-epithelial electrical resistance from the start of the experiment. This destruction of the cell layer as a barrier was also seen with the movement of FITC-Dextran from the upper chamber into the lower chamber. Scanning electron microscopy revealed that the epithelial layer had been totally removed from the membrane. These results lead to the possibility that the protease used was at too high a concentration.

Phl p treatment in the three models showed reductions in TEER, suggesting destruction of the tight junctions. In terms of the paracellular movement of FITC-Dextran, the 16HBE 14o- models showed the most movement, with little seen in the ChWk and inhibition of movement in the IOBA-NHC model. Morphologically the 16HBE 14o- cells had valleys in between the cells that would back-up the FITC-Dextran data of movement. The ChWk and IOBA-NHC morphology showed no valleys, therefore little dextran movement, the cracks seen are possibly due to some of the processing stages for electron microscopy. The surface features of the ChWk and IOBA-NHC cells showed that the allergen caused flattening of the microvilli in the ChWk and no distinguishable changes in the IOBA-NHC cells, which would explain the inhibition of movement. Phl p1 has been cited as a cysteine protease, demonstrated by

specific substrates and inhibitors and therefore could be the allergen that facilitates allergen paracellular movement as seen by the data above (Petersen *et al* 1999). Phl p1 mode of action is postulated to be similar to the major house dust mite allergen Der p1, found in house dust mite faeces, which is also a cysteine protease (Tovey *et al* 1981). Der p1 has been extensively studied, and has been shown to degrade the tight junction by cleavage of the proteins occludin, claudin-1 and ZO-1 (Wan *et al* 2000 and 1999, Schulz *et al* 1998, Roche *et al* 1997). Serine proteinases present in Timothy grass pollen allergen could also mediate increased epithelial permeability (Wan *et al* 2001, John *et al* 2000). The changes in the morphology of the 16HBE 14o- could be a result of junctional deterioration, which leads to enhanced paracellular transit (Evans *et al* 2002). Mine (2003) showed shortening of microvilli on cells post food allergen treatment, similar to the shortening seen with the Phl p treatment. House dust mite proteinase also has been shown to induce cell death, as seen in the micrographs with cell having a round shape and detaching from the membrane (Winton *et al* 1998).

Phl p + protease inhibitor treatment did not overtly affect the TEER of any of the cell models with the readings staying around the control. This was also seen in the movement of dextran, with only the ChWk showing a slight movement from the 12-hour mark until the end of the experiment. None of the cell layer morphologies was greatly affect either, with cracks being seen possibly due to the processing steps. The surface features of the cell lines did not offer any clue, with shortened microvilli seen present with increased amounts of debris also seen on the cell membranes. With Phl p1 being classified as a cysteine proteinase its action should be inhibited by E-64 (one of the constitutes of the protease inhibitor), and has been shown to inhibit the cysteine proteinase fraction of the group 1 allergen (Winton *et al* 1998). With the observation of no change in TEER or the movement of FITC-Dextran shows that the Phl p allergen may work as a cysteine protease.

Phl p + Histamine treatment in all the cell models produced a reduction in TEER without any notable movement of FITC-Dextran across the cell layer with inhibition seen in the ChWk and IOBA-NHC layers. Morphologically the 16HBE 14o- appeared to be most affected by this treatment with cell-cell contacts being lost as individual cells can be identified, this would partially explain the slight movement of dextran seen in the early part of the experiment. Surface feature analysis showed that the again, debris

deposited on the cell membranes, with the exception of the ChWk layer, which displayed a greatly flattened appearance, possibly due to the action of the treatment. Histamine has been cited as increasing paracellular permeability, possibly via disruption of E-cadherin (Zabner *et al* 2003). Although other studies have shown that histamine has no discernable effect on paracellular epithelial permeability (Devalia *et al* 1994). Histamine has also been shown to have roles in modulating cell growth and migration and regulation the inflammatory activation of epithelial cells (Leonardi *et al* 1999).

## 5.7 Conclusion

*Phleum pratense (Timothy grass) facilitate paracellular movement of non-indigenous molecules via tight junction disruption.*

So does the hypothesis hold true?

The addition of Phl p did reduce the TEER and FITC-Dextran was detected in the lower chamber, suggesting that the allergen facilitated the paracellular movement of non-indigenous molecules. The action of the Phl p has been suggested via protease action, as with the addition of protease inhibitors the effect on TEER is reduced. This would agree with Petersen (1999) who suggested Phl p 1 works via its cysteine protease motifs.

# 5.1 16HBE 14o- Allergen challenge TEER

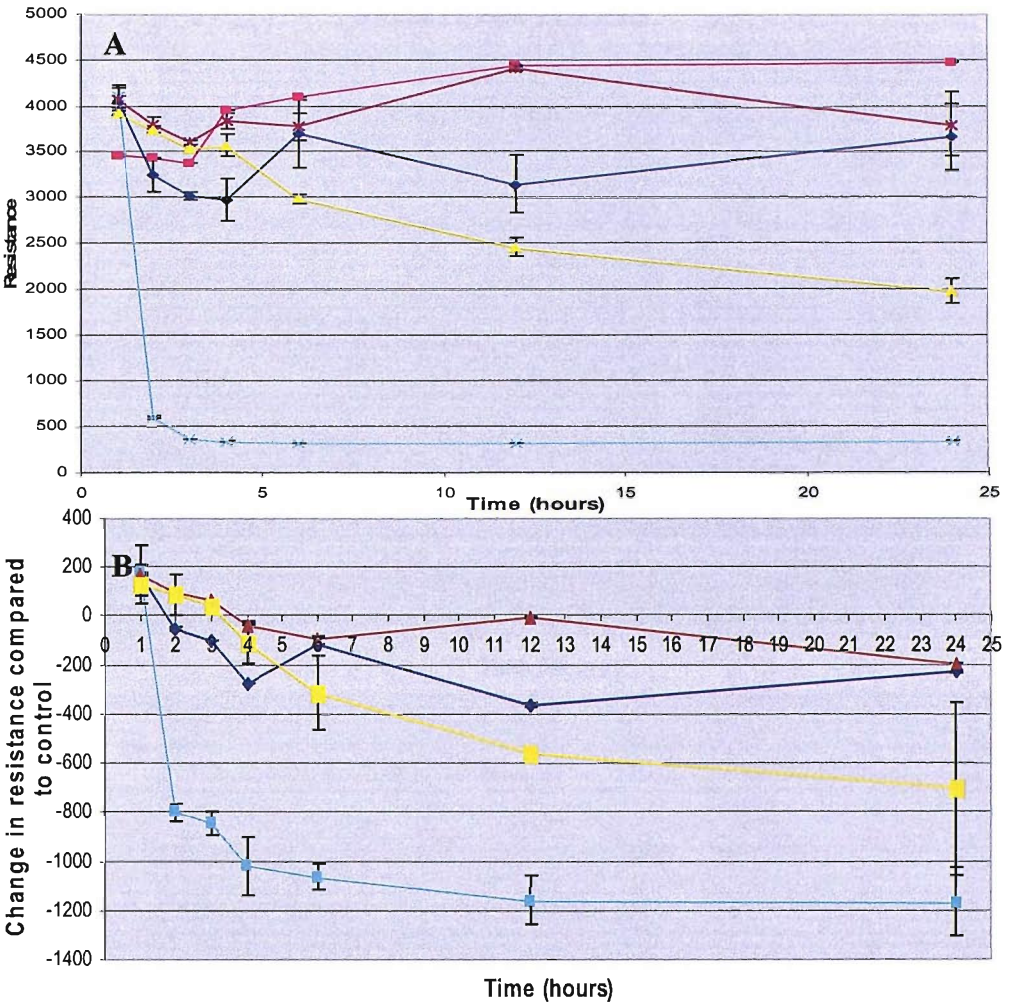


The above graphs show the Trans-Epithelial Electrical Resistance of the 16HBE 14o- cell line model when challenged with timothy grass pollen extract and other treatments.

- Control,
- Phl p,
- Protease,
- Phl p and inhibitor cocktail,
- Phl p and histamine.

Graph A shows the raw resistance values recorded throughout the course of the experiment.

Graph B shows the resistance reading when compared against the control and corrected for area, using the equation (Re - Rc) $\pi r^2$ = R (Ohms.cm$^2$). It is clear from the graph that the protease treatment rapidly reduces the electrical resistance of the cell mono-layer with no recovery seen within the 24 hour experiment time period, ending on a reading of -1167.69. The three Phl p treatments (Phl p, Phl p + inhibitor cocktail and Phl p + histamine) all started by dropping the resistance in a similar trend until the 4 to 6 hour mark, at which point the resistance in the Phl p and Phl p + inhibitor cocktail treatments recovered but ended still -229.73 and -192.61 from the control respectively (both p = n/s). The Phl p + histamine treatment showed no signs of recovery in resistance ending at -705.79 from the control ($p > 0.001$).

n = 16 for each treatment

# 5.2 16HBE 14o- allergen challenge FITC-Dextran levels

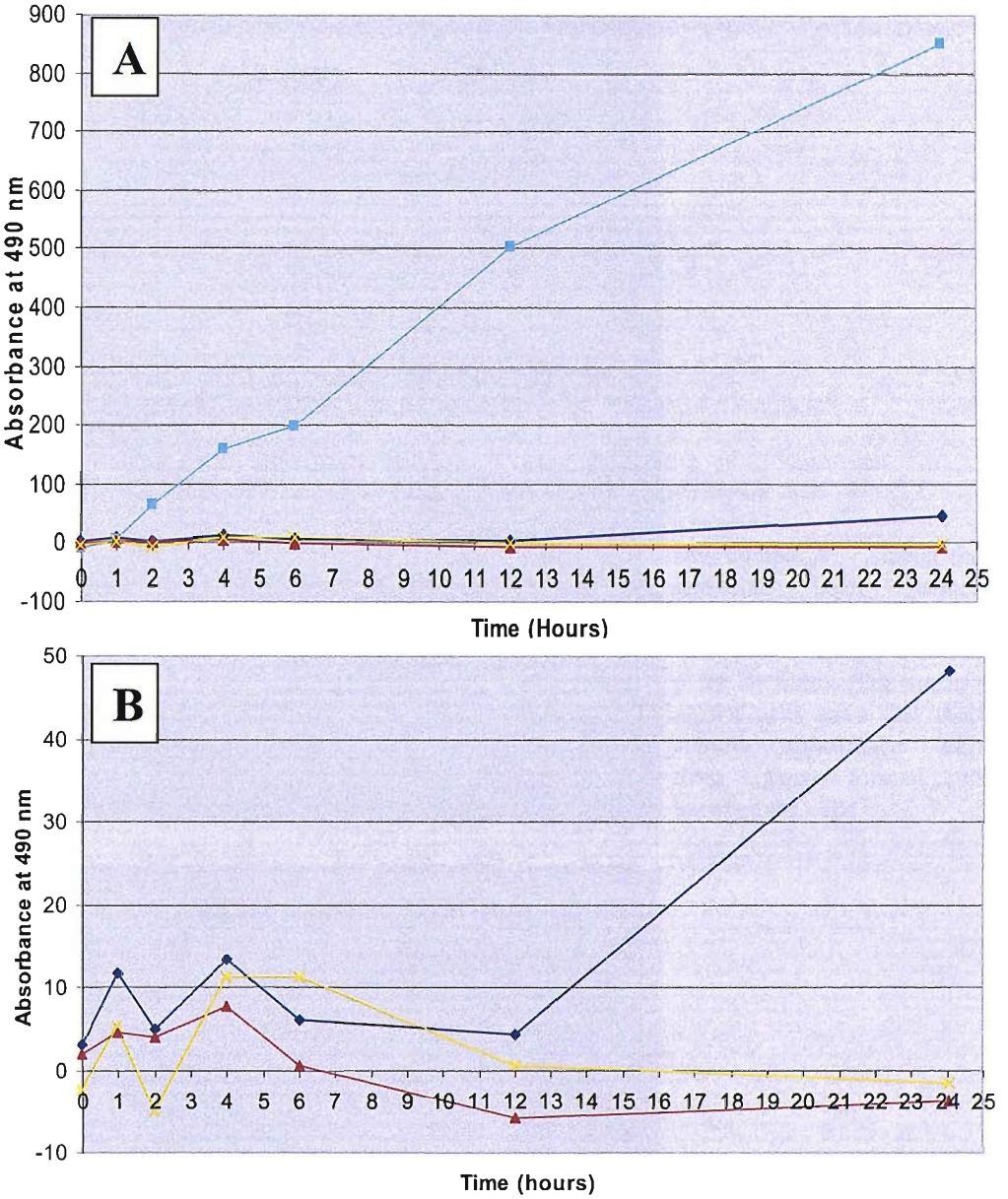


The above graph shows the movement of FITC-Dextran within the 16HBE 14o- cell line model allergen challenge.

- Phl p,
- Protease,
- Phl p and inhibitor cocktail,
- Phl p and histamine.

The above graphs show the movement of the FITC-Dextran across the 16HBE 14o- cell layer, when sampled from the lower chamber of the insert.

Graph A shows the four treatments (Phl p, Protease, Phl p + inhibitor cocktail and Phl p + histamine) that the 16HBE 14o- cell model were treated with. Clearly the protease treatment caused the greatest movement of FITC-Dextran across the cell mono-layer, ending with a final optical reading of 850 when measured at 490nm. This reading is so much higher than the others that further analysis is impossible.

Graph B shows the optical readings from the same three treatments of Phl p, Phl p + inhibitor and Phl p + histamine. Both the Phl p + inhibitor and Phl p + histamine treatments caused slight fluctuating optical readings along the experimental time line, both ending with readings that are close to the experiment control (-3.66 and -1.66 respectively). The Phl p treatment fluctuated until the 12 hour point of the experiment, at which point it rose steadily ending with a reading of 48.33.

The x axis is the experiment time line. Samples time points were 0, 1, 2, 4, 6, 12 and 24 hours.

The y axis is the absorbance at λ 490nm.

# Figure 5.3a 16HBE 14o- Phl p treatment

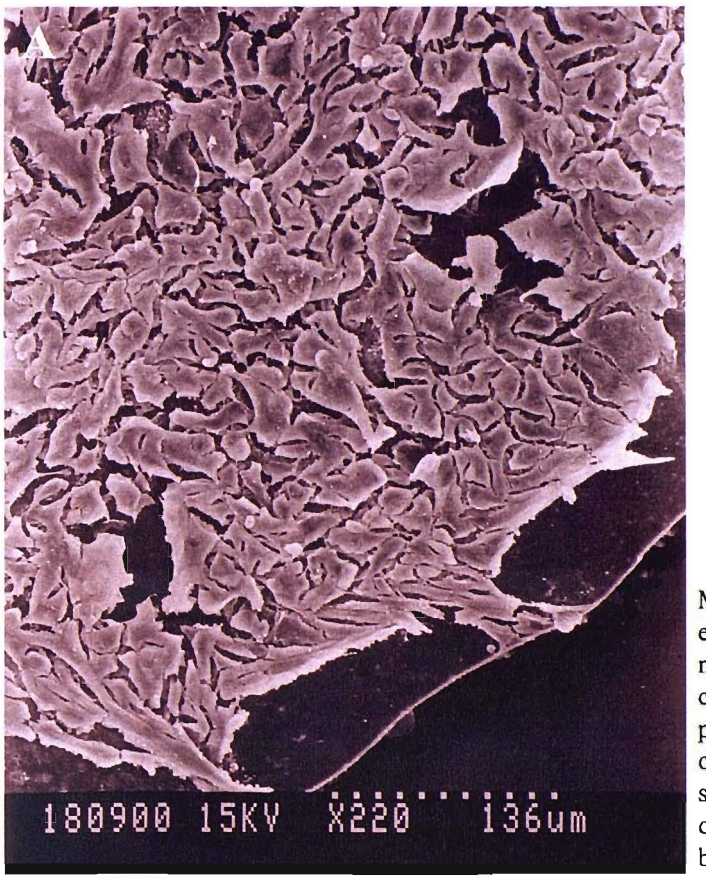


Micrograph A – shows the epithelial layer surface morphology of 16HBE 14o- cells, post treatment with Phl p for 24 hours. The surface of the cells have lost their smooth appearance with deep gaps formed in between the cells.

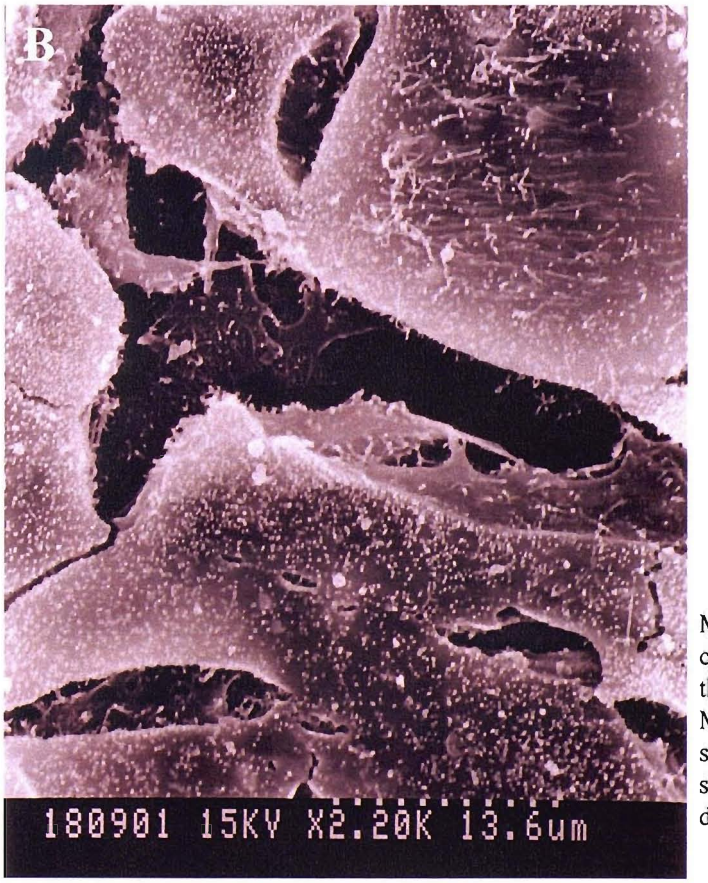


Micrograph B – shows the cell surface morphology and the loss of cell-cell contacts. Microvilli still present on the surface of the cells do not show any significant surface damage or re-distribution.

# Figure 5.3b 16HBE 14o- Phl p treatment

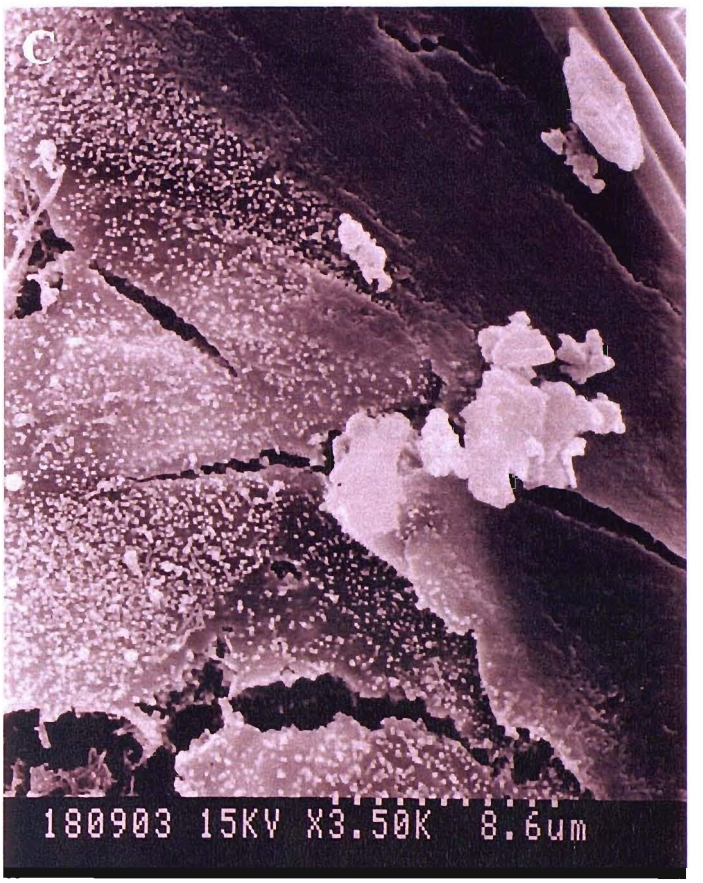


Micrograph C – shows the microvilli on the surface of the cells in greater detail and also the gaps formed between the cells.

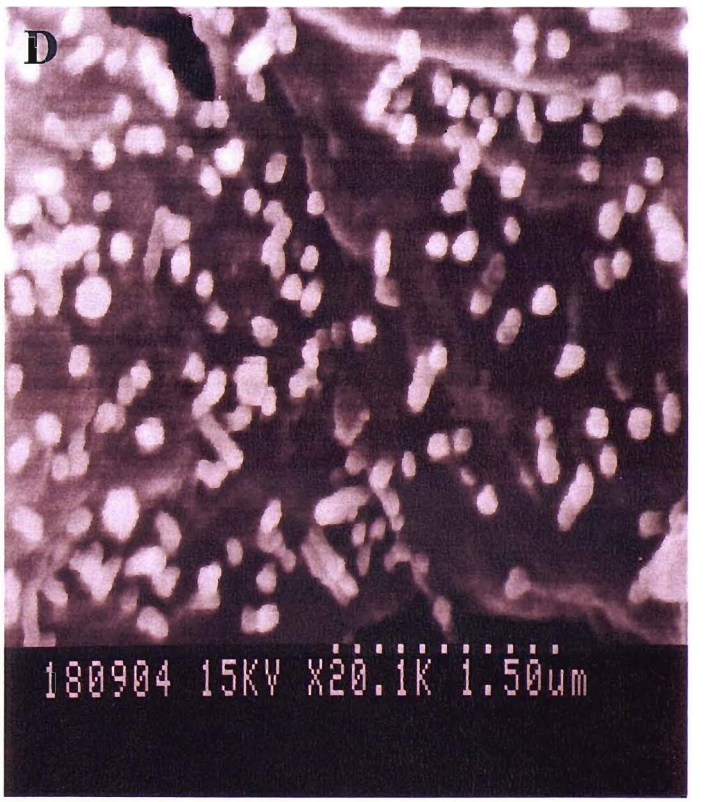


Micrograph D – shows a lack of branching can be identified in the microvilli also possible shortening of the microvilli.

# Figure 5.4 16HBE 14o- Protease treatment


Micrograph A – shows total epithelial loss from the surface of the insert membrane after protease treatment for 24 hours.

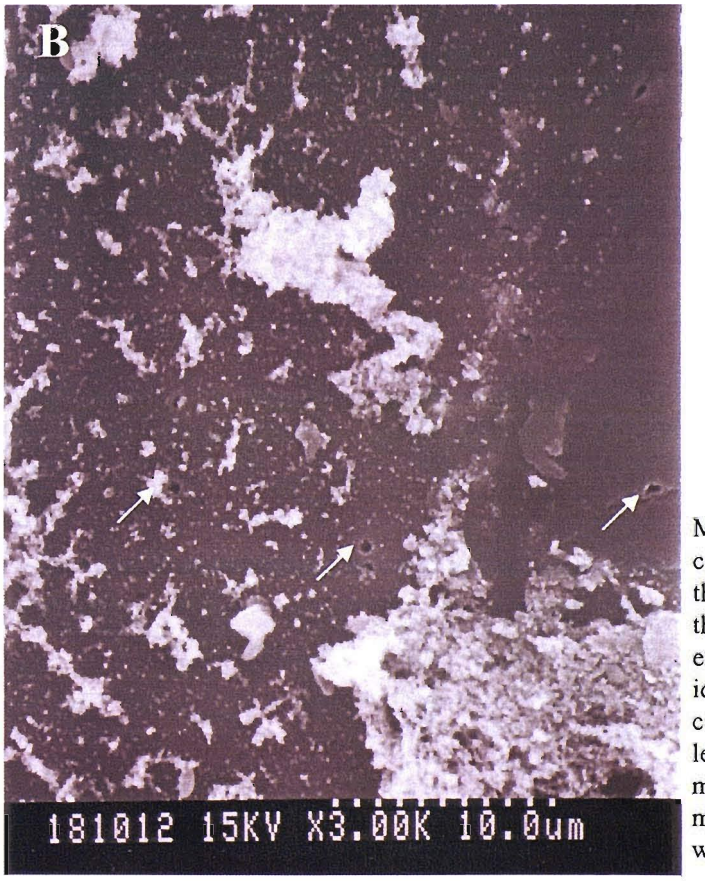


Micrograph B – shows the cellular debris remaining on the insert membrane after the protease treatment. The extent of cell damage can be identified remains of a cell can be seen in the bottom left corner of this micrograph. The pores in the membranes are highlighted with the white arrows.

# Figure 5.5a 16HBE 14o- Phl p + Protease Inhibitor treatment

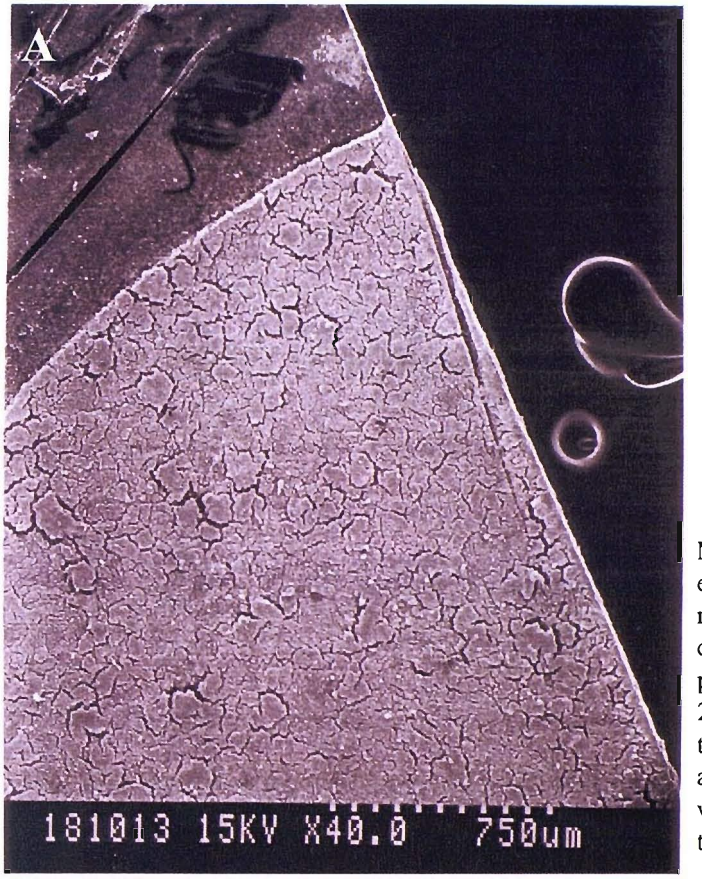


Micrograph A – shows the epithelial layer surface morphology of 16HBE 14o- cells, post treatment with Phl p and Protease Inhibitors for 24 hours. The cells have lost their smooth surface appearance with deep valleys formed in between them.

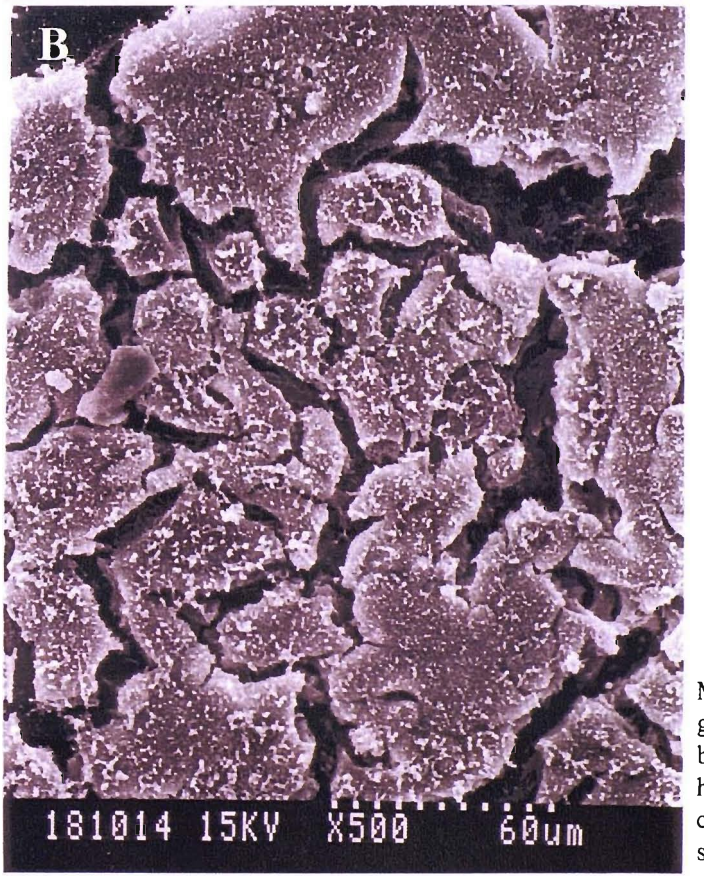


Micrograph B – shows the gaps that have formed in-between the cells after 24 hours of treatment. These cells seem to have retained some of the surface features.

# Figure 5.5b 16HBE 14o- Phl p + Protease Inhibitor treatment

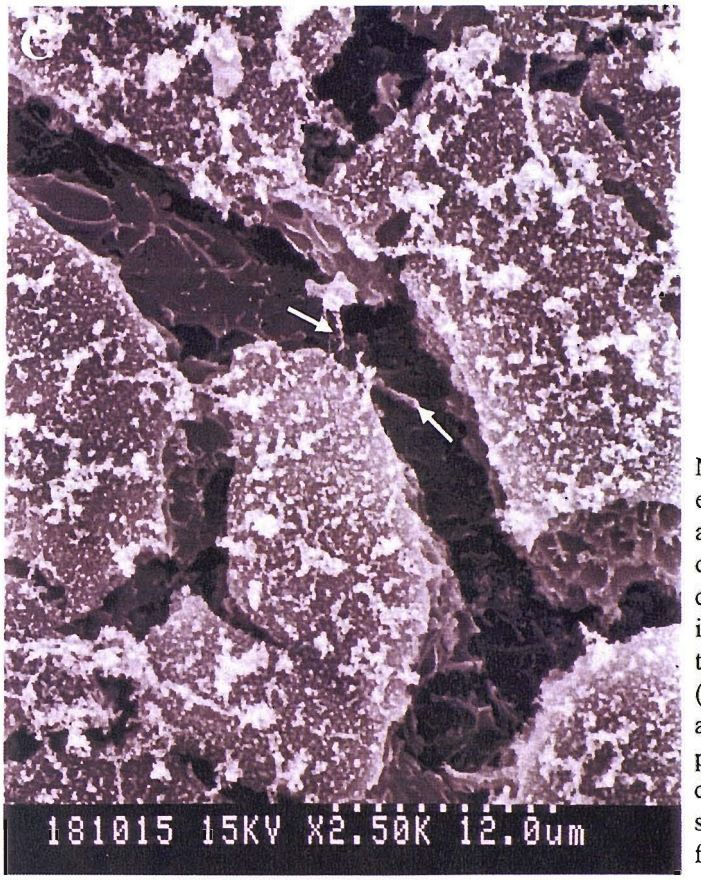


Micrograph C – shows the extent of the cell shape loss and the loss of cell-cell contacts although possible cellular processes can be identified extending from the cell membrane (highlighted with the white arrows). Microvilli are still present on the surface of the cells, but also present on the surface are clumps of fibrous material.

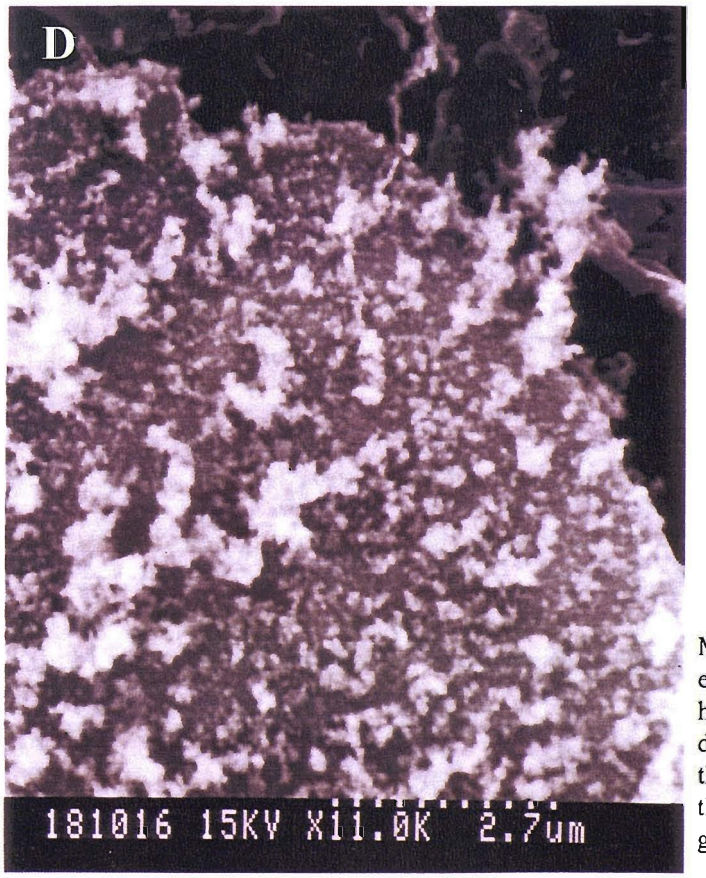


Micrograph D – shows the effect that the treatments have had on the microvilli, displaying degradation of the microvilli and debris on the surface on the cell in greater detail.

# Figure 5.6a 16HBE 14o- Phl p + Histamine treatment

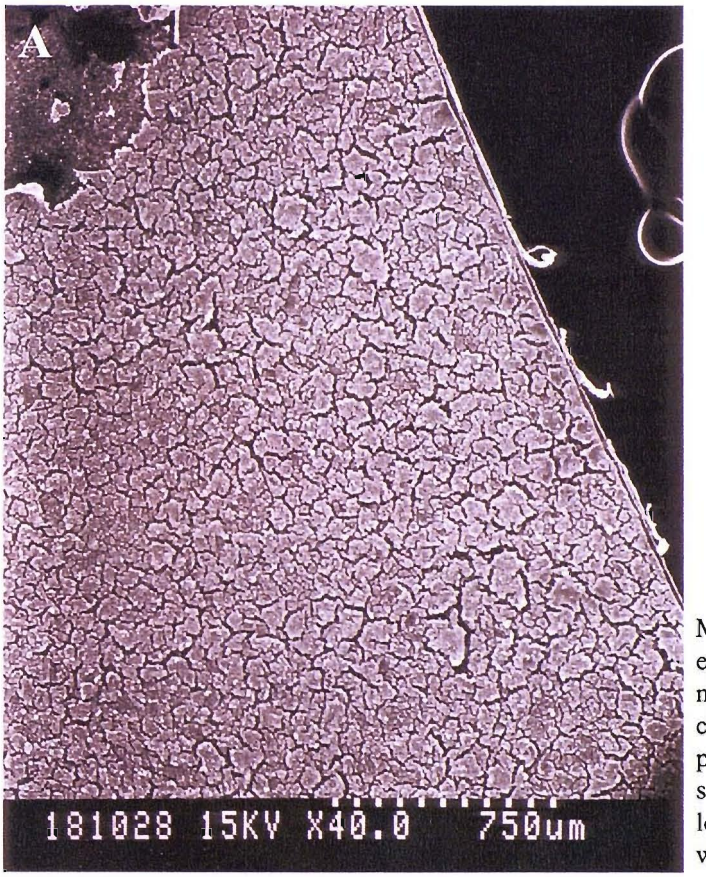


Micrograph A – shows the epithelial layer surface morphology of 16HBE 14o- cells, post treatment with Phl p and Histamine. The surface of the cell layer has lost its smooth appearance, with deep valleys formed.

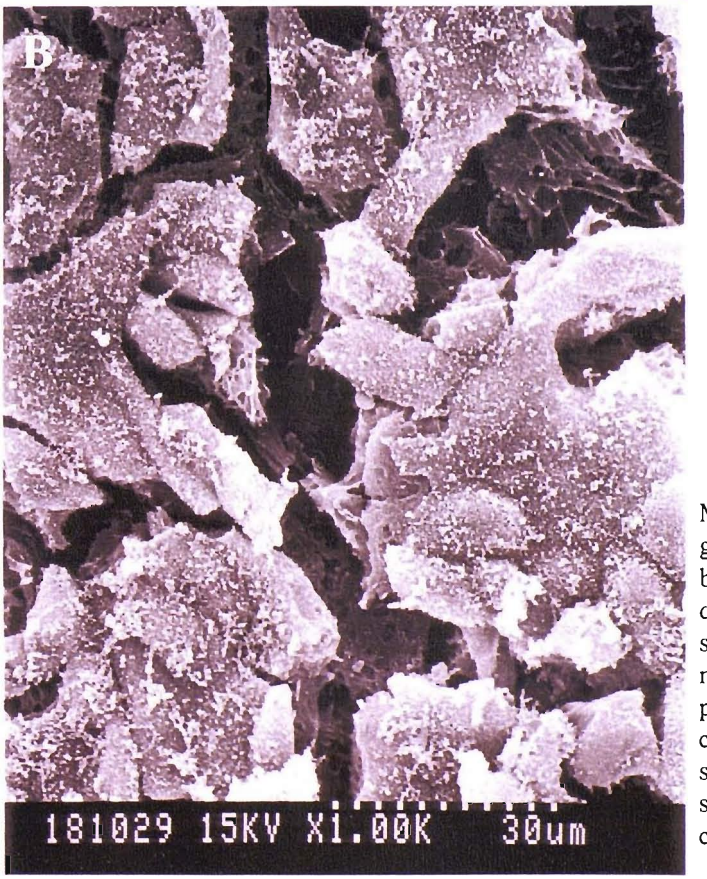


Micrograph B – shows the gaps that have formed in-between the cells in greater detail. Cells have retained surface features such as microvilli and cellular processes. Individual cells can be identified from their shape even though they are still incorporated within the cell layer.

# Figure 5.6b 16HBE 14o- Phl p + Histamine treatment

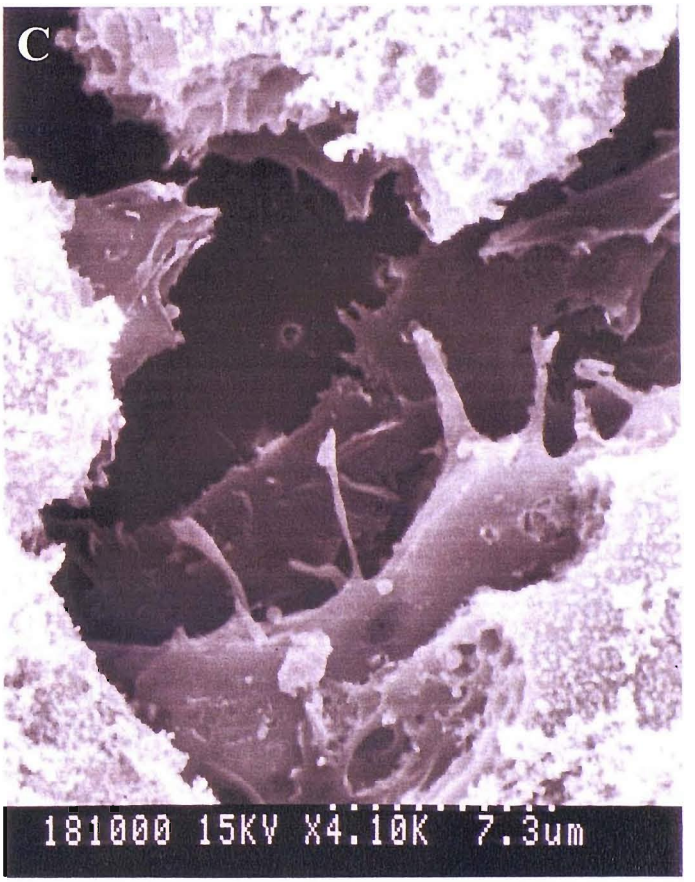


Micrograph C – shows an edge of a cell, displaying the retention of microvilli on the surface, and the presence of projecting cellular processes extending from the cell. Debris can also be identified on the cell surface although not well shown in this micrograph.

# Figure 5.7 ChWk allergen challenge TEER

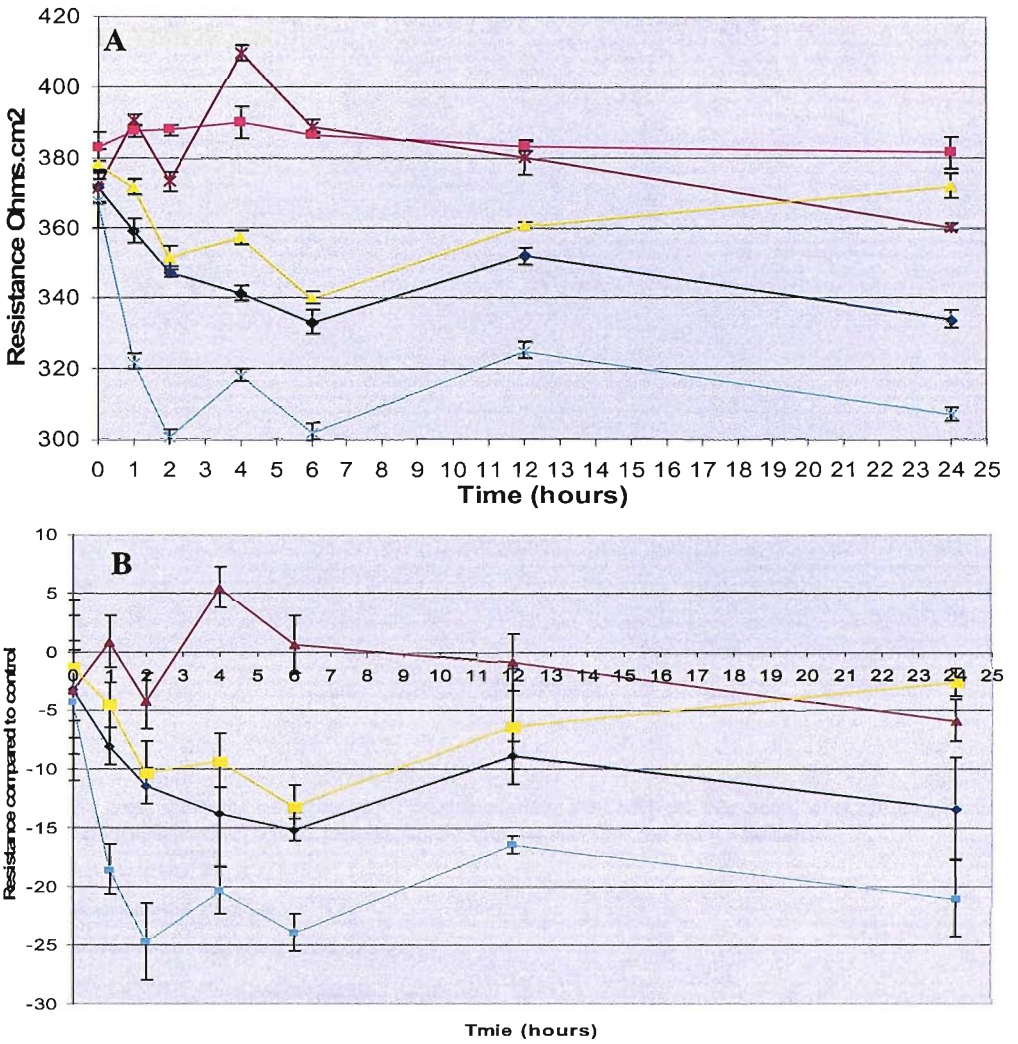


The above graph shows the Trans-Epithelial Electrical Resistance of the ChWk cell line model when challenged with timothy grass pollen and other treatments.

- Control,
- Phl p,
- Protease,
- Phl p and inhibitor cocktail,
- Phl p and histamine.

Graph A shows the raw resistance values measured throughout the experiment.

Graph B shows the resistance reading when corrected against control and area, using the equation (Re - Rc) $\pi r^2$ = R (Ohms.cm$^2$). The protease treatment reduces the resistance rapidly during the first two hours of the experiment, with no recovery in resistance seen, ending with a resistance value of -20.99 from control. The Phl p and Phl p + histamine both start by reducing the resistance until the 6 hour mark, where the Phl p + histamine recover to a final resistance of -2.61 ($p$ = n/s), the Phl p ends with a resistance of -13.37 ($p > 0.001$). The Phl p + inhibitor cocktail treatment maintains a resistance consistent with control until the 12 hour mark, and falls to a final value of -5.86.

n = 16 for each treatment.

# Figure 5.8 FITC-Dextran movement in the ChWk allergen challenge

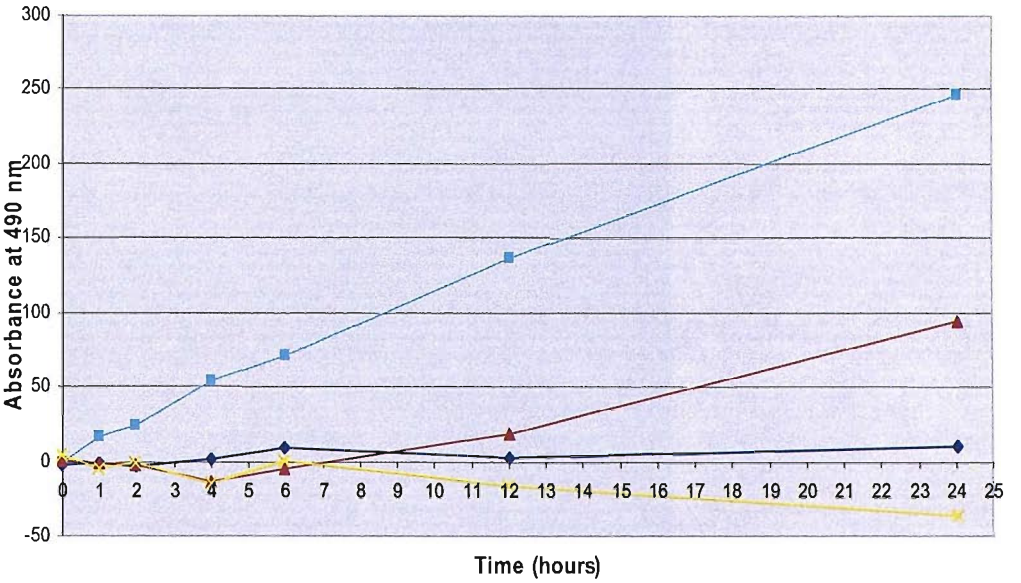


The above graph shows the movement of FITC-Dextran, within the ChWk cell line model, when challenged with timothy grass pollen extract (Phl p), protease, Phl p + protease inhibitors and Phl p + Histamine.

- Phl p,
- Protease,
- Phl p and inhibitor cocktail,
- Phl p and histamine.

The graph shows the movement of the FITC-Dextran from each of the challenge treatments across the ChWk cell layer compared against control, sampled from the lower chamber of the insert. The protease treatment allows the constant diffusion of the FITC-Dextran across the mono-layer. The Phl p and inhibitor treatment remains constant until the 6 hour mark at which point the FITC-Dextran can be seen to move across the mono-layer. The exception is the Phl p + histamine treatment which measured a final reading lower than the control 35.66.

The x axis is the experiment time line. Samples time points were 0, 1, 2, 4, 6, 12 and 24 hours.

The y axis is the absorbance at λ 490nm.

# Figure 5.9a ChWk Phl p treatment

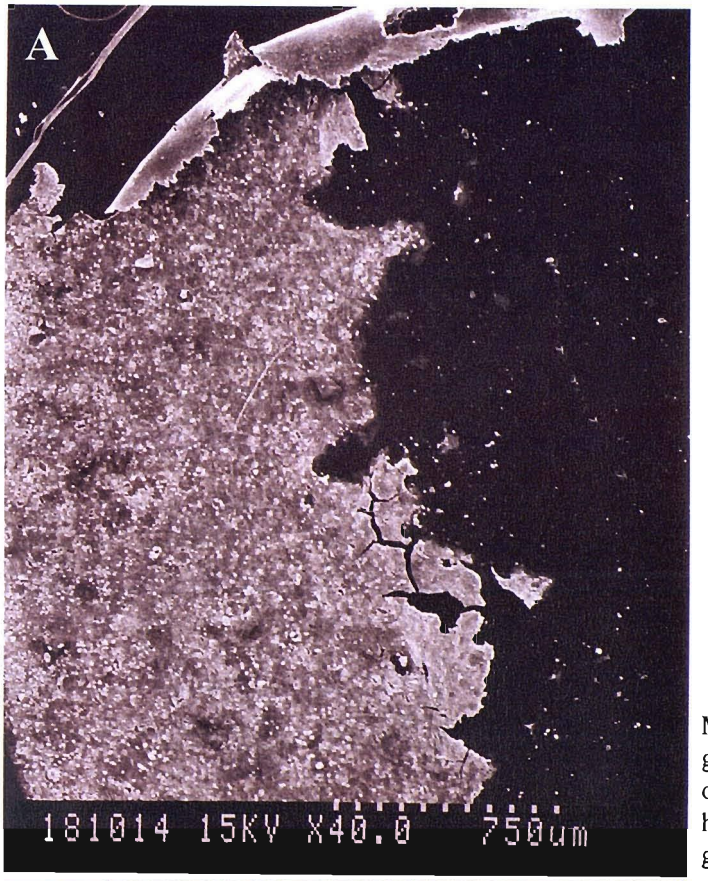


Micrograph A – shows the general surface morphology of the ChWk cells after 24 hours treatment with timothy grass pollen extract.


Micrograph B – shows the cell layer has retained their cell-cell contacts, individual cells that have started to round up and are identifiable (highlighted with the white arrows). The large cracks seen in the epithelial layer are possibly a result of the electron microscopy processing steps, rather than a direct result of the Phlp treatment.

# Figure 5.9b ChWk Phl p treatment

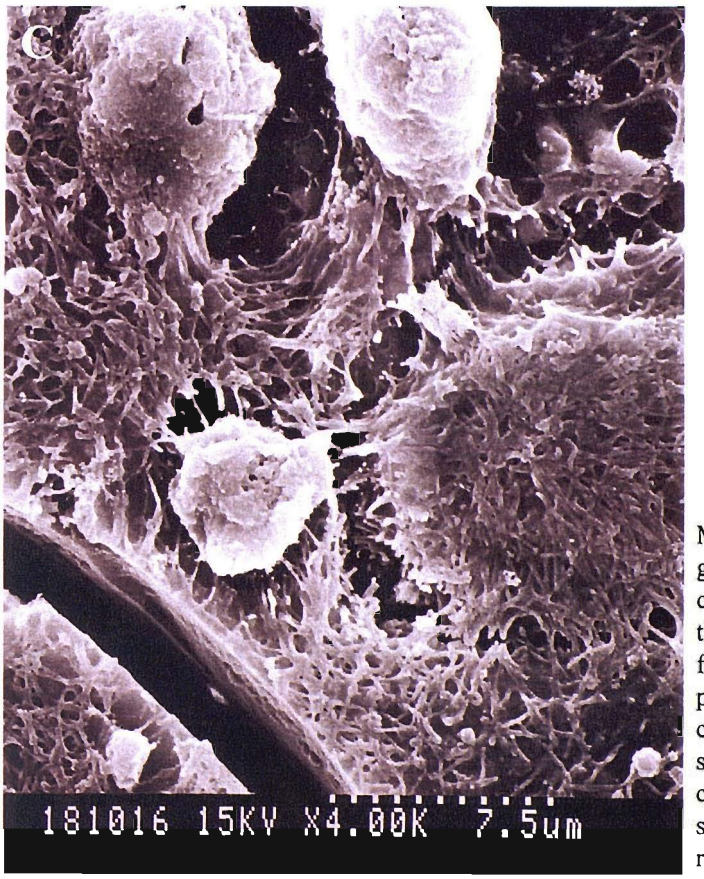


Micrograph C – shows in greater detail the ChWk cells that have started to lose their cell-cell bonds are a forming a spherical shape prior to detaching from the cell layer. On the cell surface, individual microvilli can not be identified as the surface has become more ruffled.


Micrograph D – shows that as the cell loses its classical epithelial shape the microvilli seem to flatten to the cell surface.

# Figure 5.10a ChWk Protease Treatment

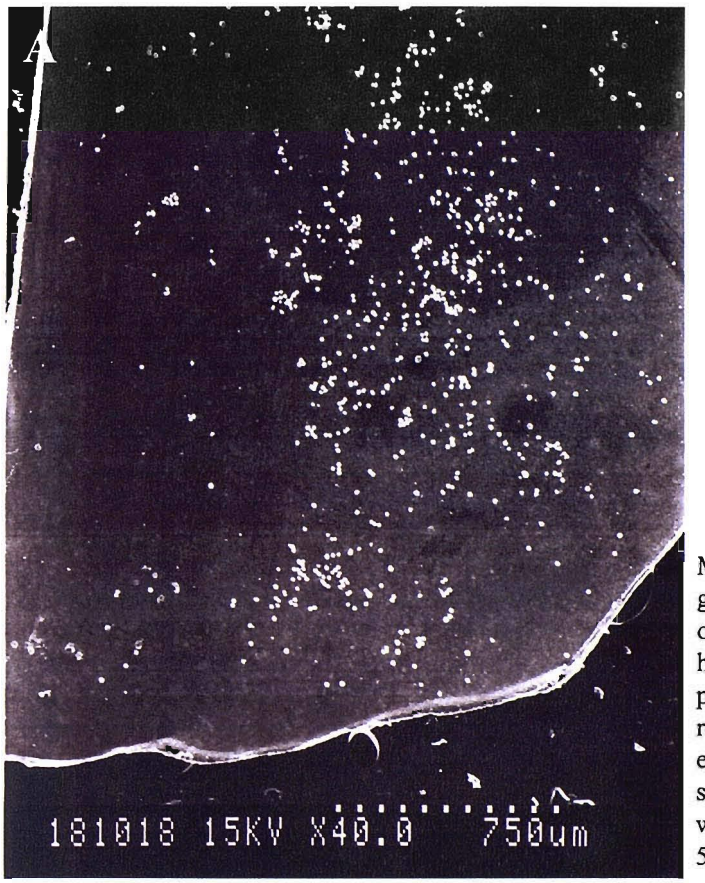


Micrograph A – shows the general surface morphology of the ChWk cells after 24 hours treatment with protease treatment and the resulting loss of the epithelial layer from the surface of the membrane when compared to figure 5.17a micrograph A.

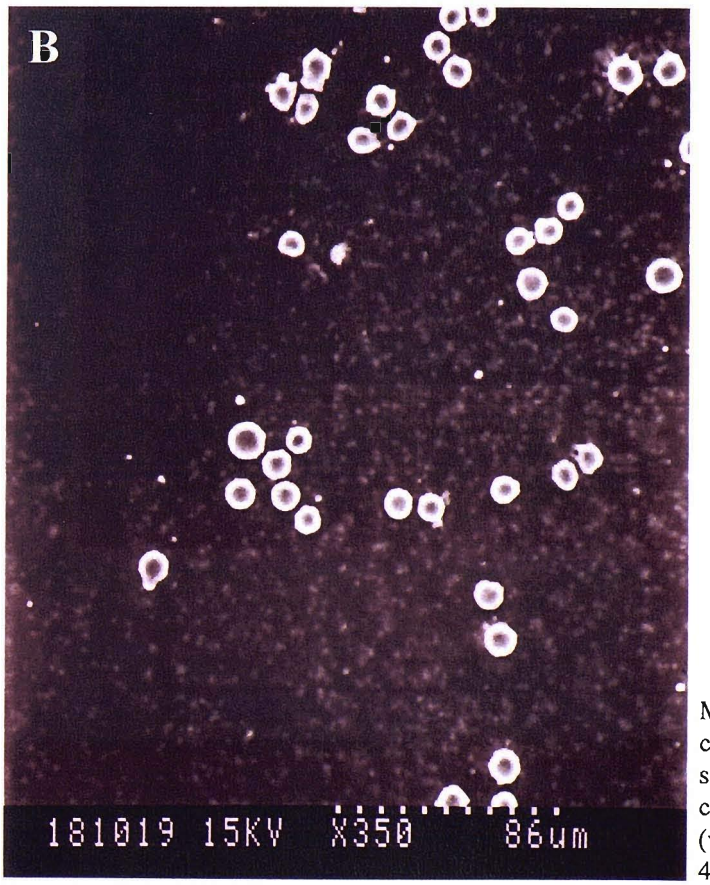


Micrograph B – shows the cells when their epithelial shape has been lost and they change to a round shape (when compared to figure 4.2 micrograph B).

# Figure 5.10b ChWk Protease Treatment

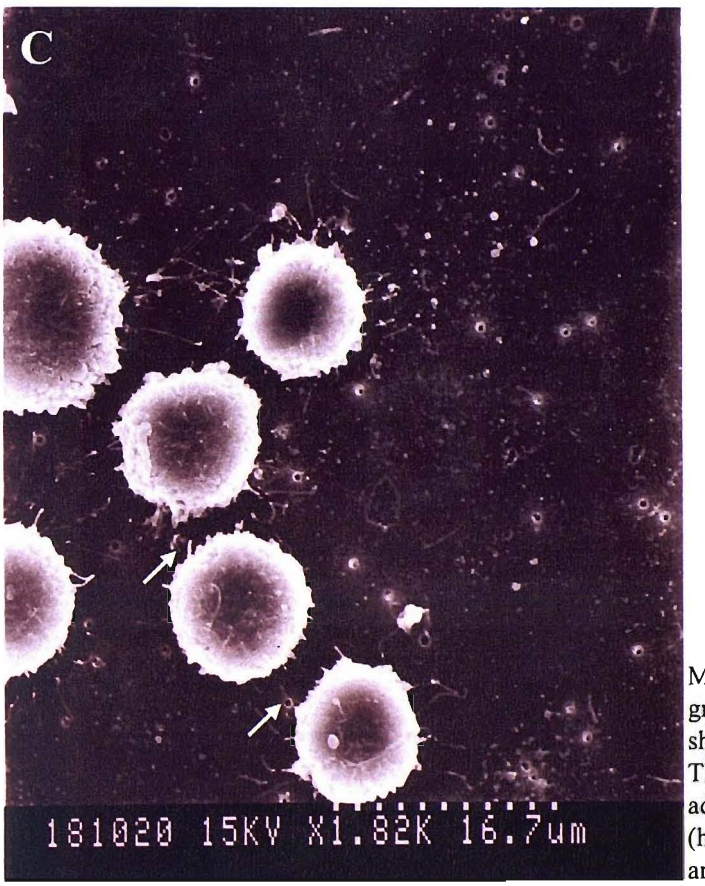


Micrograph C – shows in greater detail the loss of shape and surface features. The few remaining surface adhesion processes (highlighted with the white arrows).

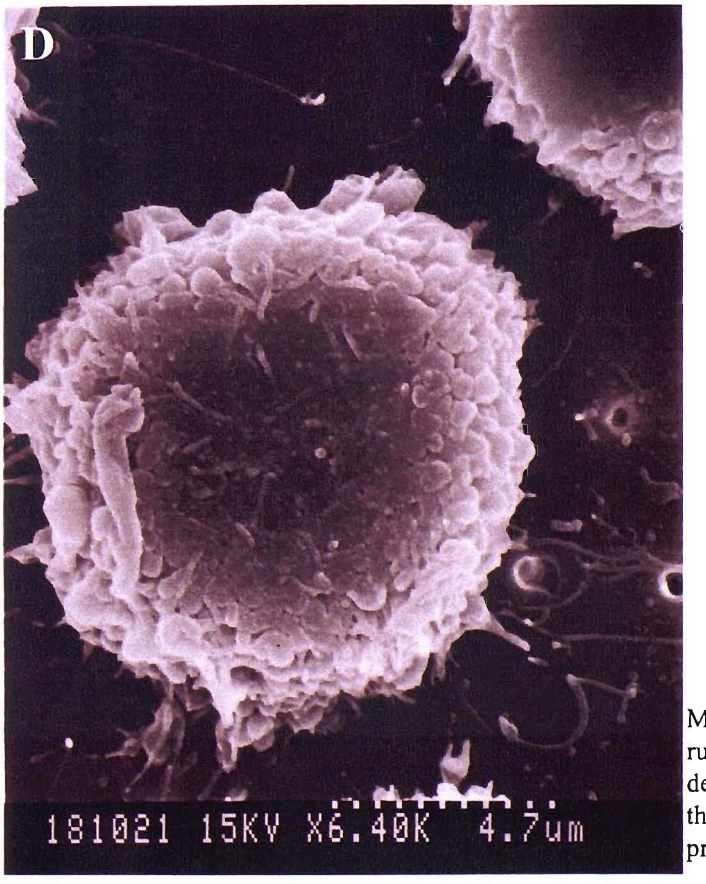


Micrograph D – shows the ruffled surface feature of the detaching epithelial cell and the surface adhesion processes.

# Figure 5.11 ChWk Phl p + Inhibitor treatment

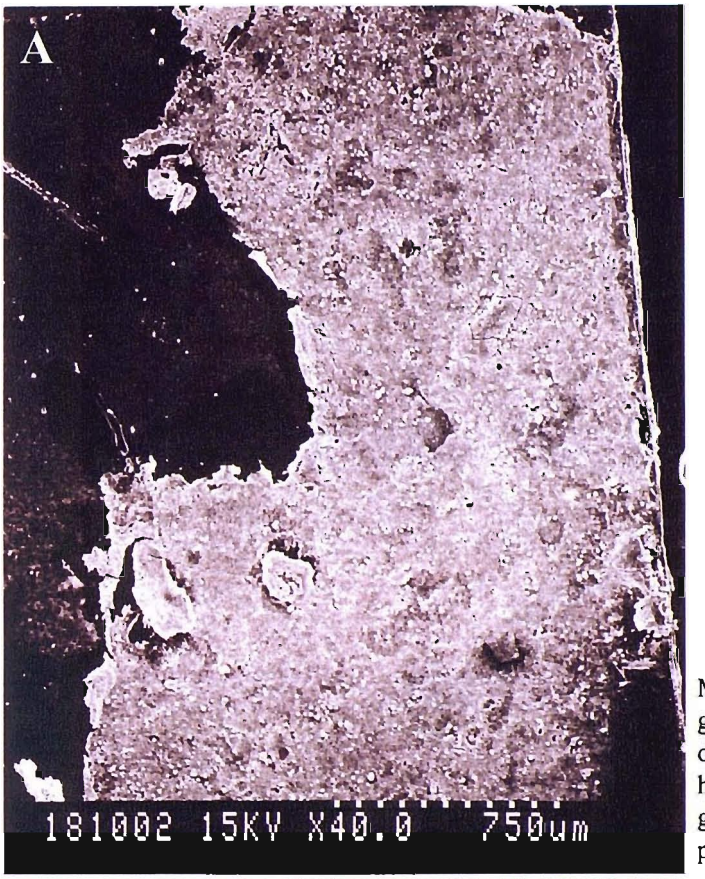


Micrograph A – shows the general surface morphology of the ChWk cells after 24 hours treatment with timothy grass pollen extract and protease inhibitor.

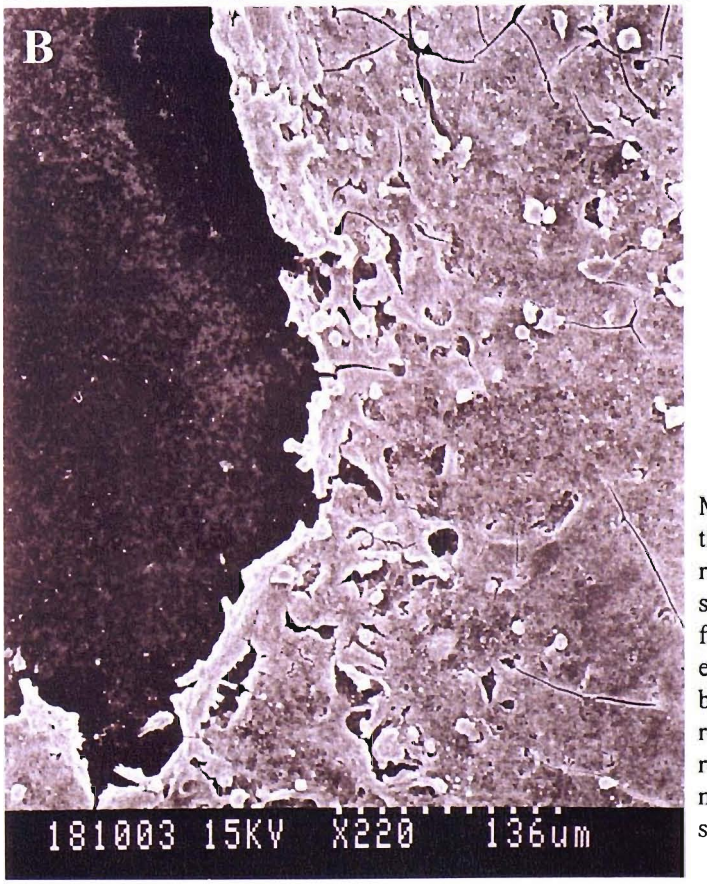


Micrograph B – shows that the ChWk cells have retained their smooth surface morphology. As in figure 5.17 micrograph B, epithelial layer cracking can be seen in the top central region of the micrograph, resulting from the electron microscopy processing steps.

# Figure 5.12a ChWk Phl p + Histamine treatment

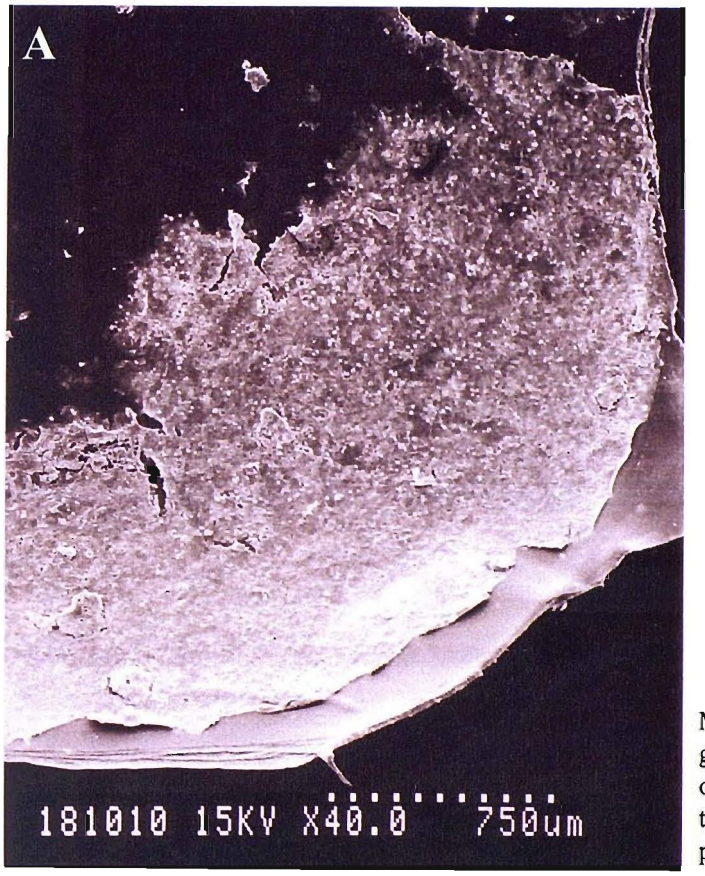


Micrograph A – shows the general surface morphology of the ChWk cells after treatment with timothy grass pollen extract and histamine.

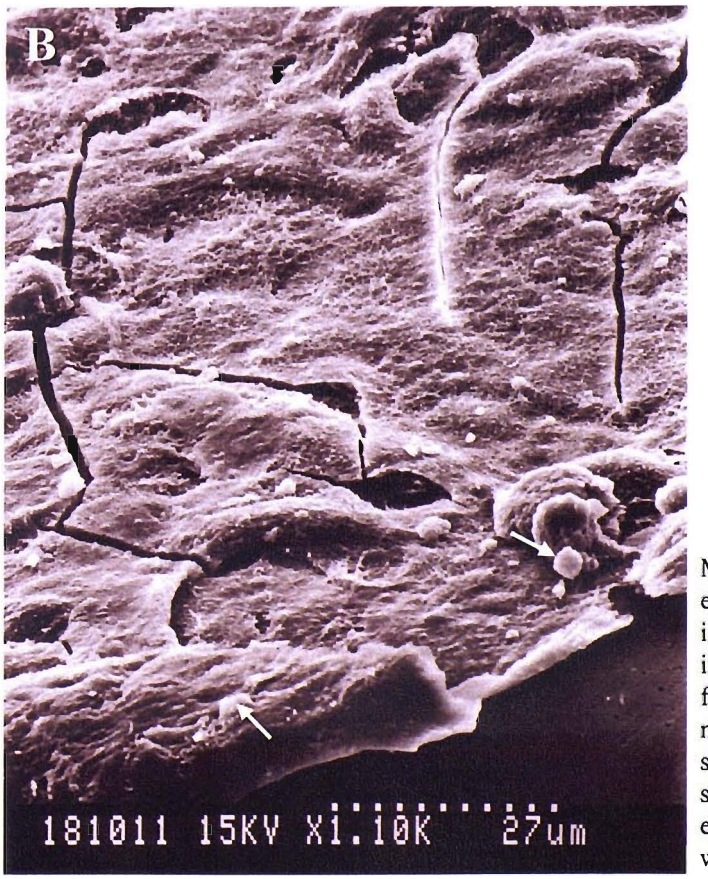


Micrograph B – shows an epithelial surface that is intact. cracking can be seen in the micrograph, resulting from the electron microscopy processing steps. Several cells have started to detach from the epithelial layer (highlighted with the white arrows)

# Figure 5.12b ChWk Phl p + Histamine treatment

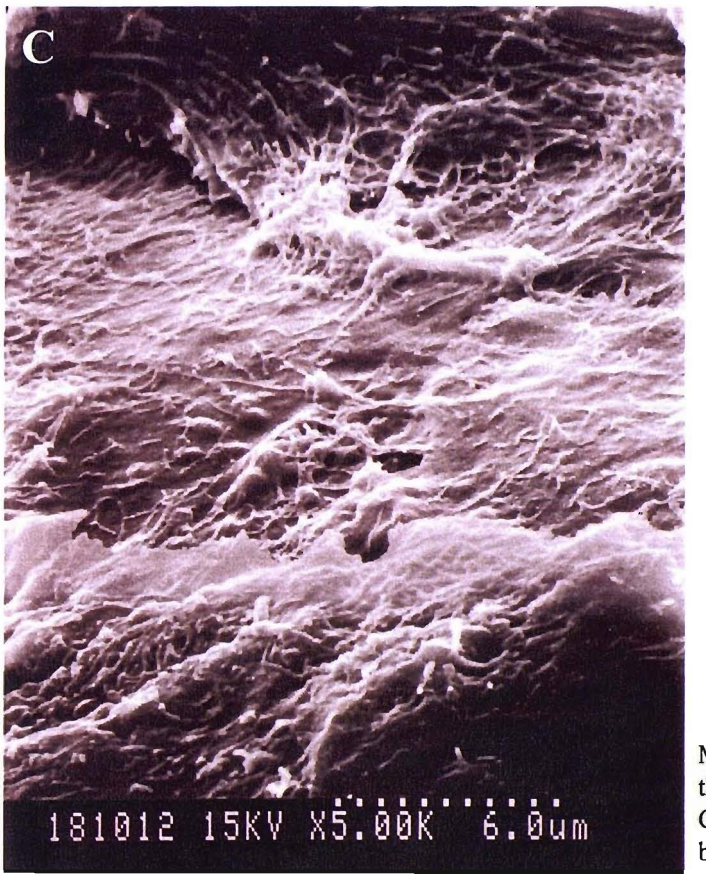


Micrograph C – shows that the surface features of the ChWk cells seem to have been flattened.


Micrograph D – shows the extent of the flattening with the microvili only identifiable as slight raises in the surface membranes of the cells.

# Figure 5.13 IOBA-NHC TEER

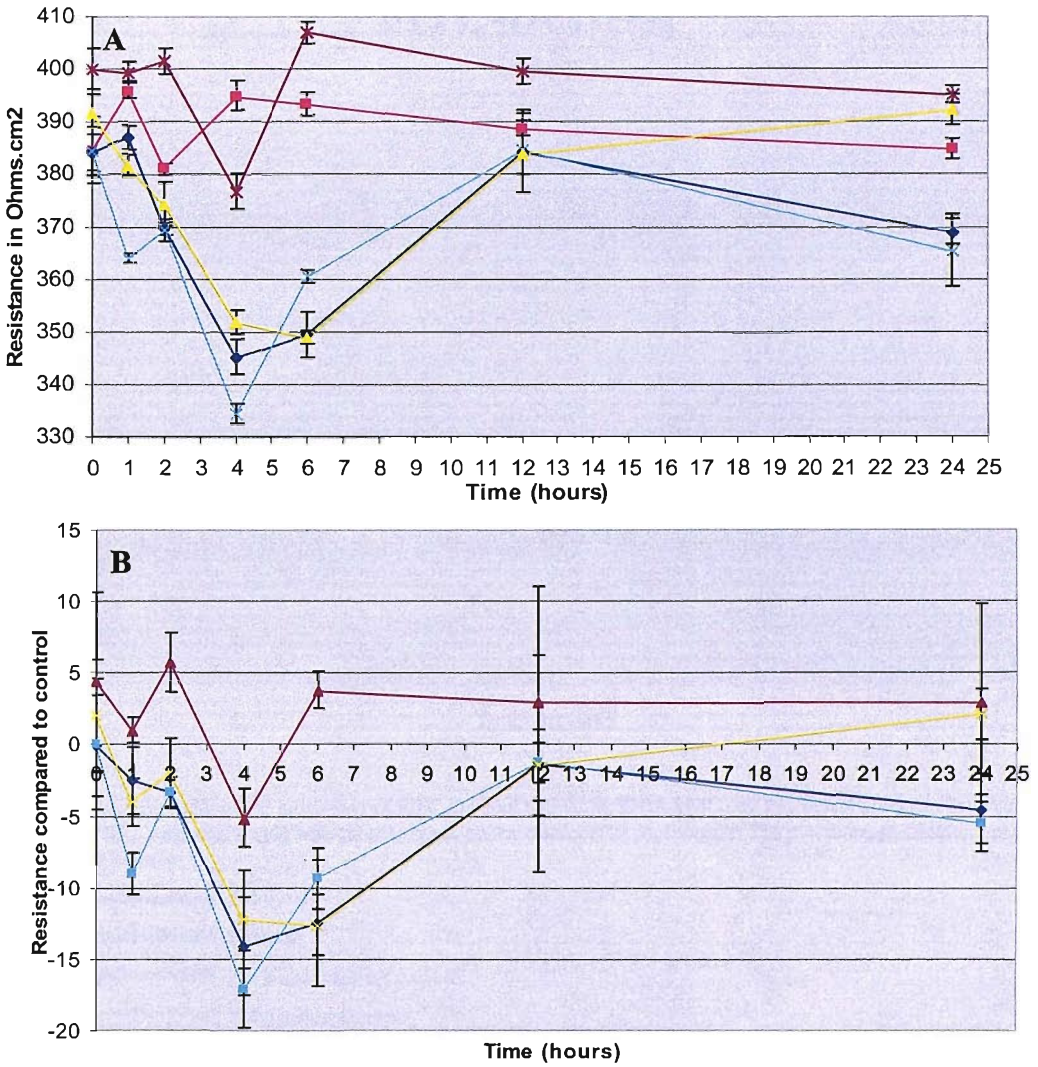


The above graph shows the Trans-Epithelial Electrical Resistance of the IOBA-NHC cell line model when challenged with timothy grass pollen extract (Phl p), Protease, Phl p + protease inhibitors and Phl p + histamine.

- Control,
- Phl p,
- Protease,
- Phl p and inhibitor cocktail,
- Phl p and histamine.

Graph A shows the raw resistance values measured throughout the experiment

Graph B shows the resistance readings when compared against control and corrected for area, using the equation (Re - Rc) $\pi$ $r^2$ = R (Ohms.cm$^2$). All four treatments start by reducing the resistance for the first hour of the experiment. The Phl p + inhibitor resistance is reduced below the control at the four hour mark but recovers back above control ending with a reading of 2.93. At the four hour mark the other treatments recover until the 12 hour mark, where Phl p + histamine finishes with a reading of 2.12 above control. The resistance of the Phl p and protease treatment reduce back down to -4.48 and -5.47 from control respectively ( both $p > 0.01$) .

n = 16 for each treatment.

# Figure 5.14 IOBA-NHC allergen challenge FITC-Dextran

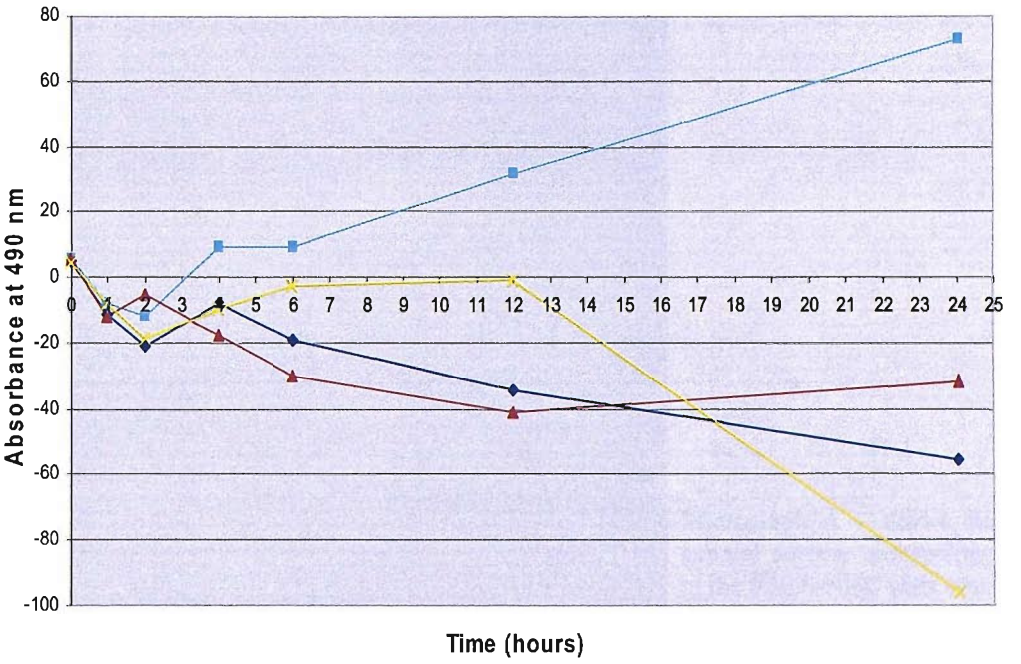


The above graph shows the movement of FITC-Dextran within the IOBA-NHC cell line model allergen challenge. IOBA-NHC were challenged with timothy grass pollen extract (Phl p), Protease, Phl p + protease inhibitors and Phl p+ histamine.

- Phl p,
- Protease,
- Phl p and inhibitor cocktail,
- Phl p and histamine.

The graph shows the movement of the FITC-Dextran recorded from each of the treatments when compared against control, across the IOBA-NHC cell layer sampled from the lower chamber of the insert. The protease treatment allowed the greatest movement of FITC-Dextran across the cell mono-layer. The other treatments caused fluctuating readings until the 12 hour mark at which point the Phl p + histamine ended with -95.66. The other treatments, Phl p and Phl + inhibitor, ended nearer the control line at -55 and -31.33 respectively.

The x axis is the experiment time line. Samples time points were 0, 1, 2, 4, 6, 12 and 24 hours.

The y axis is the absorbance at λ 490nm.

# Figure 5.15a IOBA-NHC Phl p treatment

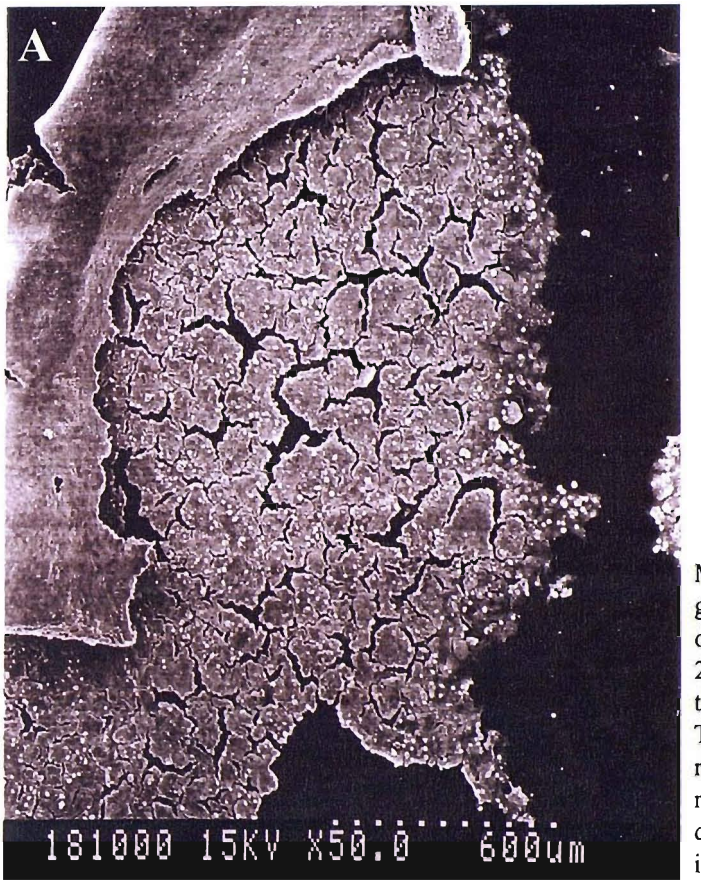


Micrograph A – shows the general surface morphology of the IOBA-NHC cells after 24 hours treatment with timothy grass pollen extract. The layer has large cracks run through it, these do not resemble those encountered during the processing stages in other specimens.

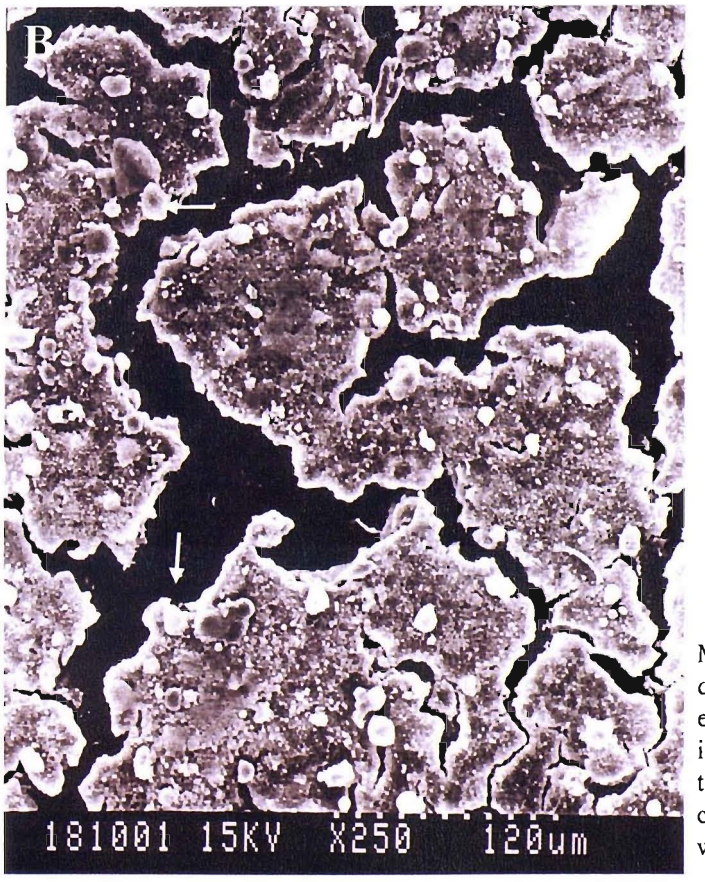


Micrograph B – shows the disassociated regions of the epithelial layer, also identified on the surface of the cell layer are detaching cells (highlighted with the white arrows).

# Figure 5.15b IOBA-NHC Phl p treatment


Micrograph C – shows the retention of the microvili on the surface of the cells.


Micrograph D – shows the cell surface features in greater detail.

# Figure 5.16 IOBA-NHC Protease treatment


Micrograph A – shows the IOBA-NHC cells after 24 hours treatment with protease treatment and the resulting loss of the epithelial layer from the surface of the insert membrane.


Micrograph B – shows the morphology of a cell still attached to the insert membrane, cell adhesion processes are highlighted with the white arrow.

# Figure 5.17a IOBA-NHC Phl p + Inhibitor treatment

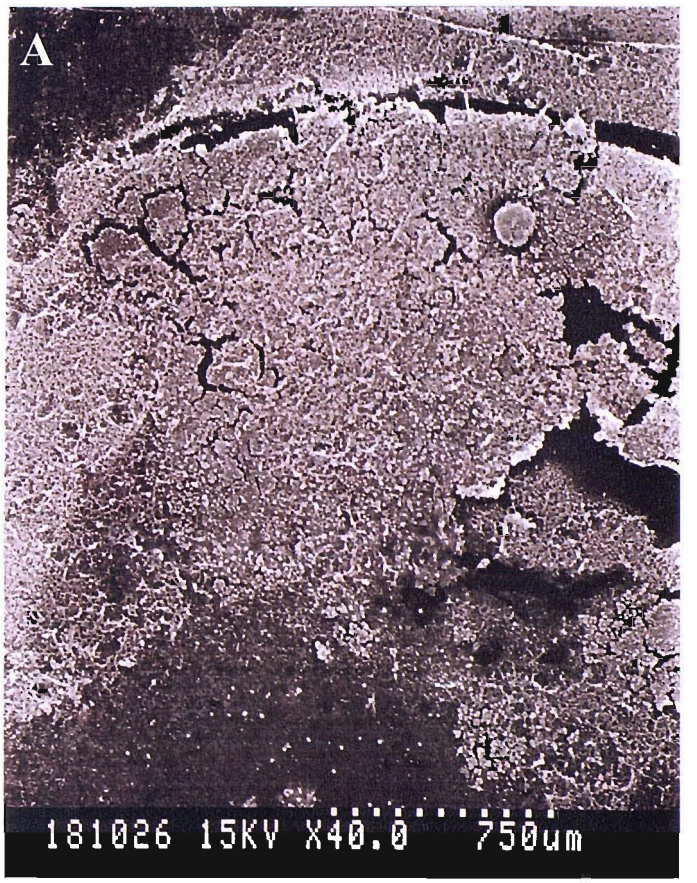


Micrograph A – shows the general surface morphology of the IOBA-NHC cells after 24 hours treatment with grass pollen extract and protease inhibitor treatment. Cracks in the epithelial layer can be identified possibly due to the treatment conditions.

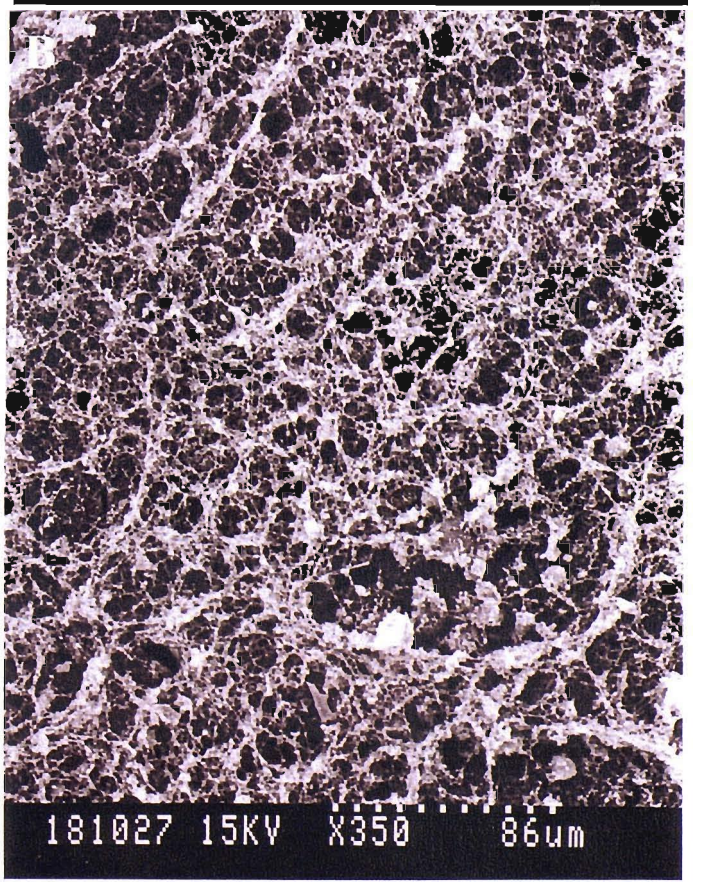


Micrograph B – shows the general surface features of the cells, although the individual cells can not be identified, also present on the surface are clumps of fibrous material.

# Figure 5.17b IOBA-NHC Phl p + Inhibitor treatment

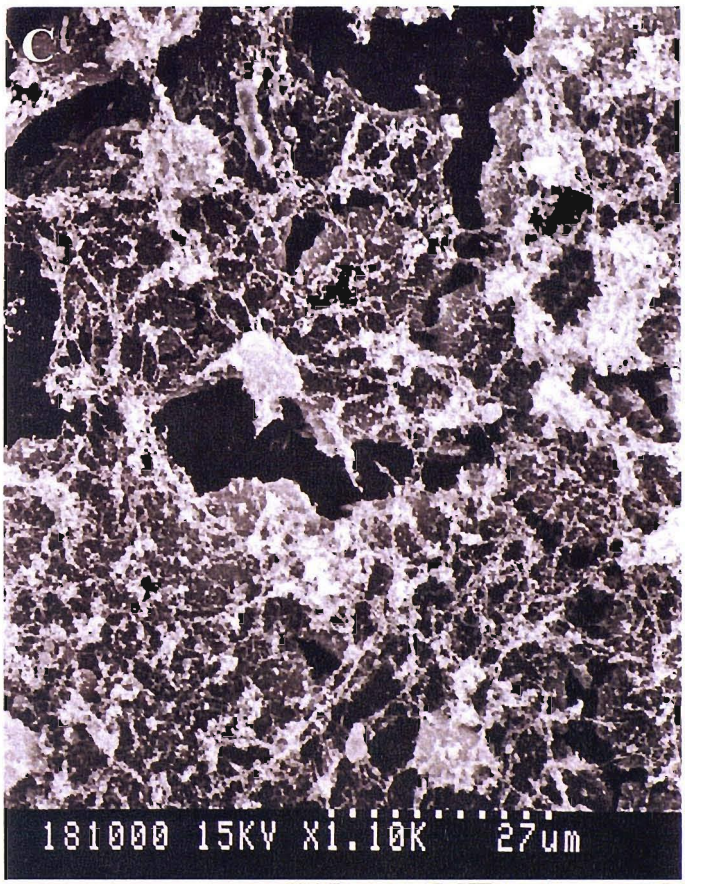


Micrograph C – shows the extent of the clumps of fibrous material present on the surface

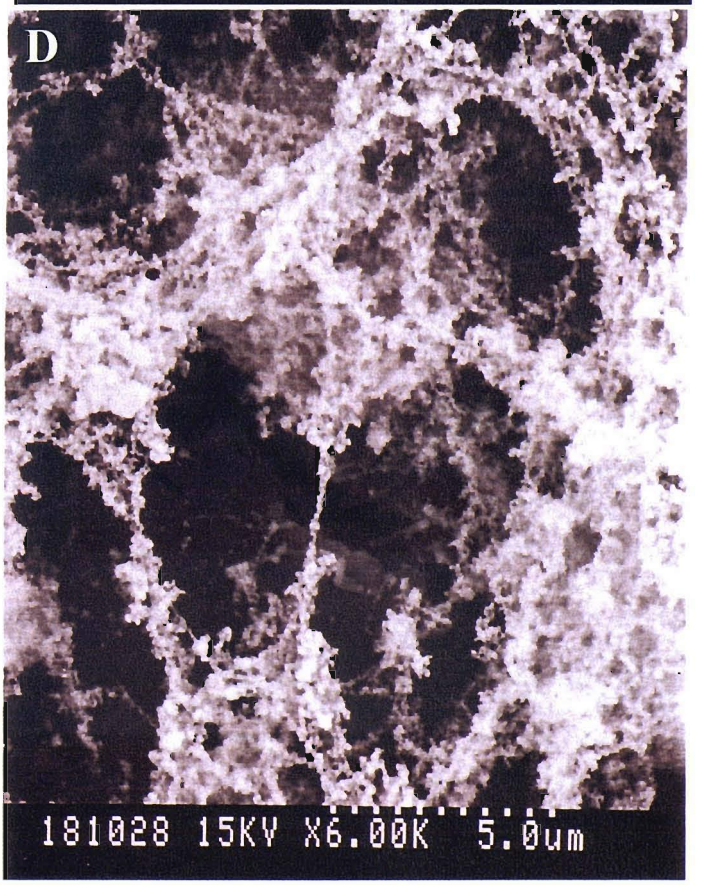


Micrograph D – shows this fibrous material in greater detail.

# Figure 5.18a IOBA-NHC Phl p + Histamine treatment

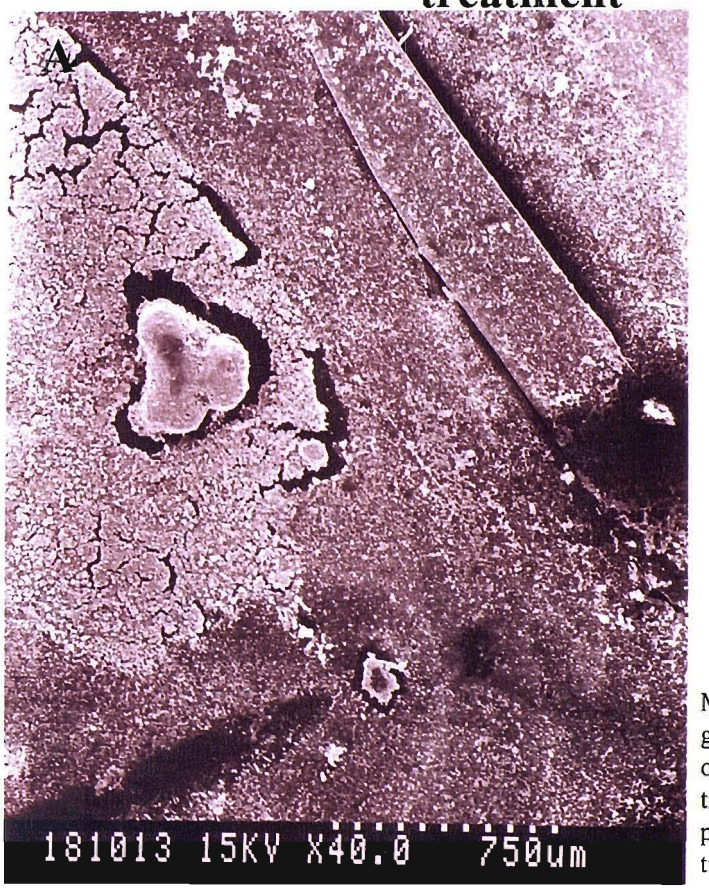


Micrograph A – shows the general surface morphology of the IOBA-NHC cells treatment with timothy grass pollen extract and histamine treatment.

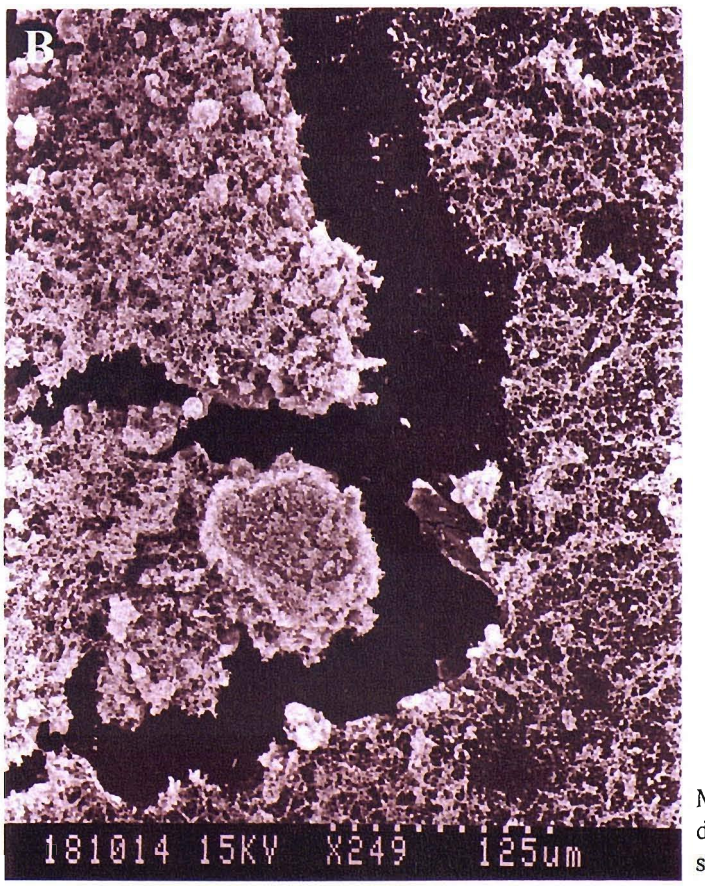


Micrograph B – shows the debris on the cell layer surface

# Figure 5.18b IOBA-NHC Phl p + Histamine treatment

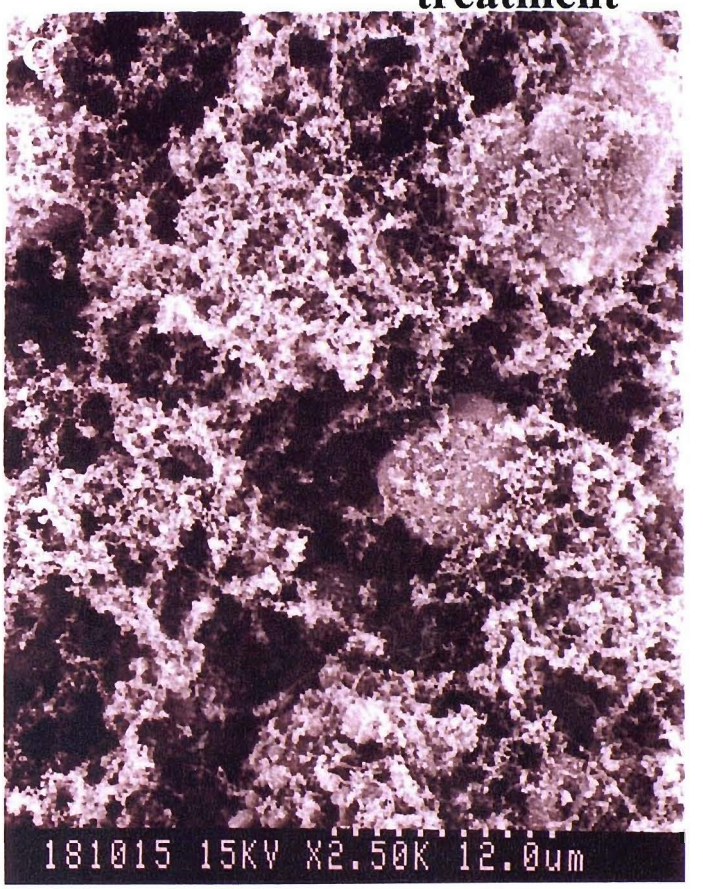


Micrograph C – shows a fibrous deposition of the surface of the cell layer, making analysis of the surface features of the cells impossible

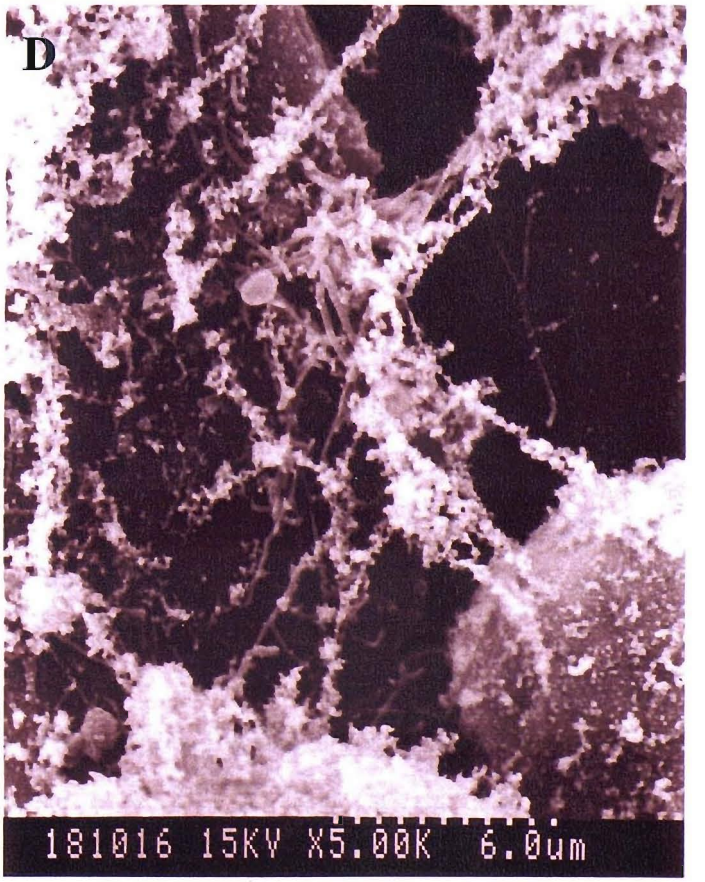


Micrograph D – shows this material in greater detail.

# 6. Localisation of Phleum pratense in allergen challenge models

## Chapter hypothesis:

***Phleum pratense (Timothy grass) pollen extract can be localised in challenged model systems and ocular allergen challenged patients with seasonal allergic conjunctivitis (SAC).***

### 6.1 Introduction

In the previous chapter, in vitro cell models were used to re-create the in vivo allergen challenge model of disease, achieved by the instillation of allergen into the eye. Ocular allergen challenges are used clinically to objectively confirm a case history suggestive of allergy and in research to re-create the signs and symptoms that patients experience during active episodes of seasonal allergic conjunctivitis; such as hyperaemia, oedema and itch, (Möller *et al* 1984, Abelson *et al* 1990).

The aim of this chapter was first to localise the Timothy grass pollen that was used as the challenge agent, in sections of the in vitro cell model of allergen challenge and then to localise Timothy grass allergen in biopsy material from patients who have undergone an ocular allergen challenge.

A sample of each in vitro cell model of allergen challenge were fixed and embedded in GMA for localisation of the Timothy grass pollen allergen and morphological assessment. Embedded sections of stored biopsy material taken from SACq patients, who underwent an ocular allergen challenge, were stained for the detection and localisation of Timothy grass pollen allergen within a stratified epithelial tissue.

The Timothy grass pollen allergen antibodies used were targeted at extracts Phl p1, Phl p5 and Phl p6. Pre-immune serum, taken before the generation of antibodies, was also used as a negative control.

The results of localisation of Timothy grass allergen within the *in vitro* and *in vivo* challenges were evaluated as well as the chapter hypothesis at the end of the chapter.

## 6.2 Localisation of Timothy grass pollen *In Vitro*

Using the insert membranes from the in vitro challenge model of the previous chapter, attempts were made to localise the Timothy grass allergen. 16HBE 14o- or ChWk or IOBA-NHC were challenged in culture for 24 hours according to section 2.2.10.1 then treated according to section 2.1.6. At the conclusion of the experiment the cell layer on the membranes were fixed and embedded in GMA for immunohistochemical staining according to section 2.2.4.

The four treatments used were, Phl p, Protease, Phl p + protease inhibitors and Phl p + histamine. A control was run simultaneously with the treatments.

Each of the epithelial layers from the challenge runs were stained and the results are described below.

Toludine blue and IgG isotype control staining runs are not shown.

### 6.2.1 16HBE 14o-

6.2.1.1 Control (figure 6.1)

Negative control showed no staining (plate A),

Keratin 18 showed staining in the epithelial layer (plate B),

Rabbit serum showed staining was included as a further control, due to the Timothy grass pollen antibody being raised in a rabbit species. Staining can be identified within the epithelial layer mainly co-localising with the folds in the GMA resin, which occur during the resin cutting stages (plates C and D),

Timothy grass pollen antibody Phl p1 was targeted against the group I allergen of Timothy grass. Staining can be identified with the Phl p1 antibody, majority of which co-localises with the folds in the resin. Small areas of staining can also be identified that are not in the folded resin (plate E and F).

6.2.1.2 Phl p treatment (figure 6.2)

Negative control showed no staining (plate A),

Keratin 18 showed staining in the epithelial layer (plate B),

Rabbit serum showed staining mainly co-localising with the folds in the GMA resin, which occur during the resin cutting stages (plates C and D),

Timothy grass pollen antibody Phl p1 staining can be identified the majority of which co-localises with the folds in the resin. Small areas of staining can also be identified that are not in the folded resin (plate E and F).

No membranes from the Phl p + protease inhibitors or Phl p + histamine treatment runs could be successfully embedded or sectioned.

**6.2.2 ChWk**

6.2.2.1 Control (figure 6.3)

Negative control showed no staining (plate A),

E-Cadherin showed staining in the epithelial layer (plate B),

Pre-immune rabbit serum showed staining mainly co-localising with the folds in the GMA resin, which occur during the resin cutting stages (plates C),

Timothy grass pollen antibody Phl p1 staining was identified with the folds in the resin (plate D).

Timothy grass pollen antibody Phl p5 staining was identified with the folds in the resin (plate E).

Timothy grass pollen antibody Phl p6 staining was identified with the folds in the resin (plate F).

6.2.2.2 Phl p treatment (figure 6.4)

Negative control showed no staining (plate A),

Keratin 18 showed staining in the epithelial layer (plate B),

Rabbit serum showed no staining (plates C and D),

Timothy grass pollen antibody Phl p1 showed very slight staining which was identified with the folds in the resin (plate E and F).

6.2.2.4 Phl p + protease inhibitors treatment (figure 6.5)

Negative control showed no staining (plate A),

Keratin 18 showed staining in the epithelial layer (plate B),

Rabbit serum showed staining in the epithelial layer (plates C and D),

Timothy grass pollen antibody Phl p1 showed no staining (plate E and F).

6.2.2.5 Phl p + histamine (figure 6.6)

Negative control showed no staining (plate A),

Keratin 18 showed staining in the epithelial layer (plate B),

Rabbit serum showed staining mainly co-localising with the folds in the GMA resin, which occur during the resin cutting stages (plates C and D),

Timothy grass pollen antibody Phl p1 staining was identified with the folds in the resin (plate E and F).

**6.2.3 IOBA-NHC**

6.2.3.1 Control (figure 6.7)

Negative control showed no staining (plate A),

Keratin 18 showed staining in the epithelial layer (plate B),

Rabbit serum showed staining mainly co-localising with the folds in the GMA resin, which occur during the resin cutting stages (plates C and D),

Timothy grass pollen antibody Phl p1 showed no staining (plate E and F).

No membranes from the Phl p, Phl p + protease inhibitors or Phl p + histamine treatment runs were successfully embedded or sectioned.

6.2.4 Protease treatment (figure 6.8)

Total loss of the epithelial layers from the insert membranes were observed with the protease treatment in all cell line model systems.

## 6.3 Localisation of Timothy grass pollen *In Vivo*

Localisation was undertaken in GMA embedded biopsies taken from SACq patients challenged with allergen. Briefly, SACq patients under went a skin prick test to ensure their atopy status, then one drop, approx. 25µl of

allergen in diluent was placed into the inferior fornix. The allergen used was a mixed grass pollen, containing Agrostis stofonisera (bent grass), Anthoxanthum odoratum (sweet vernal), Dactylis glomerata (June / orchard grass, cox foot), Lolinum perennie (rye grass), Arrhenatherum elatius (wild oat), Festuca ruba, Poa prantensis, Secale cereale, Holcus lanatus (velvet grass) and Phleum pratense (Timothy grass).

Biopsies were taken either 6 or 24 hours after challenge.

### 6.3.1 SACq 6 hour biopsy

Negative staining (omitting the primary antibody) showed no staining (figure 6.9),

Rabbit serum, as the Timothy grass pollen antibody was raised in a rabbit species; a rabbit serum was used as a species control. Strong positive staining was seen in the superbasal cell layers of the epithelium (figure 6.10, highlighted with the arrows),

Phl p1, weak positive staining was identified in the superbasal cell layers of the epithelium stained with the Timothy grass pollen antibody Phl p1 (figure 6.11).

### 6.3.2 SACq 24 hour biopsy

Negative staining (omitting the primary antibody) showed no staining (figure 6.12),

Rabbit serum, the Timothy grass pollen antibody was raised in a rabbit species; therefore a rabbit serum was used as a species control. Figure 6.13 shows patchy, full thickness, non-continuous staining in regions of the epithelial layer,

Phl p1, weak positive staining was identified in regions of the epithelial layer, with the Timothy grass pollen antibody Phl p1 (figure 6.14).

## 6.4 Discussion

The chapter hypothesis states:

*Phleum pratense (Timothy grass) pollen extract can be localised in challenged model systems and ocular allergen challenged patients with seasonal allergic conjunctivitis (SAC).*

In order to answer this, localisation studies were undertaken in allergen challenge in vitro and in vivo models of seasonal allergic conjunctivitis.

Sections of the membranes from each of the in vitro runs were fixed, immediately after the experiment had reached its conclusion, then embedded in GMA for Immunohistochemistry.

The proteins targeted for were, keratin 18 or E-Cadherin (used as the epithelial positive control) and the Timothy grass pollen group 1, 5 and 6 allergens. Also included were, a toludine blue morphological stain for assessing the morphology of the epithelial layer, a negative control (omitting primary antibody), an IgG isotype control and normal rabbit sera to assess endogenous staining.

The Timothy grass pollen antibodies were raised in a rabbit species, so a normal rabbit sera was used as a species control.

The 16HBE 14o- control run showed that the cells formed a confluent covering the surface of the insert membrane. In the control run, no endogenous staining was seen in the negative or IgG isotype controls. Staining was identified across the whole layer with keratin 18. With the normal rabbit sera and the Phl p1 staining was observed in the epithelial layer, the majority of which co-localised with folds in the GMA resin. The folds in the resin form during the cutting of resin blocks. These stains are false-positive stains as no Timothy grass pollen extract was added to the control run.

Similar patterns of staining were observed in the Phl p treated 16HBE 14 o- cells.

No membranes for the Phl p + protease inhibitor or Phl p + histamine treatments survived or could be stained, this was probably due to the nature of fixing, processing and the cutting of insert membranes which are notorious for the cell layer tearing away from the membrane and therefore being lost / unable to stain appropriately.

The ChWk control formed a confluent layer across the insert membranes. No staining in the negative or IgG isotype controls was seen. E-Cadherin showed

positive staining. Rabbit sera, Phl p 1, 5 and 6 also showed staining, of which the majority of this staining co-localised with the folds in the GMA resin. Again, no allergen was introduced in the control run, so no staining with the exception of the positive control should have been seen. This positive staining seen with the E-Cadherin is contra to the published data from De Saint Jean (2004), who stated that 'chang (ChWk) cells did not express E-Cadherin in basal conditions' – whereas figure 6.3 shows E-Cadherin staining in ChWk cells.

The pattern of staining that was seen in the treatment runs of the allergen challenge showed no staining in the negative or isotype control. Staining was seen in the keratin 18 staining runs. No staining was identified in the rabbit sera with the Phl p treatment, but staining was identified with the Phl p + protease inhibitor and Phl p + histamine treatments. No staining with Phl p 1, was observed with the Phl p + protease inhibitor treatment, but staining was observed in the Phl p and Phl p + histamine treatments.

In the IOBA-NHC control, toludine blue morphological stain showed that the epithelial layer formed a confluent layer across the insert membrane, no staining was seen in the negative or IgG isotype controls. Keratin 18 staining was seen in the epithelial layer and the rabbit sera also showed staining. No staining was seen in the Phl p 1 run.

The protease treatment stripped the epithelial cells from the membrane as seen in the previous chapter.

This the first time that allergen localisation has been undertaken with Timothy grass pollen in cell line models of disease. The staining with the Timothy grass pollen antibodies showed staining that is suggestive of localising the Timothy grass pollen extract used in the in vitro allergen challenges. With the staining seen in the rabbit sera, this result can not be ruled out as false-positive though.

In vivo – 6 hour biopsy

Embedded biopsy sections taken with SACq patient who had undergone ocular allergen challenges were stained in order to localise the Timothy grass pollen.

No staining was seen the negative or isotype controls. Staining was seen in the rabbit sera and Phl p 1 staining runs. The intensity of the staining was greater in the rabbit sera, and the both stains co-localised in the superbasal layers of the epithelium, therefore the Phl p 1 staining result in the six hour biopsy SACq patients is classed as false-positive.

24 hour biopsy

No staining was seen the negative or isotype controls. Staining was seen in the rabbit sera and Phl p 1 staining runs. The intensity of the staining was greater in the rabbit sera, and the both stains co-localised in the epithelium, therefore the Phl p 1 staining result in the 24 hour biopsy SACq patients is classed as false-positive.

## 6.5 Conclusion

*Phleum pratense (Timothy grass) pollen extract can be localised in challenged model systems and ocular allergen challenged patients with seasonal allergic conjunctivitis (SAC).*

Unfortunately, with the rabbit sera control returning positive results in both challenge models the hypothesis cannot be accepted. This said, I believe that this system still has legs, and could provide an interesting avenue for investigating the paracellular trafficking of allergen within epithelial tissues.
The in vivo experiment above has several extremely limiting factors; firstly, due to the limited stock of antibodies, dilution runs had to be restricted to a minimum. With a greater stock of antibodies, further dilutions could have been run to find the optimum concentration. Secondly, the ocular allergen challenge samples had been stored since 1992 and 1994, no data exists as to the retention of antigenicity of samples that have been in long-term storage, also these patient samples had been used in previous studies and limited sections could be cut from

each of the resin blocks. Fresh samples would have increased the number that could have been tested and negated the possible problems of resin blocks undergoing repeated episodes of freeze/thawing and cutting. Thirdly, the allergen used to challenge the patients was a mixed grass solution, with no data available on the exact concentrations of the constituting grass pollens, if a pure Timothy grass pollen extract had been used, this could have increased its detection within the epithelial layer.

# Figure 6.1 16HBE 14o- Control

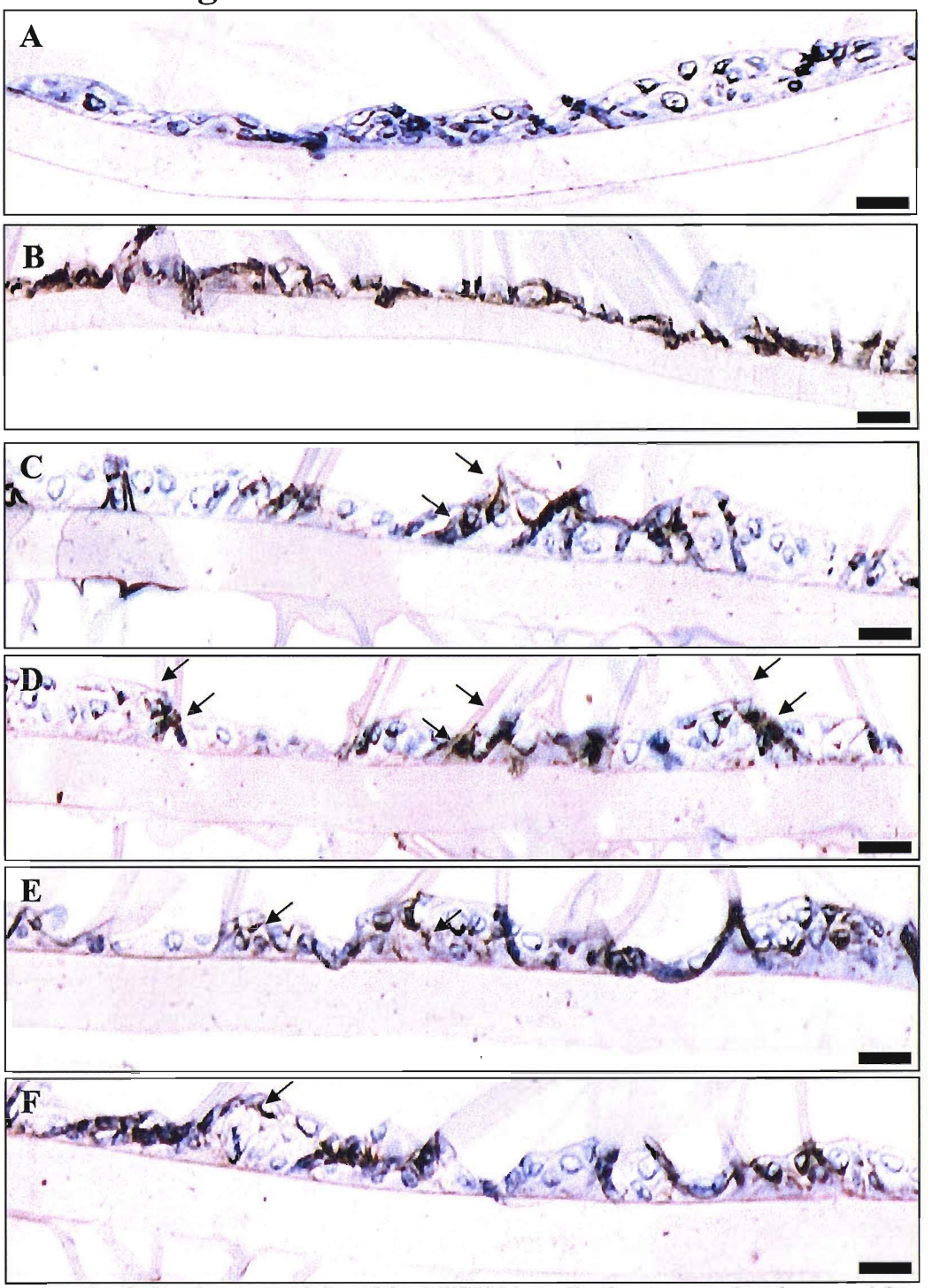


Figures A - F show immunostaining of the 16HBE 14o- cells, that were used as the control for the *in vitro* allergen challenge.

Plate A and B shows the negative control and keratin 18 staining respectively.

Plates C and D show the cells that have been treated with rabbit serum. Staining can be identified in these sections, although the majority of staining also locate with the folds created in the resin due to the cutting procedure (highlighted arrows).

Plates E and F the cells that have been stained for *Phleum pratense.* Staining can be identified in the above epithelial sections, but the majority of these sections co-localise with the folds of the resin. The regions that do not co-localise with the folds are highlighted with the arrows. Scale bar = 10 μm.

# Figure 6.2 16HBE 14o- Phl p treatment

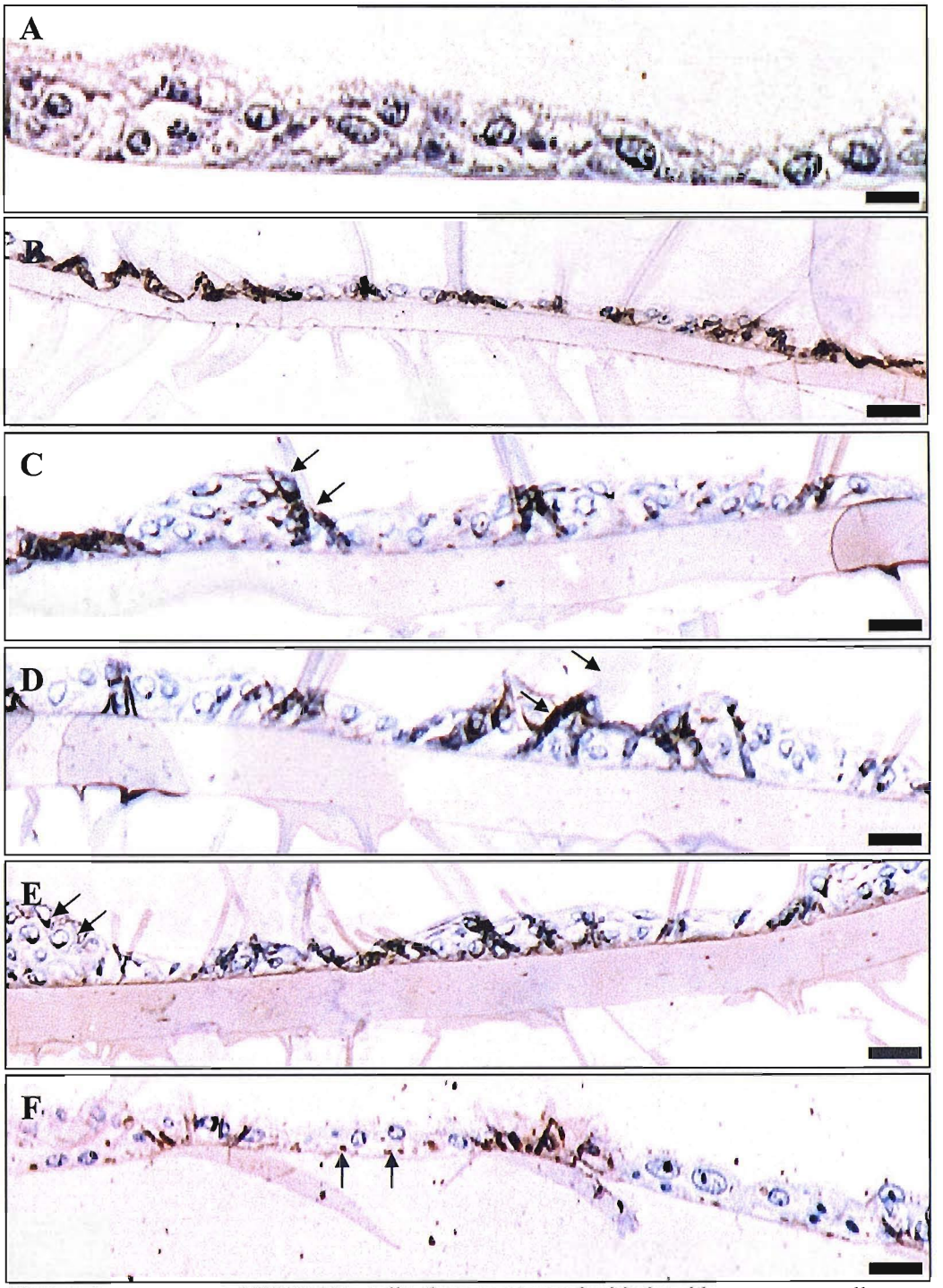


Figures A - F show the 16HBE 14o- cells, that were treated with the phleum pratense allergen extract during the *in vitro* allergen challenge.

Plates A and B show the negative control and keratin 18 staining respectively.

Plates C and D show the cells have been treated with rabbit serum. Staining can be identified in these sections, although the majority of staining also locate with the folds created in the resin due to the cutting procedure (highlighted arrows).

Plates E and F show the cells have been stained for the *Phleum pratense* allergen extract 1. Staining can be identified in the above epithelial sections, the majority of these sections are located in the folds of the resin, but small sections are located in the non-folded parts of the epithelium (highlighted with the arrows).
Scale bar = 10 μm.

# Figure 6.3 ChWk Control

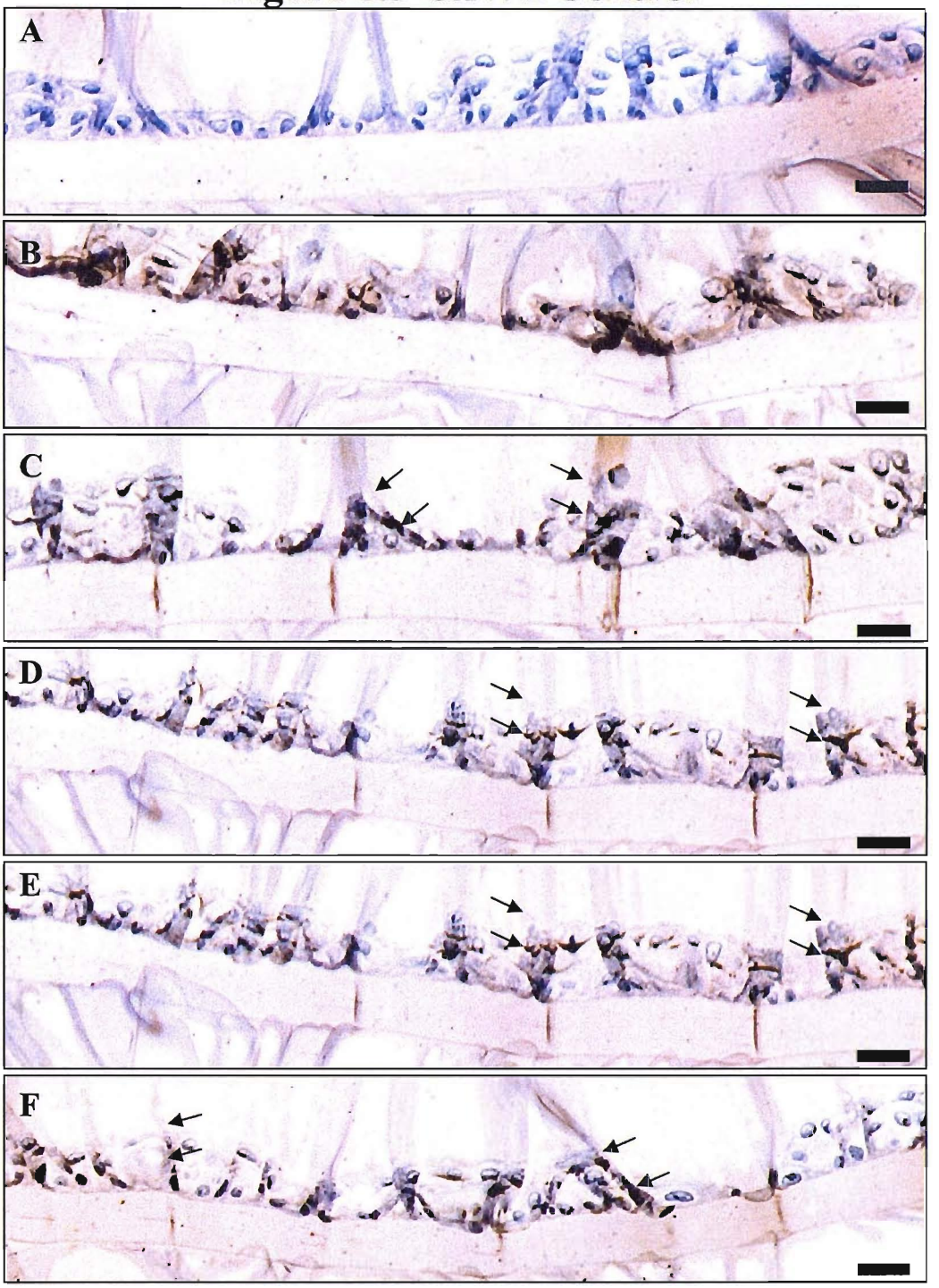


Figures A - F show the immunostaining of the ChWk cells, that were used as the control for the *in vitro* allergen challenge.

Plates A and B show the negative control and E-Cadherin staining respectively.

Plates C show the cells have been treated with a pre-immune rabbit serum obtained from the animal prior to allergen injection and therefore the production of antibodies. Staining locates with the folds created in the resin due to the cutting procedure (highlighted arrows).

Plate D, E and F show the cells have been stained for the *Phleum pratense* allergen extract 1, 5 and 6 respectively. Staining can be identified in the above epithelial sections, but these sections are located in the folds of the resin (highlighted with the arrows).

Scale bar = 10 μm.

# Figure 6.4 ChWk Phl p treatment

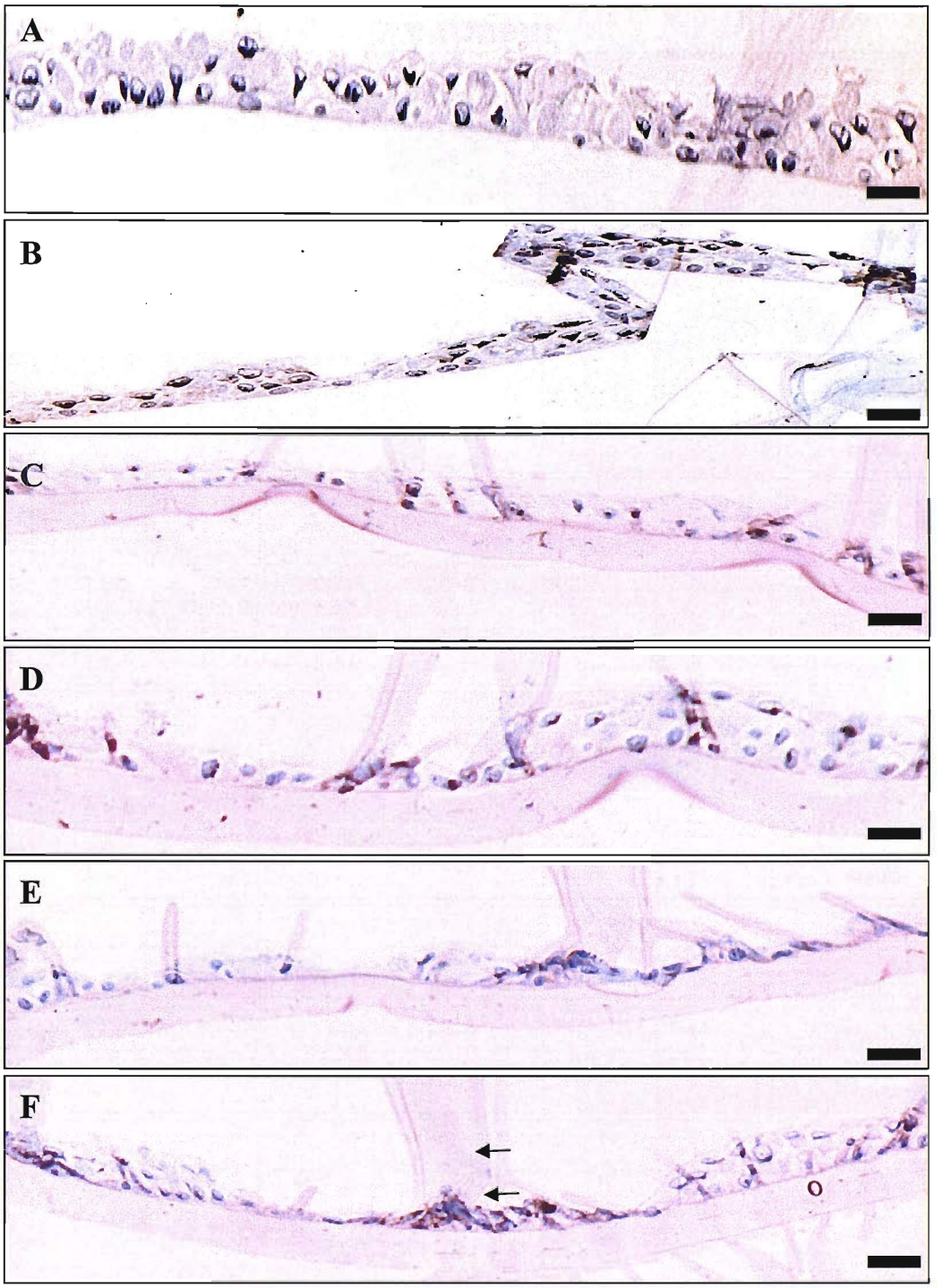


Figures A - F show immunostaining of the ChWk cells, that were treated with the *Phleum pratense* allergen extract during the *in vitro* allergen challenge.

Plates A and B show the negative control and keratin 18 staining respectively.

Plates C and D show the cells that have been treated with rabbit serum

Plates E and F show the cells have been stained for the *Phleum pratense* allergen extract 1. Staining can be localised in the folds of the resin (highlighted with the arrows).
Scale bar = 10 μm.

# Figure 6.5 ChWk Phl p + Protease inhibitors treatment

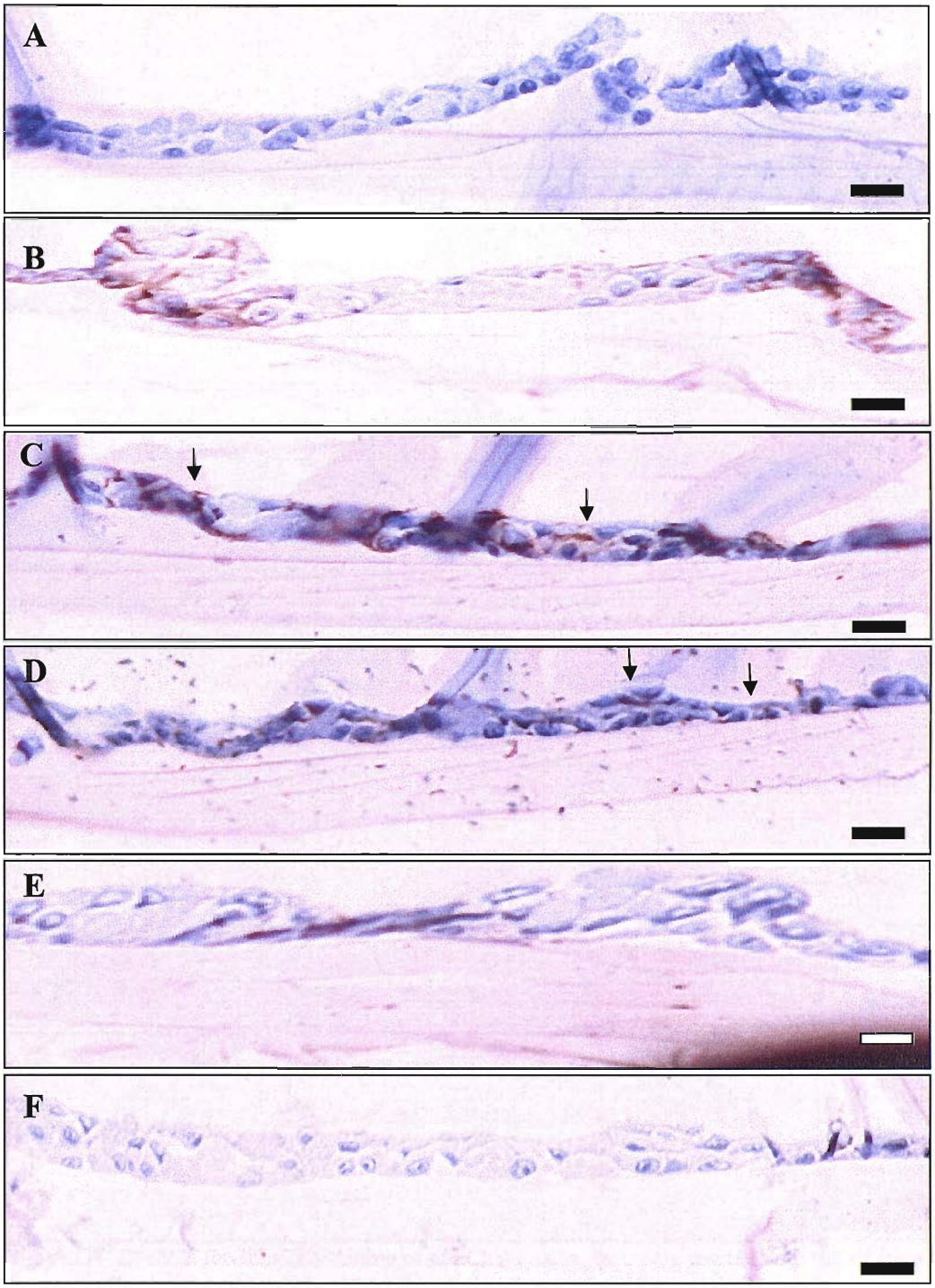


Figure A - F show the immunostaining of the ChWk cells, that were treated with the *Phleum pratense* allergen extract and then protease inhibitors during the *in vitro* allergen challenge.

Figures A and B show the negative control and keratin 18 staining respectively.

Figures C and D show the cells have been treated with rabbit serum, staining can be identified (highlighted arrows).

Figure E and F show the cells have been stained for the *Phleum pratense* allergen extract 1.

Scale bar = 10 µm.

# Figure 6.6 ChWk Phl p + Histamine treatment

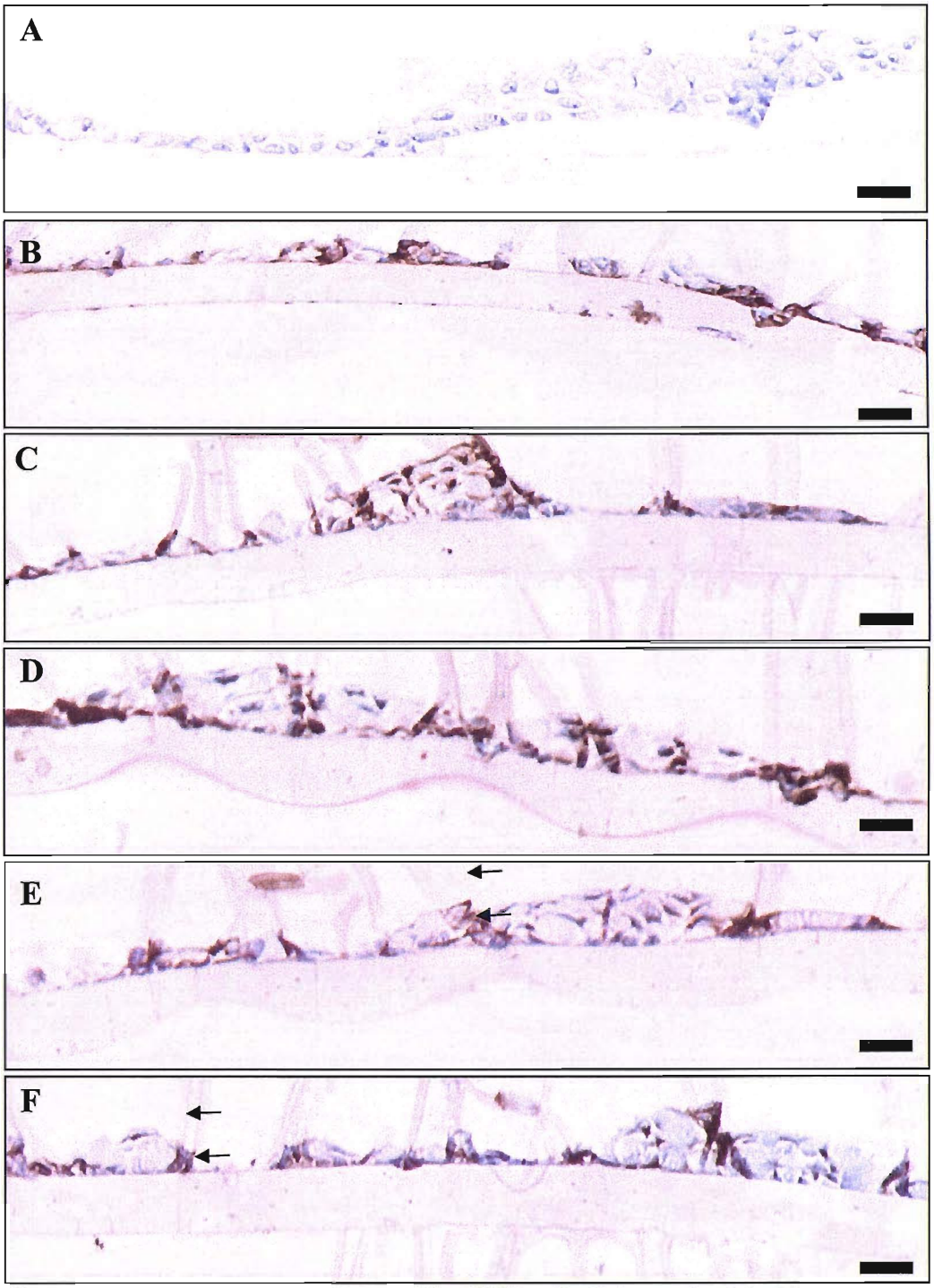


Figures A - F show the immunostaining of the ChWk cells, that were treated with the *Phleum pratense* allergen extract and then histamine during the *in vitro* allergen challenge.

Figure A and B show the negative control and keratin 18 staining respectively.

Figures C and D show the cells that have been treated with rabbit serum control. Staining can be identified in the plates, the majority of staining locates with the folds created in the resin, caused by the block cutting procedure.

Figures E and F show the cells have been stained for the *Phleum pratense* allergen extract 1. Staining can be identified in the above epithelial sections, mostly localised in the folds of the resin (highlighted with the arrows).

Scale bar = 10 μm.

# Figure 6.7 IOBA-NHC Control

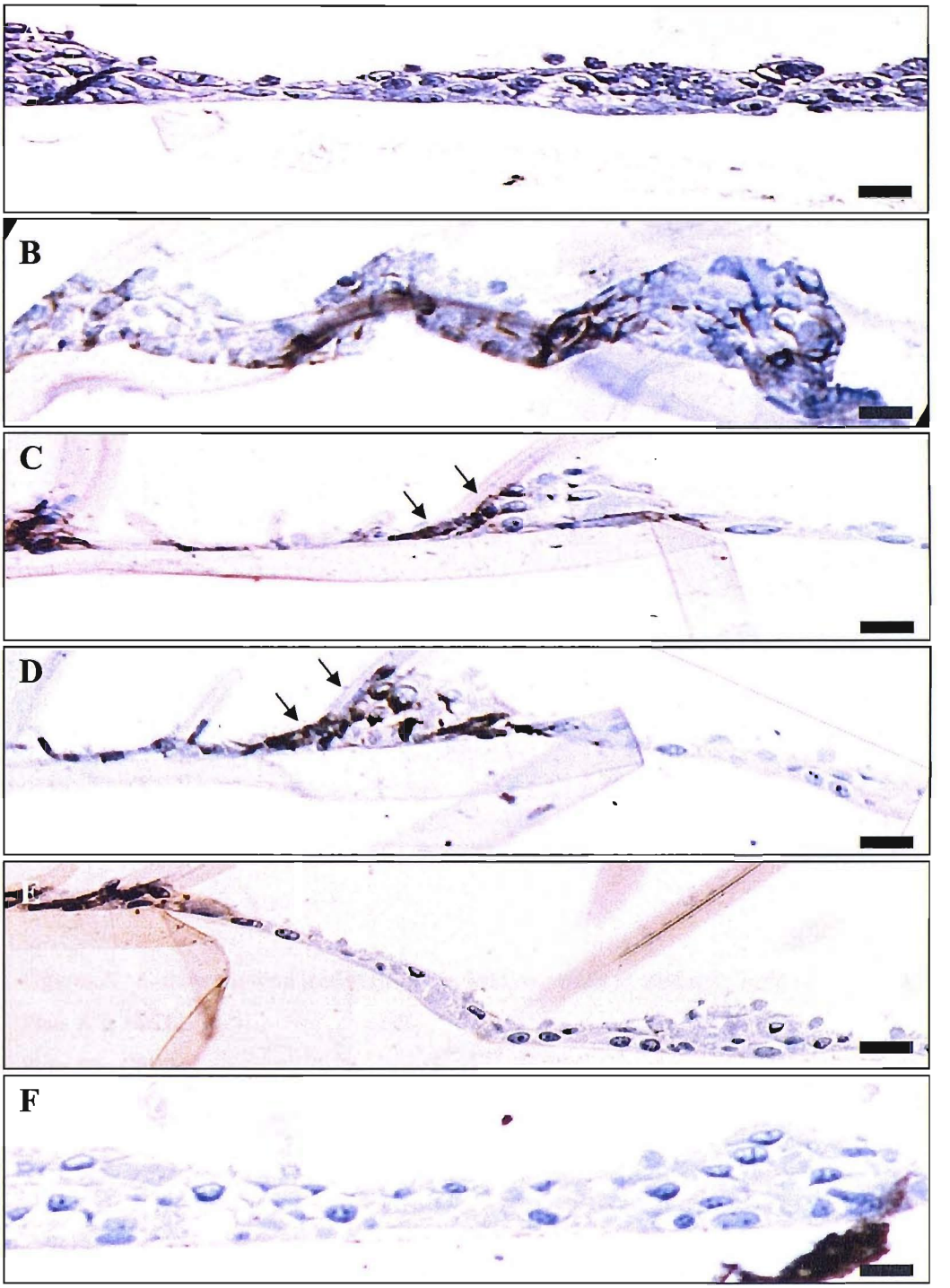


Figures A – F show of the IOBA-NHC cells, that were used as the control for the *in vitro* allergen challenge.

Plates A and B show the negative control and keratin 18 respectively.

Plates C and D show the cells that have been treated with rabbit serum. From the above plates small areas staining can be identified, although the majority of this staining locates with the folds created in the resin due to the cutting procedure (highlighted arrows).

Plates E and F show the cells have been stained for the *Phleum pratense* allergen extract 1.

Scale bar = 10 μm.

# Figure 6.8 Protease treatment

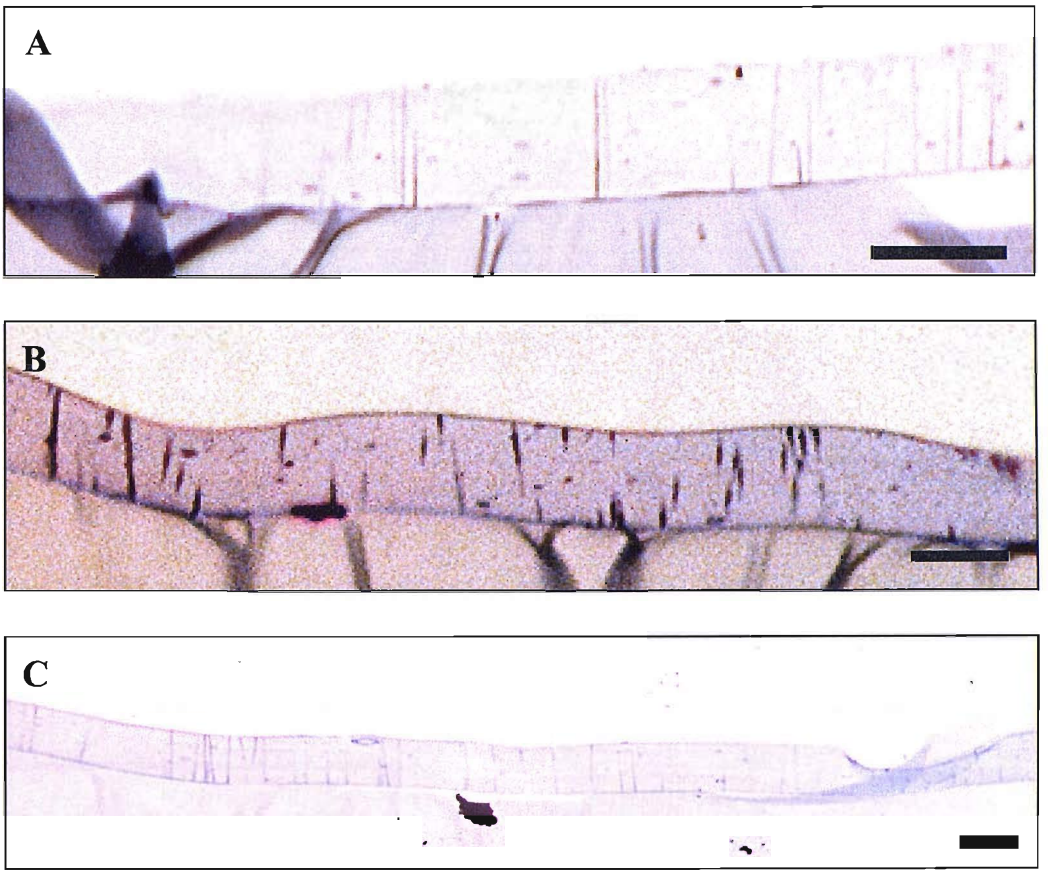


Figures A - C show the total loss of the epithelial layer when treated with protease.

Plate A is 16HBE 14o-.

Plate B is ChWk.

Plate C is IOBA-NHC

Scale bar = 10 μm.

# Figure 6.9 *In vivo* allergen challenge 6 hour Control

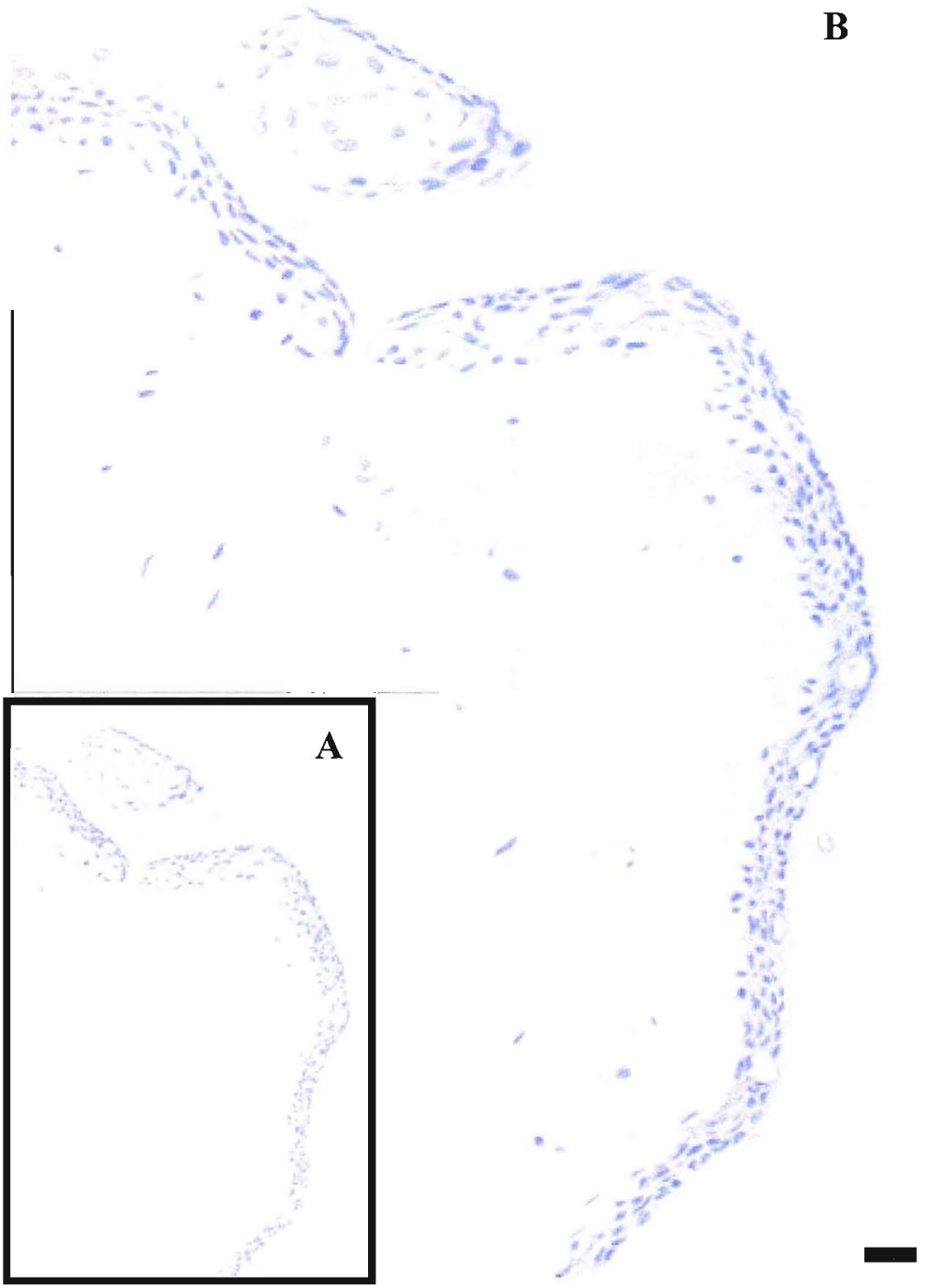


The figure above shows a section of epithelium taken from a SACq patient after an in vivo allergen challenge. The biopsy was taken after 6 hours post challenge. The patient was challenged with mixed grass allergen extracts in order to re-create the ocular symptoms observed during an active disease episode. The section was included as the negative staining control (minus primary antibody), to show that no exogenous staining occurred.

Plate A is a low magnification of the section.

Plate B shows a composite image of the section in plate A, at a higher magnification to locate if any staining had occurred.

Scale bar = 30μm.

# Figure 6.10 *In vivo* allergen challenge 6 hour – Rabbit serum

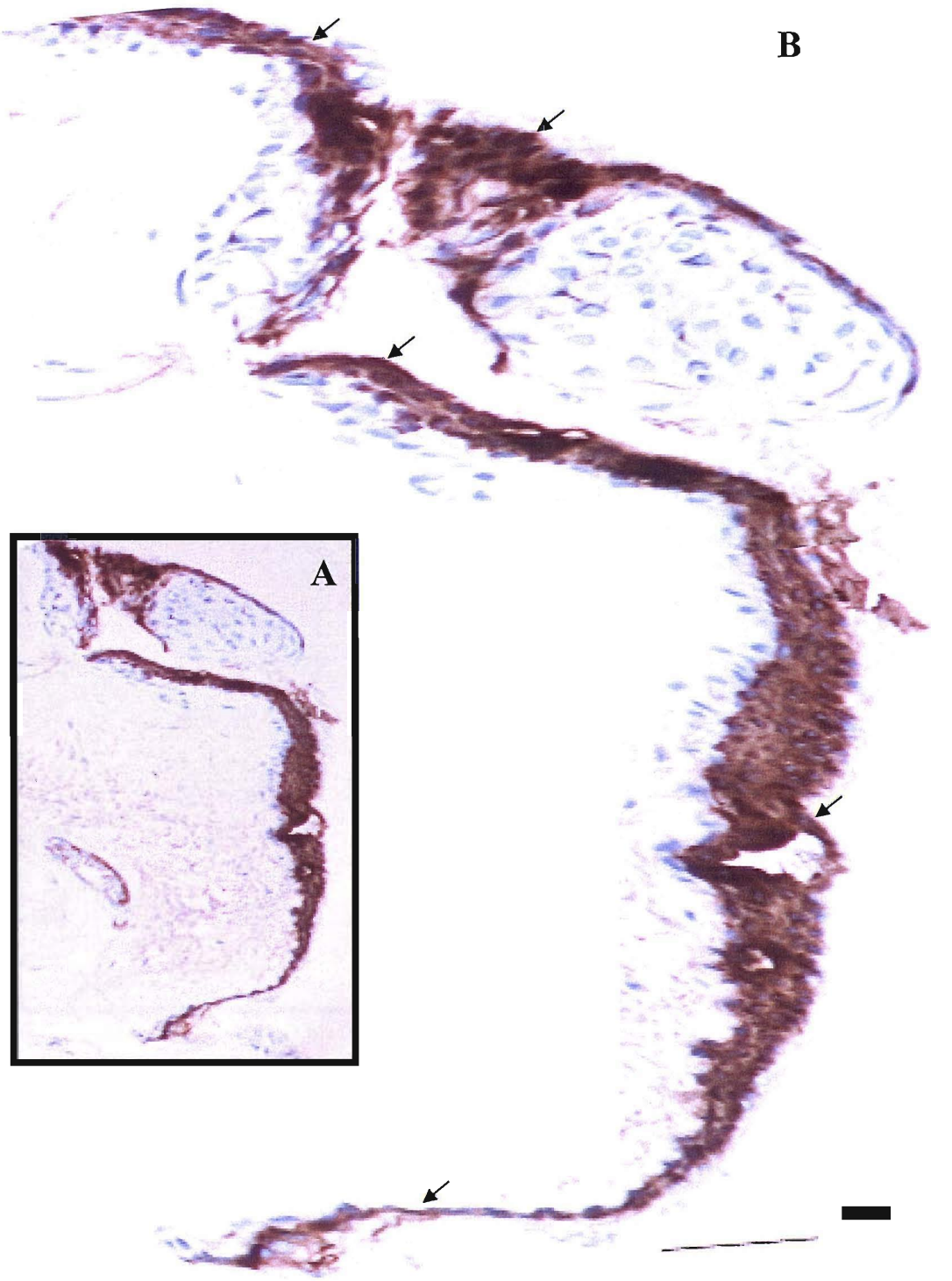


The figure above shows a section of epithelium taken from a SACq patient after an in vivo allergen challenge. The biopsy was taken after 6 hours post challenge. The patient was challenged with mixed grass allergen extracts in order to re-create the ocular symptoms observed during an active disease episode. The section was staining using the rabbit serum control. No staining was expected to occur, but staining within the epithelial layer can be clearly identified (highlighted with the arrows).

Plate A is a low magnification of the section.

Plate B shows a composite image of the section in plate A, at a higher magnification to locate the staining.

Scale bar = 30μm.

# Figure 6.11 *In vivo* allergen challenge 6 hour Phl p1

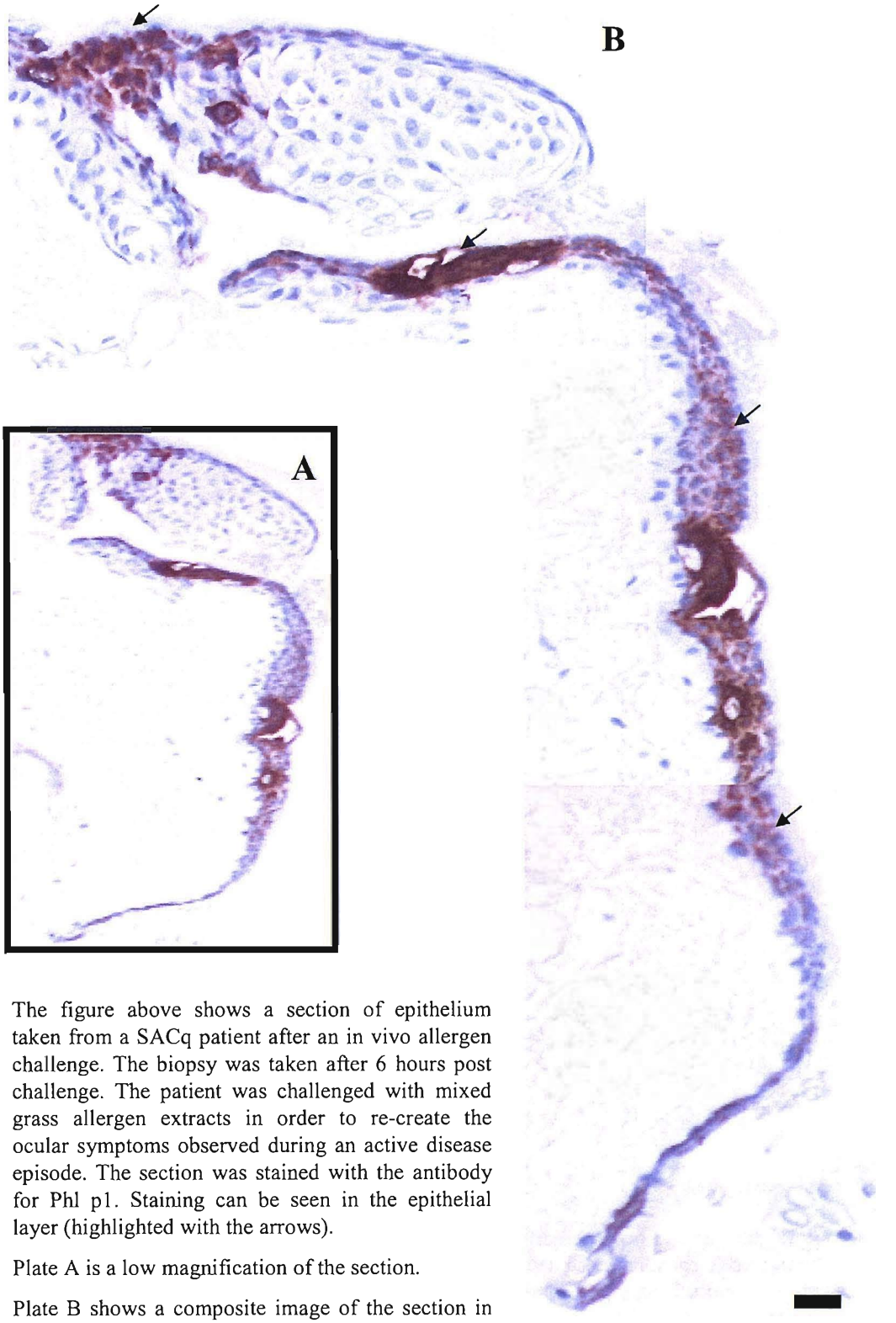


The figure above shows a section of epithelium taken from a SACq patient after an in vivo allergen challenge. The biopsy was taken after 6 hours post challenge. The patient was challenged with mixed grass allergen extracts in order to re-create the ocular symptoms observed during an active disease episode. The section was stained with the antibody for Phl p1. Staining can be seen in the epithelial layer (highlighted with the arrows).

Plate A is a low magnification of the section.

Plate B shows a composite image of the section in plate A, at a higher magnification to locate if any staining had occurred.

Scale bar = 30μm.

# Figure 6.12 *In vivo* allergen challenge 24 hour Control

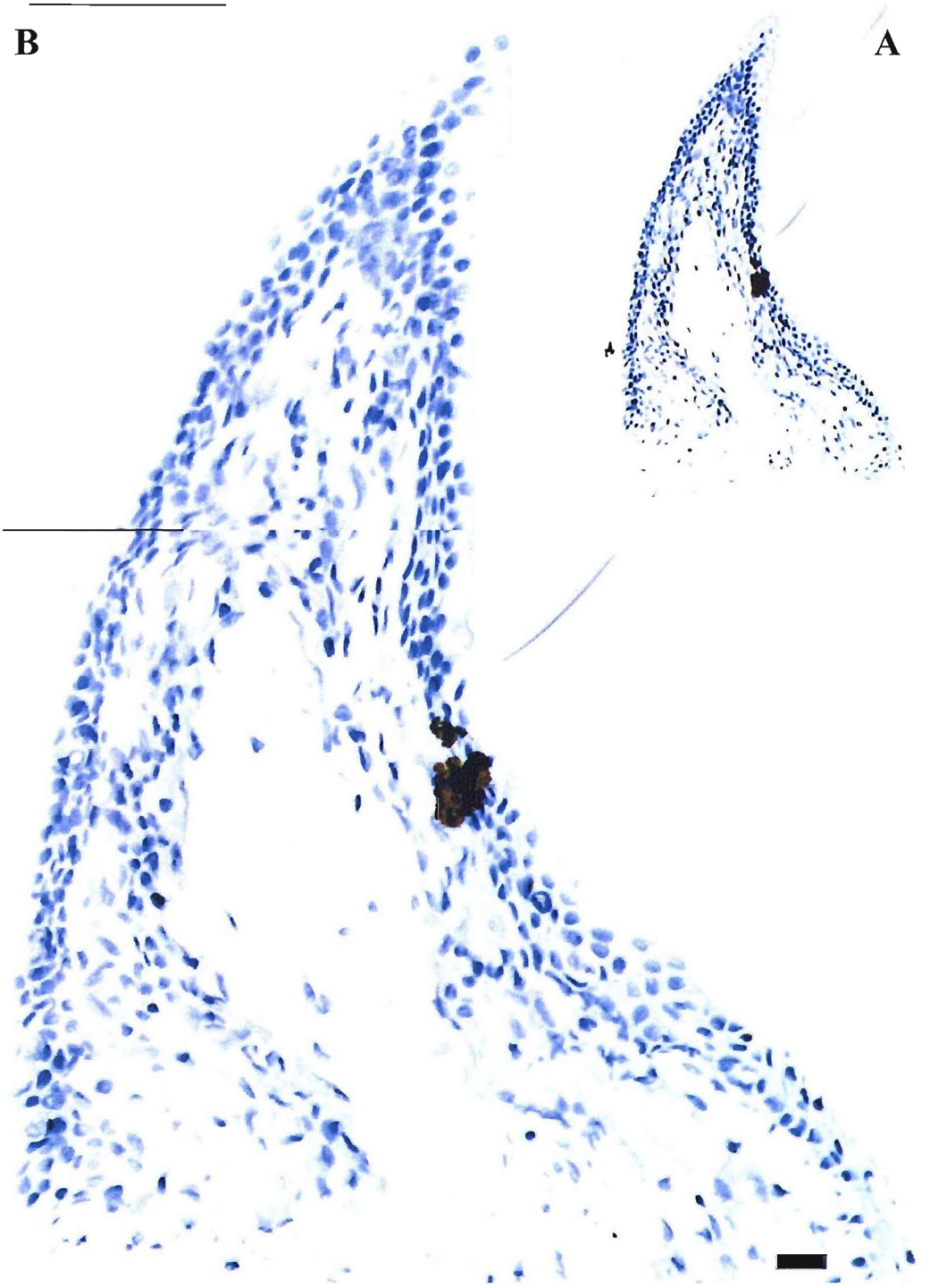


The figure above shows a section of epithelium taken from a SACq patient after an in vivo allergen challenge. The biopsy was taken after 24 hours post challenge. The patient was challenged with mixed grass allergen extracts in order to re-create the ocular symptoms observed during an active disease episode. The section was included as the negative staining control (minus primary antibody), to show that no exogenous staining occurred.

Plate A is a low magnification of the section.

Plate B shows a composite image of the section in plate A, at a higher magnification to locate if any staining had occurred.

Scale bar = 30μm.

# Figure 6.13 *In vivo* allergen challenge 24 hour Rabbit serum

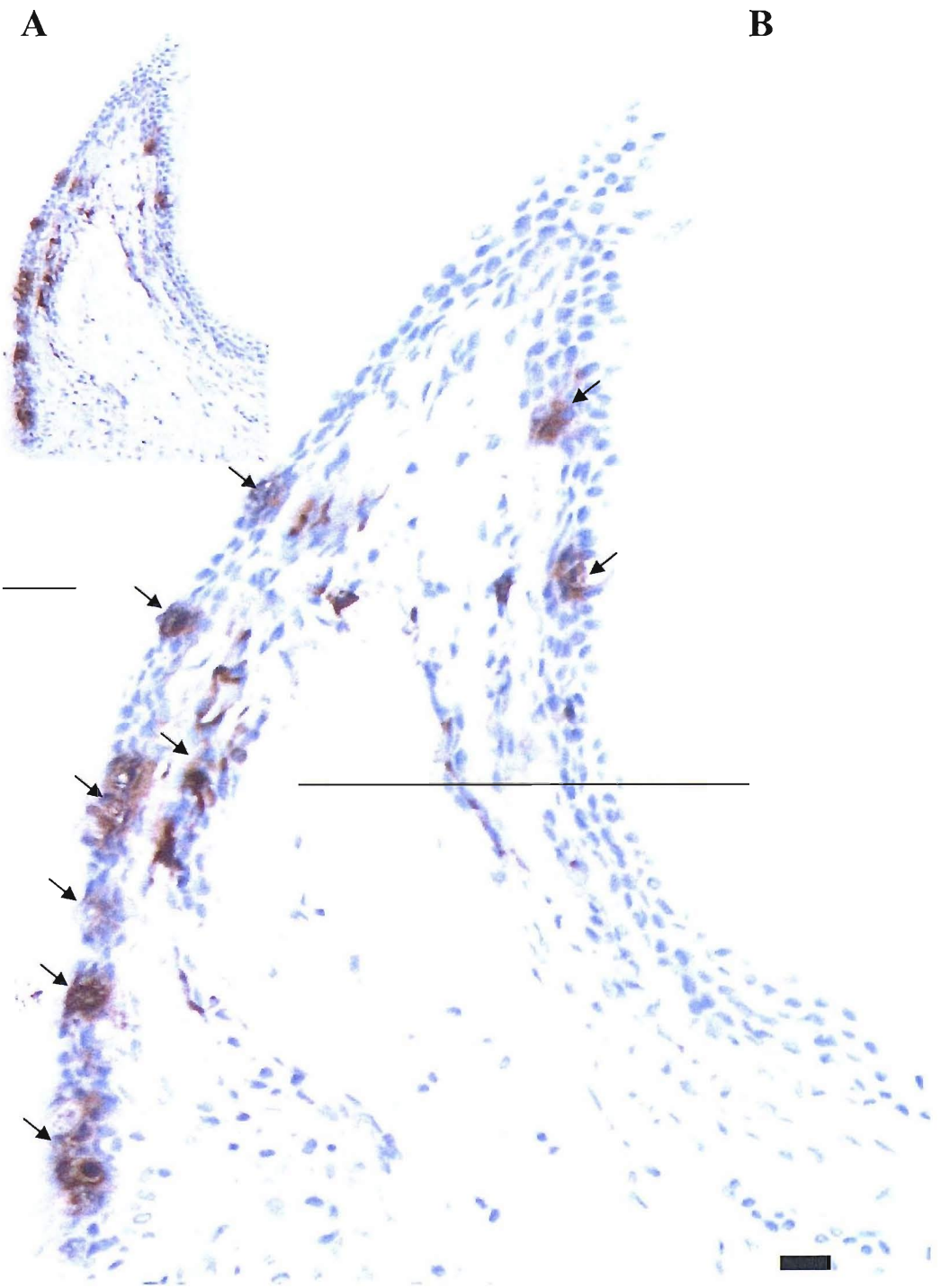


The figure above shows a section of epithelium taken from a SACq patient after an in vivo allergen challenge. The biopsy was taken after 24 hours post challenge. The patient was challenged with mixed grass allergen extracts in order to re-create the ocular symptoms observed during an active disease episode. The section was stained the rabbit serum control, no staining was expected to be seen, staining can be identified within the epithelial layer (highlighted with the arrows).

Plate A is a low magnification of the section.

Plate B shows a composite image of the section in plate A, at a higher magnification to locate if any staining had occurred.

Scale bar = 30μm.

# Figure 6.14 *In vivo* allergen challenge 24 hour Phl p1

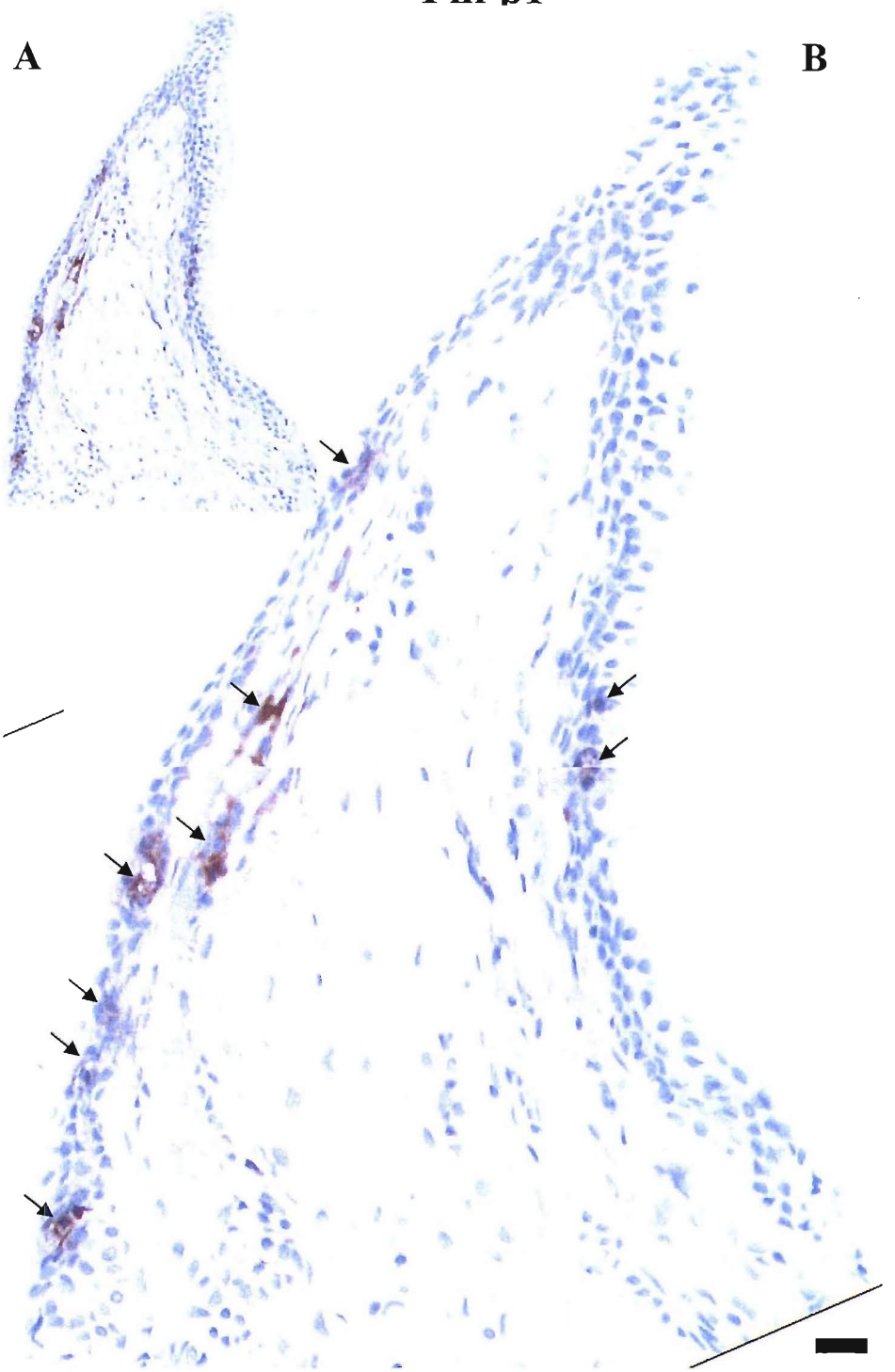


The figure above shows a section of epithelium taken from a SACq patient after an in vivo allergen challenge. The biopsy was taken after 24 hours post challenge. The patient was challenged with mixed grass allergen extracts in order to re-create the ocular symptoms observed during an active disease episode. The section was stained the Phl p1, staining can be identified within the epithelial layer (highlighted with the arrows).

Plate A is a low magnification of the section.

Plate B shows a composite image of the section in plate A, at a higher magnification to locate if any staining had occurred.

Scale bar = 30μm.

# Chapter 7 Final discussion

The hypothesis for the work in this thesis states:

*The conjunctival epithelium is altered in allergic eye disease and in the context of an inflammatory response; this facilitates the passage of allergen through the epithelium, contributing to the pathogenesis of the disease.*

In order to test this, it was subsequently divided into workable parts:

**1. Chapter three hypothesis:**

*The human conjunctival epithelium is structurally altered in patients with seasonal allergic conjunctivitis (SAC).*

Ultrastructure and morphological analysis showed that the conjunctival epithelium of subjects with seasonal allergic conjunctivitis is structurally altered when compared to the structure of non-allergic subjects.

Important questions that remain from this work are the ultrastructural features of SACa and SACq subjects. Scanning electron microscopy would shed light on the health of the microvilli. Transmission electron microscopy would assist in the classification of the epithelial layer when used in connection with the GMA embedded sections obtained previously. TEM would also assist with another important question arising from the immunostaining of desmosome spot junctions throughout the layer. Immunostaining showed decreased expression of desmoplakin 1-2, a main constitute of the desmosomal plaque. Electron microscopic study of the desmosomes in SACa and SACq, would either agree with this result, or show that desmosomes are still present but the constitutes of the desmosomal plaque is altered by either junction structural changes therefore blocking antibody binding sites or the loss of desmoplakin 1-2 from the plaque.

Other important questions concerning the barrier function of SACa and SACq conjunctival epithelium could be answered via TEM, by identifying and quantifying tight junctions within the epithelial layer. Confocal microscopy could also be employed, where targeting tight junctional proteins such as occludin, claudin or ZO-1 in biopsy samples from SACa and SACq subjects, could support the TEM identification of tight junctions. If large enough biopsies were obtained

then direct trans-epithelial electrical resistance of human stratified tissue could be measured using the Ussing chamber technique used with the *Ovis aries* stratified tissue in chapter four. A specialised chamber would need to be constructed, as currently the smallest diameter sized chamber is too large to mount human biopsy material on. Another approach would be to use mounting rings that could securely hold the material and fit into the currently available chambers.

These further investigations would conclude the characterisation work within this thesis and produce novel data on the barrier properties of the human conjunctival epithelium.

**2. Chapter four hypothesis:**

*Conjunctival epithelial cell models provide an accurate experimental model of the human conjunctival epithelium.*

Characterisation of the experimental models showed epithelial characteristics and could be included in future work investigating the pathogenesis of conjunctival disease. The *in vitro* models were the most practical model for repeated experimental work with highly reproducible results. The *ex vivo* model would produce results that are more relevant to the target tissue of interest than immortalised cell lines, but the protocol developed in this thesis and logistics of *ex vivo* culture was considered too time consuming and unreliable, in terms of culture success, for this use of such valuable tissue. The stratified tissue model showed extremely positive results in terms of characterisation and barrier functional data, which may be reflective of the barrier properties of human stratified tissue. The amount and availability of material would facilitate extensive experimental work. Unfortunately, the timing of this tissue in terms of this thesis meant that only limited work could be carried out on this model.

Several further work to fully extend the characterisation of *in vitro* experimental models such include the use of confocal microscopy to identify the junctional complex (tight junction – intermediate junction – desmosome), within the cell monolayer, which is crucial when investigating the paracellular movement of allergens. Electron microscopy would enable identification of junctional complexes and further desmosomes within the model, supporting the immunostaining data from confocal microscopy. If *ex vivo* culture is developed further then, immunostaining for the tight junction proteins would suggest the

formation of tight junctions and therefore the development of a polarised barrier, if insufficient outgrowths are obtained, the use of the polymerase chain reaction (PCR) would indicate the transcription of tight junction proteins, but not specifically their expression and therefore barrier functional data. TEM and SEM would also demonstrate whether primary cells retained original tissue cell phenotype or whether they take a more cultured cell phenotype. In addition, junctional complexes could be identified in primary cell layers suggesting polarity. If primary cells could be induced to grow on porous insert membranes, then TEER could be measured by loading the membrane in the Ussing chamber equipment for direct functional data. Electron microscopy could be further employed to investigate the cell type that divides out from the edge of the explant, therefore indicating any culture additives that could be employed to increase the success rate of culturing primary cells, such as cytokines released during wound healing processes or whether more basal cell friendly conditions influence epithelial growth. For concluding the characterisation of the stratified model, immunostaining using confocal microscopy would enable the localisation of epithelial targets within a multiple layered sample. Electron microscopy could be employed to identify junctional complexes and their structure. PCR or western blotting could also be used to identify further epithelial elements too.

**3. Chapter five hypothesis:**

*Phleum pratense (Timothy grass) facilitate paracellular movement of non-indigenous molecules via tight junction disruption.*

In vitro allergen challenges demonstrated that Phl p caused destruction of tight junctions, shown by changes in TEER and the detection of FITC-Dextran molecules in the lower chambers of insert membrane wells. Protease treatment (used as a positive control of proteolytic action on tight junctions), not only cut cell junctions and cell-cell contacts but induces cell death and lead to the loss of the epithelial layer form the surface of the membranes. With the addition of protease inhibitor cocktail, the action of the Phl p was reduced. The treatment of Phl p and histamine showed no tangible results.

In order to investigate the hypothesis thoroughly, further experiments should concentrate solely on the action of Phl p on the epithelium. The chopstick method of measuring TEER is an extremely easy and uncomplicated technique,

but with the use of an Ussing chamber, membranes could be kept in enclosed culture conditions, during reading taking, rather than introducing electrodes into the two chambers for each time point. The sampling of the medium form the basal side could also be facilitated easier using the Ussing chamber equipment. The detection of the grass pollen allergen is highly dependant on stocks of specific antibodies. Only limited detection could be utilised in this thesis due to an extremely limited stock of antibody available. The use of immunogold staining would indicate the actual location of the allergen within the epithelial layer; immunostaining could be used to locate the allergen and junctional proteins using triple labelling. Dot blot analysis of the lower chamber culture medium was piloted to detect allergen therefore proving its movement through the epithelial layer, but due to the limited stock of Phl p antibody this technique could not be further developed or applied, but this technique would give strong data about the movement of allergen. Antibody stocks were saved to be used for the localisation in embedded membrane samples and patient biopsies samples. To investigate the action of Phl p, non-cellular based assays could be employed, such as fluorescence-released cleavage assays.

**4. Chapter six hypothesis:**

*Phleum pratense (Timothy grass) pollen extract can be localised in challenged model systems and ocular allergen challenged patients with seasonal allergic conjunctivitis (SAC).*

Attempts to localise the Timothy grass pollen allergen used *in vitro* and *in vivo* challenges failed to return a positive result. The Phl p antibody was raised in a rabbit species and a pre-immune serum control was added. This control returned greater intensity of staining than the Phl p antibody.

Further dilution runs are needed to find the optimum concentration of both the rabbit serum and Phl p antibodies. The antigenicity of the *in vivo* allergen challenge samples remains unknown, the samples used had been stored since 1992 and 1994, and the samples had undergone repeated cycles of freeze / thawing so that sections could be cut. Another important factor is the allergen used as the challenge substance; a mixed grass allergen solution was used with no information on the concentrations of the grasses. In order to fully investigate whether Phl p can be localised within the epithelium of a subject who had an *in*

*vivo* allergen challenge, fresh subjects would need to be recruited and a pure Timothy grass pollen used, possibly targeted with newly raised fully validated antibodies.

## Future directions

The crux of any future investigations into the allergen-epithelial interaction in SAC is the establishment of whether the conjunctival epithelium of SAC sufferers are intrinsically different / abnormal to the conjunctival epithelium of whose who do not suffer from SAC. This should include data regarding the structural integrity during periods of quiescent disease and active disease, and how the SAC epithelium responds to inflammatory cytokines released during active disease. From data presented in this thesis, it could be postulated that during disease episodes recovery in structural elements that regulate the integrity of the epithelium, is observed through increased expression, possibly by activation of the epithelial cells. The conjunctival epithelium become activated by signals from the extracellular environment. These could be inflammatory cytokines or by the proteolytic action of allergens on the surface of the cells. In terms of inflammatory cytokines, the most extensively studied molecules are the interferons.

In SAC IFN-γ, has been shown to be produced, IFN-γ binds to surface bound receptors and initiates a cascade of protein phosphorylation events, leading to transcription-activating pathways of multiple genes. The IFN-γ interacts with the JAK kinases that then interact with the STAT (signal transducing activator of transcription) family. Once the STAT are phosphorylated they trans locate to the nucleus, bind to specific DNA sites and the transcription of neighbouring genes is activated. One known outcome of IFN-γ interaction on epithelial cells is its ability to regulate permeability, where IFN-γ has been shown to increase permeability of the epithelium via reducing ZO-1 levels (Reisinger et al 2005, Walsh *et al* 2000, Youakim and Ahdieh 1999). Other cytokines that also activate transcription pathways are GM-CSF, TNF-α and IL-4, which are released during episodes of SAC (Leonardi *et al* 2003, Breuhalm *et al* 2000, Gasbarrini and Montalto 1999, Tomic-Canic *et al* 1998). These cytokines can also by induce from the epithelium directly via proteolytic

allergens (Mattoli 2001, King *et al* 1998). To support this proposed disease pathway, is through the use of gene array technique, backed up with proteomic data, showing any possible post translational modifications that may occur (Knight 2002).

Another interesting avenue of investigation is the proposed theory of mucosal immunity. The extent at which the conjunctival epithelium acts as an 'antigen presenting tissue' for the local recognition and therefore speedy response to allergen contact. Vital to this is the expression of major histocompatibility complex (MHC) class II molecules, which are a characteristic of antigen presenting cells, and possible up-regulation of expression during episodes of disease, similar to that seen in gastric epithelial cells (Barrera *et al* 2002). Another set of receptor that could be implicated in the local immune response in the conjunctival are the Toll receptors, who are growing in their known involvement of host defences to antigens or pathogens (Imler and Hoffmann 2001).

APC migrate into the epithelial layer to sample antigen and can mediate the immune response locally, this is vital to ensuring the speed of the immune reaction to allergen contact (Neutra *et al* 1996). The level of migrating APCs and the level of activated APCs during disease episodes within the conjunctival epithelium needs to be addressed to fully understand their role in the local immune response.

One cascade of immune response regulation that occurs with the reaction to Der p1, is the proteolytic cleavage of CD23 and CD25, the low-affinity (adhesion molecule) and high-affinity receptors for human IgE. This pathway has been extensively studied, and could be relevant to the group I Timothy grass allergen Phl p1 interaction with IgE and possible negative feedback mechanism of IgE cleavage (John et al 2000, Bonnefoy *et al* 1997, Schulz *et al* 1997, Schulz *et al* 1995, Hewitt *et al* 1995).

This thesis presents novel findings regarding the structural elements of the conjunctival epithelium of patients with seasonal allergic conjunctivitis and the action of Timothy grass pollen on tight junctions, laying the foundations for further epithelium based investigations.

## References


Aalberse R.C. and Kapsenberg M.L. 2001 "Allergens", Encyclopaedia of Life Sciences, Nature Publishing Group, http://els.net

Abdel-Khalek L.M., Williamson J. & Lee W.R. 1978 "Morphological changes in the human conjunctival epithelium in the normal elderly population", *Br. J. Ophthalmol.* Vol. 62, no. 11, pp. 792-799.

Abelson M.B., Chambers W.A. & Smith L.M. 1990 "Conjunctival allergen challenge", *Arch. Ophthalmol.* Vol. 108, pp. 84-88.

Alder K.B., Akley N.J. & Glasgow W.C. 1992 "Platelet-activating factor provokes release of mucin-like glycoprotein from guinea pig respiratory epithelial cells via a lipoxygenase-dependent mechanism", *Am. J. Respir. Cell Mol. Biol.* Vol. 6, no. 5, pp. 550-556.

Anderson D.F., MacLeod J.D., Baddeley S.M., Bacon A.S., McGill J.I., Holgate S.T. & Roche W.R. 1997 "Seasonal allergic conjunctivitis is accompanied by increased mast cell numbers in the absence of leucocyte infiltration", *Clin. Exp. Allergy* Vol. 27 no. 9, pp. 1060-1066.

Anderson D.F. 2001 "Management of seasonal allergic conjunctivitis (SAC): current therapeutic strategies", *Clin. Exp. Allergy.* Vol. 31, pp. 823-826. (a)

Anderson D.F., Zhang S., Bradding P., McGill J.I., Holgate S.T. & Roche W.R. 2001 "The relative contribution of mast cell subsets to conjunctival TH2-like cytokines", *Invest. Ophthalmol. Vis. Sci.* Vol. 42, no. 5, pp. 995-1001. (b)

Anderson J.M. and van Itallie C.M. 1999 "Tight junctions: Closing in on the seal", *Curr. Biol.* Vol. 9, R922-R924.

Andersson K and Lidholm J. 2003 "Characteristics and immunobiology of grass pollen allergens", *Int. Arch. Allergy Immunol.* Vol. 130, no. 2, pp. 87-107.

Angst B.D., Nilles L.A. & Green K.J. 1990 "Desmoplapkin II expression is not restricted to stratified epithelia", *J. Cell Sci.* Vol. 97, pt. 2, pp. 247-257.

Bacon A.S., Ahluwalia P., Irani A.M., Schwartz L.B., Holgate S.T., Church M.K. & McGill J.I. 2000 "Tear and conjunctival changes during the allergen-induced early- and late-phase responses", *J. Allergy Clin. Immunol.* Vol. 106, no. 5, pp. 948-954.

Bacon A.S., McGill J.I., Anderson D.F., Baddeley S., Lightman S.L. & Holgate S.T. 1998 "Adhesion molecules and relationship to leukocyte levels in allergic eye disease", *Invest. Ophthalmol. Vis. Sci.* Vol. 39, no. 2, pp. 322-330.

Baddeley S.M., Bacon A.S., McGill J.I., Lightman S.L., Holgate S.T. & Roche W.R. 1995 "Mast cell distribution and neutral protease expression in acute and chronic allergic conjunctivitis", *Clin. Exp. Allergy.* Vol. 25, no. 1, pp. 41-50.

Balda M.S., Flores-Maldonado S., Cereijido M. & Matter K. 2000 "Multiple domains of occludin are involved in the regulation of paracellular permeability", *J. Cell Biochem.* Vol. 78, no. 1, pp. 85-96.

Balda M.S. & Matter K. 2000 "The tight junction protein ZO-1 and an interacting transcription factor regulate ErbB-2 expression", *EMBO.* Vol. 19, no. 9, pp. 2024-2033.

Ball T., Edstrom W., Mauch L., Schmitt J., Leistler B., Fiebig H., Sperr W.R., Hauswirth A.W., Valent P., Kraft D., Almo S.C. & Valenta R. 2005 "Gain of structure and IgE epitopes by eukaryotic expression of the major Timothy grass pollen allergen, Phl p1", *FEBS J.* Vol. 272, pp. 217-227.

Bannon L.J., Cabrera B.L., Stack M.S. & Green K.J. 2001 "Isoform-specific differences in the size of desmosomal cadherin/catenin complexes", *J. Invest. Dermatol.* Vol. 117, pp. 1302-1306.

Bannon G.A. 2002 "Hypersensitivity: Anaphylactic (Type I)" Encyclopaedia of Life Sciences, Nature Publishing Group, http://els.net

Barrera C., Espejo R. & Reyes V.E. 2002 "Differential glycosylation of MHC class II molecules on gastric epithelial cells: Implications in local immune responses", *Human Immunol.* Vol. 63, pp. 384-393.

Behrendt H. and Becker W-M. 1993 "Localization, release and bioavailability of pollen allergens: the influence of the environmental factors", *Curr. Opin. Immunol.* Vol. 13, pp. 709-715.

Bloor B.K., Seddon S.V. & Morgan P.R. 2000 "Gene expression of differentiation-specific keratins (K4, K13, K1 and K10) in oral non-dysplastic keratoses and lichen planus", *J. Oral Pathol. Med.* Vol. 29, no. 8, pp. 376-384.

Bonnefoy J.Y., Lacoanet-Henchoz S., Gauchat J.F., Graber P., Aubry J.P., Jeannin P. & Plater-Zyberk C. 1997 "Structure and functions of CD23", *Int. Rev. Immunol.* Vol. 16, nos. 1-2, pp. 113-128.

Bozzola J.J. 2002 "Electron microscopy" Encyclopaedia of Life Sciences, Nature Publishing Group, http://els.net

Braga V.M.M., Machesky L.M., Hall A. & Hotchin N.A. 1997 "The small GTPases Rho and Rac are required for the setanblishment of cadherin-dependent cell-cell contacts", *J. Cell Biol.* Vol. 137, no. 6, pp. 1421-1431.

Brembeck F.H., Rosário M. & Birchmeier W. 2006 "Balancing cell adhesion and Wnt signalling, the key role of $\beta$-catenin", *Curr. Opin. Genet. Dev.* Vol. 16, pp. 51-59.

Breuhaln K., Mann A., Muller G., Wilhelmi A., Schirmacher P., Enk A. & Blessing M. 2000 "Epidermal overexpression of granulocyte-macrophage colony-stimulating factor induces keratinocyte and apoptosis", *Cell Growth Differ.* Vol, 11, no. 2, pp. 111-121.

Broers J.L., de Leij L., Rot M.K., ter Haar A., Lane E.B., Leigh I.M., Wagenaar S.S., Vooijs G.P. & Ramaekers F.C. 1989 "Expression of intermediate filament proteins in fetal and adult human lung tissue", *Differentiation* Vol. 40, no. 2, pp. 119-128.

Buckley R.J. 1998 "Allergic eye disease – a clinical challenge", *Clin. Exp. Allergy.* Vol. 28, no. 6, pp. 39-43.

Canonica G.W., Ciprandi G., Passalacqua G., Pesce G., Scordamaglia A. & Bagnasco M. 1997 "Molecular events in allergic inflammation: experimental models and possible modulation", *Allergy* Vol. 52, Suppl. 34, pp. 25-30.

Carmichael R.P., McCulloch C.A. & Zarb G.A. 1991 "Immunohistochemical localisation and quantification of desmoplakin I & II and keratins 1 and 19 in plastic-embedded sections of human gingival", *J. Histochem. Cytochem.* Vol. 39, no. 4, pp. 519-528.

Carreno M.P., Rousseau Y. & Haeffner-Cavaillon N. 1995 "Cell adhesion molecules and the immune system", *Allerg. Immunol.* Vol. 27, no. 7, pp. 106-110.

Cereijido M., Shoshani L. & Contreras R.G. 2000 "Molecular physiology and pathophysiology of tight junctions I. Biogenesis of tight junctions and epithelial polarity", *Am. J. Gastrointest. Liver Physiol.* Vol. 279, G477-G482.

Chen K.H., Azar D. & Joyce N.C. 2001 "Transplantation of adult human corneal endothelium ex vivo: a morphologic study", *Cornea* Vol. 20, no. 7, pp. 731-737.

Chen Y-H., Lu Q., Schneeberger E.E. & Goodenough D.A. 2000 "Restoration of tight junction structure and barrier function by down-regulation of the mitogen-activated protein kinase pathway in ras-transformed Madin-Darby canine kidney cells", *Mol. Biol. Cell* Vol. 11, no. 3, pp. 849-862.

Chitaev N.A. and Troyanovsky S.M. 1998 "Adhesive but not lateral E-cadherin complexes require calcium and catenins for their formation", *J. Cell Biol.* Vol. 142, no. 3, pp. 837-846.

Cho B.J., Djalilian A.R., Obritsch W.F., Matteson D.M., Chan C.C. & Holland E.J. 1999 "Conjunctival epithelial cells cultured on human amniotic membrane fail to transdifferentiate into corneal epithelia-type cells" *Cornea* Vol. 18, no. 2, pp. 216-224.

Chu P.G. and Weiss L.M. 2002 "Keratin expression in human tissues and neoplasms", *Histopathology* Vol. 40, no. 5, pp. 403-439.

Clayton W.D., Harman K.T. & Williamson H. 2002 onwards "World grass species: Description, identification and information retrieval. http://.kew.org/data/grasses-db.html accessed 08/05/2006.

Colgan S.P., Resnick M.B., Parkos C.A., Delp-Archer C., McGuirk D., Bacarra A.E., Weller P.F. & Madara J.L. 1994 "IL-4 directly modulates function of a model human intestinal epithelium", *J. Immunol.* Vol. 153, no. 5, pp. 2122-2129.

Cowin P., Kapprell H.P. & Franke W.W. 1985 "The complement of desmosomal plaque proteins in different cell types", *J. Cell Biol.* Vol. 101, no. 4, pp. 1442-1454.

Cozens A.L., Yezzi M.J., Yamaya M., Steiger D., Wagner J.A., Garber S.S., Chin L., Simon E.M., Cutting G.R., Gardner P, et al. 1992 "A transformed human epithelial cell line that retains tight junctions post crisis", *In Vitro Cell Dev. Biol.* Vol. 28A, nos. 11-12, pp. 735-744.

Cozens A.L., Yezzi M.J., Kunzelmann K., Ohuri T., Chin L., Eng K., Finkbeiner W.E., Widdicombe J.H. & Gruenert D.C. 1994 "CFTR expression and chloride secretion in polarized immortal human bronchial epithelial cells", *Am. J. Respir. Cell Mol. Biol.* Vol 10, no. 1, pp. 38-47.

Cyr D.G., Robaire B. & Hermo L. 1995 "Structure and turnover of junctional complexes between principle cells of the rat epididymis", *Microsc. Res. Tech.* Vol. 30, no. 1, pp. 54-66.

Dart J.K., Buckley R.J., Monnickendan M & Prasad J. 1986 "Perennial allergic conjunctivitis: definition, clinical characteristics and prevalence. A comparison with seasonal allergic conjunctivitis", *Trans. Ophthalmol. Soc. UK.* Vol. 105, no. 5, pp. 513-520.

De Saint Jean M., Brignole F., Feldmann G., Goguel A. & Baudouin C. 1999 "Interferon-gamma induces apoptosis and expression of inflammation-related proteins in Chang conjunctival cells", *Invest. Ophthalmol. Vis., Sci.* Vol. 40, no. 10, pp. 2199-2212.

De Saint Jean M., Debbasch C., Brignole F., Rat P., Warnet J.M. & Baudouin C. 2000 "Toxicity of preserved and unpreserved antiglaucoma topical drugs in an in vitro model of conjunctival cells", *Curr. Eye Res.* Vol. 20, no. 2, pp. 85-94.

De Saint Jean M., Baudouin C., Di Nolfo M. Roman S., Lozato P. Warnet J.M. & Brignole F. 2004 "Comparison of morphological and functional characteristics of primary-cultured human conjunctival epithelium and of Wong-Kilbourne derivative of Chang conjunctival cell line", *Exp. Eye Res.* Vol. 78, pp. 257-274.

Devalia J.L., Godfrey R.W., Sapsford R.J., Severs N.J., Jeffery P.K. & Davies R.J. 1994 "No effect of histamine on human bronchial epithelial cell permeability and tight junctional integrity in vitro", Eur. *Respir. J.* Vol. 7, no. 11, pp. 1958-1965.

Diebold Y.C., Calonge M., Enriquez de Salamanca A., Callejo S., Corrales R.M. & Saez V. 2003 "Characterization of a spontaneously immortalized cell line (IOBA-NHC) from normal human conjunctiva", *Invest. Ophthalmol. Vis. Sci.,* Vol. 44, no. 10, pp. 4263-4274.

Diebold Y.C., Calonge M.C., Callejo S.C., Lazaro M.C., Bringas R.M. & Herreras J.M. 1999 "Ultrastructural evidence of mucus in human conjunctival epithelial cultures", *Curr. Eye Res.* Vol. 19, no. 2, pp. 95-105.

Diebold Y.C., Calonge M., Carretero V., Fernández N. & Herreras J. 1998 "Expression of ICAM-1 and HLA-DR by human conjunctival epithelial cultured cells and modulation by nedocromil sodium", *Journal of ocular pharmacology and therapeutics*, Vol. 14, no. 6, pp. 517-527.

Diebold Y.C., Calonge M., Fernandez N., Lazaro M.C., Callejo S., Herreras J.M. & Pastor J.C. 1997 "Characterisation of epithelial primary cultures from human conjunctiva", *Graefes Arch. Clin. Exp. Ophthalmol.* Vol. 235, no. 5, pp. 268-276.

Dogru M., Katakami C., Nakaagawa N., Tetsumoto K. & Yamamoto M. 1998, "Impression cytology in atopic dermatitis", *Ophthalmology* Vol. 105, no. 8, pp. 1478-1484.

Dota A., Nishida K., Adachi W., Nakamura T., Koizumi N., Kawamoto S., Okubo K. & Kinoshita S. 2001 "An expression profile of active genes in human conjunctival epithelium", *Exp. Eye Res.* Vol. 72, no. 3, pp. 235-241.

Duke, J., A. 1983 Handbook of Energy Crops. Unpublished. http:/hort.purdee.edu/newcrop/duke-energy/panicum-maximum html.

Easty D. & Wyse R. (Eds) 2002 "Seasonal allergic conjunctivitis and rhinoconjunctivitis", Round Table Series 78, The Royal Society of Medicine Press.

Ebato B., Friend J. & Thoft R.A. 1986 "Comparison of central and peripheral human corneal epithelium in tissue culture", *Invest. Ophthalmol. Vis. Sci.* Vol. 28, pp. 1450-1456.

Enriquez de Salamanca A., Diebold Y., Calonge M., Garcia-Vazquez C., Callejo S., Vila A. Alonso M.J. 2006 "Chitosan nanoparticles as a potential drug delivery system for the ocular surface: toxicity, uptake mechanism and in vivo tolerance", *Invest Ophthalmol. Vis. Sci.* Vol. 47, no. 4, pp. 1416-1426.

Enriquez de Salamanca A., Siemasko K.F., Diebold Y., Calonge M., Gao J., Juarez-Campo M. & Stern M.E. 2005 "Expression of muscarinic and adrenergic receptors in normal human conjunctival epithelium", *Invest. Opthalmol. Vis. Sci.* Vol. 46, no. 2, pp. 504-513.

Evans S.M., Blyth D.I., Wong T., Sanjar S. & West M.R. 2002 "Decreased distribution of lung epithelial junction proteins after intratracheal antigen or lipopolysaccharide challenge: Correlation with neutrophil influx and levels of BALF sE-Cadherin", *Am. J. Respir. Cell Mol. Biol.* Vol. 27, pp. 446-454.

Franke W.W., Moll R., Schiller D.L., Schmid E., Kartenbeck J. & Mueller H. 1982 "Desmoplakins of epithelial and myocardial desmosomes are immunologically and biochemically related", *Differentiation* Vol. 23, no. 2, pp. 115-127.

Franke W.W., Moll R., Mueller H., Schmid E., Kuhn C., Krepler R., Artlieb U. & Denk H. 1983 "Immunocytochemical identification of epithelium-derived human tumours with antibodies to desmosomal plaque proteins", *Proc. Natl. Acad. Sci.* Vol. 80, no. 2, pp. 543-547.

Freedberg I.M., Tomic-Canic M., Komine M. & Blumenberg M. 2001 "Keratins and the keratinocyte activation cycle", *J. Invest. Dermatol.* Vol. 116, no. 5, pp. 633-640.

Fritschy J-M. and Härtig W. 2002 "Indirect immunofluorescence of cultured cells", Encyclopaedia of Life Sciences, Nature Publishing Group, http://els.net

Fuchs E. & Weber K. 1994 "Intermediate Filaments: Structure, Dynamics, Function and Disease", *Annu. Rev. Biochem.* Vol. 63, pp. 345-82.

Fujishima H., Takeyama M., Takeuchi T., Saito I. & Tsubota K. 1997 "Elevated levels of substance P in tears of patients with allergic conjunctivitis and vernal Keratoconjunctivitis", *Clin. Exp. Allergy* Vol. 27, no. 4, pp. 372-378.

Furukawa F., Fujii K., Horiguchi Y., Matsuyoshi N., Fujita M., Toda K-I., Imamura S., Wakita H., Shirahama S. & Takigawa M. 1997 "Roles of E- and P- Cadherin in the human skin", *Microsc. Res. Tech.* Vol. 38, pp. 343-352.

Galli S.J. 1997 "The mast cell: A versatile effector cell for a challenging world", *Int. Arch. Allergy Immunol.* Vol. 113, pp. 14-22.

Galou M., Gao J., Humbert J., Mericskay M., Li Z., Paulin D. & Vicart P. 1997 "The importance of intermediate filaments in the adaptation of tissues to mechanical stress: evidence from gene knockout studies", *Biol. Cell.* Vol. 89, no. 2, pp. 85-97.

Gamache D.A., Dimitrijevich S.D., Weimer L.K., Lang L.S., Spellman J.M., Graff G. & Yanni J.M. 1997 "Secretion of pro-inflammatory cytokines by human conjunctival epithelial cells", *Ocul. Immunol. Inflamm.* Vol. 5. no. 2, pp. 117-128.

Gasbarrini G. and Montalton M. 1999 "Structure and function of tight junctions. Role in intestinal barrier", *Ital. J. Gastroenterol. Hepatol.* Vol. 31, no. 6, pp. 481-488.

Gipson I.K., Spurr-Michaud S.J., Tisdale A.S., Kublin C., Cintron C. & Keutmann H. 1995 "Stratified squamous epithelia produce Mucin-like glycoproteins", *Tissue Cell* Vol. 27, no. 4, pp. 397-404.

di Girolamo N., Tedla N., Kumar R.K., McCluskey P., Lloyd A., Coroneo M.T. & Wakefield D. 1999 "Culture and characterisation of epithelial cells from human pterygia", *Br. J. Ophthalmol.* Vol. 83, pp. 1077-1082.

Goebeler M., Roth J., van den Bos C., Ader G. & Sorg C. 1995 "Increase of calcium levels in epithelial cells induces translocation of calcium-binding proteins migration inhibitory factor-related protein 8 (MRP8) and MRP14 to keratin intermediate filaments", *Biochem. J.* Vol. 309, no. 2, pp. 419-424.

Goetinck P.F., Stripe N.S., Tsonis P.A. & Carlone D. 1987 "The tandemly repeated sequence of cartilage link proteins contains the sites of interaction with hyaluronic acid", *J. Cell. Biol.* Vol. 105, pp. 2403-2408.

Goller T. and Weyrauch K.D. 1993 "The conjunctival epithelium of dogs. Light and electron microscopic investigations", *Anat. Anz.* Vol. 175, no. 2, pp. 127-134.

González-Marisacl L., Betanzos A., Nava P. & Jaramillo B.E. 2003 "Tight junction proteins", *Progress Biophys. Mol. Biol.* Vol. 81, pp 1-44.

Goto Y., Uchida Y., Nomura A., Sakamoto T., Ishii Y., Morishima Y., Masuyama K. & Sekizawa K. 2000 "Dislocation of E-Cadherin in the airway epithelium during an antigen-induced asthmatic response", *Am. J. Respir. Cell Mol. Biol.* Vol. 23, pp. 712-718.

Green K.J., Geiger B., Jones J.C., Talian J.C. & Goldman R.D. 1987 "The relationship between intermediate filaments and microfilaments before and during the formation of desmosomes and adherens-type junctions in mouse epidermal keratinocytes", *J. Cell Biol.* Vol. 104, no. 5, pp. 1389-1402.

Green K.J., Parry D.A., Steinert P.M., Virata M.L., Wagner R.M., Angst B.D. & Nilles L.A. 1990 "Structure of the human desmoplakins. Implications for the function in the desmosome", *J. Biol. Chem.* Vol. 265, no. 5, pp. 2603-2612.

Green K.J., Stappenbeck T.S., Parry D.A. & Virata M.L. 1992 "Structure of desmoplakin and its association with intermediate filaments", *J. Dermatol.* Vol. 19, no. 11, pp. 765-769.

Grobe K., Wolf-Meinhard B., Schlaak M. & Petersen A. 1999, "Grass group 1 allergens (β-expansins) are novel, papain-related proteinase", *Eur. J. Biochem.*, Vol. 263, pp. 33-40.

Grobe K., Poppelmann M., Wolf-Meinhard B. & Petersen A. "Properties of group 1 allergens from grass pollen and their relation to cathepsin B, a member of the C1 family of cysteine proteinases", *Eur. J. Biochem.*, Vol. 269, pp. 2083-2092.

Groneberg D.A., Bielory L., Fischer A., Bonini S. & Wahn U. 2003 "Animal models of allergic and inflammatory conjunctivitis", *Allergy* Vol. 58, pp. 1101-1113.

Grote M., Vrtala S., Niederberger V., Wiermann R., Valenta R. & Reichelt R. 2001 "Release of allergen-bearing cytoplasm from hydrated pollen: a mechanism common to a variety of grass (Poaceae) species revealed by electron microscopy", *J. Allergy Clin. Immunol.* Vol. 108, no. 1, pp. 109-115.

Gukasyan H.J., Lee V.H.L., Kim K-J. & Kannan R. 2002 "Net glutathione secretion across primary cultured rabbit conjunctival epithelial cell layers", *Invest. Ophthalmol. Vis. Sci.* Vol. 43, no. 4, pp. 1154-1161.

Hatsell S. & Cowin P. 2001 "Deconstructing desmoplakin", *Nature Cell Biol.* Vol. 3, pp. 270-272.

Hatzfeld M., Maier G. & Franke W.W. 1987 "Cytokeratin domains involved in heterotypic complex formation determined by in-vitro binding assays", *J. Mol. Biol.* Vol. 197, no. 2, pp. 237-255.

Hatzfeld M. & Franke W.W. 1985 "Pair formation and promiscuity of cytokeratins: formation in vitro of heterotypic complexes and intermediate-sized filaments by homologous and heterologous recombinations of purified polypeptides", *J. Cell Biol.* Vol. 101 no. 5, pt. 1, pp. 1826-1841.

Heiskala M., Peteron P.A. & Yang Y. 2001 "The roles of claudin superfamily proteins in paracellular transport", *Traffic* Vol. 2, no. 2, pp. 93-98.

Herbert C.A., King C.M., Ring P.C., Holgate S.C., Steward G.A., Thompson P.J. & Robinson C. 1995 "Augmentation of permeability in the bronchial epithelium by the house dust mite allergen Der p1", *Am. J. Resp. Cell Mol.*, Vol. 12, pp. 369-378.

Herrstrom P. & Hogstedt B. 1994 "Allergic disease, dental health, and socioeconomic situation of Swedish teenagers. Allergy, dental health, and social situation", *Scand. J. Prim. Health Care* Vol. 12, no. 1, pp. 57-61.

Hewitt C.R., Brown A.P., Hart B.J. & Pritchard D.I. 1995 "A major house dust mite allergen disrupts the immunoglobulin E network by selectly cleaving CD23: innate protection by antiproteases", *J. Exp. Med. Vol.* 182, no. 5, pp. 1537-1544.

Hicks W. Jr., Hall L. 3rd., Sigurdson L., Stewart C., Hard R., Winston J. & Lwebuga-Mukasa J. 1997 "Isolation and characterization pf basal cells from human upper respiratory epithelium", *Exp. Cell Res.* Vol. 237, no. 2, pp. 357-363.

Hopkins A.M., Li D., Mrsny R.J., Walsh S.V. & Nusrat A. 2000 "Modulation of tight junction function by G protein-coupled events", *Advanced Drug Delivery Rev.* Vol. 40, pp. 329-340.

Holgate S.T., Church M.K. & Lichtenstein L.M. (Eds). 2001 "Allergy", 2nd Ed. Mosby.

Horiguchi Y., Furukawa F., Fujita M. & Imamura S. 1994 "Ultrastructural localization of E-Cadherin cell adhesion molecule on the cytoplasmic membrane of keratinocytes in vivo and in vitro", *J. Histochem. Cytochem.* Vol. 42, no. 10, pp. 1333-1340.

Howart W.J., Holgate S.T. & Lackie P.M. 2002 "TGF-beta isoform release and activation during in vitro bronchial epithelial wound repair", *Am. J. Physiol. Lung Mol. Physiol.* Vol. 282, no. 1, L115-L123.

Howarth P.H. 1998 "Is allergy increasing?- early life influences", *Clin. Exp. Allergy*, Vol. 28, Suppl. 6, pp. 2-7.

Huang A.J., Tseng S.C. & Kenyon K.R. 1989 "Paracellular permeability of corneal and conjunctival epithelia", *Invest. Ophthalmol. Vis. Sci.* Vol. 30, no. 4, pp. 684-689.

Imler J-L. and Hoffmann J.A. 2001 "Toll receptors in innate immunity", *Trends Cell Biol.* Vol. 11, no. 7, pp. 304-311.

Inai T., Kobayashi J & Shibata Y 1999 "Claudin-1 contributes to the epithelial barrier function in MDCK cells", *Eur. J. Cell Biol.* Vol. 78, no. 12, pp. 849-855.

Itoh M., Furuse M., Morita K., Kubota K., Saitou M & Tsukita S. 1999 "Direct binding of three tight junction-associated MAGUKs, ZO-1, ZO-2 and ZO-3, with the COOH termini of claudins", *J. Cell Biol.* Vol. 147, no. 6, pp. 1351-1363.

Itoh M., Sasaki H., Furuse M., Ozaki H., Kita T. & Tsukita S. 2001 "Junctional adhesion molecule (JAM) binds to PAR-3: a possible mechanism doe the recruitment of PAR-3 to tight junctions", *J. Cell Biol.* Vol. 154, no. 3, pp. 491-497.

Ivanov D.B, Philippova M.P. & Tkachuk V.A. 2001 "Structure and function of classical cadherins", *Biochemistry* Vol. 66, no. 10, pp. 1174-1186.

Jackson H.A., Orton S.M. & Hammerberg B. 2002 "IgE is present on peripheral blood monocytes and B cells in normal dogs and dogs with atopic dermatitis but there is no correlation with serum IgE concentrations", *Vet. Immunol. Immunopathol.* Vol. 73, pp. 167-182.

Jang Y.J., Kim H.G., Koo T.W. & Chung P.S. 2002 "Localization of the ZO-1 and E-Cadherin in the nasal polyp epithelium", *Eur. Arch. Otorhinolaryngol.* Vol. 259, no. 9, pp. 465-469.

John R.J., Rusznak C., Ramjee M., Lamont A.G., Abrahamson M. & Hewitt E.L. 2000 "Functional effects of the inhibition of the cysteine protease activity of the major house dust mite allergen Der p1 by a novel peptide-based inhibitor", *Clin. Exp. Allergy* Vol. 30, pp. 784-793.

Jones J.C. & Goldman R.D. 1985 "Intermediate filaments and the initiation of desmosome assembly", *J. Cell Biol.* Vol. 101, no. 2, pp. 506-517.

Joss J.D. & Craig T.J. 1999 "Seasonal allergic conjunctivitis: overview and treatment update", *J. Am. Osteopath. Assoc.* Vol. 99, Suppl. 7, s. 13-18.

Kallakury B.V., Sheehan C.E. & Ross J.S. 2001 "Co-downregilation of cell adhesion proteins alpha- and beta-catenins, p120CTN, E-Cadherin and CD44 in prostatic adenocarcinomas", *Hum. Pathol.* Vol. 32, no. 8, pp. 849-855.

Kasper M. 1991 "Heterogeneity in the Immunolocalisation of cytokeratin specific monoclonal antibodies in the rat eye: evaluation of unusual epithelial tissue entities", *Histochemistry.* Vol. 95, no. 6, pp. 613-620.

Kee S-H. and Steinert P.M. 2001 "Microtubule disruption in keratinocytes induces cell-cell adhesion through activation of endogenous E-Cadherin", *Mol. Biol. Cell* Vol. 12, pp. 1983-1993.

King C., Brennan S., Thompson P.J. & Stewart G.A. 1998 "Dust mite proteolytic allergens induce cytokine release from cultured airway epithelium", *J. Immunol.* Vol. 161, pp. 3645-3651.

Kinoshita S., Kiorpes T.C., friend J. & Thoft R.A. 1982 "Limbal epithelium in ocular surface wound healing", *Invest. Ophthalmol. Vis. Sci.* Vol. 23, no. 1, pp. 73-80.

Kivela T. & Uusitalo M. 1998 "Structure, development and function of cytoskeletal elements in non-neuronal cells of the human eye", *Prog. Retin. Eye Res.* Vol. 17, no. 3, pp. 385-428.

Klinger C., Kniesel U., Bamforth S.D., Wolburg H., Engelhardt B. & Risau W. 2000 "Disruption of epithelial tight junctions is prevented cyclic nucleotide-dependent protein kinase inhibitors", *Histochem. Cell Biol.* Vol. 112, no. 5, pp. 349-361.

Knight D. 2002 "Increased permeability of asthmatic epithelial cells to pollutants. Does this mean that they are intrinsically abnormal", *Clin. Exp. Allergy* Vol. 32, pp. 1263-1265.

Kobayashi N., Dezawa M., Nagata H., Yuasa S. & Konno A. 1998 "Imuunohistochemical study of E-Cadherin and ZO-1 in allergic nasal epithelium of the guinea pig", *Int. Arch. Allergy Immunol.* Vol. 116, mo. 3, pp. 196-205.

Koch A.E., Kronfeld-Harrington L.B., Szekanecz Z., Cho M.M., Haines G.K., Harlow L.A., Strieter R.M., Kunkel S.L., Massa M.C. & Barr W.G. 1993 "In situ expression of cytokines and cellular adhesion molecules in the skin of patients with systemic sclerosis. Their role in early and late disease", *Pathobiology*. Vol. 61 nos. 5-6, pp. 239-246.

Koizumi N., Cooper L.J., Fullwood N.J., Nakamura T., Inoki K., Tsuzuki M. & Kinoshita S. 2002 "An evaluation of cultured corneal limbal epithelial cells, using cell-suspension culture", *Invest. Ophthalmol. Vis. Sci.* Vol. 43, no. 7, pp. 2114-2121.

von Koskull H. & Virtanen I. 1987 "Induction of cytokeratin expression in human mesenchymal cells", *J. Cell Physiol.* Vol. 133, no. 2, pp. 321-329.

Kosunen T.U., Höök-Nikanne J., Salomaa A., Sarna A., Aromaa A. & Haahtela T. 2002 *Clin. Exp. Allergy*, Vol. 32, pp. 373-378.

Kouklis P.D., Hutton E. & Fuchs E. 1994 "Making a connection: direct binding between keratin intermediate filaments and desmosomal proteins", *J. Cell Biol.* Vol. 127, no. 4, pp. 1049-1060.

Kowalczyk A.P., Bornslaeger E.A., Borgwardt J.E., Palka H.L., Dhaliwal A.S., Corcoran C.M., Denning M.F. & Green K.J. 1997 "the amoni-terminal domain of desmoplakin binds to plakogloblin and clusters desmosomal cadherin-plakoglobin complexes", *J. Cell Biol.* Vol. 139, no. 3, pp. 773-784.

Kowalczyk A.P., Stappenbeck T.S., Parry D.A., Palka H.L., Virata M.L., Bornslaeger E.A., Nilles L.A. & Green K.J. 1994 "Structure and function of desmosomal transmembrane core and plaque molecules", *Biophys. Chem.* Vol. 50, nos. 1-2, pp. 97-112.

Krenzer K.L. & Freddo T.F. 1997 "Cytokeratin expression in normal human bulbar conjunctiva obtained by impression cytology", *Invest. Ophthalmol. Vis. Sci.* Vol. 38, no. 1, pp. 142-152.

Kreis T. and Vale R. 1994 "Guidebook to the extracellular matrix and adhesion proteins", Oxford University Press. Pp. 116-118.

Ku N.O., Michie S., Resurreccion E.Z., Broome R.L. & Omary M.B. 2002 "Keratin binding to 14-3-3 proteins modulates keratin filaments and hepatocyte mitotic progression", *Proc. Natl. Acad. Sci.* Vol. 99, no. 7, pp. 4373-4378.

Kubota K., Furuse M., Sasaki H., Sonoda N., Fujita K., Nagafuchi A. & Tsukita S. 1999 "Ca(2+)-independent cell-adhesion activity of claudins, a family of integral membrane proteins localised at tight junctions", *Curr. Biol.* Vol. 9, no. 18, pp. 1035-1038.

Kurpakus M.A., Stock E.L. & Jones J.C. 1992 "The role of the basement membrane in differential expression of keratin proteins in epithelial cells", *Dev. Biol.* Vol. 150, no. 2, pp. 243-255.

Lain-Chao L. & Cosgrove D. "Grass group 1 pollen allergens ($\beta$-expansins) lack proteinase activity and do not cause wall loosening via proteolysis", *Eur. J. Biochem.*, Vol. 268, pp. 4217-4226.

Lambrecht B.N. 2001 "Allergen uptake and presentation by dendritic cells", *Curr. Opin. Allergy Clin. Immunol.* Vol. 1, pp. 51-59.

Lebowitz M.D., Barbee R. & Burrows B. 1984 "Family concordance of IgE, atopy and disease", *J. Allergy Clin. Immunol.* Vol. 73, no. 2, pp. 259-264.

Lee C.Y., Matsumoto-Pon J. & Widdicombe J.H. 1997 "Cultured lung epithelium: A cellular model for lung preservation" *Cryobiology* Vol. 35, pp. 209-218.

Leir S.H., Holgate S.T. & Lackie P.M. 2003 "Inflammatory cytokines can enhance CD44-mediated airway epithelial cell adhesion independently of CD44 expression", *Am. J. Physiol. Cell Mol. Physiol.* Vol. 285, no. 6, L1305-1311.

Leonardi A., Brun P., Tavolato M., Plebani M., Abatengelo G. & Secchi A.G. 2003 "Tumor necrosis factor-alpha (TNF-alpha) in seasonal allergic conjunctivitis and vernal keratoconjunctivitis", *Eur. J. Opthalmol.* Vol. 13, no. 7, pp. 606-610.

Leonardi A., Borghesan F., Faggian D., Depaoli M., Secchi A.G. & Plebani M. 2000 "Tear and serum soluble leukocyte activation markers in conjunctival allergic diseases", *Am. J. Ophthalmol.* Vol. 129, no. 2, pp. 151-158.

Leonardi A., Radice M., Fregona I.A., Plebani M., Abatangelo G. & Secchi A. 1999 "Histamine effects on conjunctival fibroblasts from patients with vernal conjunctivitis", *Exp. Eye Res.* Vol. 68, pp. 739-746.

Lesley J., He Q., Miyake K., Hamann A., Hyman R. & Kincade P.W. 1992 "Requirements for hyaluronic acid binding by CD44: a role for the cytoplasmic domain and activation by antibody", *J. Exp. Med.* Vol. 175, no. 1, pp. 257-266.

Leung, C.L., Green K.J. & Liem R.K.H. 2002 "Plakins: a family of versatile cytolinker proteins", *Trends Cell Biol.* Vol. 12, no. 1, pp. 37-45.

Liang T.W., DeMarco R.A., Mrsny R.J., Gurney A., Gray A., Hooley J., Aaron H.L., Huang A., Klassen T., Tumas D.B. & Fong S. 2000 "Characterisation of huJAM: evidence for involvement in cell-cell contact and tight junction regulation", *Am. J. Physiol. Cell Physiol.* Vol. 279, no. 6, C1733-1743.

Lippoldt A., Liebner S., Andbjer B., Kalbacher H., Wolburg H., Haller H. & Fuxe K. 2000 "Organisation of choroid plexus epithelial and endothelial cell tight junctions and regulation of claudin-1, -2 and -5 expression by protein kinase C", *Neuroeport.* Vol. 11, no. 7, pp. 1427-1437.

Linhart B., Jahn-Schmid B., Verdino P., Keller W., Ebner C., Kraft D & Valenta R. 2002 "Combination vaccines for the treatment of grass pollen allergy consisting of genetically engineered hybrid molecules with increased immunogenicity", *FASEB J.* Vol. 16, pp. 1301-1303.

Liu Y., Nusrat A., Schnell F.J., Reaves T.A., Walsh S., Pochet M. & Parkos C.A. 2000 "Human junction adhesion molecule regulates tight junction resealing in epithelia", *J. Cell Sci.* Vol. 113, pp. 2363-2374.

Lu D.P., Tatemoto Y., Kimura T. & Osaki T. 2002 "Expression of cytokeratins (CKs) 8, 13 and 18 and their mRNA in epithelial linings of radicular cysts: implication for the same CK profiles as nasal columnar in squamous epithelial lining", *Oral Dis.* Vol. 8, no. 1, pp. 30-36.

Ma L., Xu J., Coulombe P.A. & Wirtz D. 1999 "Keratin filament suspensions show unique micromechanical properties", *J. Biol. Chem.* Vol. 274, no. 27, pp. 19145-19151.

Ma T.Y., Tran D., Hoa N., Nguyen D., Merryfield M. & Tarnawski A. 2000 "Mechanism of extracellular calcium regulation of intestinal epithelial tight junction permeability: role of cytoskeletal involvement", *Microsc. Res. Tech.* Vol. 51, no. 2, pp. 156-168.

Maciver S.K. 2001 "Polymerisation dynamics of cytoskeletal filaments" Encyclopaedia of Life Sciences, Nature Publishing Group, http://els.net

Mackay S., Booth S.H., MacGowan A. & Smith R.A. 1999 "Ultrastructural studies demonstrate that epithelial polarity is established in cultured mouse pre-Sertoli cells by extracellular matrix components", *J. Electron Microsc. (Toyko).* Vol. 48, no. 2, pp. 159-169.

MacLeod J.D., Anderson D.F., Baddeley S.M., Holgate S.T., McGill J.I. & Roche W.R. 1997 "Immunolocalization of cytokines to mast cells in normal and allergic conjunctiva", *Clin. Exp. Allergy.* Vol. 27, no. 11, pp. 1328-1334.

Magee A.I. 1995 "Cell adhesion molecules and intracellular signalling: From fly to man", *Cellular signalling* Vol. 7, no. 3, pp. 165-170.

Magone M.T., Chan C.C., Beck L., Whitcup S.M. & Raz E. 2000 "Systemic or mucosal administration of immunostimulatory DNA inhibits early and late phases of murine allergic conjunctivitis", *Eur. J. Immunol.* Vol. 30, no. 7, pp. 1841-1850.

Marceau N., Loranger A., Gilbert S., Daigle N. & Champetier S. 2001 "Keratin-mediated resistance to stress and apoptosis in simple epithelial cells in relation to health and disease", *Biochem. Cell Biol.* Vol. 79, no. 5, pp. 543-555.

Mari A. 2003 "Skin test with a timothy grass Phleum pratense pollen extract vs. IgE to a timothy extract vs. IgE to rPhl p1, rPhl p2, nPhl p4, rPhl p5, rPhl p6, rPhl p7, rPhl p11, and rPhl p 12: epidemiological and diagnostic data", *Clin. Exp. Allergy* Vol. 33, pp. 43-51.

Mattoli S. 2001 "Allergen-induced generation of mediators in the mucosa", *Environ. Health Perspect.* Vol. 109, Suppl. 4, pp. 553-557.

Mauro T., Guitard M., Behne M., Oda Y., Crumrine D., Komuves L., Rassner U., Elias P.M. & Hummler E. 2002 "The ENaC channel is required for normal epidermal differentiation", *Invest. Dermatol.* Vol. 118, no. 4, pp. 589-594.

McGill J.I., Holgate S.T., Church M.K., Anderson D.F. & Bacon A. 1998 "Allergic eye disease mechanisms", *Br. J. Ophthalmol.* Vol. 82, pp. 1203-1214.

Medina R., Rahner C., Mitic L.L., Anderson J.M. & van Itallie C.M. 2000 "Occludin localization at the tight junction requires the second extracellular loop", *J. Membr. Biol.* Vol. 178, no. 3, pp. 235-247.

Meller D. and Tseng S.C. 1999 "Conjunctival epithelial cell differentiation on amniotic membrane" *Invest. Ophthalmol. Vis. Sci.* Vol. 40, no. 5, pp. 878-886.

Meller D., Dabul V. & Tseng S.C. 2002 "Expansion of conjunctival epithelial progenitor cells on amniotic membrane" *Exp. Eye Res.* Vol. 74, no. 4, pp. 537-545.

Michelini F.M., Ramirez J.A., Berra A., Galagovsky L.R. & Alche L.E. 2005 "In vitro and in vivo antiherpetic activity of three new synthetic brassinosteroid analogues" *Steroids* Vol. 69, nos. 11-12, pp. 713-720.

Mine Y. and Zhang J.W. 2003 "Surfactants enhance the tight-junction permeability of food allergens in human intestinal epithelial Caco-2 cells", *Int. Arch. Allergy Immunol.* Vol. 130, no. 2, pp. 135-142.

Moll R., Franke W.W., Schiller D.L., Geiger B. & Krepler R. 1982 "The catalog of human cytokeratins: pattern of expression in normal epithelia, tumour and culture cells", *Cell.* Vol. 31, pp. 11-24.

Möller C., Björkstén B., Nilsson G. & Dreborg 1984, "The precision of the conjunctival provocation test", *Allergy*, Vol. 39, pp. 37-41.

Montefort S., Baker J., Roche W.R. & Holgate S.T. 1993 "The distribution of adhesive mechanisms in the normal bronchial epithelium", *Eur. Respir. J.* Vol. 6, pp. 1257-1263.

Moreno M.P-M., Jamora C. and Fuchs E. 2003 "Sticky business: orchestrating cellular signals at adherens junctions", *Cell* Vol. 112, pp. 535-548.

Morgan S.J., Williams J.H., Walls A.F., Church M.K., Holgate S.T. & McGill J.I. 1991 "Mast cell numbers and staining characteristics in the normal and allergic conjunctiva", *J. Allergy Clin. Immunol.* Vol. 87, no. 1, pp. 111-116.

Motta A., Peltre G., Dormans J. A. M. A., Withagen C. E. T., Lacroix G., Bois F. & Streerenberg P. A. 2004 "*Phleum pratense* pollen starch granules induce humoral and cell-mediated immune responses in a rat model of allergy", *Clin. Exp. Allergy*, Vol. 34, pp. 310-314.

Mueller H. & Franke W.W. "Biochemical and immunological charaterization of desmoplakins I and II, the major polpeptides of the desmosomal plaque", *J. Mol. Biol.* Vol. 163, no. 4, pp. 647-671.

van Muijen G.N., Ruiter D.J., Franke W.W., Achstatter T., Haasnoot W.H., Ponec M. and Warnaar S.O. 1986 "Cell type heterogeneity of cytokeratin expression in complex epithelia and carcinomas as demonstrated by monoclonal antibodies specific for cytokeratins nos. 4 and 13", *Exp. Cell. Res.* Vol. 162, no. 1, pp. 97-113.

Nagafuchi A. 2001 "Molecular architecture of adherens junctions", *Curr. Opin. Cell Biol.* Vol. 13, pp. 600-603.

Neame S.J. & Isacke C.M. 1993 "The cytoplasmic tail of CD44 is required for basolateral localisation in epithelial MDCK cells but does not mediate association with the detergent-insoluble cytoskeleton of fibroblasts", *J. Cell Biol.* Vol. 121, no. 6, pp. 1299-1310.

Nelson W.G. & Sun T.T. 1983 "The 50- and 58-kdalton keratin classes as molecular markers for stratified squamous epithelia: cell culture studies", *J. Cell Biol.* Vol. 97, no. 1, pp. 244-251.

Neutra M.R., Pringault E & Kraehenbuhl J.P. 1996 "Antigen sampling across epithelial barriers and induction of mucosal immune response", *Annu. Rev. Immunol.* Vol. 14, pp. 275-300.

Nichols B., Dawson C.R. & Togni B. 1983 "Surface features of the conjunctiva and cornea", *Invest. Ophthalmol. Vis. Sci.* Vol. 24, no. 5, pp. 570-576.

Niiya A., Matsumoto Y., Ishibashi T., Matsumoto K & Kinoshita S. 1997 ""Collagen gel-embedding culture of conjunctival epithelial cells", *Graefes. Arch. Clin. Exp. Ophthalmol.* Vol. 235, no. 1, pp. 32-40.

Ninan T.K. & Russell G. 1992 "Respiratory symptoms and atopy in Aberdeen schoolchildren: evidence from two surveys 25 years apart", *BMJ.* Vol. 4, no. 304(6831), pp. 873-875.

Nishimata S., Kato K., Tanaka M., Ijiri R., Toyoda Y., Kigasawa H., Ohama Y., Nakatani Y., Notohara K., Kobayashi Y., Hoire H., Hoshika A. & Tanaka Y. 2005 "Expression pattern of keratin subclasses in pancreatoblastoma with special emphasis on squamoid corpuscles", *Pathol. Int.* Vol. 55, pp. 287-302.

Nomura K. & Takamura E. 1998 "Tear IgE concentrations in allergic conjunctivitis", *Eye.* Vol 12, no. 2, pp. 296-298.

Norrman E., Rosehall L., Nystrom L., Jonsson E. & Stjernberg N. 1994 "Prevalence of positive skin prick tests, allergic asthma, and rhinoconjunctivitis in teenagers in northern Sweden", *Allergy* Vol. 49, no. 10, pp. 808-815.

North A.J., Bardsley W.G., Hyam J., Bornslaeger E.A., Cordingley H.C., Trinnaman B., Hatzfeld M., Green K.J., Magee A.I. & Garrod D.R. 1999 "Molecular map of the desmosomal plaque", *J. Cell Sci.* Vol. 112, pp. 4325-4336.

Nusrat A., Parkos C.A., Verkade P., Foley C.S., Liang T.W., Innis-Whitehouse W., Eastburn K.K. & Madara J.L. 2000 "Tight junctions are membrane microdomains", *J. Cell Sci.* Vol. 113, pt. 10, pp. 1771-1781.

Ogawa C., Iwatsuki H., Sasaki K. & Kumano I. 2001 "Keratin filaments in epithelial cells of the excretory ducts of rabbit submandibular glands—an immunohistochemical and ultraimmunohistochemical study", *Kaibogaku Zasshi*, Vol. 76, no. 4, pp. 389-398.

Ohkawara Y., Yamauchi K., Tanno Y., Tamura G., Ohtani H., Nagura H., Ohkuda K. & Takishmia T. 1992 "Human lung mast cells and pulmonary macrophages produce tumour necrosis factor-alpha in sensitized lung tissue after IgE receptor triggering", *Am. J. Respir. Cell Mol. Biol.* Vol. 7, no. 4, pp. 385-392.

O'Keefe E.J., Erickson H.P. & Bennett V. 1989 "Desmoplakin I and desmoplakin II. Purification and characterization", *J. Biol. Chem.* Vol. 264, no. 14, pp. 8310-8318.

Omary M.B., Ku N.O., Liao J. & Price D. 1998 "Keratin modifications and solubility properties in epithelial cells and in vitro", *Subcell. Biochem.* Vol. 31, pp. 105-140.

Ono S.J. 2000 "Molecular genetics of allergic diseases", *Annu. Rav. Immunol.* Vol 18, pp. 647-366.

Oshima R.G., Baribault H. & Caulin C. 1996 "Oncogenic regulation and function of keratins 8 and 18", *Cancer Metastasis Rev.* Vol. 15, no. 4, pp. 445-471.

Ozawa M., Ringwald M. & Kemler R. 1990 "Uvomorulin-catenin complex formation is regulated by a specific domain in the cytoplasmic region of the cell adhesion molecule", *Proc. Natl. Acad. Sci.* Vol. 87, pp. 4246-4250.

Ozawa M. and Kemler R. 1998 "Altered cell adhesion activity by pervanadate due to the dissociation of α-catenin from the E-cadherin-catenin complex", *J. Biol. Chem.* Vol. 273, no. 11, pp. 6166-6170.

Pasdar M. & Nelson W.J. 1988 "Kinetics of desmosome assembly in Madin-darby canine kidney epithelial cells: temporal and spatial regulation of desmoplakin organisation and stabilisation upon cell-cell contact. I. Biochemical analysis", *J. Cell Biol.* Vol. 106, no. 3, pp. 677-685. (a).

Pasdar M. & Nelson W.J. 1988 "Kinetics of desmosome assembly in Madin-darby canine kidney epithelial cells: temporal and spatial regulation of desmoplakin organisation and stabilisation upon cell-cell contact. II. Morphological analysis", *J. Cell Biol.* Vol. 106, no. 3, pp. 687-695. (b).

Pasdar M., Li Z. & Chan H. 1995 "Desmosome assembly and disassembly are regulated by reversible protein phosphorylation in cultured epithelial cells", *Cell Motil. Cytoskeleton* Vol. 30, no. 2, pp. 108-121.

Petersen A., Grobe K., Schramm G., Vieths S., Altmann F., Schlaak M. & Becker W.M. 1999 "Implications of the grass group I allergens on the sensitization and provocation process", *Int. Arch. Allergy Immunol.* Vol. 118, no. 4, pp. 411-413.

Pfister R.R. 1974 "The normal surface of conjunctiva epithelium. A scanning electron microscopic study", *Invest. Ophthalmol.* Vol. 14, no. 4, pp. 267-279.

Pigott R. & Power C. 1993 "The adhesion molecule facts book". Academic press, Harcourt Brace & Company, Publishers. Pp 6-8, 57-59.

Polosa R., Prosperini G., Leir S.H., Holgate S.T., Lackie P.M. & Davies D.E. 1999 "Expression of c-erbB receptors and ligands in human bronchial mucosa", *Am. J. Respir. Cell Mol.* Vol. 20, no. 5, pp. 914-923.

Porter R.M. & Lane E.B. 2003 "Phenotypes, genotypes and their contribution to understanding keratin function", *Trends in Genetics*, Vol. 19, pp. 278-285.

Pur E. & Cuff C.A. 2001 "A crucial role for CD44 in inflammation", *Trends Mol. Med.* Vol. 7, no. 5, pp. 213-221.

Presland R.B. & Dale B.A. 2000 "Epithelial structural proteins of the skin and oral cavity: function in health and disease", *Crit. Rev. Oral. Biol. Med.* Vol. 11, no. 4, pp. 383-408.

Presland R.B., Kuechle M.K., Lewis S.P., Fleckman P. & Dale B.A. 2001 "Regulated expression of human filaggrin in keratinocytes results in cytoskeletal disruption, loss of cell-cell adhesion and cell cycle arrest", *Exp. Cell Res.* Vol. 270, no. 2, pp. 199-213.

Presland R.B. & Jurevic R.J. 2002 "Making sense of epithelial barrier: What molecular biology and genetics tell us about the functions of oral mucosal and epidermal tissues", *J. Dent. Educ.* Vol. 66, no. 4, pp. 564-574.

Quinlan R.A., Schiller D.L., Hatzfeld M., Achtstatter T., Moll R., Jorcano J.L., Magin T.M. & Franke W.W. 1985 "Patterns of expression and organisation of cytokeratin intermediate filaments", *Ann. N. Y. Acad. Sci.* Vol. 455, pp. 585-306.

Quinlan M.P. and Hyatt J.L. 1999 "Establishment of the circumferential actin filament network is a prerequisite for the localisation of the cadherin-catenin complex in epithelial cells", *Cell Growth Differ.* Vol. 10, pp. 839-854.

Raviola G. 1983 "Conjunctival and episcleral blood vessels are permeable to blood-borne horseradish peroxidase", *Invest. Ophthalmol. Vis. Sci.* Vol. 24, no. 6, pp. 725-736.

Reischl I.G., Coward W.R. & Church M.K. 1999 "Molecular consequences of human mast cell activation following immunoglobulin E-high-affinity immunoglobulin E receptor (IgE-FcεRI) interaction", *Biochem. Pharm.* Vol. 58, pp. 1841-1850.

Reisinger J., triendl A., Kuchler E., Bohle B., Krauth M.T., Rauter I., Valent P., Koeing F., Valenta R. & Niederberger V. 2005 "IFN-gamma-enhanced allergen penetration across respiratory epithelium augments allergic inflammation", *J. Allergy Clin Immunol.* Vol. 115, no. 5, pp. 973-981.

Renard G., Pouliquen Y. & Savoldelli M. 1980 "Epithelial invasion of the anterior chamber: exploration by scanning electron microscopy", *J. Fr. Ophthalmol.* Vol. 3, no. 10, pp. 571-578.

Ring J. 1997 "Allergy and modern society: Does 'western life style' promote the development of allergies", *Int. Arch. Allergy Immunol.* Vol. 113, pp. 7-10.

Risse Marsh B.C., Massaro-Giodano M., Marshall C.M., Lavker R.M. & Jensen P.J. 2002 "Initiation and characterization of keratinocyte cultures from biopsies of normal human conjunctiva", *Exp. Eye Res.* Vol. 74, pp. 61-69.

Roat M.I., Ohji M., Hunt L.E. & Thoft R.A. 1993 "Conjunctival epithelial cell hypermitosis and goblet cell hyperplasia in atopic keratoconjunctivitis", *Am. J. Ophthalmol.* Vol. 116, no. 4, pp. 456-463.

Roche N., Chinet T.C. & Huchon G.J. 1997 "Allergic and non-allergic interactions between house dust mite allergens and airway mucosa", *Eur. Respir. J.* Vol. 10, pp. 719-726.

Rubinstein N. & Stanely J.R. 1987 "Pemphigus foliaceus antibodies and a monoclonal antibody to desmoglein I demonstrates stratified squamous epithelial-specific epitopes of desmosomes", *Am. J. Dermatopathol.* Vol. 9, no. 6, pp. 510-514.

Ryder M.I. & Weinreb R.N. 1990 "Cytokeratin patterns in corneal, limbal and conjunctival epithelium. An immunofluorescence study with PKK-1, 8.12, 8.60 and 4.62 anticytokeratin antibodies", *Invest. Ophthalmol Vis Sci.* Vol. 31, no. 11, pp. 2230-2240.

Ryeom S.W., Paul D. & Goodenough D.A. 2000 "Truncation mutants of the tight junction protein ZO-1 disrupt corneal epithelial cell morphology", *Mol. Biol. Cell* Vol. 11, no. 5, pp. 1687-169.

Saha C., Nigam S.K. & Denker B.M. 2001 "Expanding roles of G proteins in tight junction regulation: Galpha(s) stimulates TJ assembly", *Biochem. Biophys. Res. Commun.* Vol. 285, no. 2, pp. 250-256.

Sanderson R.D. and Bernfield M. 1988 "Molecular polymorphism of a cell surface proteoglycan: distinct structures on simple and stratified epithelia", *Proc. Natl. Acad. Sci.* Vol. 85, no. 24, pp. 9562-9566.

Savani R.C. & Turley E.A. 1995 "The role of hyaluronan and its receptor in restenosis after balloon angioplasty: development of a potential treatment", *Int. J. Tissue React.* Vol. 17, no. 4, pp. 141-151.

Schulz O., Sewell H.F. & Shakib F. 1998 "A sensitive fluorescent assay for measuring the cysteine protease activity of Der p1, a major allergen from the dust mite *Dermatophagoides pteronyssinus*", *J. Clin. Pathol: Mol. Pathol.* Vol. 51, pp. 222-231.

Schulz O., Sutton B.J., Beavil R.L., Shi J., Sewell H.F., Gould H.J., Laing P. & Shakib F. 1997 "Cleavage of the low-affinity receptor for human IgE (CD23) by a mite cysteine protease: nature of the cleaved fragment in relation to the structure and function of CD23", *Eur. J. Immunol.* Vol. 27, no. 3, pp. 584-588.

Schulz O., Laing P., Sewell H.F. & Shakib F. 1995 "Der p I, a major allergen of the house dust mite, proteolyically cleaves the low-affinity receptors for human IgE (CD23)", *Eur. J. Immunol.* Vol. 25, no. 11, pp. 3191-3194.

Schwartz L.B. & Austen K.F. 1984 "Structure and function of the chemical mediators of mast cells", *Prog. Allergy.* Vol. 34, pp. 271-321.

Scott R.A.H., Lauweryns B., Snead D.M.J., Haynes R.J., Mahida Y. & Dua H.S. 1997 "E-cadherin distribution and epithelial basement membrane characteristics of normal human conjunctiva and cornea", *Eye* Vol. 11, Pt. 5, pp. 607-12.

Scott R.A.H., Dua H.S., Joseph A., Haynes R., Snead D & Hand N.M. 2002 "E-Cadherin distribution in normal and dysplastic conjunctival epithelium", *Eye* Vol. 16, pp. 198-200.

Shen J., Taylor N., Duncan L., Kovesdi I., Bruder J.T., Forrester J.V. & Dick A.D. 2001 "Ex-vivo mediated gene transfection of human conjunctival epithelium", *Br. J. Ophthalmol.* Vol. 85, pp. 861-867.

Sheu H.M., Kitajima Y. & Yaoita H. 1989 "Involvement of protein kinase C in translocation of desmoplakins from cytosol to plasma membrane during desmosome formation in human squamous cell carcinoma grown in low to normal calcium concentration", *Exp. Cell Res.* Vol. 185, no. 1, pp. 176-190.

Simon B., Podolsky D.K., Moldenhauer G., Isselbacher K.J., Gattoni-Celli S. & Brand S.J. 1990 "Epithelial glycoprotein is a member of a family of epithelial cell surface antigens homologous to nidogen, a matrix adhesion protein", *Proc. Natl. Acad. Sci.* Vol. 87, pp. 2755-2579.

Sly R.M. 1999 "Changing prevalence of allergic rhinitis and asthma", *Ann. Allergy Asthma Immunol.* Vol. 82, no. 3, pp. 233-248.

Stacey G. 2001 "Primary cell cultures and immortal cell lines", Encyclopaedia of Life Sciences, Nature Publishing Group, http://els.net

Stefanovic L., Bogic M., Balaban J., Mitrovic O., Stosovic R. & Andrejevic S. 1998 "The role of endothelial cells in allergic inflammation reactions", *Srp. Arh. Celok. Lek.* Vol. 126, no. 3-4, pp. 138-144.

Steuhl K.P. & Knorr M. 1990 "The second, mucus-secreting system of the conjunctiva. Ultrastructural findings", *Fortschr. Ophthalmol.* Vol. 87, no. 2, pp. 492-496.

Stewart M. 1993 "Intermediate filament structure and assembly", *Curr. Opin. Cell Biol.* Vol. 5, no. 1, pp. 3-11.

Suck R., Hagen S., Cromwell O. & Fiebig H. 1999 "Rapid and efficient purification of *Phleum pratense* major allergens Phl p 1 and group Phl p 2/3 using a two-step procedure", *J. Immunol. Methods* Vol. 229, pp. 73-80.

Sun T.T. and Green H. 1977 "Cultured epithelial cells of cornea, conjunctiva and skin: absence of marked intrinsic divergence of their differentiated states", *Nature* Vol. 269, no. 5628, pp. 489-493.

Sun T.T., Eichner R., Nelson W.G., Tseng S.C.G., Weiss R.A., Jarvinen M. & Woodcoock-Mitchell J. 1983 "Keratin classes: Molecular markers for different types of epithelial differentiation", *J. Invest. Dermatol.* Vol. 81, Suppl. 1, pp. 109s-115s.

Sun T-T., Tseng S.C.G., Huang A.J.W., Cooper D., Schermer A., Lynch M.H., Weiss R.A. & Eichner R. 1985 "Monoclonal antibody studies of mammalian epithelial keratins: A review", *Ann. N.Y. Acad. Sci.* Vol. 455, pp. 307-329.

Takada M., Yamamoto M. & Saitoh Y. 1994 "The significance of CD44 in human pancreatic cancer: II. The role of CD44 in human pancreatic adenocarcinomas invasion", *Pancreas.* Vol. 9, no. 6, pp. 753-757.

Thie M., Fuchs P., Butz S., Sieckmann F., Hoschutzky H., Kemler R. & Denker H.W. 1996 "Adhesiveness of the apical surface of uterine epithelial cells: the role of junctional complex integrity", *Eur. J Cell Biol.*, vol. 70, no. 3, pp. 221-232.

Toivola D.M., Ku N.O., Ghori N., Lowe A.W., Michie S.A. & Omary M.B. 2000 "Effects of keratin filament disruption on exocrine pancreas-stimulated secretion and susceptibility to injury", *Exp. Cell. Res.* Vol. 15, no. 255/2, pp. 156-170.

Tomic-Canic M., Komine M., Freedberg I.M. & Blumenberg M. 1998 "Epidermal signal transduction and transcription factor activation in activated keratinocytes", *J. Dermatol. Sci.* Vol. 17, pp. 167-181.

Toole B.P. 1990 "Hyaluronan and its binding proteins, the hyaladherins", *Curr. Opin. Cell. Biol.* Vol. 2, pp. 839-844.

Tovey E.R., Chapman M.D. & Platts-Mills T.A.E. "Mite faeces are a major source of house dust allergens", *Nature* Vol. 289, pp. 592-593.

Trejdosiewicz L.K., Trejdosiewicz A.J., Ling N.R. & Dykes P.W. 1979 "Growth enhancing property of human monocytes from normal donors and cancer patients", *Immunology*, vol. 37, no. 1, pp. 247-252.

Tsai R.J., Ho Y.S. & Chen J.K. 1994 "The effects of fibroblasts on the growth and differentiation of human bulbar conjunctival epithelial cells in an in vitro conjunctival equivalent", *Invest. Ophthalmol. Vis. Sci.* Vol. 35, no. 6, pp. 2865-2875.

Twell D. 2001 "Pollen: Structure, Development and Function" Encyclopaedia of Life Sciences, Nature Publishing Group, http://els.net

Underhill C. 1992" CD44: The hyaluronan receptor", *J. Cell Sci.* Vol. 103, pp. 293-298.

Vrtala S., Grote M., Duchene M., van Ree K., Kraft D., Scheiner O. & Valenta R., 1993 "Properties of tree and grass pollen allergens: reinvestigation of the linkage between solubility and allergenicity", *Int. Arch. Allergy Immunol.* Vol. 102, no. 2, pp. 160-169.

Walsh S.V., Hopkins A.M., Chen J., Narumiya S., Parkos C.A. & Nusrat A. 2001 "Rho kinase regulates tight junction function and is necessary for tight junction assembly in polarized intestinal epithelia", *Gastroenterology* Vol. 121, no. 3, pp. 566-579.

Walsh S.V., Hopkins A.M. & Nusrat A. 2000 "Modulation of tight junction structure and function by cytokines", *Adv. Drug Del. Rev.* Vol. 14, pp. 303-313.

Waseem A., Alam Y., Dogan B., White K.N., Leigh I.M. & Waseem N.H. 1998 "Isolation, sequence and expression of the gene encoding human keratin 13", *Gene* Vol. 215, pp. 269-279.

Watanabe H., Fabricant M., Tisdale A.S., Spurr-Michaud S.J., Lindberg K. & Gipson I.K. 1995 "Human corneal and conjunctival epithelia produces a mucin-like glycoprotein for the apical surface", *Invest. Ophthalmol. Vis. Sci.* Vol. 36, no. 2, pp. 337-344.

Wan H., Winton H.L., Soeller C., Taylor G.W., Gruenert D.C., Thompson P.J., Cannell M.B., Stewart G.A., Garrod D.R. & Robinson C. 2001 "The transmembrane protein occludin of epithelial tight junctions is a functional target for serine peptidases from faecal pellets of *Dermatophagoides pteronyssinus*", *Clin. Exp. Allergy* Vol. 31, no. 2, pp. 279-294.

Wan H., Winton H.L., Soeller C., Gruenert D.C., Thompson P.J., Cannell M.B., Stewart G.A., Garrod D.R. & Robinson C. 2000 "Quantitative structural and biochemical analyses of tight junction dynamics following exposure of epithelial cells to house dust mite allergen Der p1", *Clin. Exp. Allergy* Vol. 30, no. 5, pp. 685-698.

Wan H., Winton H.L., Soeller C., Stewart G.A., Thompson P.J., Gruenert D.C., Cannell M.B., Garrod D.R. & Robinson C. 2000 "Tight junction properties of the immortalized human bronchial epithelial cell lines Calu-3 and 16HBE 14o-", *Eur. Respir. J.* Vol. 15, no. 6, pp. 1058-1068.

Wan H., Winton H.L., Soeller C., Tovey E.R., Gruenert D.C., Thompson P.J., Stewart G.A., Taylor G.W., Garrod D.R., Cannell M.B. & Robinson C. 1999 "Der p1 facilitates transepithelial allergen delivery by disruption of tight junctions", *J. Clin. Invest.* Vol. 104, no. 1, pp. 123-133.

Weaver E.J., McCue P.A., Bagley D.H., Kovatich A.J. & Bibbo M. 2001 "Expression of cytokeratin 20 and CD44 protein in upper urinary tract transitional cell carcinoma: cytologic-hitsologic correlation", *Anal. Quant. Cytol. Histol.* Vol. 23, no. 5, pp. 339-344.

Wei Z.G., Cotsarelis G., Sun T.T. & Lavker R.M. 1995 "Label-retaining cells are preferentially located in fornical epithelium: implications on conjunctival epithelial homeostasis", *Invest. Ophthalmol. Vis. Sci.* Vol. 36, No. 1, pp. 236-246.

Weyrauch K.D. 1983 "The conjunctival epithelium in the domestic ruminants. I. Lightmicroscopic investigations", *Z. Mikrosk. Anat. Forsch.* Vol. 97 No. 4, pp. 565-572.

Weyrauch K.D. 1983 "The conjunctival epithelium in the domestic ruminants. II. Electronmicroscopic investigations", *Z. Mikrosk. Anat. Forsch.* Vol. 97 No. 4, pp. 573-588.

Weyrauch K.D. 1984 "The surface of the conjunctiva in domestic ruminants. A scanning electron microscopic investigation", *Acta. Anat. (Basel).* Vol. 119, no. 1, pp. 27-32.

Whitlock N.V., Eady R.A.J. & McGrath J.A. 2000 "Genomic organisation and amplification of the human keratin 15 and keratin 19 genes", *Biochem. Biophys. Res. Comm.* Vol. 267 pp. 462-465.

Widelitz R. 2005 "Wnt signalling through canonical and non-canonical pathways: Recent progress", *Growth Factors* Vol. 23, no. 2, pp. 111-116.

Wilson A.K., Colulombe P.A. & Fuchs E. 1992 "The roles of K5 and K14 head, tail, and R/K L L E G E domains in keratin filament assembly *in vitro*", *J. Cell Biol.* Vol. 119, no. 2, pp. 401-414.

Winton H.L., Wan H., Cannell M.B., Gruenert D.C., Thompson P.J., Garrod D.R., Stewart G.A. & Robinson C. 1998 "Cell lines of pulmonary and non-pulmonary origin as tools to study the effects of house dust mite proteinases on the regulation of epithelial permeability", *Clin. Exp. Allergy* Vol. 28, pp. 1273-1285.

Winton H.L., Wan H., Cannell M.B., Thompson P.J., Garrod D.R., Stewart G.A. & Robinson C. 1998 "Class specific inhibition of house dust mite proteinase which cleave cell adhesion, induce cell death and which increase the permeability of lung epithelium", *Br. J. Pharmacol.* Vol. 124, no. 6, pp. 1048-1059.

Winkel G.K., Ferguson J.E., Takeichi M. & Nuccitelli R. 1990 "Activation of protein kinase C triggers premature compaction in the four-cell stage mouse embryo", *Dev. Biol.* Vol. 138, no. 1, pp. 1-15.

Woolcock A.J. & Peat J.K. 1997 "Evidence for the increase in asthma worldwide", *Ciba Found. Symp.* Vol. 206, pp. 122-134.

Wüthrich R.P. 1999 "The proinflammatory role of hyaluronan – CD44 interactions in renal injury", *Nephrol. Dial. Transplant*; Vol. 14, pp. 2554-2556.

Yamano T., Shimada M., Okada S., Yutaka T., Yabuuchi H. & Nakao Y. 1979 "Electron microscopic examination of skin and conjunctival biopsy specimens in neuronal storage diseases", *Brain Dev.* Vol. 1, no. 1, pp. 16-25.

Youakim A and Ahdieh M. 1999 "Interferon-gamma decreases barrier function in T84 cells by reducing ZO-1 levels and disrupting apical actin", *Am. J. Physiol.* Vol. 276, no. 5, pt. 1, G1279-1288.

Zanbner J., Winter M., Excoffon K.J., Stoltz D., Ries D., Shasby S. & Shasby M. 2003 "Histamine alters E-cadherin cell adhesion to increase human airway epithelial permeability", *J. Appl. Physiol.* Vol. 95, no. 1, pp. 394-401.

Zahraoui A., Joberty G., Arpin M., Fontaine J.J., Hellio R., Tavitian A. & Louvard D. 1994 "A small rab GTPase is distributed in cytoplasmic vesicles in non polarized cells but colocalizes with the tight junction marker ZO-1 in polarized epithelial cells", *J. Cell Biol.* Vol. 124, nos. 1-2, pp. 101-115.

Zhan H., Towler H.M.A.T. & Calder V.L. 2003, "The immunomodulatory role of the human conjunctival epithelial cells", *Invest. Ophthalmol. Vis. Sci.* Vol. 44, no. 9, pp. 3906-3910.

Zhang S., Anderson D.F., Bradding P., Coward W.R., Baddeley S.M., MacLeod J.D., McGill J.I., Church M.K., Holgate S.T. & Roche W.R. 1998 "Human mast cells express stem cell factor", *J. Pathol.* Vol. 186, no. 1, pp. 59-66.

Zhang M., Liu Z. & Xie Y. 2000 "The study on the expression of keratin proteins in pterygial epithelium", *Yan Ke Xue Bao*, Vol. 16, no. 1, pp. 48-52.

# Appendices

## A. Patient details.

**GMA embedded biopsies**

Control samples

| Code | Age / DOB | Sex | Biopsy date |
|---|---|---|---|
| 63 | 63 | F | 19/08/1993 |
| 64 | 90 | M | 19/08/1993 |
| 91 | 72 | M | 06/10/1994 |
| 100 | 51 | F | 09/01/1995 |
| 101 | 91 | F | 20/02/1995 |
| 102 | 50 | F | 06/03/1995 |
| 103 | 67 | F | 16/03/1995 |
| 104 | 77 | F | 16/03/1995 |
| 105 | 73 | F | 11/05/1995 |
| 110 | 82 | F | 14/06/1995 |
| 112 | 75 | M | 21/06/1995 |
| 114 | 74 | M | 21/09/1995 |
| 115 | 80 | F | 21/06/1995 |
| 116 | 89 | F | 23/06/1995 |
| 117 | 79 | M | 23/06/1995 |
| 121 | 26 | F | 03/08/1995 |
| 122 | 48 | F | 02/08/1995 |
| 0.00041 | - | M | - |
| 0.01003 | - | - | - |
| 0.02001 | - | M | 28/02/2002 |
| 0.02002 | - | M | 28/02/2002 |
| 0.02028 | 62 | F | 17/09/2002 |
| 0.02031 | 73 | M | 15/10/2002 |
| 0.02032 | 86 | M | 15/10/2002 |
| 0.02034 | 83 | M | 24/10/2002 |
| 0.02035 | 22 | F | 24/10/2002 |

SACq samples

| | | | |
|---|---|---|---|
| 31 | 59 | M | 27/07/1991 |
| 45 | 27 | F | 10/02/1992 |
| 47 | 28 | F | 10/02/1992 |
| 53 | 46 | M | 24/02/1992 |
| 65 | 70 | M | 12/01/1994 |
| 66 | 24 | M | 12/01/1994 |
| 67 | 71 | F | 20/01/1994 |
| 69 | 38 | F | 26/01/1994 |
| 70 | 19 | M | 26/01/1994 |
| 0.02027 | 65 | M | 10/09/2002 |
| 0.02044 | 23 | M | 21/11/2002 |
| 0.02043 | 31 | M | 21/11/2002 |

SACa samples

| | | | |
|---|---|---|---|
| 11C | 55 | M | 23/04/1991 |
| 24A | - | F | 20/05/1991 |
| 27A | - | M | 20/05/1991 |
| 28A | - | - | 03/06/1991 |
| 79 | 68 | F | 01/06/1994 |
| 81 | 28 | M | 13/07/1994 |
| 82 | 28 | M | 02/06/1994 |
| 83 | 72 | M | 02/06/1994 |
| 84 | 58 | F | 15/06/1994 |
| 85 | 79 | M | 15/06/1994 |
| 86 | 44 | M | 16/06/1995 |

Primary culture

| Code | Age / DOB | Sex | Biopsy date |
|---|---|---|---|
| Overnight SEU | | | |
| 02/003 | 80 | M | 30/05/2002 |
| 02/004 | 70 | F | 30/05/2002 |
| 02/005 | 66 | F | 30/05/2002 |
| 02/006 | 77 | F | 30/05/2002 |
| 02/007 | 70 | M | 30/05/2002 |
| 02/008 | 84 | F | 30/05/2002 |
| 02/009 | 85 | F | 30/05/2002 |
| 02/010 | 27 | M | 30/05/2002 |
| 02/011 | 68 | F | 30/05/2002 |
| 02/012 | 70 | M | 30/05/2002 |
| 02/013 | 57 | M | 30/05/2002 |
| 02/014 | 79 | M | 30/05/2002 |
| 02/015 | 79 | F | 09/07/2002 |
| 02/016 | 39 | F | 09/07/2002 |
| 02/017 | 55 | F | 09/07/2002 |
| 02/018 | 85 | M | 30/07/2002 |
| 02/019 | 83 | F | 06/08/2002 |
| 02/020 | 60 | M | 13/08/2002 |
| 02/021 | 77 | M | 13/08/2002 |
| 02/022 | 55 | M | 20/08/2002 |
| 02/023 | 82 | M | 27/08/2002 |
| 02/024 | 73 | F | 27/08/2002 |
| Mediums | | | |
| 02/025 | 57 | M | 29/08/2002 |
| 02/026 | 65 | M | 29/08/2002 |
| 02/027 | 65 | M | 10/09/2002 |
| 02/028 | 62 | F | 17/09/2002 |
| 02/029 | 63 | F | 01/10/2002 |
| 02/030 | 66 | F | 01/10/2002 |
| 02/031 | 73 | M | 15/10/2002 |
| 02/032 | 86 | M | 15/10/2002 |
| 02/033 | 74 | M | 22/10/2002 |
| 02/038 | 74 | M | 05/11/2002 |
| 02/039 | 70 | M | 05/11/2002 |
| 02/040 | 70 | M | 05/11/2002 |
| 02/045 | 91 | M | 26/11/2002 |
| 02/046 | 70 | M | 05/12/2002 |

| | | | |
|---|---|---|---|
| 02/047 | 79 | M | 05/12/2002 |
| 02/048 | 56 | M | 05/12/2002 |
| 02/049 | 71 | F | 10/12/2002 |
| 03/001 | 52 | F | 07/01/2003 |
| 03/002 | 70 | F | 07/01/2003 |
| 03/003 | 81 | F | 07/01/2003 |
| 03/004 | 87 | F | 14/01/2003 |
| 03/005 | 88 | M | 14/01/2003 |
| 03/006 | 44 | M | 16/01/2003 |
| 03/007 | 89 | F | 16/01/2003 |
| 03/008 | 73 | M | 21/01/2003 |
| 03/009 | 72 | M | 21/01/2003 |
| 03/010 | 72 | F | 28/01/2003 |
| 03/011 | 54 | M | 28/01/2003 |
| 03/012 | 34 | F | 30/01/2003 |
| 03/013 | 36 | F | 30/01/2003 |
| 03/014 | 68 | F | 30/01/2003 |
| 03/015 | 69 | M | 04/03/2003 |
| 03/016 | 74 | M | 04/03/2003 |
| 03/017 | 83 | F | 11/03/2003 |
| 03/018 | 50 | M | 18/03/2003 |
| 03/019 | 49 | F | 01/04/2003 |
| 03/020 | 70 | F | 08/04/2003 |
| 03/021 | 83 | M | 10/04/2003 |
| 03/022 | 88 | M | 10/04/2003 |
| 03/023 | 48 | M | 22/04/2003 |
| BEGM | | | |
| 03/024 | 59 | M | 29/04/2003 |
| 03/025 | 76 | F | 13/05/2003 |
| 03/026 | 77 | F | 03/06/2003 |
| 03/028 | 42 | M | 15/07/2003 |
| 03/029 | 74 | F | 15/07/2003 |
| 03/030 | 77 | M | 04/11/2003 |
| M199 | | | |
| 03/031 | 75 | M | 04/11/2003 |
| 03/032 | 63 | M | 18/11/2003 |
| 03/033 | 81 | F | 25/11/2003 |
| 03/034 | 72 | F | 27/11/2003 |
| 03/035 | 71 | M | 27/11/2003 |
| 03/036 | 87 | F | 04/12/2003 |
| 03/037 | 73 | M | 04/12/2003 |
| 04/001 | 72 | F | 06/01/2004 |
| 04/002 | 56 | M | 06/01/2004 |
| 04/003 | 47 | M | 08/01/2004 |
| 04/004 | 58 | F | 27/01/2004 |
| 04/005 | 72 | M | 29/01/2004 |
| 04/006 | 55 | M | 29/01/2004 |
| 04/007 | 72 | M | 29/01/2004 |
| 04/008 | 44 | M | 03/02/2004 |
| 04/009 | 52 | M | 03/02/2004 |
| 04/010 | 59 | F | 03/02/2004 |
| 04/012 | 47 | M | 12/07/2004 |

| | | | |
|---|---|---|---|
| 04/013 | 66 | M | 10/08/2004 |
| 04/014 | 63 | M | 10/08/2004 |

Allergen challenged

| | | | |
|---|---|---|---|
| 40 | - | M | 28/01/1992 |
| 54 | - | M | 24/02/1992 |
| 71 | 30/03/1936 | M | 09/03/1994 |
| 72 | 25/06/1960 | M | 09/03/1994 |

Samples were stored airtight at -20°C.

# B. Solutions

Piperazine (PIPES) buffer

| | |
|---|---|
| Piperazine-NN'-bis-2-ethanesulphonic acid (PIPES) | 60.48g |
| Sodium hydroxide (NaOH) (10mM) | |

- Mix piperazine with 900ml of distilled water,
- Add NaOH up to pH 7.2,
- Make up to 1 litre with distilled water to produce a 0.2M solution.

Phosphate-buffered saline (PBS)

| | |
|---|---|
| $NaH_2PO_4$ (anhydrous) (1.9mM) | 0.23g |
| $Na_2HPO_4$ (anhydrous) (8.1mM) | 1.15g |
| NaCl (154mM) | 9.00g |

- Mix with 900ml distilled water,
- Adjust pH to 7.2 using 1M NaOH or 1M HCl,
- Make up to 1 litre.

Formaldehyde fixative solution

| | |
|---|---|
| Paraformaldehyde | 4g |
| Glutaraldehyde | 3g |

- Add to 100ml of PBS/PIPES,
- Warm to 60-70°C,
- Cool to room temperature,
- Adjust pH to 7.2,
- Filter and store ready to use within two weeks.

Mowiol mounting solution with Citifluor

| | |
|---|---|
| Mowiol | 20g |
| Citifluor | One tablet |

- Mix with 80ml PBS,
- Warm to 60°C,
- Add 40ml of glycerol and mix for 8 hours,
- Centrifuge at 12,000 rpm for 15 minutes,
- Store at 4°C,
- For Citifluor dissolve tablet in 300$\mu$l then add to mixture after glycerol step.

# C. Statistical results

Chapter Five – allergen challenge of the *in vitro* epithelial cell model. Each of the treatments are represented by two columns down the page. Each value at each time point was tested against the value at zero hours. (zero versus 1, 2, 4, 6, 12 and 24 hours (six rows across)).

Statistics for the ChWk allergen challenge studies. Figure 5.7.

| t-Test: Paired Two Sample for means | phl p | | con | | phl p + his | | pro | | phl p + in | |
|---|---|---|---|---|---|---|---|---|---|---|
| | *zero* | *1 hr* | *zero* | *1 hr* | *Variable 1* | *Variable 2* | *Variable 1* | *Variable 2* | *Variable 1* | *Variable 2* |
| Mean | 371.6875 | 359.1875 | 383 | 387.625 | 378.125 | 371.625 | 367.875 | 322 | 371.375 | 390.625 |
| Variance | 324.89583 | 191.3625 | 139.42857 | 19.410714 | 158.125 | 35.410714 | 470.98214 | 39.428571 | 157.69643 | 29.410714 |
| Observations | 16 | 16 | 8 | 8 | 8 | 8 | 8 | 8 | 8 | 8 |
| Pearson Correlation | 0.775081 | | 0.730444 | | -0.321926 | | 0.7642259 | | 0.356867 | |
| Hypothesized Mean Difference | 0 | | 0 | | 0 | | 0 | | 0 | |
| df | 15 | | 7 | | 7 | | 7 | | 7 | |
| t Stat | 4.3897948 | | -1.437271 | | 1.1825164 | | 7.4649644 | | -4.626482 | |
| P(T<=t) one-tail | 0.0002638 | | 0.0968983 | | 0.1378027 | | 7.071E-05 | | 0.0012038 | |
| t Critical one-tail | 1.753051 | | 1.8945775 | | 1.8945775 | | 1.8945775 | | 1.8945775 | |
| P(T<=t) two-tail | 0.0005276 | | 0.1937967 | | 0.2756054 | | 0.0001414 | | 0.0024077 | |
| t Critical two-tail | 2.1314509 | | 2.3646226 | | 2.3646226 | | 2.3646226 | | 2.3646226 | |

| | *zero* | *2 hr* | *Variable 1* | *Variable 2* | *Variable 1* | *Variable 2* | *Variable 1* | *Variable 2* | *Variable 1* | *Variable 2* |
|---|---|---|---|---|---|---|---|---|---|---|
| Mean | 371.6875 | 347.625 | 383 | 388 | 378.125 | 351.625 | 367.875 | 300.75 | 371.375 | 373.25 |
| Variance | 324.89583 | 41.716667 | 139.42857 | 18 | 158.125 | 82.839286 | 470.98214 | 44.214286 | 157.69643 | 57.928571 |
| Observations | 16 | 16 | 8 | 8 | 8 | 8 | 8 | 8 | 8 | 8 |
| Pearson Correlation | 0.3465189 | | 0.1767997 | | -0.235441 | | 0.6570871 | | 0.2425098 | |
| Hypothesized Mean Difference | 0 | | 0 | | 0 | | 0 | | 0 | |
| df | 15 | | 7 | | 7 | | 7 | | 7 | |
| t Stat | 5.6920867 | | -1.19645 | | 4.365008 | | 10.522479 | | -0.407623 | |
| P(T<=t) one-tail | 2.135E-05 | | 0.135234 | | 0.001647 | | 7.639E-06 | | 0.3478642 | |
| t Critical one-tail | 1.753051 | | 1.8945775 | | 1.8945775 | | 1.8945775 | | 1.8945775 | |
| P(T<=t) two-tail | 4.27E-05 | | 0.2704679 | | 0.003294 | | 1.528E-05 | | 0.6957284 | |
| t Critical two-tail | 2.1314509 | | 2.3646226 | | 2.3646226 | | 2.3646226 | | 2.3646226 | |

| | *zero* | *4 hr* | *Variable 1* | *Variable 2* | *Variable 1* | *Variable 2* | *Variable 1* | *Variable 2* | *Variable 1* | *Variable 2* |
|---|---|---|---|---|---|---|---|---|---|---|
| Mean | 371.6875 | 341.4375 | 383 | 390.125 | 378.125 | 357.25 | 367.875 | 318 | 371.375 | 409.625 |
| Variance | 324.89583 | 85.4625 | 139.42857 | 161.83929 | 158.125 | 31.071429 | 470.98214 | 22.857143 | 157.69643 | 42.553571 |
| Observations | 16 | 16 | 8 | 8 | 8 | 8 | 8 | 8 | 8 | 8 |
| Pearson Correlation | 0.4725717 | | 0.1350431 | | -0.114642 | | 0.6071938 | | 0.1955354 | |
| Hypothesized Mean Difference | 0 | | 0 | | 0 | | 0 | | 0 | |
| df | 15 | | 7 | | 7 | | 7 | | 7 | |
| t Stat | 7.6092101 | | -1.248137 | | 4.1210796 | | 7.3552738 | | -8.341516 | |
| P(T<=t) one-tail | 7.934E-07 | | 0.1260546 | | 0.0022268 | | 7.761E-05 | | 3.486E-05 | |
| t Critical one-tail | 1.753051 | | 1.8945775 | | 1.8945775 | | 1.8945775 | | 1.8945775 | |
| P(T<=t) two-tail | 1.587E-06 | | 0.2521093 | | 0.0044535 | | 0.0001552 | | 6.973E-05 | |

| | | | | | | | | | | |
|---|---|---|---|---|---|---|---|---|---|---|
| t Critical two-tail | 2.1314509 | | 2.3646226 | | 2.3646226 | | 2.3646226 | | 2.3646226 | |

| | *zero* | *6 hr* | *Variable 1* | *Variable 2* | *Variable 1* | *Variable 2* | *Variable 1* | *Variable 2* | *Variable 1* | *Variable 2* |
|---|---|---|---|---|---|---|---|---|---|---|
| Mean | 371.6875 | 333.125 | 383 | 386.75 | 378.125 | 340.125 | 367.875 | 302.25 | 371.375 | 389.125 |
| Variance | 324.89583 | 189.58333 | 139.42857 | 7.3571429 | 158.125 | 20.982143 | 470.98214 | 48.214286 | 157.69643 | 26.410714 |
| Observations | 16 | 16 | 8 | 8 | 8 | 8 | 8 | 8 | 8 | 8 |
| Pearson Correlation | 0.6625821 | | 0.7850262 | | -0.211122 | | 0.6477263 | | -0.304095 | |
| Hypothesized Mean Difference | 0 | | 0 | | 0 | | 0 | | 0 | |
| df | 15 | | 7 | | 7 | | 7 | | 7 | |
| t Stat | 11.322467 | | -1.079724 | | 7.5356829 | | 10.312258 | | -3.359259 | |
| P(T<=t) one-tail | 4.763E-09 | | 0.1580284 | | 6.663E-05 | | 8.731E-06 | | 0.0060483 | |
| t Critical one-tail | 1.753051 | | 1.8945775 | | 1.8945775 | | 1.8945775 | | 1.8945775 | |
| P(T<=t) two-tail | 9.526E-09 | | 0.3160569 | | 0.0001333 | | 1.746E-05 | | 0.0120966 | |
| t Critical two-tail | 2.1314509 | | 2.3646226 | | 2.3646226 | | 2.3646226 | | 2.3646226 | |

| | *zero* | *12 hr* | *Variable 1* | *Variable 2* | *Variable 1* | *Variable 2* | *Variable 1* | *Variable 2* | *Variable 1* | *Variable 2* |
|---|---|---|---|---|---|---|---|---|---|---|
| Mean | 371.6875 | 352.0625 | 383 | 383.25 | 378.125 | 360.875 | 367.875 | 325.125 | 371.375 | 380.125 |
| Variance | 324.89583 | 100.32917 | 139.42857 | 11.357143 | 158.125 | 4.4107143 | 470.98214 | 46.125 | 157.69643 | 193.83929 |
| Observations | 16 | 16 | 8 | 8 | 8 | 8 | 8 | 8 | 8 | 8 |
| Pearson Correlation | 0.5787336 | | -0.506187 | | 0.2386887 | | -0.166588 | | 0.1500382 | |
| Hypothesized Mean Difference | 0 | | 0 | | 0 | | 0 | | 0 | |
| df | 15 | | 7 | | 7 | | 7 | | 7 | |
| t Stat | 5.3381601 | | -0.051155 | | 3.9846657 | | 5.0814856 | | -1.431086 | |
| P(T<=t) one-tail | 4.141E-05 | | 0.4803156 | | 0.0026462 | | 0.0007143 | | 0.0977481 | |
| t Critical one-tail | 1.753051 | | 1.8945775 | | 1.8945775 | | 1.8945775 | | 1.8945775 | |
| P(T<=t) two-tail | 8.283E-05 | | 0.9606312 | | 0.0052923 | | 0.0014287 | | 0.1954961 | |
| t Critical two-tail | 2.1314509 | | 2.3646226 | | 2.3646226 | | 2.3646226 | | 2.3646226 | |

| *phl p* | *zero* | *24 hr* | *Variable 1* | *Variable 2* | *Variable 1* | *Variable 2* | *Variable 1* | *Variable 2* | *Variable 1* | *Variable 2* |
|---|---|---|---|---|---|---|---|---|---|---|
| Mean | 371.6875 | 334.0625 | 383 | 381.375 | 378.125 | 372.125 | 367.875 | 307.125 | 371.375 | 360.625 |
| Variance | 324.89583 | 99.795833 | 139.42857 | 153.69643 | 158.125 | 87.553571 | 470.98214 | 24.410714 | 157.69643 | 10.553571 |
| Observations | 16 | 16 | 8 | 8 | 8 | 8 | 8 | 8 | 8 | 8 |
| Pearson Correlation | 0.7913133 | | 0.109298 | | -0.039004 | | 0.7262825 | | 0.4031447 | |
| Hypothesized Mean Difference | 0 | | 0 | | 0 | | 0 | | 0 | |
| df | 15 | | 7 | | 7 | | 7 | | 7 | |
| t Stat | 12.732462 | | 0.2844292 | | 1.0630357 | | 9.3235227 | | 2.613442 | |
| P(T<=t) one-tail | 9.578E-10 | | 0.3921558 | | 0.1615285 | | 1.694E-05 | | 0.0173695 | |
| t Critical one-tail | 1.753051 | | 1.8945775 | | 1.8945775 | | 1.8945775 | | 1.8945775 | |
| P(T<=t) two-tail | 1.916E-09 | | 0.7843116 | | 0.323057 | | 3.388E-05 | | 0.034739 | |
| t Critical two-tail | 2.1314509 | | 2.3646226 | | 2.3646226 | | 2.3646226 | | 2.3646226 | |

## Statistics for the IOBA-NHC allergen challenge studies. Figure 5.13

| t-Test: Paired Two Sample for means | phl p | | con | | phl p + his | | pro | | phl p + in | |
|---|---|---|---|---|---|---|---|---|---|---|
| | *Variable 1* | *Variable 2* | *Variable 1* | *Variable 2* | *Variable 1* | *Variable 2* | *Variable 1* | *Variable 2* | *Variable 1* | *Variable 2* |
| Mean | 384.25 | 387.1875 | 384.5 | 396 | 391.625 | 381.875 | 384.75 | 364.125 | 400.125 | 399.5 |
| Variance | 199.93333 | 89.229167 | 165.71429 | 16.571429 | 107.41071 | 34.125 | 311.92857 | 6.125 | 122.69643 | 22.285714 |
| Observations | 16 | 16 | 8 | 8 | 8 | 8 | 8 | 8 | 8 | 8 |
| Pearson Correlation | 0.2996021 | | 0.4007369 | | -0.654499 | | -0.361964 | | 0.4630655 | |
| Hypothesized Mean Difference | 0 | | 0 | | 0 | | 0 | | 0 | |

| | | | | | |
|---|---|---|---|---|---|
| df | 15 | 7 | 7 | 7 | 7 |
| t Stat | -0.812513 | -2.746225 | 1.8559408 | 3.1195601 | 0.179904 |
| P(T<=t) one-tail | 0.2146023 | 0.0143298 | 0.0529201 | 0.008427 | 0.4311625 |
| t Critical one-tail | 1.753051 | 1.8945775 | 1.8945775 | 1.8945775 | 1.8945775 |
| P(T<=t) two-tail | 0.4292045 | 0.0286596 | 0.1058403 | 0.0168541 | 0.8623251 |
| t Critical two-tail | 2.1314509 | 2.3646226 | 2.3646226 | 2.3646226 | 2.3646226 |

| | *Variable 1* | *Variable 2* | *Variable 1* | *Variable 2* | *Variable 1* | *Variable 2* | *Variable 1* | *Variable 2* | *Variable 1* | *Variable 2* |
|---|---|---|---|---|---|---|---|---|---|---|
| Mean | 384.25 | 369.6875 | 384.5 | 381.25 | 391.625 | 374.375 | 384.75 | 369.5 | 400.125 | 401.625 |
| Variance | 199.93333 | 15.9625 | 165.71429 | 9.6428571 | 107.41071 | 133.69643 | 311.92857 | 34.571429 | 122.69643 | 46.267857 |
| Observations | 16 | 16 | 8 | 8 | 8 | 8 | 8 | 8 | 8 | 8 |
| Pearson Correlation | -0.151937 | | 0.3001915 | | -0.755652 | | 0.6754562 | | 0.7458527 | |
| Hypothesized Mean Difference | 0 | | 0 | | 0 | | 0 | | 0 | |
| df | 15 | | 7 | | 7 | | 7 | | 7 | |
| t Stat | 3.8155727 | | 0.7471828 | | 2.3744752 | | 3.0036925 | | -0.564076 | |
| P(T<=t) one-tail | 0.0008443 | | 0.239647 | | 0.0246404 | | 0.0099191 | | 0.2951545 | |
| t Critical one-tail | 1.753051 | | 1.8945775 | | 1.8945775 | | 1.8945775 | | 1.8945775 | |
| P(T<=t) two-tail | 0.0016886 | | 0.479294 | | 0.0492808 | | 0.0198383 | | 0.590309 | |
| t Critical two-tail | 2.1314509 | | 2.3646226 | | 2.3646226 | | 2.3646226 | | 2.3646226 | |

| | *Variable 1* | *Variable 2* | *Variable 1* | *Variable 2* | *Variable 1* | *Variable 2* | *Variable 1* | *Variable 2* | *Variable 1* | *Variable 2* |
|---|---|---|---|---|---|---|---|---|---|---|
| Mean | 384.25 | 345.1875 | 384.5 | 395 | 391.625 | 351.875 | 384.75 | 334.5 | 400.125 | 376.875 |
| Variance | 199.93333 | 187.3625 | 165.71429 | 57.714286 | 107.41071 | 38.410714 | 311.92857 | 32.285714 | 122.69643 | 94.696429 |
| Observations | 16 | 16 | 8 | 8 | 8 | 8 | 8 | 8 | 8 | 8 |
| Pearson Correlation | 0.196422 | | 0.0365191 | | 0.352796 | | -0.754475 | | -0.600202 | |
| Hypothesized Mean Difference | 0 | | 0 | | 0 | | 0 | | 0 | |
| df | 15 | | 7 | | 7 | | 7 | | 7 | |
| t Stat | 8.8563878 | | -2.019391 | | 11.214995 | | 6.3840552 | | 3.5313223 | |
| P(T<=t) one-tail | 1.204E-07 | | 0.0416025 | | 5E-06 | | 0.0001865 | | 0.0047904 | |
| t Critical one-tail | 1.753051 | | 1.8945775 | | 1.8945775 | | 1.8945775 | | 1.8945775 | |
| P(T<=t) two-tail | 2.408E-07 | | 0.0832051 | | 9.999E-06 | | 0.0003729 | | 0.0095808 | |
| t Critical two-tail | 2.1314509 | | 2.3646226 | | 2.3646226 | | 2.3646226 | | 2.3646226 | |

| | *Variable 1* | *Variable 2* | *Variable 1* | *Variable 2* | *Variable 1* | *Variable 2* | *Variable 1* | *Variable 2* | *Variable 1* | *Variable 2* |
|---|---|---|---|---|---|---|---|---|---|---|
| Mean | 384.25 | 349.5 | 384.5 | 393.5 | 391.625 | 349 | 384.75 | 360.5 | 400.125 | 407 |
| Variance | 199.93333 | 309.46667 | 165.71429 | 36.285714 | 107.41071 | 12.571429 | 311.92857 | 13.428571 | 122.69643 | 36.571429 |
| Observations | 16 | 16 | 8 | 8 | 8 | 8 | 8 | 8 | 8 | 8 |
| Pearson Correlation | -0.108814 | | 0.4034579 | | -0.711438 | | -0.686467 | | 0.4777086 | |
| Hypothesized Mean Difference | 0 | | 0 | | 0 | | 0 | | 0 | |
| df | 15 | | 7 | | 7 | | 7 | | 7 | |
| t Stat | 5.8553788 | | -2.155816 | | 9.1855943 | | 3.370111 | | -1.992253 | |
| P(T<=t) one-tail | 1.582E-05 | | 0.0340135 | | 1.867E-05 | | 0.0059593 | | 0.0433015 | |
| t Critical one-tail | 1.753051 | | 1.8945775 | | 1.8945775 | | 1.8945775 | | 1.8945775 | |
| P(T<=t) two-tail | 3.163E-05 | | 0.0680269 | | 3.735E-05 | | 0.0119185 | | 0.0866031 | |
| t Critical two-tail | 2.1314509 | | 2.3646226 | | 2.3646226 | | 2.3646226 | | 2.3646226 | |

| | *Variable 1* | *Variable 2* | *Variable 1* | *Variable 2* | *Variable 1* | *Variable 2* | *Variable 1* | *Variable 2* | *Variable 1* | *Variable 2* |
|---|---|---|---|---|---|---|---|---|---|---|
| Mean | 384.25 | 384.1875 | 384.5 | 388.875 | 391.625 | 383.875 | 384.75 | 384.5 | 400.125 | 399.625 |
| Variance | 199.93333 | 912.5625 | 165.71429 | 14.982143 | 107.41071 | 110.98214 | 311.92857 | 508.28571 | 122.69643 | 49.982143 |
| Observations | 16 | 16 | 8 | 8 | 8 | 8 | 8 | 8 | 8 | 8 |
| Pearson Correlation | 0.0880656 | | -0.104647 | | -0.799943 | | 0.7577298 | | -0.537462 | |
| Hypothesized Mean Difference | 0 | | 0 | | 0 | | 0 | | 0 | |
| df | 15 | | 7 | | 7 | | 7 | | 7 | |

| | | | | | |
|---|---|---|---|---|---|
| t Stat | 0.0077624 | -0.895085 | 1.1056329 | 0.0480253 | 0.0882407 |
| P(T<=t) one-tail | 0.4969544 | 0.2002356 | 0.1527155 | 0.4815188 | 0.4660784 |
| t Critical one-tail | 1.753051 | 1.8945775 | 1.8945775 | 1.8945775 | 1.8945775 |
| P(T<=t) two-tail | 0.9939089 | 0.4004713 | 0.3054311 | 0.9630376 | 0.9321567 |
| t Critical two-tail | 2.1314509 | 2.3646226 | 2.3646226 | 2.3646226 | 2.3646226 |

| | *Variable 1* | *Variable 2* | *Variable 1* | *Variable 2* | *Variable 1* | *Variable 2* | *Variable 1* | *Variable 2* | *Variable 1* | *Variable 2* |
|---|---|---|---|---|---|---|---|---|---|---|
| Mean | 384.25 | 369 | 384.5 | 384.875 | 391.625 | 392.375 | 384.75 | 365.5 | 400.125 | 395.25 |
| Variance | 199.93333 | 94 | 165.71429 | 32.125 | 107.41071 | 66.839286 | 311.92857 | 381.42857 | 122.69643 | 23.642857 |
| Observations | 16 | 16 | 8 | 8 | 8 | 8 | 8 | 8 | 8 | 8 |
| Pearson Correlation | 0.1235196 | | -0.059717 | | -0.347109 | | 0.7719936 | | 0.7181323 | |
| Hypothesized Mean Difference | 0 | | 0 | | 0 | | 0 | | 0 | |
| df | 15 | | 7 | | 7 | | 7 | | 7 | |
| t Stat | 3.7825745 | | -0.073801 | | -0.138951 | | 4.2939007 | | 1.6601651 | |
| P(T<=t) one-tail | 0.0009032 | | 0.4716168 | | 0.446701 | | 0.0017967 | | 0.0704202 | |
| t Critical one-tail | 1.753051 | | 1.8945775 | | 1.8945775 | | 1.8945775 | | 1.8945775 | |
| P(T<=t) two-tail | 0.0018065 | | 0.9432337 | | 0.8934019 | | 0.0035934 | | 0.1408404 | |
| t Critical two-tail | 2.1314509 | | 2.3646226 | | 2.3646226 | | 2.3646226 | | 2.3646226 | |

## Statistics for the 16HBE-14o- allergen challenge studies. Figure 5.1

t-Test: Paired Two Sample

for means

| | *Variable 1* | *Variable 2* | *Variable 1* | *Variable 2* | *Variable 1* | *Variable 2* | *Variable 1* | *Variable 2* | *Variable 1* | *Variable 2* |
|---|---|---|---|---|---|---|---|---|---|---|
| Mean | 4050.8333 | 3245.8333 | 3462.5 | 3430 | 3920 | 3740 | 4098.75 | 607.5 | 4066.25 | 3790 |
| Variance | 239208.33 | 401808.33 | 225 | 66.666667 | 6628.5714 | 10400 | 115212.5 | 1791.7143 | 18369.643 | 59200 |
| Observations | 12 | 12 | 4 | 4 | 8 | 8 | 8 | 8 | 8 | 8 |
| Pearson Correlation | -0.457809 | | 0.8164966 | | 0.9944963 | | -0.855546 | | 0.9946325 | |
| Hypothesized Mean Difference | 0 | | 0 | | 0 | | 0 | | 0 | |
| df | 11 | | 3 | | 7 | | 7 | | 7 | |
| t Stat | 2.8996353 | | 6.7890286 | | 22.449944 | | 26.242908 | | 7.1417836 | |
| P(T<=t) one-tail | 0.0072273 | | 0.0032666 | | 4.401E-08 | | 1.493E-08 | | 9.335E-05 | |
| t Critical one-tail | 1.7958837 | | 2.353363 | | 1.8945775 | | 1.8945775 | | 1.8945775 | |
| P(T<=t) two-tail | 0.0144545 | | 0.0065332 | | 8.803E-08 | | 2.986E-08 | | 0.0001867 | |
| t Critical two-tail | 2.2009863 | | 3.1824493 | | 2.3646226 | | 2.3646226 | | 2.3646226 | |

| | *Variable 1* | *Variable 2* | *Variable 1* | *Variable 2* | *Variable 1* | *Variable 2* | *Variable 1* | *Variable 2* | *Variable 1* | *Variable 2* |
|---|---|---|---|---|---|---|---|---|---|---|
| Mean | 4050.8333 | 3020 | 3462.5 | 3372.5 | 3920 | 3536.25 | 4098.75 | 375.125 | 4066.25 | 3600 |
| Variance | 239208.33 | 23527.273 | 225 | 25 | 6628.5714 | 17541.071 | 115212.5 | 5.5535714 | 18369.643 | 3828.5714 |
| Observations | 12 | 12 | 4 | 4 | 8 | 8 | 8 | 8 | 8 | 8 |
| Pearson Correlation | -0.96169 | | 0.7777778 | | 0.9803827 | | 0.5699369 | | 0.9863063 | |
| Hypothesized Mean Difference | 0 | | 0 | | 0 | | 0 | | 0 | |
| df | 11 | | 3 | | 7 | | 7 | | 7 | |
| t Stat | 5.5971601 | | 15.588457 | | 19.728885 | | 31.151281 | | 17.536133 | |
| P(T<=t) one-tail | 8.05E-05 | | 0.0002868 | | 1.074E-07 | | 4.536E-09 | | 2.414E-07 | |
| t Critical one-tail | 1.7958837 | | 2.353363 | | 1.8945775 | | 1.8945775 | | 1.8945775 | |
| P(T<=t) two-tail | 0.000161 | | 0.0005737 | | 2.148E-07 | | 9.073E-09 | | 4.829E-07 | |
| t Critical two-tail | 2.2009863 | | 3.1824493 | | 2.3646226 | | 2.3646226 | | 2.3646226 | |

| | *Variable 1* | *Variable 2* | *Variable 1* | *Variable 2* | *Variable 1* | *Variable 2* | *Variable 1* | *Variable 2* | *Variable 1* | *Variable 2* |
|---|---|---|---|---|---|---|---|---|---|---|
| Mean | 4050.8333 | 2971.6667 | 3462.5 | 3950 | 3920 | 3568.75 | 4098.75 | 346.875 | 4066.25 | 3833.75 |
| Variance | 239208.33 | 616524.24 | 225 | 0 | 6628.5714 | 110783.93 | 115212.5 | 119.83929 | 18369.643 | 59826.786 |
| Observations | 12 | 12 | 4 | 4 | 8 | 8 | 8 | 8 | 8 | 8 |
| Pearson Correlation | -0.750588 | | #DIV/0! | | 0.9847602 | | 0.8980534 | | -0.995819 | |
| Hypothesized Mean Difference | 0 | | 0 | | 0 | | 0 | | 0 | |
| df | 11 | | 3 | | 7 | | 7 | | 7 | |
| t Stat | 3.1237286 | | -65 | | 3.9258349 | | 32.193017 | | 1.7316218 | |
| P(T<=t) one-tail | 0.0048427 | | 4.012E-06 | | 0.0028531 | | 3.608E-09 | | 0.0634748 | |
| t Critical one-tail | 1.7958837 | | 2.353363 | | 1.8945775 | | 1.8945775 | | 1.8945775 | |
| P(T<=t) two-tail | 0.0096854 | | 8.023E-06 | | 0.0057061 | | 7.217E-09 | | 0.1269497 | |
| t Critical two-tail | 2.2009863 | | 3.1824493 | | 2.3646226 | | 2.3646226 | | 2.3646226 | |

| | *Variable 1* | *Variable 2* | *Variable 1* | *Variable 2* | *Variable 1* | *Variable 2* | *Variable 1* | *Variable 2* | *Variable 1* | *Variable 2* |
|---|---|---|---|---|---|---|---|---|---|---|
| Mean | 4050.8333 | 3691.0833 | 3462.5 | 4090 | 3920 | 2985 | 4098.75 | 327.75 | 4066.25 | 3775 |
| Variance | 239208.33 | 1651691.5 | 225 | 0 | 6628.5714 | 21714.286 | 115212.5 | 141.07143 | 18369.643 | 187485.71 |
| Observations | 12 | 12 | 4 | 4 | 8 | 8 | 8 | 8 | 8 | 8 |
| Pearson Correlation | -0.677694 | | #DIV/0! | | -0.975221 | | 0.7819622 | | -0.995735 | |
| Hypothesized Mean Difference | 0 | | 0 | | 0 | | 0 | | 0 | |
| df | 11 | | 3 | | 7 | | 7 | | 7 | |
| t Stat | 0.7524715 | | -83.66667 | | 11.626029 | | 32.299183 | | 1.4500849 | |
| P(T<=t) one-tail | 0.2337825 | | 1.882E-06 | | 3.931E-06 | | 3.527E-09 | | 0.095159 | |
| t Critical one-tail | 1.7958837 | | 2.353363 | | 1.8945775 | | 1.8945775 | | 1.8945775 | |
| P(T<=t) two-tail | 0.467565 | | 3.763E-06 | | 7.861E-06 | | 7.053E-09 | | 0.1903179 | |
| t Critical two-tail | 2.2009863 | | 3.1824493 | | 2.3646226 | | 2.3646226 | | 2.3646226 | |

| | *Variable 1* | *Variable 2* | *Variable 1* | *Variable 2* | *Variable 1* | *Variable 2* | *Variable 1* | *Variable 2* | *Variable 1* | *Variable 2* |
|---|---|---|---|---|---|---|---|---|---|---|
| Mean | 4050.8333 | 3153.3333 | 3462.5 | 4432.5 | 3920 | 2460 | 4098.75 | 332.875 | 4066.25 | 4406.25 |
| Variance | 239208.33 | 1198642.4 | 225 | 91.666667 | 6628.5714 | 77400 | 115212.5 | 19.553571 | 18369.643 | 2483.9286 |
| Observations | 12 | 12 | 4 | 4 | 8 | 8 | 8 | 8 | 8 | 8 |
| Pearson Correlation | -0.920153 | | 0.4061812 | | -0.978213 | | -0.587371 | | -0.987905 | |
| Hypothesized Mean Difference | 0 | | 0 | | 0 | | 0 | | 0 | |
| df | 11 | | 3 | | 7 | | 7 | | 7 | |
| t Stat | 1.99721 | | -137.1787 | | 11.526886 | | 31.140583 | | -5.20009 | |
| P(T<=t) one-tail | 0.0355716 | | 4.271E-07 | | 4.162E-06 | | 4.547E-09 | | 0.0006264 | |
| t Critical one-tail | 1.7958837 | | 2.353363 | | 1.8945775 | | 1.8945775 | | 1.8945775 | |
| P(T<=t) two-tail | 0.0711432 | | 8.541E-07 | | 8.325E-06 | | 9.094E-09 | | 0.0012529 | |
| t Critical two-tail | 2.2009863 | | 3.1824493 | | 2.3646226 | | 2.3646226 | | 2.3646226 | |

| | *Variable 1* | *Variable 2* | *Variable 1* | *Variable 2* | *Variable 1* | *Variable 2* | *Variable 1* | *Variable 2* | *Variable 1* | *Variable 2* |
|---|---|---|---|---|---|---|---|---|---|---|
| Mean | 4050.8333 | 3662.5 | 3462.5 | 4475 | 3920 | 1978.75 | 4098.75 | 345.125 | 4066.25 | 3793.75 |
| Variance | 239208.33 | 1606384.1 | 225 | 33.333333 | 6628.5714 | 149412.5 | 115212.5 | 6.4107143 | 18369.643 | 991141.07 |
| Observations | 12 | 12 | 4 | 4 | 8 | 8 | 8 | 8 | 8 | 8 |
| Pearson Correlation | -0.686771 | | 0.1924501 | | 0.9855039 | | 0.0002078 | | -0.995507 | |
| Hypothesized Mean Difference | 0 | | 0 | | 0 | | 0 | | 0 | |
| df | 11 | | 3 | | 7 | | 7 | | 7 | |
| t Stat | 0.8191287 | | -135 | | 17.907446 | | 31.27769 | | 0.681739 | |
| P(T<=t) one-tail | 0.2150514 | | 4.481E-07 | | 2.091E-07 | | 4.41E-09 | | 0.2586587 | |
| t Critical one-tail | 1.7958837 | | 2.353363 | | 1.8945775 | | 1.8945775 | | 1.8945775 | |
| P(T<=t) two-tail | 0.4301028 | | 8.962E-07 | | 4.182E-07 | | 8.821E-09 | | 0.5173173 | |
| t Critical two-tail | 2.2009863 | | 3.1824493 | | 2.3646226 | | 2.3646226 | | 2.3646226 | |